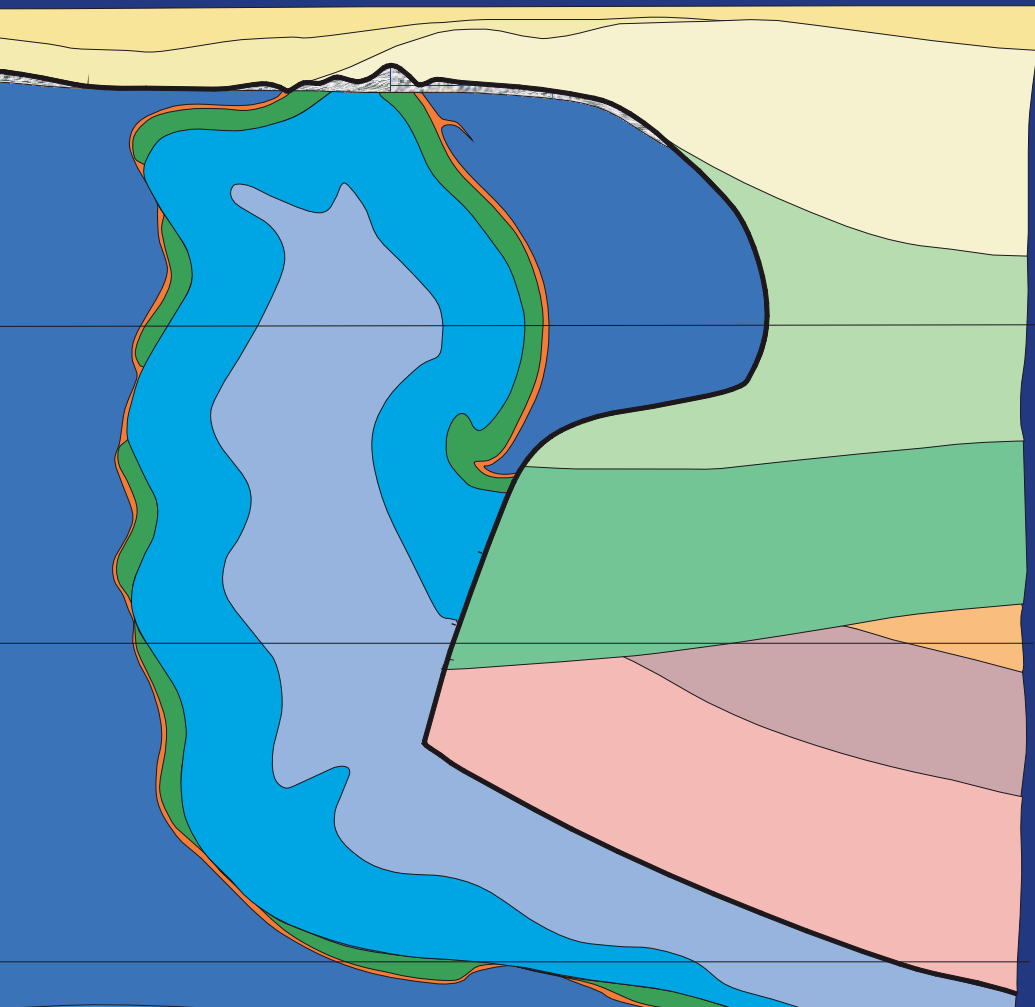


Description of the Gorleben Site Part 3:

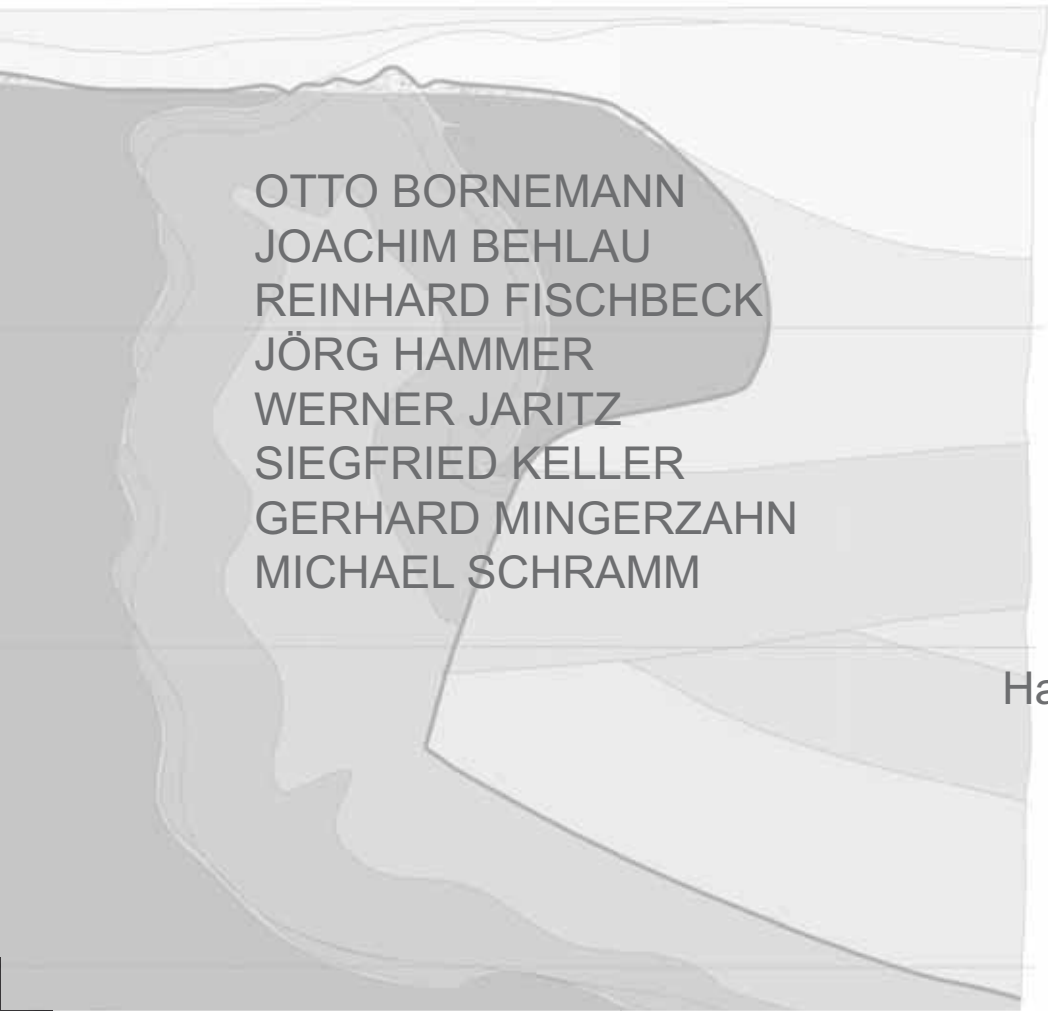
Results of the geological surface and underground exploration of the salt formation



Description of the Gorleben Site
Part 3:
Results of the geological surface
and underground exploration of
the salt formation

Description of the Gorleben Site
Part 3:

Results of the geological surface
and underground exploration of the
salt formation

A faint, grayscale geological map of the Gorleben site is visible in the background. It shows various geological features, including a large, irregularly shaped area that is shaded in a darker gray, likely representing the salt formation mentioned in the title. The map includes contour lines and other geological symbols.

OTTO BORNEMANN
JOACHIM BEHLAU
REINHARD FISCHBECK
JÖRG HAMMER
WERNER JARITZ
SIEGFRIED KELLER
GERHARD MINGERZAHN
MICHAEL SCHRAMM

Hannover, 2008

German edition:

Standortbeschreibung Gorleben Teil 3
Ergebnisse der über- und untertägigen Erkundung des Salinars

ISBN 978-3-510-95964-8, Price: 64.00 €

More information/Purchase: <http://www.schweizerbart.de/9783510959648>

© Bundesanstalt für Geowissenschaften und Rohstoffe (BGR)
Geozentrum Hannover
Stilleweg 2
30655 Hannover
Germany

www.bgr.bund.de

ISBN 978-3-9813373-6-5

Foreword

Research has been carried out since 1979 on the Gorleben salt dome, located in the rural district of Lüchow-Dannenberg in Lower Saxony, to investigate its suitability as a geologic repository for radioactive waste. The investigation programme consists of surface and underground geological and mine engineering exploration, as well as analysing and evaluating all of the issues necessary to competently assess its suitability and long-term safety. The Gorleben site was investigated in detail for a period of more than twenty years to understand the internal structure of the salt dome, the overburden and the adjoining rock. The preliminary results of these investigations were published in interim reports in 1983, 1990 and 1995. The findings published in these reports substantiated the potential suitability of the salt dome as a geologic repository for radioactive waste.

The investigation work at the Gorleben site was suspended as a consequence of the agreement reached on 14 June 2000 between the German government and the power supply industry. This moratorium applied for a period of at least three years, but a maximum of ten years. Notwithstanding the moratorium, the German government issued a statement on Gorleben which confirmed that the previous findings from its investigation did not contradict the site's potential suitability.

It is now possible after the termination of the surface investigation programme, and for the purpose of documenting the results of the extensive underground exploration, to present the findings of the geoscientific investigation of the Gorleben site in an overall report. The first part presents the hydrogeology of the overburden. The second part presents the results of the geological and structural geological exploration of the overburden and the adjoining rock, and the third part covers the results of the exploration of the salt itself. These findings are supplemented in the fourth part by a description of the geotechnical investigations.

This compilation of the data, and the presentation of the technical evaluation of the geoscientific investigation results, as well as the documentation, should also help to bring more objectivity into the controversially discussed public and political debate concerning the Gorleben site.



(Volkmar Bräuer)

- Repository Project Manager -

Abstract

This report describes the geological investigations of the salt formation of the Gorleben salt dome performed during surface and underground exploration up to the beginning of the moratorium on October 1, 2000, summarizes their results and evaluates their meaning for the long-term safety of the planned repository for radioactive waste.

In the course of the exploration, a new high-resolution stratigraphic subdivision of the Zechstein period was created for certain stratigraphic horizons, which to a certain degree applies to the whole Zechstein Basin. Combined with the development of standard bromide profiles for the Stassfurt-Folge and Leine-Folge and their integration in a 3D geological deposit model, this high resolution stratigraphy facilitates better planning of the excavation of exploration and repository drifts, whilst leaving the geological barrier largely intact.

Estimates of subsidence rates at the top of the diapir, the epigenetic development of the region and the salt diapirism show that the thickness of the geological barrier consisting of the host rock salt will still be large enough for sustainable prevention of radionuclide transport to the biosphere from a future repository even after a period of a million years. The occurrence of hazards during or after operation of the repository arising from the inflow of gases and solutions can also be excluded.

Although the exploration of Exploration Area 1 (EB1) has not been concluded yet, the results of the exploration of the salt dome carried out to date support the conclusion that none of the geoscientific findings rule out the suitability of the Gorleben salt dome with regards to the long-term safe storage of radioactive waste. As predicted on the basis of the evaluation of the surface exploration boreholes, the unjointed and undisturbed Hauptsalz body of the Stassfurt-Folge is sufficiently large to act as a potential host rock for the final disposal of radioactive waste.

Contents		Page
1	Introduction	9
2	Sequence and objectives of the exploration and methods employed	12
2.1	Chronological order and objectives of the exploration	12
2.2	Seismic reflection and refraction surveys	15
2.3	Surface exploration boreholes	16
2.3.1	Salt dome exploration boreholes	16
2.3.2	Shaft pilot boreholes	27
2.3.3	Salt table boreholes	34
2.4	Underground mapping	43
2.4.1	Shafts Gorleben 1 and Gorleben 2	44
2.4.2	Drifts and chambers	45
2.5	Underground exploration boreholes	45
2.6	Electromagnetic survey methods	50
2.6.1	Electromagnetic reflection surveys	50
2.6.2	High-frequency absorption surveys	53
2.7	Mineralogical and geochemical investigations	54
2.7.1	Sample preparation and analysis to determine the qualitative mineralogical composition	55
2.7.2	Determining the quantitative mineralogical composition	56
2.7.3	Determining the bromide content in the evaporites	57
3	Salt dome exploration results	59
3.1	Composition, extent and genesis of the cap rock	59
3.1.1	Late Mesozoic to Cenozoic cap rock development	60
3.1.1.1	Quaternary subsidence	64
3.1.1.2	Cretaceous and Tertiary subsidence	71
3.1.2	Middle Mesozoic cap rock formation	73
3.2	Salt table and selective subsidence	75
3.3	Composition and structure of the salt dome	79
3.3.1	Stratigraphy and petrography	79
3.3.1.1	Stassfurt-Folge (Zechstein 2)	81
3.3.1.2	Leine-Folge (Zechstein 3)	89
3.3.1.3	Aller-Folge (Zechstein 4)	120
3.3.2	Structure of the Gorleben salt dome	124
3.3.2.1	Large-scale folding in the Gorleben salt dome	124
3.3.2.2	Investigation of the structural geology in the shafts	129
3.3.2.3	Geological structure of the infrastructure section	132
3.3.2.4	Structural geology of Exploration Area 1 (EB 1)	135

3.3.3	Mineralogy and geochemistry of the salt rocks	141
3.3.3.1	Bromide standard profile of the Stassfurt-Folge (Zechstein 2)	141
3.3.3.2	Bromide standard profile of the Leine-Folge (Zechstein 3)	146
3.3.3.3	Mineralogical and geochemical investigations of the Kaliflöz Stassfurt	150
3.3.4	Hydrocarbons, gases and brines in the Gorleben salt dome	160
3.3.4.1	Gaseous hydrocarbons and condensates	160
3.3.4.2	Other gas inclusions in the salt formation	167
3.3.4.3	Brines	169
3.3.4.4	Pressures in solution and gas reservoirs	177
3.3.4.5	Permeabilities of the rock salt in the vicinity of solution and gas reservoirs	177
3.3.5	Water content of the rock salt	178
4	Evaluation of the results	179
4.1	Size of the Hauptsalz as the host medium for a potential repository	179
4.2	Fissures and potential migration paths for saline solutions and gases	180
4.3	Consequences of subsrosion for the long-term safety of a repository	182
5	Summary	185
	References	189
	Abbreviations	215
	List of tables	217
	List of figures	218
	List of appendices	223

1 Introduction

The Federal Institute for Geosciences and Natural Resources (BGR), as the German government's central authority on geoscientific issues, works on the geoscientific aspects of the investigation of the Gorleben site as part of the geological repository measures of the Federal Ministry for the Environment, Nature Conservation and Nuclear Safety (BMU) and the Federal Office for Radiation Protection (BfS). All of the investigation findings resulting from the surface and underground geological exploration activities are interpreted and presented by the BGR. The results of the exploration and the safety analysis form the basis for the assessment of the site and the subsequent approval procedures conducted pursuant to the Atomic Energy Act.

This report summarizes the results of the various surface and underground exploration operations (mapping, drilling, mineralogical and geochemical analyses, electromagnetic reflection surveys, etc.) carried out until October 1, 2000 in the form of a geological model of the Gorleben salt dome. The geological and tectonic mapping of the shafts, drifts and chambers in the Gorleben salt dome, and the surveying and preparation of the well logs for the shafts, the exploration and drift pilot boreholes were carried out by the DBE (Deutsche Gesellschaft zum Bau und Betrieb von Endlagern für Abfallstoffe mbH, Peine; German Company for the Construction and Operation of Waste Repositories, Ltd.) under the geoscientific supervision and quality control of the BGR. The BGR, acting on behalf of the BfS, is responsible for integrating all results into a geological model of the deposit.

The investigation results have been recorded in numerous internal interim and final reports, and in dissertations and theses, which are not available to a wide readership. In order to document authorship as well as to facilitate identification of the primary data and further use of the investigation results, these reports have been included in the references under the separate heading "Unpublished reports".

The Gorleben salt dome strikes from NE to SW and is approx. 14 km long and a maximum of 4 km wide. The structure continues for another 16 km to the NE of the River Elbe as the Rambow salt dome, although with reduced width. The salt table is approx. 250 m below ground level whilst the base of the Zechstein lies at a depth of between 3200 and 3400 m. The salt dome has a large overhang on its SE flank and a very small overhang on its NW flank.

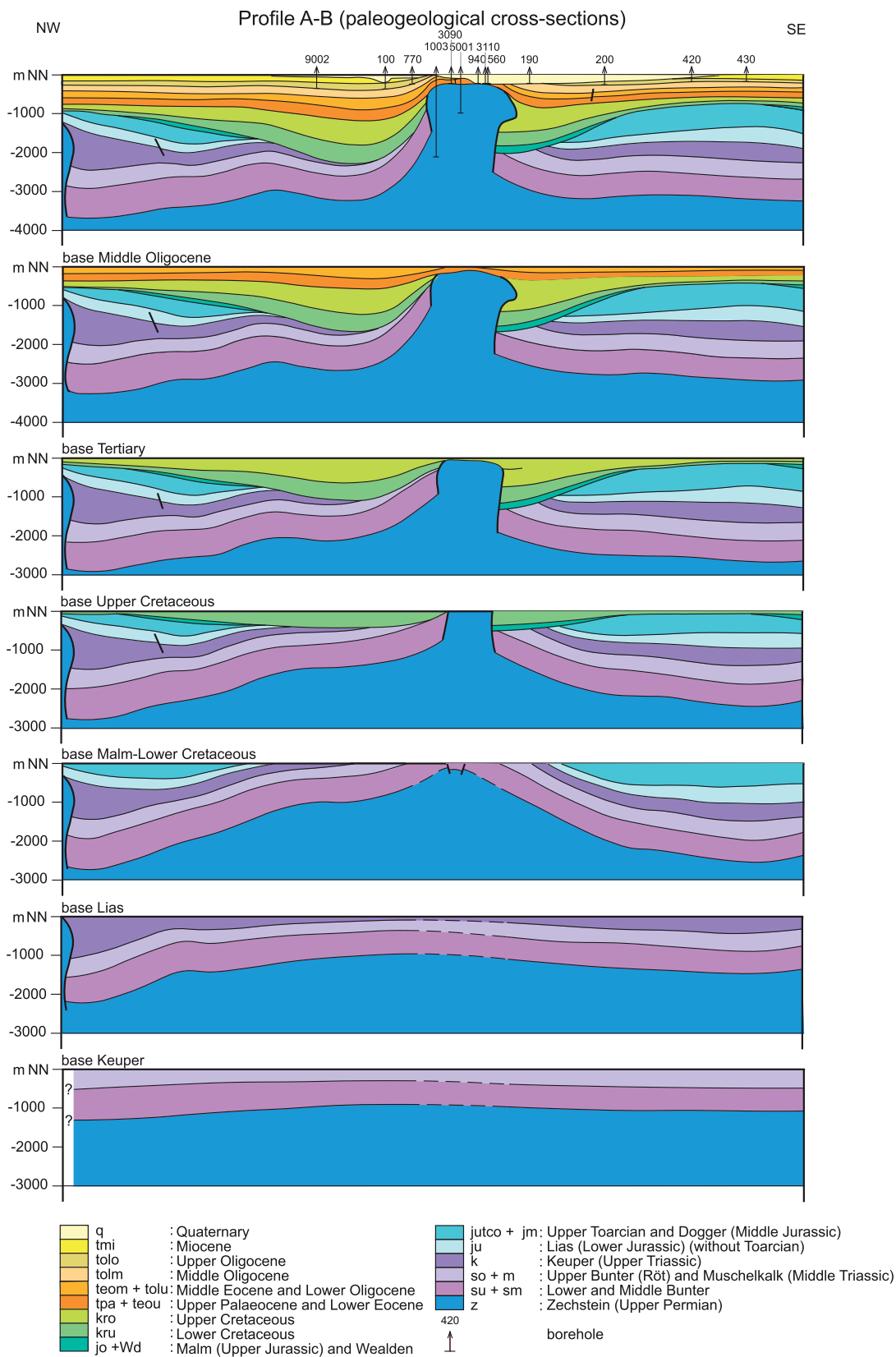


Figure 1: Geochronological scheme of the salt dome formation at the Gorleben site shown as a cross section (after JARITZ 1980; ZIRNGAST 1985, 1991).

The first indication of salt pillow formation was during the Upper Bunter to Muschelkalk period (Fig. 1). Pillow formation reached its maximum during the Keuper, Lias and Dogger periods. From the Malm to the Lower Cretaceous, the salt accumulated within the salt pillow began to penetrate the overburden and form a salt dome. The structure developed further in the Upper Cretaceous and Tertiary (JARITZ 1980; ZIRNGAST 1985; 1991).

The sequence of strata within the Gorleben salt dome consists mostly of rock salt. However, anhydrite, mudstone and carnallite can also be found. Homogeneous, continuous bodies of halite primarily occur in the Stassfurt-Folge (z2). These salt rocks are called Hauptsalz (z2HS). During the formation of the salt dome they travelled a distance of several thousand metres. They occur as mostly homogeneous rock salt that, due to the transport-induced alteration processes, only very rarely contain brines or gases.

The Hauptsalz of the Stassfurt-Folge contains approx. 95 % halite and on average 5 % anhydrite. The Leine-Folge and Aller-Folge (z3, z4) display more frequent changes in their mineral components (JARITZ 1993).

The Hauptsalz of the Stassfurt-Folge forms the core of a central upright anticline in the salt dome. The younger layers of the Leine-Folge and Aller-Folge occur mainly in the outer regions of the salt dome. In the inner region they occur in narrow synclines of extensive depth and are sometimes overlaid by overturned folds of the Hauptsalz in the overhangs (see Chapter 3.3.2).

The gas exploration borehole "Gorleben Z1" (Go Z1, see Fig. 2) drilled on the NW flank of the salt dome in 1957 showed flat layers of the Werra-Folge and lower Stassfurt-Folge that are unrelated to the formation of the salt dome.

2 Sequence and objectives of the exploration and methods employed

2.1 *Chronological order and objectives of the exploration*

A multitude of geological data is necessary to assess the suitability of the Gorleben salt dome as a repository for radioactive waste. The geological data result from extensive surface and underground exploration work.

The objectives of the **geological exploration from the surface** can be summarized as follows:

Salt table boreholes

- Determine subsrosion behaviour of the salt dome
- Create a geological map of the salt table level
- Determine subsrosion rate of the Kaliflöz Stassfurt cropping out at the salt table
- Designate two shaft drilling locations that penetrate mainly layers of the lower Leine-Folge to a depth of approx. 1000 m

Exploration boreholes

- Determine and describe the stratigraphy of the Zechstein period in the salt dome
- Determine the mineralogical and geochemical components of the Zechstein layers
- Elaborate preliminary findings on gas and brine occurrences in the sequences of the salt dome
- Develop an idea of the inner structure of the salt dome
- Create a preliminary geological map of the designated exploration level (840 m-level)

The main objective of the **subsurface geological exploration** was to create a geological model of the salt dome as well as to prove that the Hauptsalz (z2HS) body of the Stassfurt-Folge:

- is sufficiently large in area and volume to serve as a repository and
- contains neither significant volumes of gas or brines nor secondary minerals such as carnallite

and furthermore that

- there is no connection via fluid migration paths between the exploration level and the aquifer above the salt dome,
- the brine reservoirs found in the Hauptanhydrit have no longrange interconnections.

The surface exploration of the western part of the Gorleben-Rambow salt dome (study area Gorleben-Süd) started in 1979 and ended in 1985 (see BfS 1990; BÖHME et al. 1995; BORNEMANN et al. 1988). Supplementary shallow seismic surveys followed between 1994 and 1997. The area around Dömitz-Lenzen (eastern part of the structure) was the object of exploration operations from 1996 to 1998.

The surface exploration programme involved the following tasks (see KLINGE et al. 2003, 2007; KÖTHE et al. 2003, 2007; ZIRNGAST et al. 2003):

- Hydrogeological exploration
over an area of approx. 390 km² involving 322 water-level observation boreholes and 4 wells for long-term pump tests in the Gorleben-Süd area, and 22 exploration boreholes, 76 water-level observation boreholes and one well with 12 additional observation points for a pump test in the Dömitz-Lenzen area. Additionally, 5 boreholes were drilled to explore the structural geology of the transition zone between the Gorleben and Rambow salt domes (KLINGE et al. 2001).
- Mapping of the Quaternary geology
- Geophysical surveys
comprising 549 deep soundings and 16 seismic reflection profiles along and across the salt dome, with a total length of 150 km as well as 82 high-resolution seismic profiles with a total length of 312 km.
- The installation and operation of a seismographic array
to continuously monitor any local earthquake activity at the site starting in February 1986.
- 44 salt table drillings
to investigate the contact zone and transition zone between the salt dome and the overburden/cap rock.
- 4 deep boreholes
penetrating the flanks of the salt dome drilled to a depth of approx. 2000 m to investigate the material components and structure of the salt dome.
- 2 pilot shaft boreholes to a depth of almost 1000 m to prepare the sinking of the mine shafts for the underground exploration. The salt table boreholes GoHy 3151 to 3155 were used for a more detailed exploration of the shaft drilling locations.

The subsurface exploration programme started with the sinking of Shafts Gorleben 1 and Gorleben 2, spaced approx. 400 m apart, from 1986 to 1997 and 1989 to 1995 respectively. Subsurface exploration continued with drift excavation for the mine infrastructure and Exploration Area 1 (EB 1). This was started by setting up the bottom landings at the 840m-level on October 4, 1995 for Shaft 1 and on November 18, 1995 for Shaft 2. Connection of both shafts via the main drift was achieved on October 21, 1996.

Drifting continued with the construction of the infrastructure area with workrooms, operational areas and storerooms. The shaft sinking and the drift and chamber mining work were accompanied by detailed geological mapping. Numerous exploration and geotechnical boreholes were drilled in order to plan the mining operations and to gain information on the geological structure, geophysical properties, as well as the mineral and structural inventory of the salt dome (App. 3). A broad spectrum of logging carried out in the boreholes added to the information gained. Logging methods used in selected **exploration boreholes** were the following:

- Borehole deviation logs
- Temperature logs
- Permeability tests and
- Electromagnetic reflection surveys (EMR)

In the **geotechnical boreholes** the following measurement methods were carried out:

- Extensometer and inclinometer measurements
- Temperature measurements
- Convergence measurements
- Short-term and long-term stress measurements

In addition to this, measurement locations for deformation recording were installed in the shafts and drifts. EMR surveys were carried out in numerous boreholes, as well as in the shafts, underground drifts and chambers. The surface and underground exploration was also accompanied by the collection of a comprehensive series of samples to determine the mineralogical and geochemical composition of the rocks.

On October 1, 2000, exploration was suspended due to the politically motivated moratorium that was agreed upon by the Federal Government and the energy supply companies. Due to the suspension of the underground exploration, this report is still incomplete

with regards to a comprehensive and firm assessment of the suitability of the salt dome for a potential repository for radioactive wastes. The results of the hydrogeological and geotechnical investigations at the Gorleben site are covered in detail by the following reports: KLINGE et al. (2007); ZIRNGAST et al. (2003); KLINGE et al. (2001); ALBRECHT et al. (1991). The investigations with regard to the geology and tectonics of the salt dome carried out to date are summarized below.

2.2 *Seismic reflection and refraction surveys*

In the first quarter of 1984, investigation of the Gorleben site involved seismic reflection, refraction and salt dome undershooting surveys of the salt dome. The BGR was responsible for planning the positioning and orientation of the survey lines. The field surveys and the subsequent digital processing were performed by contractors. The seismic reflection profiles were then evaluated and geologically interpreted by the BGR.

These surveys were performed in order to determine the structure and boundaries of the salt dome, using reflection seismics, and to determine the structure and shape of the salt dome surface, using reflection and refraction seismics. Another objective was to define the base of the salt body by seismic reflection methods, as far as technically feasible. With this aim, undershooting of the salt dome was carried out on selected lines (ZIRNGAST 1985, 1990). These field surveys were carried out from mid-January until the end of March 1984. Digital processing of the field data as well as the preliminary geological interpretation required for some of the processing steps were carried out from the beginning of February 1984 to the beginning of June 1985.

In total, 549 deep soundings were carried out and 16 seismic reflection profiles with a total length of 150 km were surveyed along and across the salt dome. Several separate reports have already presented the results, e.g. with regard to the structural development of the salt dome (ZIRNGAST 1991; ZIRNGAST et al. 2003). From 1994 to 1996, two high-resolution seismic reflection survey campaigns involving the acquisition of 312 kilometres of profiles were surveyed in the Gorleben-Süd and Dömitz-Lenzen areas as part of complementary structural and hydrogeological investigations of the overburden. The aim of these investigations was a more precise definition of the bedding of the Tertiary and Quaternary layers and of the upper surface of the Gorleben-Rambow salt dome and the identification of outcrops of the Kaliflöz Stassfurt at the salt table to determine selective subsrosion areas.

Downhole seismic surveys were carried out in 42 boreholes to provide the data necessary to interpret the time sections and determine the seismic velocities required for depth conversion. Based on this information, the profiles were depth converted and geologically interpreted. The results of these profile interpretations and the borehole data were used to create detailed structural maps of the Quaternary base, of six horizons of Tertiary rock units, and of the salt dome surface (see also KÖTHE et al. 2007, 2003; ZIRNGAST et al. 2003). The data on the salt dome and overburden obtained by seismic methods were integrated into the geological 3D model of salt dome.

2.3 Surface exploration boreholes

In order to determine the stratigraphic sequences and salt tectonics in the area of the planned repository location, 4 exploration boreholes, 44 salt table boreholes, and two shaft pilot boreholes were drilled into the salt dome. The results are presented in the following chapters and are taken mainly from reports by BORNEMANN (1991) and ALBRECHT et al. (1991).

2.3.1 Salt dome exploration boreholes

The exploration of the sequence of strata and the structures in the salt dome began with the 4 exploration boreholes Go 1002, Go 1003, Go 1004, and Go 1005 with final depths of approx. 2000 m. Boreholes Go 1002 and Go 1003 were sunk on the NW side of the salt dome and boreholes Go 1004 and Go 1005 on the SE flank of the salt dome (Fig. 2).

The structure of salt domes in northern Germany is often divided into two subzones. The Hauptsalz of the Stassfurt-Folge (z2HS) is the oldest stratigraphic member and forms the core of the salt domes whilst the younger strata of the Leine-Folge and Aller-Folge (z3, z4) form the outer regions of the salt domes.

Based on the data of earlier seismic profiles, the extent and shape of the Gorleben salt dome was sufficiently known to allow a well-founded selection of the locations for the exploration boreholes. Considering the general salt dome structure, the four salt dome exploration boreholes were drilled in areas where the younger as well as the older salt dome sequences could be expected. This was done to ensure that a range of sequences would be penetrated without unnecessarily damaging the Hauptsalz (z2HS), the host rock for the prospective repository. The peripheral positions of the boreholes had the additional advantage of allowing a more precise analysis of the strata shapes and structure than would have been possible with boreholes merely penetrating the uniform sequences of the Hauptsalz.

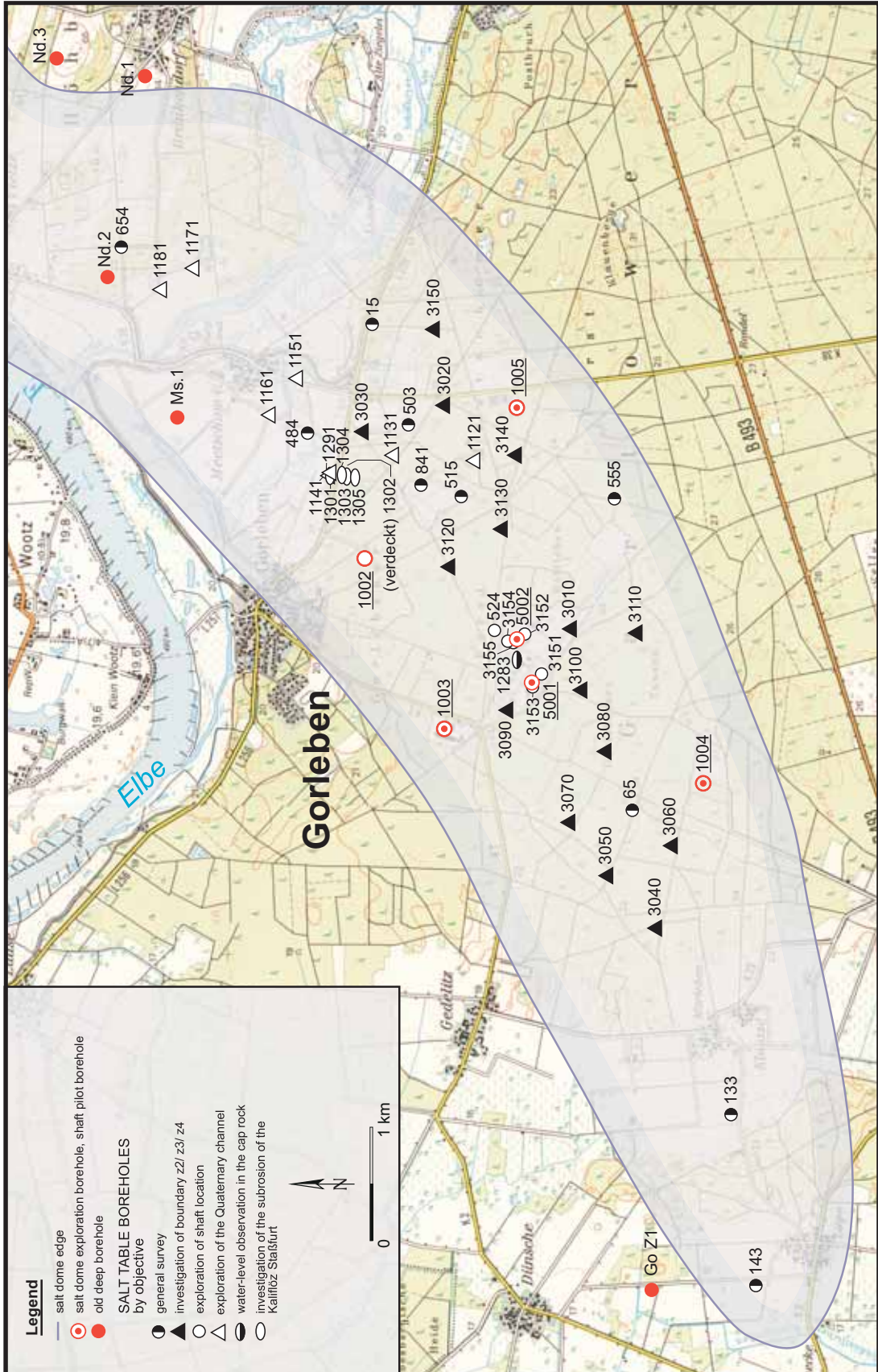


Figure 2: Borehole map – surface boreholes with exposures in the salt formation (abbreviations used for surface boreholes: GoHy - salt table boreholes, Go - pilot shaft boreholes and exploration boreholes).

Each salt dome exploration borehole was driven through the overburden down to the top of the cap rock as a full-hole, non-core well and then continued to final depth as a core drilling producing an almost continuous stretch of cores with a diameter of approx. 100 mm. The exception is borehole Go 1003: In this borehole coring was started at the salt table. Only some small sections in the cap rock and the salt formation were not cored as the homogeneous rock could easily be identified.

Different drilling muds were used depending on the rock type encountered. The overburden was drilled using a clay/freshwater mud. At the top of the cap rock this was replaced by mud containing clay, a salt-mix and water to ensure that even in the layers containing potassium and magnesium minerals cores could be cut with as little subsidence as possible. Borehole Go 1003 was cored from the salt table to final depth with an oil-based mud with the idea of creating a good rock interface for future electromagnetic reflection surveys (EMR) via the oil, and with the additional aim of cutting costs. However, the oil interfered with the handling of the cores as these had to be cleaned laboriously before they could be analysed. Thus, using oil-based mud turned out to be unsuitable for the drilling stage. In the other salt dome exploration boreholes, the clay/salt-mix/water mud was replaced with oil-based mud only after final depth had been reached in order to facilitate high-frequency absorption (HFA) surveys and electromagnetic reflection surveys (EMR). Due to brine inflow, the oil-based mud in Go 1003 had to be refreshed.

Casing of the boreholes was started with a 30" conductor pipe except for borehole Go 1003 which was started with a 20" conductor pipe. After reaching the cap rock, a 13-3/8" casing was set in the cap rock and cemented up to the surface. This was followed by a 9-5/8" anchor casing to approx. 100 m below the salt table, which was also cemented up to the surface. In borehole Go 1003, an additional 7" casing was set at 550 m and cemented up to the surface after reaching final depth because of brine inflow.

To interpret the structure of the salt dome, core samples, most with a length of 18 m, are available from all boreholes. Oriented cores were also taken after every 50 to 70 metres of drilling. The following geophysical logs were also run in the exploration wells to provide additional information on the geology of the salt dome (see BORNEMANN 1991: Apps. 2-5):

- **Go 1002**
Temperature log, density log, borehole geometry log, calliper log, gamma-ray log
- **Go 1003**
Temperature log, neutron log, borehole geometry log, sonic log, calliper log, salinity log to 1280 m, gamma-ray log, density log

- **Go 1004**
Temperature log, neutron log, borehole geometry log, sonic log, calliper log, continuous dipmeter log, gamma-ray log, density log
- **Go 1005**
Temperature log, density log, borehole geometry log, sonic log, calliper log, neutron log, gamma-ray log

Furthermore, in all boreholes electromagnetic reflection surveys (EMR) as well as geothermal surveys to determine the natural temperature field were performed. In boreholes Go 1002 and Go 1003, high-frequency absorption (HFA) and seismic reflection methods (downhole seismic surveys) were used. The latter were used to determine the NW flank of the salt dome (ALBRECHT et al. 1991).

After replacing the drilling mud, the borehole heads were sealed in order to monitor head pressure and potential brine discharges. The time periods involved for each borehole were:

- Go 1002: from July 1980 to January 1983
- Go 1003: from April 1980 to August 1983
- Go 1004: from November 1980 to April 1982
- Go 1005: from March 1981 to February 1982

Subsequently, packer tests were carried out in the boreholes to identify any brine or gas discharges. This was followed by successive backfilling of the boreholes. The results of the tests and the backfilling procedures were described in detail in several DBE reports (ENKE 1982 a and b; 1983 a and b; GRÜBLER & REPPERT 1985; REPPERT 1982 a and b; 1983 c).

For the records, each core sample was photographed; the photographs were used to create core sequential photo logs. The descriptions in the stratigraphic logs were based on analyses of the cores using reflected and transmitted light. Powder samples were taken every 1 or 2 metres of the core in order to partially back up the macroscopic mineralogical analysis by microscopic analysis. In addition to this, more than 100 roentgenographic analyses were carried out for precise petrographic identification. The stratigraphic logs were also based on the results of the geophysical borehole logs.

The data on each of the exploration boreholes is briefly summarized below (cf. ALBRECHT et al. 1991; BORNEMANN 1991). A detailed geological evaluation of the exploration results of boreholes Go 1002 to 1005 can be found in Chapter 3.3.

Gorleben 1002

Eighty-one core samples each 18 m long and 3 core samples of between 1 and 12 m in length were extracted. In 26 core samples core orientation was carried out; measurements on 2 of these were unsuccessful. The sections from 1251 to 1296 m, 1314 to 1359 m, 1377 to 1422 m, 1440 to 1485 m, 1784 to 1830 m, 1848 to 1882 m, 1890 to 1932 m, and 1950 to 1982 m were drilled as non-core full holes.

The overburden consists of 215 m of Quaternary, 13 m of Tertiary and 9 m of Upper Cretaceous sediments (BORNEMANN 1991: Table 2). The thick Quaternary and thin Tertiary strata indicate the peripheral location with respect to the Quaternary Gorleben Channel. The Upper Cretaceous sequence is interpreted as an erosion residue, which was preserved during the Tertiary transgression. The borehole reached the top of the cap rock at 237 m, which has a thickness of 16.9 m. The uppermost cap rock stretch of 7 m was drilled as a full hole, the salt formations below 244 m were cored.

Borehole **Go 1002** penetrated the boundary of the Stassfurt- (z2) and Leine-Folge (z3) (BORNEMANN 1991: App. 1 and Table 5) on the NW flank of the salt dome. Below overfolded beds of the Stassfurt-Folge a major syncline of intensely folded strata of the Leine-Folge was found from 646.5 to 1254 m. Further down, strata of the Stassfurt-Folge were found again. The youngest stratigraphic member is the Anhydritmittelsalz (z3AM1-3/ah) occurring in two isoclinally folded separate synclines within the large syncline at 1015.2 to 1041.25 m and 1514.35 to 1531 m.

The following points describe the mineralogical, stratigraphic and tectonic differences between borehole Go 1002 and the normal stratigraphic sequence:

- From approx. 333 m to approx. 405 m, the Hauptsalz (z2HS1-2) contains minor amounts of hydrocarbon gases.
- In the Kieseritische Übergangsschichten (z2UE), langbeinite and some sylvite crystals were found, proving brine conversion.
- The partly intensely folded Liniensalz (z3LS) from 728 to 815 m, 829.4 to 999 m, 1248.6 to 1493.6 m, and 1564.45 to 1596.2 m contains scattered carnallite layers with thicknesses ranging from some centimetres to a maximum of some decimetres, which occur mostly parallel to bedding above the anhydrite bands. All carnallite beds contain hydrocarbon gases (crackling carnallite, i.e. carnallite that releases pressurised, enclosed gases with a crackling sound when struck or dissolving in water).

- The Gorleben-Bank (z3OSM, Mittleres Orangesalz) has a thickness normal to the bedding of approx. 3.5 m at the intersection between 1009.5 and 1013.8 m. This contrasts with intersections at 1080.5 to 1081.15 m, 1096.6 to 1096.95 m, and 1559.25 to 1559.45 m where the maximum thickness of the Gorleben-Bank is only approx. 30 to 40 cm. The significant increase in thickness of the Gorleben-Bank from 1009.5 to 1013.8 m is due to tectonics. The anhydrite has been squeezed in this halokinetic position. This is indicated by striations, stylolites and disruptions of the primary sedimentary structure.
- The Kaliflöz Ronnenberg is missing at the boundary between the Orangesalz and the Bank-/Bändersalz. The borehole penetrated this boundary four times. There is no sign of any remains of the potash seam or of any halite facies which might represent the potash seam. It is therefore assumed that no primary sedimentary deposition of the potash seam took place. This finding was the same in all surface exploration boreholes.
- There is a fault zone from 1612.4 to 1619.9 m in the lower intersection of the Hauptanhydrit from 1611.3 to 1650.9 m which has been healed with coarse-crystalline multi-coloured carnallite, which contains some floating lumps of the Hauptanhydrit. Some of the carnallite crystals are up to 4 cm long and have distinct crystal surfaces. The carnallite occurs in the form of crackling carnallite, i.e. it contains hydrocarbon gases. This fault zone marks a shear-off in the Hauptanhydrit, creating a gap in the sequence of 20 to 30 m. Throughout Appendix 1 in BORNEMANN (1991), the Hauptanhydrit is shown as an undisrupted bed except in those places where faults have been identified. However, on the basis of the latest exploration results (cf. BORNEMANN et al. 2001; e.g. 40 ff., Apps. 5, 6), it must be assumed that the Hauptanhydrit has been broken into individual blocks during the salt uplift by many of the aforementioned disruptions or is missing altogether.
- The lowest section of the Kaliflöz Stassfurt is intensely folded. It stretches from 1654.7 to 1832.8 m (i.e. 178.1 drilling meters) with some enfolded units of halite of the Stassfurt- Folge. This accumulation of the potash seam is probably due to the fracturing of the overlying Hauptanhydrit causing an inflow of the highly mobile potash seam into the resulting low pressure zone.

Gorleben 1003

Sixty-two core samples each 18 m long and 42 core samples of 2.1 to 9 m length were extracted. Twenty-four oriented core samples were extracted; measurements on 3 of these were unsuccessful. The depth zones from 366.5 to 367 m, 592 to 622 m, 631 to 661 m, 670 to 700 m, 1238 to 1278 m, 1764 to 1824 m, 1842 to 1871 m, 1942 to 1982 m, 2000 to 2040 m, and 2058 to 2098 m were not cored.

The borehole hit the cap rock at 263 m beneath 37 m of Quaternary and 226 m of Tertiary overburden. The cap rock is only 8.5 m thick at this location. This small thickness is probably due to the large amount of Tertiary cover that protected the salt dome from subsidence at this location. As the borehole was not cored to 279 m, the structure and petrography of the cap rock, salt table and underlying rock salt could only be roughly reconstructed from log interpretations and the analysis of drill cuttings.

As in Go 1002, borehole **Go 1003** penetrated the boundary zone between the Zechstein 2 and Zechstein 3 sequences on the NW side of the salt dome (BORNEMANN et al. 2001: App. 1). Beneath overturned and folded beds belonging to the Stassfurt-Folge, the borehole penetrated a syncline with beds belonging to the Leine-Folge from 813.5 to approx. 1123.1 m, followed by an anticline with beds of the Stassfurt-Folge reaching down to approx. 1275 m. From this point downwards to the final depth of 2116 m, the borehole penetrated an intensely folded sequence belonging to the Leine-Folge. The youngest horizon penetrated by this borehole is the Kaliflöz Bergmannsseggen. Due to intense folding, this potash seam was penetrated as a dual layer in the lower part of the borehole from 1603.3 to 1631.7 m and again from approx. 1855 to 1898.8 m. The potash seam was initially interpreted in the preliminary stratigraphic log as the Kaliflöz Ronnenberg. However, counting the anhydrite bands in the Liniensalz and Orangesalz revealed that this potash seam lies above the Bank-/Bändersalz and thus corresponds to the Kaliflöz Bergmannsseggen. Hence, the Kaliflöz Ronnenberg is absent in this borehole as well.

The following special mineralogical, stratigraphic and tectonic features were encountered in borehole Go 1003:

- From 452.8 to 470.9 m and from 708.3 to 729.6 m, the borehole penetrated dual layers of the isoclinally folded Kaliflöz Stassfurt and its accompanying layers (Hangendsalz and Kieseritische Übergangsschichten) where it intrudes far into the Hauptsalz. It is not known whether this structure ends within the Hauptsalz or whether it is truncated at the salt table. The base of this double-layered potash seam is probably located between approx. 1244 m and 1273 m. This is also indicated by the electromagnetic reflection survey data. The reason for the potash seam intrusion may be the fracturing of the underlying Hauptanhydrit, which was found from approx. 1280.2 to 1337.9 m.
- From 432.1 to approx. 450 m, many fissures and small faults were encountered in the upper Kristallbrockensalz (z2HS3) to Hangendsalz (z2HG). At 478.3 m and 485.9 m single fissures were found in the Hangendsalz. The fissures and minor faults occur in the halite above and below the double-layered Kaliflöz Stassfurt. They have a maximum width of 5 cm, are mainly open and coated on the insides with idiomorphic halite crystals. Subsidiary fissures are also healed with coarse

crystalline halite. In the zone containing the fissures and minor faults, stratigraphy is mainly steep (70° to 90°). The fissures and minor faults are mostly horizontal or dip slightly against the strata. At 439.8 m, i.e. 7.7 m below the first occurrence of fissures and minor faults, the borehole encountered a significant brine inflow. The occurrence and origin of the aforementioned fissures and minor faults was analysed by FISCHBECK & BORNEMANN (1988).

- The Hauptanhydrit was found in three sections: from 816.2 m to 902.4 m, from 1041.8 m to 1119.1 m, and from 1280.2 to 1337.9 m. The two upper sections are undisturbed but show a difference in thickness normal to the bedding of approx. 20 m in their primary sediments. This proves cliff formation of the Hauptanhydrit during sedimentation. Two faults occur in the lower section of the Hauptanhydrit. The upper fault caused a gap in the bedding of the Hauptanhydrit of 5 to 10 m concerning the beds z3HA1-4. The faulting also destroyed the structure of the adjacent sequence from Gebänderter Deckanhydrit (z2DA) to Leine-Karbonat (z3LK). The second fault occurs from 1309.9 to 1310.3 m and represents an overthrust, doubling the bedding by 10 m to 15 m. The fault zone is healed with halite and traces of carnallite.
- Small faults were encountered at 1360.2 m and from 1380.1 to 1380.2 m in the Basissalz (z3BS) and Liniensalz (z3LS) having a dislocation of only a few centimetres to decimetres. Both faults are healed with halite. As in borehole Go 1002, there are irregular occurrences of carnallite layers parallel to the bedding with a thickness in the order of centimetres in the Liniensalz and in some parts of the Orangesalz above the anhydrite bands.

Gorleben 1004

Exploration borehole **Go 1004** produced 91 core samples of 16.7 to 18 m length and 4 core samples of 6.5 to 10.4 m length. Twenty-five oriented core samples were extracted; measurements on 4 of these were unsuccessful. The borehole was drilled as a full hole from 1227 to 1233 m, 1332 to 1400 m, 1742 to 1757 m, and from 1968 to 1970 m.

The cap rock was encountered at 224 m beneath 97 m of Quaternary and 127 m of Tertiary overburden (BORNEMANN 1991: Table 2). The uppermost 9 m of the cap rock were not cored, from 233 m onwards coring was resumed. The cap rock sequence from top to bottom consists of Flaser-/Knollengips, Liniengips, Sprengelgips and Geschichtetes Gips-, Anhydritgestein (cf. Chapter 3.1). With a thickness of 3.45 m, the Geschichtetes Gips-, Anhydritgestein is very thick. As there is no cap rock breccia, it is very difficult to determine the boundary to the overlying Sprengelgips, which means that the said thickness of 3.45 m is only an estimate.

Borehole Go 1004 penetrated the upper part of the salt formation in the salt overhang, and the lower part of the salt formation in the SE side of the salt dome containing the youngest beds. Below the salt table at 258.8 m, the sequence down to the core of the large syncline at approx. 1200 m consists of inverted beds of the Stassfurt-Folge, Leine-Folge and Aller-Folge. The layers of the Stassfurt-Folge have a southerly dip; the layers of the Leine-Folge and Aller-Folge have a northerly dip, with the Hauptanhydrit acting as a kind of hinge (BORNEMANN 1991: App. 1).

The syncline containing layers of the Aller-Folge stretching from 1036.5 to approx. 1375 m (with minor fold inclusions of Tonmittelsalz in the core) is followed by an anticline from approx. 1375 to 1755.8 m containing steeply dipping beds of the Leine-Folge. The oldest layers in the anticline were encountered from 1460.3 to 1556.7 m, consisting of the upper layers of the Anhydritmittelsalz. In the section from 1755.8 m down to the edge of the salt dome at 1881.4 m, layers of the Aller-Folge were encountered again. These are intensely folded close to the edge of the salt dome. The adjoining rock consists of intermittently strongly faulted halite with anhydrite banks of the Röt (Upper Bunter) (cf. BORNEMANN 1991: Fig. 3). The base of the Upper Bunter salt formation is marked by a dolomite bank. Beds of the Middle Bunter (Solling-Folge) follow from 1944.8 m to the final depth of 1970 m. The stratigraphic classification of these beds was confirmed by log analysis, palynological analysis, and sulphur isotope analysis.

The following special mineralogical, stratigraphic and tectonic features were encountered in borehole Go 1004:

- The borehole penetrated nearly all Zechstein sequences known in the Gorleben salt dome. The Tonbrockensalz (z4TS) penetrated at the edge of the salt dome is the youngest Zechstein bed known in the Gorleben salt dome.
- From the salt table at 258.8 to approx. 304 m, the Knäuel-/Streifensalz (z2HS1/2) contains small amounts of hydrocarbon gas.
- Red carnallite inclusions with a maximum size of 1 cm are irregularly dispersed within the Kristallbrockensalz (z2HS3) from 452 m downwards, and from approx. 500 m, the otherwise light-grey Kristallbrockensalz shows a colour range from orange or light orange to greyish brown due to dispersed polyhalite. This discoloration continues within the Hangendsalz (z2HG) down to the transition to the Kaliflöz Stassfurt at 549 m. The presence of carnallite clusters and the stains of the Kristallbrockensalz and Hangendsalz indicate that deformation of the rock strata in this zone was associated with major brine impregnation.

- From 596.3 m to 626.8 m, the borehole encountered the Hauptanhydrit. The lower part from 600.5 to 603.7 m consists of a fault zone healed with multi-coloured carnallite. The carnallite contains hydrocarbon gas (crackling carnallite). Isolated chunks of Hauptanhydrit and Leine-Karbonat float in the carnallite. Despite the thickness of the fault zone, only a few metres of the sequence are missing (BORNEMANN 1991: App. 8). Another fault was encountered at 626.8 m, causing a gap in the sequence of approx. 30 to 40 m. Only approx. 3 m of z3HA8 remain, whilst the overlying layers z3HA9-11 have been tectonically ripped out and are completely absent. The Kaliflöz Stassfurt above the Hauptanhydrit has moved in through the fault and filled the space made available above the Hauptanhydrit by the missing sequence. Thus the Kaliflöz Stassfurt lies directly on the Basissalz of the Leine-Folge at 645.8 m. The structure of the squeezed potash seam is completely destroyed. The former rock salt banks are completely broken up to form nodules of 1-5 cm in size, which are either irregularly dispersed or partly lined up in pseudo-bedding. The carnallite is rich in gas (crackling carnallite).
- A few isolated anhydrite chunks of sizes of up to 5 cm are located along the boundary between the Kaliflöz Stassfurt and the Basissalz (z3BS). These chunks have been torn off the Hauptanhydrit (z3HA11) and transported along with the intruding potash seam.
- Unlike in boreholes Go 1002 and Go 1003, where carnallite layers parallel to the bedding frequently occur above the anhydrite bands in the Liniensalz and Orangesalz, carnallite layers in this borehole are very rare.

Gorleben 1005

Exploration borehole **Go 1005** produced 76 core samples of 18 m length and 19 core samples of 2.2 to 16.4 m length. Twenty-seven oriented core samples were extracted; measurements on 2 of these were unsuccessful. The borehole was not cored from 401 to 403 m, 1546 to 1592 m, 1610 to 1656 m, and 1909 to 1911.5 m.

The borehole hit the cap rock of the salt dome at approx. 272.8 m after drilling through 95 m of Quaternary and 177.8 m of Tertiary overburden (BORNEMANN 1991: Table 2). The cap rock has a thickness of 22.8 m and consists of gypsum and anhydrite in the upper part. It was not possible to subdivide it into different zones as done by BORNEMANN & FISCHBECK (1986). However, one zone of Geschichtetes Gips-, Anhydritgestein with a thickness of 1.9 m was identified above salt table.

In the upper part of the salt formation, the borehole provided information on the structure and shape of the overhang on the SE side of the salt dome (see borehole Go 1004). The overhang consists of overfolded layers of the Stassfurt-Folge. Underneath, a syncline consisting of layers of the Leine-Folge was encountered, the centre of which is formed by the youngest bed, the Anhydritmittelsalz, from 857 to 1194.3 m. This is followed by a special anticline, which also consists of layers of the Leine-Folge with a core of dual-layer Hauptanhydrit from 1318.2 to 1518.8 m. The anticline can be traced by the layers of the Leine-Folge to the salt dome edge at 1894.5 m. Underneath, adjoining rock consisting of a sequence of halite, anhydrite, claystone, siltstone and sandstone was found (BORNEMANN 1991: Fig. 4). The borehole reached a final depth of 1930 m.

The following special mineralogical, stratigraphic and tectonic features were encountered in borehole Go 1005:

- The updoming of the cap rock (BORNEMANN 1991: App. 1) observed where the Hauptanhydrit crops out at the salt table is confirmed by the electromagnetic reflection survey and by a seismic profile.
- From the salt table at 295.6 down to approx. 365 m, small amounts of hydrocarbon gases were identified in the Knäuelsalz and in parts of the Streifensalz (z2HS1 to 2).
- The double bedded Kaliflöz Stassfurt with its accompanying layers intrudes into the Hauptsalz of the Stassfurt-Folge from 430.8 to 436.7 m. The Kieseritische Übergangsschichten are missing due to salt tectonics. The root, i.e. the place from where the seam thrusts from the normally bedded potash seam into the Hauptsalz, is unknown. The cause is assumed to be a break in the Hauptanhydrit as seen in borehole Go 1003.
- The double bedded potash seam is superimposed by steeply dipping and folded Hangendsalz (z2HG) containing fissures and small faults from 421.75 to 425.25 m. They occur in the same tectonic position as those encountered in borehole Go 1003. The fissures and small faults are either horizontal or dip slightly against the steeply dipping bedding. In some cases, they create an offset between the overlying and underlying layers so that minor dislocations are assumed but cannot be estimated precisely. The fissures and small faults are 10 to 20 cm wide and are healed with coarse crystalline clear halite, unlike those in borehole Go 1003. Bromide analysis of the halite in the fissures and of the halite in the adjoining rock revealed that the fissure fillings grew from bromide-rich metamorphic brines formed in the salt dome (FISCHBECK & BORNEMANN 1988).

- The section of Hauptanhydrit penetrated from 1318.2 to 1518.8 m is double bedded and forms an anticline at the borehole. The core of the anticline consists of Flaseranhydrit (z3HA4) and is located between 1450.5 m and 1469 m. In the crest zone of the anticline the sequence of strata is interspersed with fissures and faults and is regionally brecciated. Packer tests in this zone confirmed brine inflows (REPPERT 1982 a). Comparison of the thickness of the Hauptanhydrit on both sides of the fold revealed a difference in thickness of 20 to 30 m. This is due to a reduction or a gap in the sequence of Bündelanhydrit to Bänderanhydrit layers (z3HA8-11), as found in Go 1003. However, as there are no typical tectonic structures which could cause missing or doubled layers, it must be assumed that the sharp transitions in thickness were formed during primary sedimentation.
- A halite horizon was encountered above the Bank-/Bändersalz from 1682.2 to 1691.3 m, which is contaminated mainly with kieserite and some small amounts of polyhalite and anhydrite. It also contains irregularly dispersed red carnallite. This halite horizon presumably corresponds to the Kaliflöz Bergmannsseggen.
- From 1821.3 to 1823.7 m Tonmittelsalz (z3TM1/t) was encountered, which is the youngest layer found in this borehole. This layer consists of halite increasingly interspersed lower down with grey and brown clay. The sequence shows a severe faulting in the lower 1.3 m. This zone reflects an overthrust zone lying parallel to the edge of the salt dome which thrusts Anhydritmittel 9 (z3AM9/ah), for instance, by approx. 60 m from the original bedded sequence (BORNEMANN 1991: App. 1).

2.3.2 Shaft pilot boreholes

The objective of the shaft pilot boreholes Go 5001 and Go 5002 was to find the most favourable location for the shafts of the exploration mine. According to JARITZ (1983), favourable locations are those which allow the shafts to be sunk exclusively in rock salt of the Stassfurt-Folge or through the lower layers of the Leine-Folge from the salt table down to final depth; where the overburden and cap rock are not too thick, and which allow the sinking of two shafts with a separation of 200 to 500 m in a central location with respect to the mine layout.

It was decided to sink the Gorleben shafts over their whole lengths through the lower layers of the Leine-Folge, if possible. From the potash mines in the Hanover area it was already well known that shafts within the Leine-Folge are much more stable than those in layers of the Stassfurt-Folge. Thus, extensive scaling can be avoided. In order to find the optimal locations for the shafts, five salt table boreholes were drilled (GoHy 3151 to GoHy 3155) (BORNEMANN 1991: Fig. 2). These were drilled to provide additional information on the boundary between the Stassfurt-Folge and Leine-Folge at the salt table in the area

of the shaft locations. The positions of the salt table boreholes and shaft pilot boreholes are shown in Figure 2. The basic data of both shaft pilot boreholes, including coordinates, borehole depths, etc. are listed in BORNEMANN (1991: Table 2).

Unlike in the exploration boreholes, the overburden was cored in both shaft pilot boreholes, from 22.9 m in borehole Go 5001 and from 7 m in borehole Go 5002. These boreholes provided the data on the overburden required to plan the freezing process for the sinking of the shafts, for the selection and design of the type of shaft lining in the frozen shaft section, and to plan the shaft sinking. Due to technical problems, both boreholes had so many core losses, particularly in the sandy Quaternary sections, that the obtained cores were only of limited use for petrostratigraphic analysis. Conditions improved when the boreholes penetrated the Tertiary formation. Only minor core losses were incurred in both boreholes from top of the Tertiary to final depth. However, due to excessive mud pressure most of the argillaceous inclusions were flushed out of the cap rock cores. The overburden was drilled using a clay/freshwater mud. At the top of the cap rock the clay/freshwater mud was switched to a clay/salt-mix/water mud to prevent subsidence of the cores in the saliniferous layers.

In borehole Go 5001, increased levels of hydrocarbon gases and condensate were encountered from 870.3 m downwards, which ejected some of the drilling mud. To permit drilling to continue to final depth, barite was added to increase the weight of the NaCl mud to max. 1.7 kg/l (GRÜBLER & REPPERT 1983). During the sinking of borehole Go 5002, hydrocarbon gases were also encountered from the salt table down to the final depth. However, the amount of inflow was so low that weighting of the drilling mud was not necessary.

The boreholes were cased as follows:

In borehole Go 5001, a 20" conductor pipe was driven to a depth of 21.8 m. A casing string of 13-3/8" diameter was set in the Tertiary layers at 214.4 m and cemented up to the surface. This was followed by the installation of an anchor casing string set in the Liniensalz (z3LS) at 356.9 m, which was cemented up to 198.13 m.

In borehole Go 5002, a 24-1/2" conductor pipe was driven to a depth of 21 m, followed by an 18-5/8" casing string set at 82.1 m in the Quaternary layers, which was cemented up to the surface. A second casing string of 13-3/8" diameter had to be set in the Tertiary layers and cemented upwards to 69 m. Finally, a 9-5/8" anchor casing string was set at 359.4 m at the transition from the Orangesalz to the Bank-/Bändersalz, and cemented up to 195 m.

The cutting of oriented cores mainly of a length of 9 m was planned for approx. every 50 to 70 m during coring in both boreholes to facilitate better interpretation of the salt structure. The technical extraction of the oriented cores was in some cases unsatisfactory and the orientation of the cores was difficult to assess. This applies particularly to shaft pilot borehole Go 5001 because only 5 of the 12 oriented cores could be used to interpret the structure of the salt dome.

The following geophysical borehole logs were carried out in the shaft pilot boreholes:

- **Go 5001**
Temperature log, density log, calliper log, 4-arm dip log, acoustic log, borehole deviation log, resistivity log, gamma-ray log.
- **Go 5002**
Temperature log, gamma-ray log, resistivity log, 4-arm dip log, calliper log, neutron log, density log, acoustic log, borehole deviation log.

After reaching final depth and performing the logging mentioned above, the clay/salt-mix/water mud was replaced by an oil-based mud to create optimum conditions for the high frequency absorption survey and the electromagnetic reflection survey. Only a few reflections were useful for the structural geological evaluation of the salt dome (ALBRECHT et al. 1991: Figs. 14, 15).

The single packer test series carried out from June 6 to June 7, 1982 and from June 13 to June 20, 1982 (REPPERT 1983 b), while drilling the Go 5001 borehole, provided information on the hydrocarbon gases and condensates flowing into the borehole. Subsequently, the well head was sealed and head pressure was monitored from June 26, 1982 to April 18, 1983. A third test series was carried out in 1984 from April 6 to April 14 before partial backfilling of the borehole.

When Go 5002 reached final depth, only one packer test was run over the whole uncased section of the borehole as only minor inflows of hydrocarbon gas had been measured during drilling.

The results of the packer tests and the occurrence of hydrocarbon gases and condensates in the boreholes are described in detail in three DBE reports (GRÜBLER & REPPERT 1983; REPPERT 1983 a and b). After all tests had been concluded, both boreholes were partially backfilled (Go 5001 to 255 m, Go 5002 to 278.3 m). The remaining mud was replaced with freshwater in the remaining open sections of the boreholes. During the freeze sinking of the shafts, both boreholes were used as centre holes to reduce the pressure in the ice cylinder.

For documentation purposes, all cores were photographed. The photographs were used to create photo logs organised by core sequence. Core description was performed in the same way as for exploration boreholes Go 1002 to 1005.

Gorleben 5001

The shaft pilot borehole **Go 5001** was cored from 22.9 m down to final depth at 967.8 m, producing a total of 219 cores. Core lengths in the overburden and the cap rock varied between 0.25 and 7.5 m, the average being between 1 and 2 m. Within the salt formation, cores were usually 9 m long, although some were shorter due to drilling problems. Twelve oriented cores were extracted, most of them being 12 m long. Due to drilling problems, it was necessary to employ full-hole drilling for a short section from 360 to 361.3 m.

The layers of the overburden consist of 158 m of Quaternary, 77.67 m of Tertiary and 0.78 m of Upper Cretaceous. The borehole penetrated the cap rock at 236.45 m encountering a sequence of Liniengips, Sprenkelgips and Hutgesteinsbrekzie with a thickness of 18.1 m. There was no Geschichtetes Gips-, Anhydritgestein above the salt table. Below the salt table, the upper part of the shaft pilot borehole penetrated the z2-z3 interface, which represents the SE side of the main anticline of the salt dome, consisting of rock salt of the Stassfurt-Folge. Intensely folded beds of lower to middle Leine-Folge were encountered underneath. The youngest unit of this sequence was the Anhydritmittelsalz (z3AM1/ah to z3AM3/na) between 748.7 and 803.3 m (BORNEMANN 1991: App. 1).

The following special mineralogical, stratigraphic and tectonic features were encountered in borehole Go 5001:

- The subroded Kaliflöz Stassfurt crops out as a seam horizon at the salt table. Due to the tight folding of the beds, it was intersected again between 268.85 and 272.1 m. Due to inflow of freshwater into the potash seam during the Elsterian Glacial period, all easily soluble potassium/magnesium minerals were removed. The former potash seam is now a dense, fine-grained crystalline halite horizon. What remains of the former potash seam are the poorly soluble components such as various borate minerals and haematite scales, which were originally embedded in the carnallite. The anhydrite has largely turned into gypsum. This potash seam horizon was also encountered at a depth between 292.05 and 295.9 m in salt table borehole GoHy 3153, which was a pilot hole for the Go 5001 shaft pilot borehole.
- At 272.1 m, the subroded Kaliflöz Stassfurt is directly followed by the Liniensalz (z3LS) of the Leine-Folge. Due to salt tectonics, the beds of the upper Stassfurt-Folge (Gebänderter Deckanhydrit) are missing, having remained rigid during

deformation, as are the bottom layers of the lower Leine-Folge (Grauer Salzton to Hauptanhydrit). The Basissalz (z3BS) and a few metres of the Liniensalz (z3LS), which usually follow in the normal sequence, have also been squeezed off. A total stratigraphic gap with a thickness normal to bedding of approx. 100 m can be assumed (cf. Chapter 3.3.2).

- The Gorleben-Bank (z3OSM) was penetrated five times because of the intense folding. Using this easily identifiable anhydrite bed, the intense folding of the sequence penetrated by the borehole could be reconstructed. From 474.55 to 491.8 m and 573 to 590.65 m, the Gorleben-Bank expected in these beds was absent. This is due to halokinetic processes, which caused a thinning of the Orangesalz and squeezed out the Gorleben-Bank at these two locations.
- In the centre of the syncline, the Anhydritmittelsalz was the youngest unit that was penetrated between 748.7 and 803.3 m. The Anhydritmittel 1 to 5 were penetrated, the thickest being Anhydritmittel 1 with a thickness of approx. 10 cm perpendicular to the layer. The borehole penetrated a dual-layer halite sequence between 910 and 964.7 m, which was interpreted as a seam horizon equivalent to the Kaliflöz Ronnenberg due to its mineral composition (FISCHBECK 1984). In general, the beds form a striped structure which is roughly equivalent to that of the Orangesalz. However, the stripes do not consist of anhydrite but of polyhalite with some zones of langbeinite, kieserite, and idiomorphic anhydrite crystals up to 2 cm long. In addition to this, scattered brick-red sylvite crystals with a length of up to 2 cm were found. The mineral distribution and composition reveals that this section has suffered major solution transfer combined with the formation of new minerals. This finding is confirmed by numerous bromide analyses from this shaft level.
- Irregularly scattered milky-opaque and red sylvite clusters some millimetres to 1 cm in size occur in the Bank-/Bändersalz (z3BK/BD) and the Orangesalz (z3OS) from 357.45 to 411.1 m, 428.9 to 446.9 m, 503.9 to 560.8 m, and from 712.87 to 738.7 m. A major solution transfer combined with secondary precipitation of sylvite must be assumed for these zones. At 859.9 to 868.8 m, four irregularly scattered small faults or fissures were found within the Unteres Orangesalz (z3OSU). They are between 5 and 20 cm wide and healed with clear coarse-crystalline halite.
- While penetrating the sections from 285 to 327 m and 361 to 376 m small amounts of hydrocarbon gases were observed in the drilling mud. However, drilling was not impeded. The quantities of hydrocarbon gases flowing into the borehole between 864.5 and 870 m and between 960.2 m and final depth at 967.8 m were so high that they caused partial mud blowouts (GRÜBLER & REPPERT 1983). The hydrocarbon inflows originate from the strongly folded and thickened Gorleben-Bank at approx. 857 m which, in this case, acts as a large but limited reservoir.

Gorleben 5002

Shaft pilot borehole **Go 5002** was cored from 7 m downwards. In total, 271 cores were cut down to the final depth of 967.8 m. One hundred and sixty-three cores were extracted from the overburden and cap rock. Core lengths varied between 10 cm and 5 m with an average length of 2 to 3 m. One hundred and eight cores were extracted from the salt formation, most of them being 9 m long, including 32 oriented cores. The oriented cores were extracted in groups of three, each core with a length of 3 m, resulting in a length of 9 m for an oriented core interval. Due to drilling problems, coring was not possible between 373 and 382 m, and thus only drill cuttings could be sampled in this section.

The overburden consists of 176 m of Quaternary and 24.2 m of Tertiary sediments. A notable feature of the Quaternary sediments is the accumulation of Lauenburg Tonkomplex to a thickness of approx. 55 m, which is probably due to glacio-tectonic effects. As the base of the Tertiary at borehole Go 5002 and the neighbouring boreholes is almost horizontal, there is no connection between the accumulation of the Lauenburg Tonkomplex and the underlying reef-like updoming of the cap rock between 200.2 and 254.8 m (BORNEMANN 1991: App. 1). The marked increase in thickness of the cap rock in borehole Go 5002 and pilot borehole GoHy 3155 is due to the inclusion of an isolated, partially gypsified block of Hauptanhydrit.

The overall structure of this cap rock dome is oriented roughly N to S. The northern and southern boundaries are unknown. As the beds in the gypsified Hauptanhydrit dip to the W, the cap rock surface also has a relatively slight dip to the W. Due to the rupture of the Hauptanhydrit layers, a long stretch of the eastern side is marked by a steep reef-like slope of the cap rock surface, which is aligned N to S.

The normally bedded Hauptanhydrit block is superimposed by Liniengips and Sprengelgips. A layer of Hutgesteinsbrekzie originating from the Elsterian Glacial period lies underneath. A sequence of Geschichtetes Gips-, Anhydritgestein with a thickness of 0.9 m deposited after the Elsterian Glacial period follows. Below the Hauptanhydrit block, remains of the Leine-Karbonat (z3LK), and the Grauer Salzton (z3GT) were found.

The borehole penetrated a tectonic position in the salt dome that is similar to the Go 5001 shaft pilot borehole. This well also penetrates the intensely folded beds of the lower and middle Leine-Folge that form the SE flank of the Hauptsalz dome anticline, which is made up of Stassfurt rock salt. The boundary between the Leine-Folge and the Stassfurt-Folge crops out at the salt table about 80 to 100 m north of borehole Go 5002 in the direction of the salt table borehole GoHy 3154.

The following mineralogical, stratigraphic and tectonic characteristics were encountered in borehole Go 5002:

- The Anhydritmittelsalz, which is the youngest stratigraphic unit penetrated by borehole Go 5002, was encountered from 902.4 m to final depth.
- With the exception of a few sections (359.25 to 428.1 m: Bank-/Bändersalz; 824.1 to 965 m: Bank-/Bändersalz to Anhydritmittelsalz) the borehole penetrated intensely folded beds of the Orangesalz. Consequently, the Gorleben-Bank, which made stratigraphic identification and reconstruction of the folding possible in the first place, was penetrated eight times.
- Irregularly scattered sylvite flakes with sizes of some millimetres to 1 cm occur in the halite from 254.8 (salt table) to 350 m, 434 to 461 m, 576 to 598 m, 646 to 656 m, 789 to 806 m, 821 to 839 m, 860 to 876 m, 890 to 899 m, and 902 to 911 m. Some are associated with carnallite flakes. The flakes do not occur in any preferential stratigraphic horizon. Major solution transfer must be assumed for the above-mentioned zones, which led to the secondary precipitation of sylvite.
- Like borehole Go 5001, this borehole encountered fissures and small faults in the Oberes Orangesalz (z3OSO), which are up to 10 cm wide and healed with clear coarse-crystalline halite. In addition to this, fissures 1 to 4 cm wide or small faults healed with carnallite also occur in the Oberes Orangesalz (z3OSO) at 805.55 and 822.25 m.
- As in borehole Go 5001, hydrocarbon gases flowed out of the borehole Go 5002. In this case, however, the outflow began at the salt table and continued down to final depth with only short intermissions. Although measurable, the volumes were mostly low and did not have any effect on drilling operations. Compared to the normal background values, slightly increased gas levels were only encountered between 301 and 310 m, 335 and 342 m, 353 and 362 m, 461 and 468 m, 563 and 585 m, and between 700 and 703 m.

2.3.3 Salt table boreholes

Salt table boreholes are defined as boreholes that are cored through the cap rock and a few tens of metres into the salt to provide information on the beds at this level (see Fig. 2).

The salt table boreholes were drilled with the following objectives:

- Explore the cap rock and salt table, thus facilitating assessment of subsrosion processes affecting the salt dome
- Investigate the uppermost sections of the rock salt strata in order to gain an impression of the spatial distribution of the rock salt layers, i.e. the construction of a geological map of the salt table
- Find suitable shaft locations

To achieve these objectives, the salt table boreholes (cf. BORNEMANN 1991: Fig. 2) were drilled in groups during separate phases as:

- General exploration wells
- Boreholes to explore the z2/z3/z4 boundaries
- Boreholes to explore potential shaft locations
- Boreholes to explore the Quaternary channel
- Water-level observation hole in the cap rock and
- Boreholes to investigate subsrosion of the Kaliflöz Stassfurt

Borehole GoHy 1283 is a water-level observation hole and is not to be regarded as a salt table borehole in the proper sense even though almost all of the cap rock was cored.

Drilling cuttings were sampled every 3 m for stratigraphic interpretation. As the salt table boreholes were drilled with a large cross-roller bit, the mud samples allowed only a rough assessment of the stratigraphy. Due to this, 17 salt table boreholes (Table 1) were preceded by exploration boreholes drilled with an open crown in order to facilitate stratigraphic assessment. Drilling was stopped as soon as the first gypsiferous rock was encountered. Despite the small distance between the exploration boreholes and the salt table boreholes the determined cap rock depth often varied by some metres to tens of metres. This depth variation is due to isolated altered gypsum blocks in the overlying Tertiary. Thus, only the depth record of the salt table borehole is valid for the respective area.

At the first sign of cap rock, drilling of the salt table borehole was suspended to set a 9-5/8" casing, which was anchored in the cap rock and cemented to about 50 m above the casing shoe. The clay/freshwater mud used to drill through the overburden was then replaced by a clay/salt-mix mud. Subsequently, the cap rock and salt formation were continuously cored all the way down to final depth. At least one oriented core was extracted, a few metres below the salt table; in deeper boreholes several oriented cores were extracted. The depth of penetration of the salt formation depended on the exploration objective for each individual borehole and varied between 6.1 and 229.7 m (BORNEMANN 1991: App. 9).

Table 1: Salt table boreholes and associated exploration boreholes nearby.

Exploration borehole	Salt table borehole	Exploration borehole	Salt table borehole
GoHy 60	GoHy 65	GoHy 850	GoHy 3010
GoHy 130	GoHy 133	GoHy 1120	GoHy 1121
GoHy 140	GoHy 143	GoHy 1131	GoHy 1131
GoHy 480	GoHy 484	GoHy 1140	GoHy 1141
GoHy 500	GoHy 503	GoHy 1150	GoHy 1151
GoHy 510	GoHy 515	GoHy 1160	GoHy 1161
GoHy 520	GoHy 524	GoHy 1170	GoHy 1171
GoHy 650	GoHy 654	GoHy 1180	GoHy 1181
GoHy 840	GoHy 841		

Slow or total drilling mud losses occurred in the cap rock in boreholes GoHy 15, 503, 515, 3010, 3020, 3040, 3100, 3153, 3154, and 3155. To prevent further mud losses the zones in question were fortified with cementation or additional casing. The boreholes were geophysically logged after reaching final depth. The following logs were run:

- Calliper log
- Gamma-ray log
- Density log
- Neutron-neutron-log
- Temperature log

Subsequently, the boreholes were backfilled in several stages. The casing strings were cut off 1.3 m below ground level, leaving the rest in the borehole. The boreholes were capped by a 30-cm-thick concrete slab. For documentation purposes, each core sample was photographed and the photographs were used to create photo logs organized by core sequence.

Salt table boreholes penetrating the Hauptsalz (z2HS) of the Stassfurt-Folge

Boreholes GoHy 15, 133, 555, 3050, 3060, 3070, 3110, 3140, and 3150 (BORNEMANN 1991: Apps. 9, 10, 11, 21) encountered only the Hauptsalz (z2HS). With the exception of GoHy 555, which encountered Streifensalz (z2HS2), no further classification of the beds was possible because of the limited penetration of the salt formation. In relation to the structure, boreholes GoHy 133, 3050, 3060, 3070, 3110, 3140, and 3155 are located on the main anticline of the salt dome whilst boreholes GoHy 15, 555, and 3150 are located above the SE salt dome overhang, which also consists of the Hauptsalz of the Stassfurt-Folge. No traces of freshwater effects in the form of mineralogical transformations of the salt formations were encountered in these boreholes.

Nine additional salt table boreholes (GoHy 65, 143, 524, 841, 1161, 1181, 3030, 3040, and 3080) also penetrated the Hauptsalz of the Stassfurt-Folge (see BORNEMANN 1991: Apps. 9, 10, 11). In these cases, it was mainly Kristallbrockensalz (z2HS3), the youngest unit of the Hauptsalz, which indicates the nearby presence of the Kaliflöz Stassfurt and the boundary between the Stassfurt-Folge and the Leine-Folge.

In borehole GoHy 3080, the Kristallbrockensalz (z2HS3) is underlain by the inverted Hangendsalz (z2HG). The Kaliflöz Stassfurt is only decimetres to metres away from the final depth of this borehole. In this borehole, the effects of slightly mineralised groundwater on the salt beds were observed in the form of clay flakes from the overburden, scattered occurrences of calcite, as well as local gypsification of the sulphates (Table 2). The effects extend down to the bottom of the borehole, i.e. 28.7 m below the salt table. The subrosive changes in the Kaliflöz Stassfurt are due to an inflow of water from the overburden.

Borehole GoHy 1181 encountered a normally bedded sequence of Kieseritische Übergangsschichten (z2UE) and Hangendsalz to Hauptsalz (z2HG/HS) beneath the salt table, which means that the Kaliflöz Stassfurt must crop out at the salt table in the vicinity of the borehole. The beds penetrated by the borehole show the effects of water from the overburden in the form of partial gypsification of the sulphates and the formation of kainite, affecting a zone down to approx. 15 m below the salt table (Table 2). This is another proof that the neighbouring Kaliflöz Stassfurt has been affected by subrosive changes.

Salt table boreholes penetrating the Kaliflöz Stassfurt (z2SF)

The following eight boreholes penetrated the Kaliflöz Stassfurt and/or the boundary between the Stassfurt-Folge and the Leine-Folge: GoHy 1151, 1171, 1302, 1303, 1304, 1305, 3153, and 3154 (BORNEMANN 1991: Apps. 9, 10, 11, 21).

Due to intense folding of the beds, borehole GoHy 1151 penetrated the subroded Kaliflöz Stassfurt three times. The uppermost section (315 to 321.15 m) is a red coloured halite horizon marked by haematite scales and inclusions of clay flakes and sandstone from the overburden. The lower approx. 3 m contain traces of carnallite and kieserite. The Hangendsalz (z2HG), which underlies the seam horizon and forms an anticline, has seven fissures or faults approx. 10 to 30 cm wide, healed with clear coarse-crystalline halite. This halite contains locally clay flakes and small rock fragments from the overburden as well as isolated blue-violet halite crystals. Isolated occurrences of astrakanite and glauberite were identified in the Hangendsalz.

The middle seam section (342.15 to 344.15 m) has a petrographic structure similar to the upper seam section but contains no inclusions from the overburden. Like the two other seam sections, the lowest seam section (354.6 to 355.9 m) consists mainly of halite but also has flaky lines and layers with kainite, kieserite and astrakanite. These minerals indicate a decreasing intensity of subsrosion of the potassium/magnesium minerals with increasing depth. Lath-shaped anhydrite crystals of up to 2 cm length and isolated clay flakes were encountered in the underlying Kristallbrockensalz (z2HS3) down to a depth of approx. 367 m. This indicates that water from the overburden affected the salt rocks down to a depth of approx. 52 m below the salt table (Table 2).

In borehole GoHy 1171, the Kaliflöz Stassfurt is normally bedded at the salt table and altered by subsrosion effects. Below this, the Kieseritische Übergangsschichten (z2UE), the Hangendsalz (z2HG) and the Hauptsalz (z2HS) form the sequence down to final depth. The form of subsrosive alteration is identical to that in borehole GoHy 1151. Transformation caused by water from the overburden was found to a depth of approx. 26 m below the salt table. Boreholes GoHy 1302 to 1305 revealed that the potassium and magnesium minerals in the Kaliflöz Stassfurt are completely subroded down to approx. 90 to 130 m below the salt table (Fig. 3). In some places the seam is replaced by a halite horizon tinted red by haematite flakes, which in some regions is heavily impregnated with clastic material from the overburden (MINGERZAHN 1987).

Table 2: Penetration depth of water from the overburden below the salt table and lithological changes in the adjacent formations caused by subsrosion.

Borehole GoHy, Go	Depth*	Altered salt beds	Type of alteration
515	a few metres	z2SF/na ?, z2HS ?, z3LS	subsrosion of z2SF, rock salt lumps (z2HS) in the cap rock, inclusions of material from the overburden
1131	approx. 14	z3BS	partial gypsification and discoloration, hopper crystals in the rock salt
1141	? ≥ 32	z2DA, z3LK, z3HA	fissure with clay filling, gypsum crystals in z3HA, subsrosion of carnallite-filled cavities in the z3HA
1151	approx. 52	z2HS3, z2HG, z2SF/na	subsrosion of z2SF, kainite, blue rock salt crystals, anhydrite lathes, inclusion of material from the overburden
1171	approx. 26	z2HS, z2HG, z2SF/na	subsrosion of z2SF, inclusion of material from the overburden (clay flakes, polyhalite?)
1181	approx. 15	z2UE	partial gypsification, kainite
1291	like GoHy 1141?	z2DA ?, z3GT ?, z3LK ?, z3HA	partial gypsification of z2DA - z3LK, subsrosion of carnallite-filled cavities in the z3HA?
1301	a few metres?	z2DA, z3GT, z3LK, z3HA	partial gypsification of z2DA - z3LK, subsrosion of carnallite-filled cavities in the z3HA?
1302	approx. 41	z2HS, z2SF/na, z2DA	subsrosion of z2SF, inclusion of material from the overburden, partial gypsification of the z2HS, z2SF/na, and z2DA
1303	approx. 91	like 1302	like 1302
1304	approx. 140	like 1302, 1303	like 1302, 1303, but kainitite from approx. 130 m below the salt table
1305	approx. 170	like above	like above, from approx. 170 m below the salt table non-altered brecciated carnallite
3080	> 28.7	z2HS3, z2HG	few inclusions of material from the overburden, occurrences of calcite, partial gypsification
3130	approx. 12	z3AM	several fissures with fillings of clay and fine sand from the overburden
3153	approx. 38	z2HS3, z2HG, z2SF/na	subsrosion of z2SF, partial gypsification
5001	approx. 25	z2HS3, z2HG, z2UE, z2SF/na, z3LS	subsrosion of z2SF, inclusions of material from the overburden, partial gypsification

*below the salt table, measured in metres

Detailed analysis and interpretation of the completely cored boreholes revealed that the original stratigraphic sequence is still recognisable despite intense faulting and the filling with overburden material. The section is an extremely folded part of the Kaliflöz Stassfurt associated with a thickening of the layers. Borehole GoHy 1304 encountered the potash seam in the form of kainitite. This rock is a conversion product of carnallitite affected by groundwater. Borehole GoHy 1305 encountered the potash seam in the form of brecciated carnallitite. This zone was not affected by groundwater. Between boreholes GoHy 1304 and 1305, the lower boundary of groundwater effects on the potash seam is approx. 445 m, i.e. approx. 140 to 170 m below the salt table (Table 2). The boreholes mentioned are in the NE part of the Gorleben salt dome (Fig. 2) at a distance of approx. 2 to 3 km from the planned Repository Area 1.

In borehole GoHy 3153, the Kaliflöz Stassfurt was found beneath 33.2 m of Kristallbrockensalz (z2HS3) and 6.15 m of Hangendsalz (z2HG) at a depth of 292.05 to 295.9 m in the form of a subroded halite horizon (BORNEMANN 1991: Apps. 1, 11). The halite consists of dense, fine crystals and, in addition to anhydrite, contains gypsum crystals, polyhalite and haematite flakes of up to 2 cm in size. No effect of water from the overburden was found in the underlying Liniensalz (z3LS) down to final depth. In the overlying Hauptsalz and Hangendsalz (z2HS+HG), the sulphates are partially gypsified by the effect of water from the overburden. In summary, the salt formation shows alteration down to a depth of approx. 38 m below the salt table (Table 2) in this borehole. However, the depth of subsrosion in this area is not known yet because the Kaliflöz Stassfurt in the form of brecciated carnallitite was not reached.

Borehole GoHy 3154 is only 450 m NE of salt table borehole GoHy 3153. It penetrated the Kaliflöz Stassfurt from 279.15 to 281.85 as a dual layer in the form of brecciated carnallitite (BORNEMANN 1991: Apps. 1, 11), i.e. 25.95 m below the salt table. As in the potash seam itself, no alteration in the Hauptsalz (z2HS) above and below the potash seam due to water from the overburden was found. Comparison of these findings with salt table borehole GoHy 3153 reveals major relief differences over short distances with respect to the subsrosion of the Kaliflöz Stassfurt, i.e. the depth of penetration of water from the overburden into the salt formation.

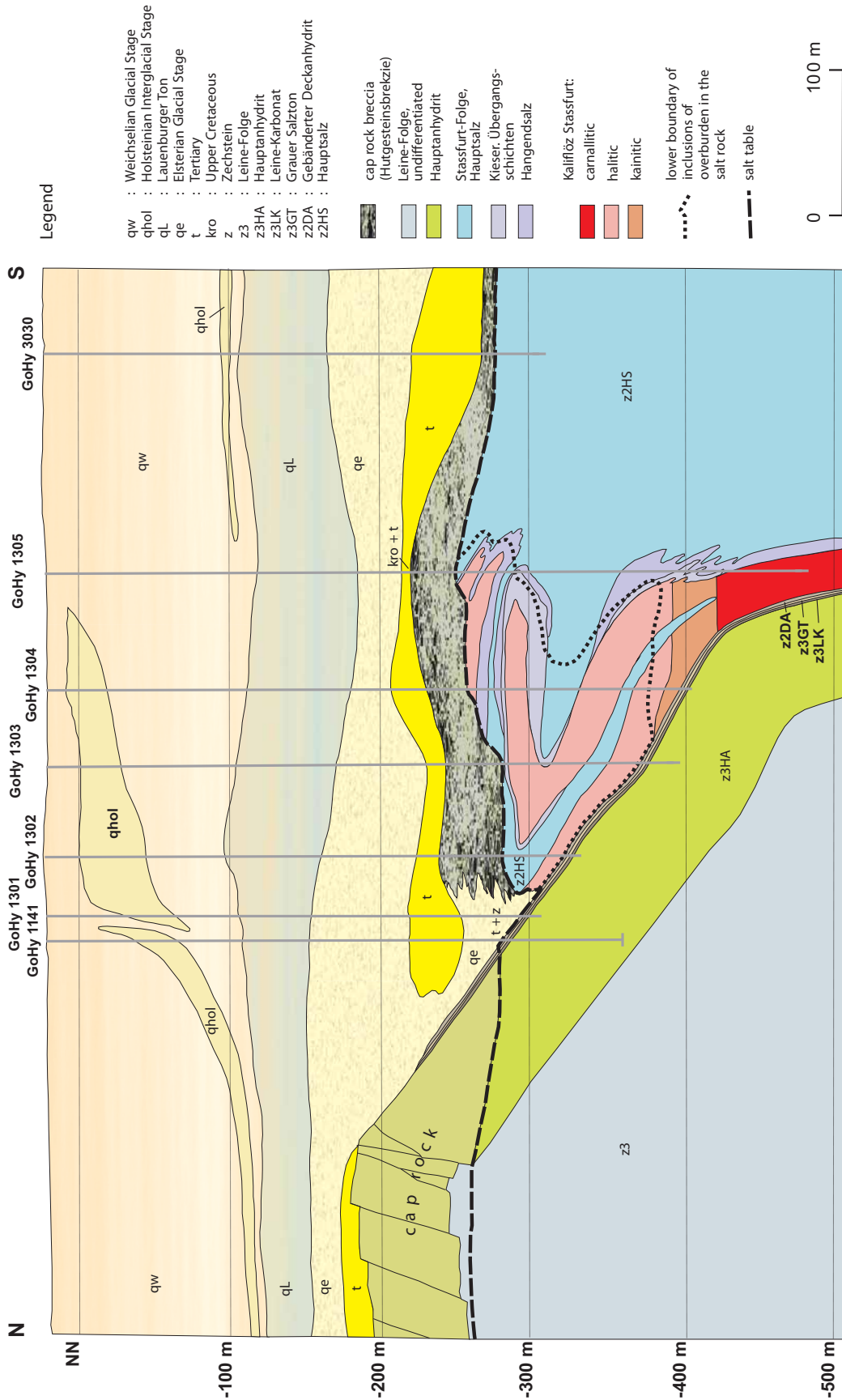


Figure 3: Subrosion of the Kaliflöz Stassfurt in the area of the Gorleben Channel as found in the salt table boreholes GoHy 1301 to 1305 and GoHy 1141.

Salt table boreholes with Gebänderter Deckanhydrit (z2DA), Grauer Salzton (z3GT), Leine-Karbonat (z3LK) and Hauptanhydrit (z3HA)

In three of the boreholes (GoHy 1121, 1141, 1291), almost the whole sequence of strata mentioned above was penetrated. Four other boreholes (GoHy 1301, 1302, 1303, and 1304) penetrated the z2DA, z3GT and z3LK units completely but cut only a few metres into the Hauptanhydrit. The stratigraphic sequence perpendicular to the strata penetrated by boreholes GoHy 1121, 1141, and 1291 is shown in BORNEMANN (1991: App. 8) with the subdivision of the Hauptanhydrit. It is difficult to identify the salt table because these three boreholes encountered no or only questionable evidence of cap rock, and because the beds are not or only partially gypsified.

The fissure fillings found in borehole GoHy 1121 illustrate how deeply the water from the overburden penetrates the carbonate and sulphate rocks cropping out at the salt table. Gebänderter Deckanhydrit, Grauer Salzton and Leine-Karbonat were penetrated from 298.2 to 302.1 m. The fissure fillings consist of clays from the overburden and further down partially of halite. In the underlying Hauptanhydrit, the fissures down to approx. 304 m are filled with clay and halite, in the lower region also partially with sylvite. Beneath this, some isolated open fissures, some of which contain halite or sylvite fillings, are found down to approx. 328 m. From approx. 328 m to the final depth at 381.6 m, the fissures are mainly sealed by carnallite and to a lesser extent also by halite or sylvite. This indicates that the water from the overburden penetrated the carbonate and sulphate rocks approx. 31 m down to a depth of approx. 328 m.

Boreholes penetrating rock salt of the Leine-Folge

In addition to the salt table borehole GoHy 3153 (see above), 12 boreholes (BORNEMANN 1991: Apps. 9, 10, 11) penetrated rock salt belonging to the Leine-Folge (GoHy 484, 503, 515, 654, 1131, 3020, 3100, 3110, 3130, 3151, 3152, and 3155). Only boreholes GoHy 515, 1131, and 3130 are described in detail because only these show subsivive alteration of the potash seam caused by water from the overburden penetrating the salt formation.

Borehole GoHy 515 reached the salt table at 299.8 m before penetrating inverted layers of Liniensalz (z3LS) and Unteres Orangesalz (z3OSU). No explicit evidence of the effect of water from the overburden on these rock salt layers was found. However, there were indications of subsivion of the Kaliflöz Stassfurt, which was assumed to be in the immediate vicinity:

- The salt table is approx. 20 m lower than in the surrounding area.

- Despite the presence of Elsterian channel formation, the overburden also contains a Tertiary block. This Tertiary block was probably preserved because the depression formed at the salt table by the subsidence of the potash seam acted as a sediment trap.
- From 275.6 m (i.e. 24.2 m above the salt table) down to the salt table the Hutgesteinsbrekzie contains irregularly scattered rock salt lumps originating from the Hauptsalz (z2HS). These are probably isolated halite lumps which dropped as a result of subsidence of the potash seam and which were then incorporated in the Hutgesteinsbrekzie. The borehole may also have penetrated the edge of a steep slope created by the trough-like depression of the salt table caused by subsidence of the potash seam. Erosion processes taking place on the slope during breccia formation could also have been the source of the halite lumps.

Borehole GoHy 1131 penetrated inverted Basissalz (z3BS) beneath the salt table at 304.6 m, and then cut through Liniensalz (z3LS) down to final depth (BORNEMANN 1991: Apps. 9, 10). The overlying cap rock is exclusively formed of partially gypsified Hauptanhydrit. This did not protect the underlying rock salt layers from the penetration of water from the overburden.

The zones of the Basissalz down to approx. 14 m below the salt table are altered as follows (Table 2):

- Occurrences of gypsum crystals of a length of up to 1 cm
- Local occurrences of anhydrite pseudomorphs of gypsum, up to 4 cm long
- Halite crystals with partial zonation (hopper crystals as a result of skeletal growth)
- The inclusion of green-grey clay flakes from the overburden
- Alteration of the colour of the halite from grey-brown to red-brown

In borehole GoHy 3130 the Anhydritmittelsalz (z3AM) was penetrated from the salt table (262.6 m) to final depth at 306.1 m (BORNEMANN 1991: Apps. 9, 11). Due to the folding of the bedding, the Anhydritmittel 9 (z3AM9/ah) was penetrated twice from 274.15 to 280.8 m and from 301.3 to 302.75 m. Beneath the lower Anhydritmittel is a zone of 1.4 m consisting of carnallite. This carnallite is missing in the upper intersection of the middle Anhydritmittel due to subsidence. The resulting void was filled with fine sandy clayey silt from the overburden. Several fissures up to 2 cm wide filled with dark-grey fine sand occur within the underlying Anhydritmittelsalz. The effects of water from the overburden were found in this borehole down to approx. 12 m below the salt table (Table 2).

Salt table boreholes containing rock salt of the Aller-Folge

Rock salt belonging to the Aller-Folge was encountered only in salt table borehole GoHy 3010 (BORNEMANN 1991: Apps. 9, 11). No alterations attributable to water from the overburden were observed.

2.4 *Underground mapping*

Geological mapping of the shafts and underground drifts and chambers was performed by the DBE geologists, while the BGR was responsible for geoscientific supervision and quality assurance. The underground mapping was the main source of information for the geological model of the Gorleben deposit.

The findings are documented for:

Shaft Gorleben 1:

AMELUNG 1998, 1999 b; AMELUNG & ZBRANCA 1996 a, c, 1997 a, d; BAUER 2001 a; DBE 1985 a; ENSTE 1990; ENSTE & GÖBEL 1989, 1990; FLECKENSTEIN 1993 b; GÖBEL 1991; GROTE 1996; ISLINGER 1992 b; KUTOWSKI et al. 1996; MARTIN 1995 a; MEYER 1993 a, 1994 a, c; MEYER & ISLINGER 1993; ZBRANCA & PETZOLD 1995 a.

Shaft Gorleben 2:

AMELUNG 1999 a; AMELUNG & ZBRANCA 1996 b, d, 1997 b, c, 1998; BAUER 2001 b; DBE 1985 b; FLECKENSTEIN 1993 a, c; GROTE 1997; ISLINGER 1992 a; MARTIN 1995 b; MEYER 1993 b, 1994 b, d; SCHUBERT 1996, 2001; ZBRANCA 1998, 1999 a; ZBRANCA & PETZOLD 1995 b.

Underground exploration:

AMELUNG 2001; AMELUNG & SCHUBERT 2000; HAMPE & KUTOWSKI 2002; KUTOWSKI 2002.

The information gained through the mapping and the subsurface exploration boreholes up to the beginning of the moratorium on October 1, 2000 is documented in the 2nd Geological Report by BORNEMANN et al. (2002 a).

As a supplement to Table 7 (see Appendices), Figure 4 provides an overview of the stratigraphic position, thickness and lithological composition of the Zechstein layers encountered in the infrastructure area and in Exploration Area 1.

Area	Division	Group	Formation	Thickness [m]	Symbol		
Infrastructure Area	Zechstein 3	Anhydritmittelsalz		60	z3AM	approx. 170 m	
		Buntes Salz		12	z3BT		
		Bank-/Bändersalz		14	z3BK/BD		
		Orangesalz		50	z3OS		
		Liniensalz		31	z3LS		
Exploration Area 1	Zechstein 3	Basissalz		16	z3BS	approx. 80 m	
		Hauptanhydrit		40 bis 80	z3HA		
		Leine-Karbonat		1,5	z3LK		
		Grauer Salzton		2,5	z3GT		
	boundary Zechstein 2 / Zechstein 3						
	Zechstein 2	Gebänderter Deckanhydrit		1,5	z2DA		
		Decksteinsalz		0,5	z2DS		
		Kaliflöz Staßfurt		0 bis 17	z2SF		
Kieseritische Übergangsschichten			2,5	z2UE			
Zechstein 1	Hangendsalz		10	z2HG	approx. 800 m		
	Hauptsalz		700 bis 800	z2HS			
	Kristallbrockensalz			z2HS3			
	Streifensalz			z2HS2			
	Knäuelsalz			z2HS1			


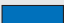
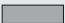

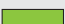
Legend		 anhydrite
 predominantly rock salt	 Salzton	
 potash	 carbonate	

Figure 4: Overview of the stratigraphic position, thickness and lithological composition of the Zechstein layers encountered in the infrastructure area and in Exploration Area 1.

2.4.1 Shafts Gorleben 1 and Gorleben 2

The mapping of the shaft walls was performed continuously, and the mapping steps followed the mining progress so that on completion a continuous geological map of the shaft cylinder at a scale of 1:50 was available (App. 2). The length of the mapping steps varied, the maximum being 4 m (BORNEMANN et al. 2002). The mapping comprises every tectonic and sedimentary feature that can be displayed at a scale of 1:50, including faults, fissures, B-axes and bedding horizons. Zones of secondary recrystallization are mapped as interpolated areas. Mapping of the Liniensalz and Orangesalz was based on line counts, which made a distinction between anticlines and synclines possible. Where possible, every tenth line was shown on the maps (HAMPE & KUTOWSKI 2002).

For parts of the cap rock and the salt formation the shaft floor was mapped in order to improve the spatial presentation of the geological findings. The documentation of the shaft walls includes continuous sets of photographs and additional photographs to characterise the structure of individual beds.

2.4.2 Drifts and chambers

As with the mapping of the shafts, the geological mapping of the underground cavities was carried out continuously in step with the excavation progress. The maps of drifts and chambers were mainly created at a scale of 1:100. Detailed maps of scale 1:25 were made in significant areas, e.g. where seams were intersected. These maps also include all tectonic and sedimentary features that can be displayed at the respective map scales, such as faults, fissures, B-axes, bedding and schistose surfaces, secondary mineralisation, hydrocarbon occurrences, etc. The mapping was performed on blasted or cut walls and over lengths of 13 to 45 metres for each step, depending on the speed of advance. Due to the rounded profile of the drifts, the maps show a two-dimensional view of the roofs and walls (HAMPE & KUTOWSKI 2002). The mapping results were digitally converted into horizontal projections and then directly incorporated into the geological 3D model by the BGR.

In addition to normal geological mapping, a mapping of the hydrocarbon occurrences in the Knäuelsalz and Streifensalz (Hauptsalz of the Stassfurt-Folge) was performed using ultraviolet light in order to reveal the distribution of the occurrences and to identify any potential changes in their outflow rates (BORNEMANN et al. 2001). As UV light causes hydrocarbons to fluoresce, they can easily be distinguished from areas free of hydrocarbons (see Fig. 49). This special mapping was conducted in both cross-cuts for the whole outcrop of the Knäuelsalz (z2HS1) and Streifensalz (z2HS2). The remaining beds of the Hauptsalz were also examined under UV light in all drifts to ensure that all condensate occurrences had been identified.

During the UV mapping, four classes of fluorescence intensity could be distinguished. Two types of occurrences that were visible under normal light, i.e. where the walls were clearly moistened by hydrocarbons, were classified as “strongly visible” and “weakly visible”. The other two types of occurrences on the wall that were only visible under UV light were classified as “strongly fluorescent” and “weakly fluorescent”.

2.5 *Underground exploration boreholes*

The location of the underground exploration boreholes is shown in Appendix 3. Before excavation of the shaft-landing for the 840 m-level in Shaft 1, the northern part of the planned shaft-landing was explored by core borehole 00YES01 RA777. On the 820 m-level in Shaft 2 a similar exploration in the direction of the planned drift was performed with borehole 00YES02 RA274, as well as to the SW with borehole 00YES02 RA272 (BORNEMANN et al. 2002: App. 1; BORNEMANN et al. 1998: Apps.).

From January 22, 1996 to April 26, 1996, seven boreholes drilled from the northern and southern shaft-landings in Shaft 1 (840 m-level) provided additional information on the geology and structure of the surrounding salt formation:

- Borehole 01YEF11 RB058 (substitute for 02YEF11 RB011)
- Borehole 02YEF11 RB003
- Borehole 02YEF11 RB012
- Borehole 02YEF11 RB004
- Borehole 02YEF11 RB013
- Borehole 02YEF11 RB001
- Borehole 02YEF10 RB001

Another seven boreholes were drilled from the northern shaft-landing in Shaft 2 (820 m-level) (App. 3, BORNEMANN, et al. 2002b: App. 1):

- Borehole 01YEF20 RB059
- Borehole 01YEF20 RB014
- Borehole 01YEF20 RB003
- Borehole 01YEF20 RB002
- Borehole 01YEF20 RB004
- Borehole 01YEF20 RB015
- Borehole 01YEF20 RB001

The objective of this drilling programme was to find rock salt in the Leine-Folge suitable for the construction of infrastructure rooms and drifts in the vicinity of the shaft, and to identify zones virtually free of Hauptanhydrit at the boundary between the Leine-Folge and Stassfurt-Folge to construct the two cross-cuts to the north in the direction of Exploration Area 1 (EB1).

During the drilling programmes, a significant structural element between the shafts, consisting of an anticlinal updoming of the Kaliflöz Stassfurt, was encountered. The core of this updoming contains beds of the Stassfurt-Folge.

An additional drilling programme consisting of five boreholes was executed from August 6, 1996 to October 9, 1996 in order to analyse this structure in more detail. The objective was to precisely determine the extent and geology of the Zechstein 2 updoming and to explore the Zechstein 3 strata assumed to follow to the SW. The following boreholes were drilled from the access drift to the machine workshop:

- Borehole 02YEA04 RB021
- Borehole 02YEA04 RB022
- Borehole 02YEA04 RB023
- Borehole 02YEA04 RB024
- Borehole 02YEA04 RB025

Boreholes 02YEA04 RB029 and 02YEA24 RB030 were drilled to provide more information on deeper lying zones. They were drilled with a dip of -25 gon and -35 gon respectively. The remaining boreholes have only a slight dip of -1 to -17 gon. Unlike the other boreholes, 02YEA24 RB030 was drilled from the tank store. The lengths of the boreholes varied between 60.9 m and 373.1 m depending on the exploration objectives. In these boreholes, the orientation of the strata was logged regularly every 50 m or at other intervals depending on the structure penetrated. The sequence penetrated by the drilling programme ranged from the Hauptsalz of the Stassfurt-Folge to the Anhydritmittelsalz of the Leine-Folge.

By mid 1997, after major parts of the underground infrastructure had been excavated, sufficient information was available to plan the drifting of cross-cut 1 West through the boundary zone between the Leine-Folge and the Stassfurt-Folge (z3/z2). The exploration results of borehole 03YEF20 RB004 indicated that drifting through the z3/z2 boundary zone in the area of cross-cut 1 East would be possible without encountering any Hauptanhydrit. Thus, further exploration in this zone was not deemed necessary at the time.

Due to the complicated stratigraphy and the frequently encountered blocks of Hauptanhydrit in the area of cross-cut 1 West, however, a sequence of four additional boreholes was drilled to provide sufficient geological information to plan the drifting of a cross-cut through the z3/z2 boundary zone (BORNEMANN et al. 2001: 8):

- 02YER02 RB032
- 02YER02 RB033
- 02YER02 RB031
- 02YER02 RB233

The boreholes were drilled from August 15, 1997 to November 25, 1997. After evaluation of the drilling results and detailed discussions of a Hauptanhydrit block with a length of approx. 10 m, which was proven to be isolated, the decision was made to drift cross-cut 1 West through the z3/z2 boundary along the line of borehole 02YER02 RB032.

In order to map the southern z3/z2 boundary, another five horizontal and downward boreholes were drilled to approx. 150 m beneath the 840 m-level between February 1998 and September 2000. These concluded the exploration of the southern boundary of EB1. The exploration boreholes were as follows (BORNEMANN et al. 2001: 10 ff., Table 3, App.1):

- 02YEQ02 RB264 (SW edge of EB 1, inclined borehole)
- 02YER02 RB261 (southern edge, centre of EB 1, inclined borehole)
- 02YEQ01 RB194 (SE edge of EB 1, inclined borehole)
- 02YER02 RB154 (southern edge, centre of EB 1, horizontal borehole)
- 02YER20 RB500 (SE edge of EB 1, horizontal borehole)

The following exploration boreholes were drilled from September 1997 to June 2000 in order to investigate the northern z3/z2 boundary zone of EB 1 and to explore the central part of this zone consisting of Hauptsalz:

- 02YEQ01 RB119
- 02YEQ01 RB120
- 02YEQ01 RB427
- 02YER20 RB254
- 02YER20 RB488

In order to prevent any brine intrusion, boreholes 02YEQ01 RB119, 02YEQ01 RB120, 02YEQ01 RB427, and 02YER20 RB488 were terminated in the Hangendsalz or in the Kieseritische Übergangsschichten when drilling came close to the Kaliflöz Stassfurt or the Hauptanhydrit. With increased knowledge of the stratigraphy in this zone, it was possible to estimate the location of the z2/z3 boundary with an accuracy of a few metres. This policy could not be followed in borehole 02YER20 RB254. As drilling progressed, a fold with intense fracturing of the Hauptanhydrit into separate blocks was encountered before reaching the z2/z3 boundary. This indicated the presence of a drag fold in front of the boundary. The actual z2/z3 boundary therefore had to lie further to the north. The risk of brine intrusion was thus taken deliberately to achieve the exploration objectives of the borehole.

In addition to the exploration boreholes, the following geotechnical boreholes were drilled from drilling locations 3, 3.1, and EL 4 (Exploration Location 4) to map the anticline of the Hauptsalz and to analyse the geological structure:

Drilling location 3

- 02YEQ01 RB206,
- 02YEQ01 RB210,

Drilling location 3.1

- 02YEQ01 RB208,

Exploration location (EL) 4

- 02YER20 RB184,
- 02YER20 RB186.

Boreholes 01YEF20 RB217 and 02YEA12 RB218 were drilled from the underground infrastructure area to provide further information on the structure of the Zechstein 2 updoming, particularly on its flanks (BORNEMANN et al. 2001: Table 4). The older borehole 02YEA24 RB030 and these additional boreholes together provided information from three directions (NE, E and SW) on the downward geometry of the flanks. The two geotechnical boreholes 02YEA06 RB170 and 02YEA06 RB171 also provided valuable information on the impoverishment of the Kaliflöz Stassfurt in the Zechstein 2 updoming.

The results of the underground exploration boreholes are given in ZBRANCA (1997 a to u, 1998 a to f, 1999 a, 2000 a to c, 2001 a, b). The interpretation of each of the boreholes can be found in separate reports by BORNEMANN et al. (1998), BORNEMANN et al. (2001) and BORNEMANN et al. (2002 a). These reports are one of the major sources for the summary of the exploration results in this report.

2.6 *Electromagnetic survey methods*

2.6.1 **Electromagnetic reflection surveys**

Electromagnetic reflection surveying (EMR) to investigate the geology of salt deposits has been standard practice in potash and rock salt mines since the 1970s. This measuring technique locates geoelectrical unconformities that are mostly associated with boundaries between different rocks and thus with lithostratigraphic horizons and other petrophysical heterogeneities (wet zones, clay mineral concentrations, etc.). During the first years after the introduction of this method, surveys were conducted from drifts and chambers. The development of borehole radar probes shifted a great part of EMR surveying to advance exploration of the stratigraphy from boreholes.

Several different types of EMR borehole probes are available, which:

- can be used in surface boreholes down to depths of several thousand metres, for the exploration of undeveloped salt domes
- are suitable for underground exploration in boreholes of a length of up to 1000 m.

An EMR system consists of the borehole probe, recording unit and cable winch or tool pusher. One of the major advances was the development of directional borehole aeriels facilitating spatial location of reflectors. At the Gorleben site, pulse radar probes were used for EMR surveys. In normal operation, a pulse with a selectable centre frequency of 20 to 300 MHz is transmitted into the rock via a transmitting antenna.

The electromagnetic wave penetrates the surrounding medium and is reflected by several geoelectrical unconformities. The travel time of the reflected wave front is recorded at each measuring point. The distance to the reflecting horizon can be determined from the wave travel time using the known propagation velocity of the electromagnetic wave.

Media through which the electromagnetic waves can pass with little attenuation offer good conditions for successful EMR surveys. Rock salt and potash deposits with their extremely low electrical conductivity are therefore suited to this exploration technique (MUNDRY et al. 1985). Depending on the frequency used, ranges of several hundred metres can be achieved. Boundaries where the gradients of the electrical parameters conductivity and dielectric constant are high can easily be identified because of the associated high reflectivity. Claystones, anhydrite, dolomite, potash salts, potash deposits and basalts can be easily identified in evaporites if the aforementioned physical conditions are met. Wet rock zones and fissures containing brine show up particularly well due to their high conductivity.

EMR surveys in surface boreholes

As part of the surface exploration of the salt dome, EMR surveys were carried out in the four exploration boreholes Go 1002, Go 1003, Go 1004, Go 1005 and in the two shaft pilot boreholes Go 5001 and Go 5002 (ALBRECHT et al. 1991). The surveys were usually run shortly after completion of the drilling operation or after replacing the drilling mud by oil-based mud. Changing the mud was necessary because the high conductivity of the complex mixed-salt solutions used in the drilling mud would have reduced or blocked the propagation of the waves. All measurements began beneath the casing shoe because the casing above this point absorbs the electromagnetic waves completely.

EMR surveys underground

EMR surveys in the shafts

In both shafts, the sections within the salt formation were surveyed down to final depth using geo-radar. Due to the moistening caused by the frost crack injection work, surveying was not possible in the whole salt formation section, but started below 371 m in Shaft 1 and below 381 m in Shaft 2. For technical reasons, full-circle surveys began in Shaft 1 only below 523 m. The EMR surveys were performed by BGR in cooperation with DBE from July 28, 1994 to November 17, 1997. BGR interpreted the EMR surveys and presented their findings in reports (EISENBURGER & GUNDELACH 1995 a to e, 1996) as well as in the final report (EISENBURGER et al. 2000).

Four profiles were recorded in each shaft. Each profile was offset from the next by 100 gon. This ensured that all the rock surrounding the shaft was optimally surveyed, and this layout also permitted directional identification of the recorded reflections. In order to determine the direction of the reflectors more precisely, full-circle surveys were carried out every 10 to 15 m in the shafts from approx. 520 m downwards. The directional measurement ensured an angular accuracy of a few gon.

The majority of the reflectors are located to the north of the shafts. South of the shafts as well as west of Shaft 1 and east of Shaft 2, fewer reflectors were recorded. Between the shafts, only a few reflectors were recorded from the salt table to approx. 480 m. Almost none were found from approx. 480 to 680 m. Below 680 m, a large number of reflectors were recorded around both shafts, which means that the beds dip at steep angles relative to the shafts. In the zone between 480 m and 680 m, however, the absence of reflectors indicates that the beds in the zone between the shafts are almost horizontal.

Reflections with a sharp first arrival were interpreted as anhydrite beds, such as the Gorleben-Bank or the anhydrite bands in the Anhydritmittelsalz. Major anhydrite bands such as those in the Liniensalz sometimes also caused distinct reflections. As the Gorleben-Bank has the greatest reflectivity in this area, some of these reflectors reached lengths of up to 200 m. Reflectors from the Anhydritmittel reached lengths in the order of tens of metres. Isolated anhydrite bands produce only short or relatively weak reflectors. Most of the reflectors belong to the Gorleben-Bank. A large proportion of these reflectors is located to the north of the shafts. This corresponds to the main occurrence of the Gorleben-Bank. The distribution of the reflectors indicates that the Gorleben-Bank also occurs to the west of Shaft 1 and east of Shaft 2, but not as often as to the north of the shafts. Reflectors classified as Anhydritmittel of the Anhydritmittelsalz were found to the south of the shafts.

Due to its good reflection properties and its widespread extent, the Gorleben-Bank has become a key mapping horizon for the geological interpretation of the radar data. It can be identified in the radargrams because of its relatively large reflection amplitude and the clarity of the arrivals. Calibration of the return signal of the Gorleben-Bank to the outcrop in the shaft is reliable because the reflectors often reach the shaft walls. As the Gorleben-Bank is a key horizon for geological mapping and elaborating the geological site model, geological mapping and geophysical surveying complement each other very well in this case. The same applies to the Anhydritmittel even though the interpretation of the reflectors is not quite as clear and the reflectors are not as long.

In addition to this, a multitude of reflectors were located at the boundary between Zechstein 2 and Zechstein 3. The return signals have much lower amplitudes than those of, for example, the Gorleben-Bank. This indicates that the returns are coming from the Kaliflöz Stassfurt (probably in the form of brecciated carnallite). The reflection amplitudes are rarely high enough to suggest that the Grauer Salzton is the origin. A notable aspect is that the reflection arrivals are not sharp but “smeared” over a certain range. This indicates that the Zechstein 2/Zechstein 3 boundary is strongly affected by small-scale folding and thus, only small sections of the boundary have favourable reflection properties.

The geology around the shafts can be identified by EMR surveys up to a distance of approx. 85 m (measured from the central axis of the shafts). Any further projection of the geology is unwise. Some reflectors were detected at a distance of up to 250 m. However, an angular deviation of only 10 gon at this distance leads to a horizontal measurement error of some 40 m. Thus, a longer-range projection is only viable when the data is supplemented by the geological mapping of the 820 m-, 840 m-, 880 m-, and 930 m-levels and the EMR surveys conducted there. Geo-radar provided valuable information concerning the bedding orientation and location for the assessment of the stratigraphy in the vicinity of the shafts.

EMR surveys in drifts and exploration boreholes

The whole underground drift network was surveyed using EMR. The same method as in the shafts was applied, including full-circle surveys (EISENBURGER & GUNDELACH 2002 a). EMR surveys were also conducted in the underground exploration boreholes drilled in the flanks of the Hauptsalz anticline and the Zechstein 2 updoming (EISENBURGER & GUNDELACH 1999, 2000 a to f, 2001, 2002 b to e).

Naturally, the reflectors recorded in these underground surveys are caused by the same lithological boundaries or unconformities as in the shaft surveys. In the central infrastructure area and on the flanks of the Hauptsalz anticline, distinct reflections of the Hauptanhydrit, the Grauer Salzton and the Kaliflöz Stassfurt were recorded as well. Thus, the z2/z3 boundary could be adequately mapped, particularly the zone from the Hauptsalz anticline to the northern flank. The EMR survey, combined with the results of the exploration boreholes, revealed a much higher degree of fracturing of the Hauptanhydrit into clasts or blocks on the northern flank of the z2 anticline.

In the Hauptsalz of the central z2 anticline some distinct and long reflectors were also recorded. Most of these EM reflectors (EISENBURGER & GUNDELACH 1999) reveal the internal bedding within the Streifensalz. The reflections were interpreted as residual anhydrite bands bordering the halite banks. This permitted a reliable face extrapolation beneath and above the Hauptsalz anticline.

2.6.2 High-frequency absorption surveys

In addition to the EMR surveys, high-frequency absorption surveys were conducted in the surface exploration boreholes. High-frequency absorption surveying (HFA method) involves the investigation of the presence, position and size of electrically responsive inclusions in a rock zone by radiating several electromagnetic sinus waves in the megahertz range. The amplitude of the voltage induced in the receiving antenna is used to interpret the electrical structure of the rock penetrated by the wave. The interpretation is based on wave propagation laws, i.e. the energy reaching the receiving antenna not only comes from the direct wave (energy losses which occur due to geometrical propagation, eddy currents, and scattering in the rock) but also from reflected and refracted waves (ALBRECHT et al. 1991: 47 ff.).

In the course of research project WAK 1527 0 by BMFT (1978-1980), two probes were developed for the application of this method in deep boreholes. These probes have a frequency range of 10 to 30 MHz and are suitable for depths of up to 3000 m. The method involves using two boreholes, which have to be filled with oil-based mud. Logging can

be done by either simultaneous vertical movement of both borehole probes or with one fixed probe and a mobile second probe.

In the Gorleben salt dome, the objective of HFA surveying was to detect and localise beds of anhydrite and/or saliniferous clay. Based on the receiving amplitude of the direct wave as a function of the logging distance and frequency, the rock salt beds were to be analysed with regard to their absorption behaviour, thus allowing the interpretation of their electrical conductivity. Dry salt rocks have an extremely low electrical conductivity and thus cause very low attenuation of the electromagnetic wave. Brine inclusions increase conductivity and therefore increase the absorption of wave energy considerably. The results of the trial surveys were not sufficiently conclusive for geological interpretation and therefore these surveys were discontinued in the course of further explorations.

2.7 Mineralogical and geochemical investigations

For salt rocks, data on mineralogy and geochemistry are necessary for the interpretation of their genesis, especially with regard to metamorphic and alteration processes in the salt formation or changes caused by external solutions. Mineralogical and geochemical data are also used to characterise the sequence of strata of the salt formation and subsequently to analyse the structure of the salt dome (BORNEMANN et al. 2002 b).

The qualitative mineralogical composition of the samples was primarily determined by using X-ray-diffraction analysis (XRD), occasional use of microscopic analysis on thin sections or loose rock samples and by means of geochemical analysis. The quantitative mineralogical composition was determined mathematically from the proportions of the main chemical components (cf. Chapter 2.7.2), with the exception of the kainite-bearing sections of the Kaliflöz Stassfurt where the composition was determined by using quantitative XRD.

The cores were sampled after detailed description of the rock types encountered in the borehole. Zones of different structure or colour were sampled separately. Sampling involved cutting specimens of approx. 2 to 3 cm in size from the centres of the cores using a band saw. Intersections of the potash seam were completely sampled, i.e. over their whole length. Each zone sampled was weighed so that an assessment of the overall composition of the rocks in each borehole could also be made by taking into account the mass proportions.

2.7.1 Sample preparation and analysis to determine the qualitative mineralogical composition

After crushing with a laboratory disk mill, 2500 mg of each sample were dissolved in 250 ml demineralised water. This was diluted to 1:10, and aliquot samples were taken for cation and anion analysis. Subsequent analysis determined the main components sodium (Na), potassium (K), calcium (Ca), magnesium ($Mg_{(total)}$), sulphate (SO_4) and chloride (Cl).

If analysis results for $Mg_{(total)}$ were greater than 500 $\mu\text{g/g}$, the $Mg_{(alc.ex.)}$ was also determined in alcohol extraction. The ICP-OES was used according to DIN 38406 (Part 22, EN ISO 11885: 1997) to analyse Na, K, Ca and Mg, whilst an ion chromatograph according to DIN 38406 (Part D19) was used to determine the SO_4 and Cl.

The cations were detected on the basis of five measurements using the ICP-OES "Spectro". The anion contents were measured using an ion chromatograph "Dionex As 12", in each case by comparison with matrix-adjusted standard calibration solutions. X-ray fluorescence spectroscopy (XRF) was used to determine the trace elements strontium (Sr) and rubidium (Rb). Bromide (Br) was measured by XRF as well as by ion chromatography (according to EN ISO 10304-1: 1995).

Alcohol extraction had to be performed before determining the magnesium chemically bound in carnallite. This involved the extraction of 1000 mg of sample for 2 hours in 50 ml absolute alcohol. Subsequently, 20 ml were removed, evaporated, dissolved in 0.5 ml concentrated nitric acid, and finally diluted to 50.5 ml with demineralised water. Analysis was carried out using ICP-OES (EN ISO 11885: 1997). No alcohol extraction was carried out on those samples which were macroscopically identified as pure carnallite as it can be assumed that the whole Mg content is attributable to the carnallite. The value of $Mg_{(total)}$ in these cases corresponds to $Mg_{(alc.ex.)}$.

The geochemical analyses were based on one chemical analysis per sample (in some cases six analyses per sample for the Kaliflöz Stassfurt). The standard deviation of the main component analyses is less than 1 % whilst the anion/cation balance shows an error tolerance of mostly less than 1 %. The results of the geochemical analysis usually differ from the total sample weight. This is due to chemically bounded water, and/or due to water-insoluble residues which were not included.

The analytic error for determining Na, Cl, and SO_4 is ± 1 %, for Ca ± 0.5 %, for K and Mg ± 0.1 %. Determination of Sr, Rb, and Br by XRF with contents of ~ 100 $\mu\text{g/g}$ incurred an error of ± 1 %.

2.7.2 Determining the quantitative mineralogical composition

The ZECHMIN-7 software (SCHRAMM & BORNEMANN 2004) was used to determine the quantitative mineralogical composition of each sample based on the concentrations of the main geochemical components. This software quantifies the mineral associations of halite, anhydrite (or gypsum), polyhalite, kieserite, carnallite, sylvite and langbeinite on the basis of the main geochemical components Na, K, Ca, $Mg_{(total)}$, $Mg_{(alc.ex.)}$, Cl and SO_4 .

In principle, the aforementioned minerals can be explicitly calculated using a simple template (Fig. 5) if no langbeinite is present. Langbeinite is selectively calculated from K, Mg or SO_4 by the program if there is an excess of these components or if the distribution into polyhalite, anhydrite and kieserite leaves large remainders of the main components so that the total mineralogical composition differs too much from the actual total sample weight.

All calculations seek an optimal distribution of main components to minerals so that the residue of non-assigned main components is kept as small as possible (total approximates to 100 %). The main priority is to avoid negative values for the main components as well as for the minerals. The calculations are usually carried out in iterative steps in order to weight the element distributions to the associated minerals. For instance, halite is not necessarily calculated solely by Na content but also automatically weighted again with the residual Cl after the first complete calculation sequence. The other minerals are calculated using the same procedure. Very lengthy iteration runs are required if langbeinite is identified.

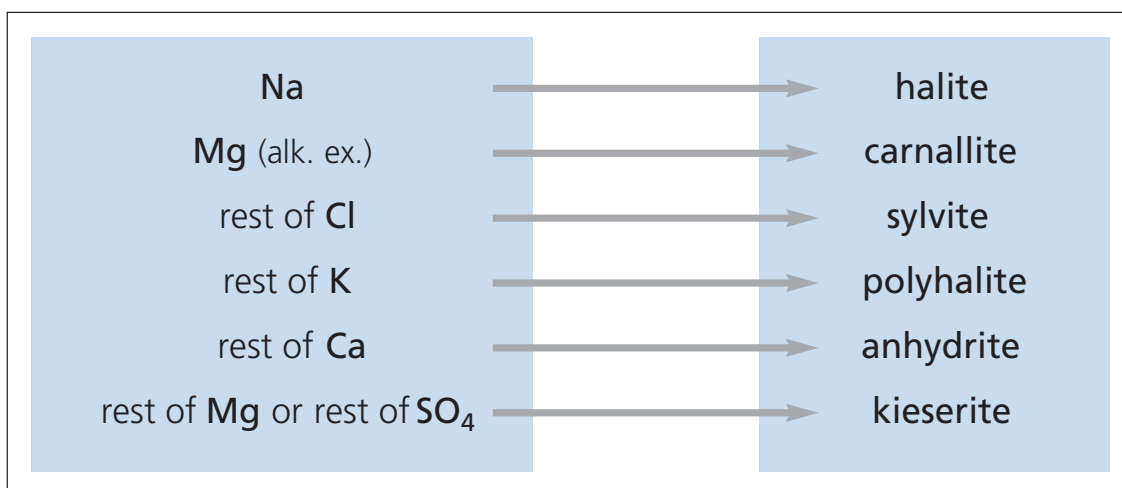


Figure 5: Simplified calculation template of the ZECHMIN-7 software to quantify the mineralogical composition.

The XRD results are always used to check (qualitatively) the calculated results to make sure that all detected minerals were actually calculated. As the detection limit of XRD analysis varies between 0.1 and 1 wt% depending on the mineral in question, the calculation method also enables minerals to be determined which were not detected by XRD. Additional control measures involved comparative calculations conducted on standard samples and the use of the quantitative XRD (Rietveld method).

This resulted in the following error analysis for ZECHMIN-7:

- Error for determining halite and carnallite < 1 wt% (corresponding to the geochemical analysis error).
- If no langbeinite was calculated (in approx. 99 % of all cases), the quantitative values for anhydrite, polyhalite, kieserite, and sylvite also have an error of approx. 1 wt%.
- If langbeinite was calculated and the mineral total was < 100 wt%, the error for anhydrite, polyhalite and kieserite can amount to several percent. In very rare cases, the mineral total was > 100 wt% when both langbeinite and anhydrite had been calculated. In these cases it is possible that no polyhalite is calculated by the program even though it was detected. Where possible, the XRD results were used to correct the calculations (<< 1 % of analysed samples).
- Calculated mineral contents of < 0.1 wt% were disregarded. These can arise mathematically from small analysis errors and/or from small brine inclusions within the rock.

2.7.3 Determining the bromide content in the evaporites


Bromide content analysis proved a useful means of interpreting the genesis of the rocks and brines, the subsidence processes, and the stratigraphic definition of the evaporite sequence, and therefore the structural analysis of the salt dome (BORNEMANN et al. 2002b).

Today's seawater has a bromide concentration of 0.00671 wt% (BRULAND 1983). As bromide does not form any discrete minerals, it becomes enriched in the residual solution by evaporation even though it is incorporated within chloride minerals to a small extent. The bromide distribution between crystallising halite (and other chlorides) and the solution is determined by the distribution coefficient b where:

$$b = \frac{\text{wt.}\%Br_{\text{crystal}}}{\text{wt.}\%Br_{\text{solution}}}$$

The distribution coefficient b for Br is < 1 . As evaporation progresses, the bromide concentration in the seawater solution initially rises to 0.054 wt% when halite first begins to form (0.0075 wt% Br in halite). As evaporation continues, the distribution coefficient b drops from 0.14 ± 0.01 down to 0.073 ± 0.004 when carnallite starts to form (BRAITSCH & HERRMANN 1963).

According to KÜHN (1955), who first determined the correlation between primary mineral associations and bromide concentration in the halites in a standard section of the Hauptsalz of the Stassfurt-Folge (z2), the following mineral regions in the rock salt of the Stassfurt-Folge are associated with specific bromide concentrations:

carnallite region	280 - 480 $\mu\text{gBr/g}$ in halite		rising degree of evaporation
kieserite region	230 - 280 $\mu\text{gBr/g}$ in halite		
polyhalite region	170 - 230 $\mu\text{gBr/g}$ in halite		
anhydrite region	60 - 170 $\mu\text{gBr/g}$ in halite		

BÄUERLE (2000) confirmed that the values of these mineral regions can be extrapolated to the z3- Liniensalz sequence in the Gorleben salt dome. Each of these mineral regions is characterised by their bromide concentration in the halite and by the first occurrence of the newly formed minerals (anhydrite or polyhalite, etc.).

Samples for bromide analysis were taken at the smallest possible spacing normal to the bedding, each from a single bed so that only halite of a single genetic origin was present in each sample. Special care was taken that a sample did not contain secondary halite and matrix halite. It was often only possible to sample mineral associations, which also contained carnallite and sylvite instead of sampling pure halite. These two minerals also incorporate bromide into their crystal lattices in place of chloride. Bromide analysis for halite within halite and carnallite mineral associations is only viable below a certain ratio. As the distribution ratio of bromide in halite to bromide in carnallite may vary between 1:7 (primary paragenetic ratio) and 1:14.7 (MATTENKLOTT 1994), the bromide content of the halite is only calculated if halite is the main mineral phase (more than 50 wt%) and the carnallite concentration of the sample is ≤ 0.4 wt%. At this mass percent ratio of 99.6:0.4 ($\approx 250:1$) the relative maximum deviation in the bromide concentration of the halite to the calculated bromide concentration from the primary paragenetic ratio is 3 %. This corresponds to the usual tolerable range of geochemical analysis. For bromide content calculations in carnallites in association with halite a maximum mass percent ratio of 1:7 between carnallite and halite is tolerable.

The distribution ratio of Br in halite to Br in sylvite varies between 1:8.8 and 1:10 (Mattenklott 1994). For the bromide calculation from the bromide analysis of the total sample of a mineral association involving halite and sylvite, there is a relative deviation of 3 % in the bromide content for a sylvite concentration of up to 3.2 wt.% compared to the bromide content calculated from a ratio factor of 8.8. The bromide content of halite with higher sylvite concentrations was not calculated because the deviation exceeds the 3 % limit. For instance a ratio of halite 1: sylvite 99 may cause a maximum error of 12 %. A maximum mass percent ratio of 1:2.85 is viable for calculating the bromide content in sylvite in a mineral association with halite. The bromide concentration of pure halite is calculated from the total bromide concentration analysed in the sample. If the sample contained neither carnallite (total Mg content of the sample < 500 µg/g) nor sylvite, the analysed bromide concentrations were related to the normative NaCl concentration.

If the sample contained carnallite, the theoretical paragenetic ratio $Br_{\text{halite}}:Br_{\text{carnallite}} = 1:7$ according to BRAITSCH & HERRMANN (1963) was assumed. Thus, the carnallite concentration was multiplied by 7 and normalized to 100 % together with the halite concentration of the sample. The product of the normalized halite proportion in percent and the analysed bromide concentration gives the bromide concentration in the halite.

In the case of samples containing sylvite, the bromide correction was carried out with the theoretical paragenetic ratio $Br_{\text{halite}}:Br_{\text{sylvite}} = 1:10$ according to BRAITSCH & HERRMANN (1963) in a similar fashion to the calculation method for samples containing carnallite.

3 Salt dome exploration results

3.1 *Composition, extent and genesis of the cap rock*

During the development of the salt pillow into a diapir, from the Malm onwards, the salt rocks rose up into the higher parts of the Mesozoic sedimentary cover (Fig. 1; JARITZ 1980; ZIRNGAST 1991, 1996). By the Early Cretaceous at the latest, the top of the salt dome lay at or near the surface resulting in increased subsidence and erosion of the updoming salt rocks. The strong salt uplift continued into the early Tertiary before declining from the late Tertiary to the Quaternary. Before the salt dome was covered by cohesive and impermeable sediments in the last stage of the Tertiary, the cap rock was subjected to local erosion and karstification (JARITZ 1994). As a result of subglacial channel formation above the NE part of the salt dome (Gorleben Channel) during the Elsterian Glacial period, the subsidence and erosion of the upper parts of the salt dome again reached a local, short-term maximum.

The results of the cap rock core analyses from salt table boreholes and deep boreholes permitted the identification of lithologically well-differentiated subrosion rocks that can be used to interpret the extent and development over time of the salt dome cap rock and thus the subrosion history of the salt dome top.

The exploration of the cap rock was of particular importance for the site investigation, due to the need to determine the extent of potentially ongoing subrosion processes and the history of earlier subrosion events. The results of the investigation are based on circa 50 boreholes, which provided continuous core sequences in the cap rock and the underlying salt formation (BORNEMANN & FISCHBECK 1986). The spatial development of the thicknesses and shape of the cap rock formation are shown in Appendix 1.

3.1.1 Late Mesozoic to Cenozoic cap rock development

Depth maps (see KÖTHE et al. 2003, 2007) of the cap rock surface reveal a significant relief of approx. 200 m (highs: approx. -100 m; troughs: approx. -300 m). This is attributable to the varying thickness of the cap rock (due to lithological or structural causes) and the presence of a Quaternary channel partially cutting across the salt dome from NE to SW in which the cap rock was partially or completely eroded. However, the relief of the salt table is less distinctive. Nevertheless, the structure of the salt dome is partially discernible depending on the salt rocks exposed at the salt table. The salt table is at approx. -230 m in the SW and slopes downward to the NE to approx. -350 m (see Chapter 3.2).

The cap rock of a salt dome is created by the dissolution of easily soluble salt minerals, transformation of poorly soluble minerals and by crystallization of new minerals out of the liquid phase, as well as by the deposition of poorly soluble or insoluble constituents at the salt table. Thus, the youngest beds created by dissolution are located at the base close to the salt table, while the oldest parts of the cap rock lie at the top of the cap rock sequence.

Hauptanhydrit, Pegmatitanhydrit, the Anhydritmittel from the Anhydritmittelsalz, as well as all clay-rich sequences are incorporated within the cap rock without losing their sedimentary textures. This applies even if anhydrite is converted to gypsum (BORNEMANN & FISCHBECK 1986). Despite having different original mineralogical compositions, rocks rich in halite all create cap rocks of similar texture. Large cap rock thicknesses indicate the presence of Hauptanhydrit blocks embedded within the cap rock sequence.

The exploration revealed that certain sequences with characteristic textures occur repeatedly within the cap rock above the whole salt dome. In the standard sequence, the following textures can be distinguished from top (old) to bottom (young) (see Fig. 6):

- **Flasergips, Knollengips:**
Fine-crystalline, dark particles rich in gypsum and light to white nodules containing relatively high amounts of anhydrite or consisting completely of anhydrite. The flasers contain minor amounts of clay. The layer can be up to approx. 10 m thick. It may be locally absent as a result of erosion or subrosion.
- **Liniengips:**
Fine-crystalline, abundant, paper-thin, slightly clay and carbonate-bearing, partially sigmoidally twisted gypsum layers which can intersect at tight and strongly varying angles. In some areas, broken or mostly corroded dolomite crystal clasts of 0.5 cm in size occur. The average thickness of the Liniengips is approx. 10 m.
- **Sprenkelgips:**
Banks of mainly coarse-crystalline but also fine-crystalline and medium-crystalline gypsum are interbedded throughout the whole Sprenkelgips sequence. The gypsum crystals are 0.5 cm to 1 cm long, semi-idiomorphic, slightly bent and suffered pressure stress according to microscopic analysis. They must have grown mainly from a solution phase. The thickness of the Sprenkelgips ranges from a few metres to approx. 15 m.

A common feature of the three uppermost cap rock units is that they only contain isolated fissures and faults or cavities. The rare exceptions are filled with material from the overlying overburden (see exposures in Shafts Gorleben 1 and 2; KUTOWSKI et al. 1996; SCHUBERT 1996). Fragmentation increases only in the lowermost few meters of the Sprenkelgips. This is the transition zone to the next deeper-lying cap rock type:

- **Hutgesteinsbrekzie:**
This rock type consists of a clayey-sandy and gypsiferous matrix as well as fragments of different gypsum types such as Liniengips, Flasergips and Knollengips. In addition to fragments of altered overburden, the matrix contains Nordic till with diameters ranging from a few millimetres to larger than the core diameter (MINGERZAHN 1987).
- **Geschichtetes Gips-, Anhydritgestein:**
This rock type lies at the base of the cap rock and is therefore the youngest member of the cap rock sequence. It is grey to light-grey and fine-crystalline to medium-crystalline. Zones with randomly oriented lath-shaped anhydrite crystals are interbedded with beds of almost idiomorphic gypsum crystals of 0.5 cm to 1 cm thickness. These may contain anhydrite residues.

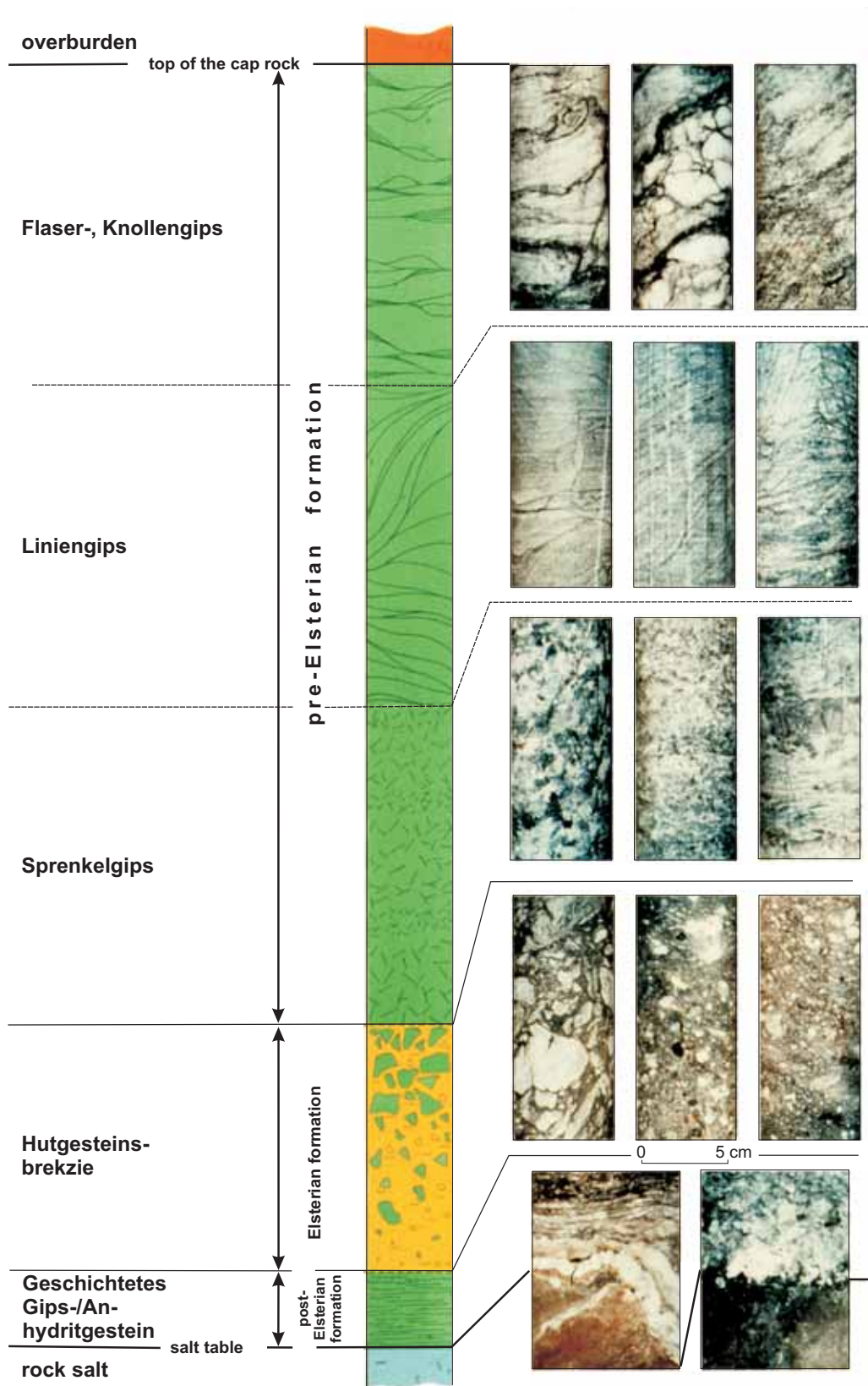


Figure 6: Non-scale illustration of the sequence of strata in the cap rock (according to BORNEMANN & FISCHBECK 1986).

Unlike the Flasergips, Knollengips, Liniengips, Sprenkelgips and Geschichtetes Gips-, Anhydritgestein which originated from the conversion of anhydrite into gypsum as a result of subrosion at the surface of the salt dome, the creation of the Hutgesteinsbrekzie is associated with the formation of the Elsterian Gorleben Channel.

There are two causes for the formation of glacial channels. They can form when meltwater dammed up by a glacier is suddenly released, causing erosion at the base of the glacier, or they are formed by the removal of sediment by glacial movement (e.g. KUSTER & MEYER 1979; EHLERS et al. 1984). The former explanation is assumed to be true for the formation of the Gorleben Channel because ground moraines at the base of the channel are rare, and the few occurrences are clearly allochthonous.

The high-pressure meltwaters responsible for carving the channel also penetrated the flanks of the channel and also intruded into the boundary between the cap rock and the salt table, which was then a weak point in terms of salt mechanics. The water penetrating this boundary altered the existing cap rock material. The typically angular gypsum fragments indicative of short transport paths, as well as the glacial sediments and rocks of the overburden flushed in by the meltwater formed the characteristic Hutgesteinsbrekzie. As the breccia was not encountered in some boreholes, the erosive meltwater appears to have selectively penetrated the salt table zone depending on pressure conditions and lithological features. Additionally, the processes involved in the formation of the Hutgesteinsbrekzie appear to have taken place in several successive stages as indicated by sequences of beds with graded bedding and other sedimentary structures (MINGERZAHN 1987: 37 ff.). A reduction in breccia formation and a decrease in the amount of glacial material is also observed with increasing distance from the channel centre.

As the age of the Hutgesteinsbrekzie can be derived from the time the channel was formed during the Elsterian Glacial (later glacials did not cause the formation of any channels in the Gorleben area) this information can be used to estimate the age of the underlying younger cap rock layers as well as the overlying older layers. This is also confirmed by analyses of the gypsum crystal water from samples of gypsum-rich rocks in each of the five cap rock layers, which determined the composition of the oxygen and hydrogen isotopes (HERBERT et al. 1990). Low δD - and $\delta^{18}O$ values of the source water can be interpreted under certain circumstances as evidence for low ambient temperatures during gypsum formation.

These conditions apply to the water involved in gypsum formation in the Hutgesteinsbrekzie. Samples from the other cap rock types had higher values, which suggest gypsum formation by water during warmer climatic periods. The only exceptions are the fractured parts of the

lower Sprenkelgips sequence lying directly above the breccia. According to the isotope values, these gypsums also have glacial signatures. Apparently, water from the events forming the Hutgesteinsbrekzie also affected these lower zones.

3.1.1.1 Quaternary subsosion

Due to the positive dating of the breccia as being formed during the Elsterian Glacial, the layers of the Geschichtetes Gips-, Anhydritgestein sequence become very important for estimating the age and intensity of the latest subsosion processes affecting the salt table. Depending on the composition of the underlying salt sequence, the thicknesses of the Geschichtetes Gips-, Anhydritgestein layers reflect the extent of post-Elsterian subsosion provided that the anhydrite conversion is complete.

The thickness of the subroded salt can be calculated for a particular location if the thickness of the Geschichtetes Gips-, Anhydritgestein at this point and the anhydrite concentration in the underlying salt dome are known. Thus, subsosion rates valid for particular locations can be derived for the period from the Elsterian Glacial to today.

Table 3 shows the results of some simple calculations. If the rock salt contained 2.8 wt% anhydrite for example, one metre of subroded rock salt would leave behind 2.0594 cm of anhydrite available for forming Geschichtetes Gips-, Anhydritgestein (conversions see Table 6, Appendix). As the deep groundwater at the top of the salt dome is saturated with sulphates in some places (KLINGE 1994), it can be assumed that the sulphate originates from the dissolved anhydrite originally contained in the salt rock at this location (2.8 wt% in this example) in addition to other sulphate sources.

According to D'ANS & LAX (1949), approx. 0.7 wt% anhydrite dissolves in a saturated NaCl solution. If 2.8 wt% anhydrite of the initial rock salt represent 2.0594 cm of Geschichtetes Gips-, Anhydritgestein, as in borehole GoHy 15, and if 0.7 % of this anhydrite (= 0.0144 cm) dissolve and the remaining anhydrite is available for forming the Geschichtetes Gips-, Anhydritgestein, then the resulting thickness of the Geschichtetes Gips-, Anhydritgestein is too small to calculate the subsosion at the salt table. On the other hand, the "missing" thickness (0.7% of 2.0594 = 0.0144 → 2.045 cm Geschichtetes Gips-, Anhydritgestein) is so small that it can be ignored for the rough estimate to deduce the height of the subroded salt column or the subsosion rate (for instance, GoHy 15: $130/2.0594 = 63.13$ m versus 63.57 m subroded salt column and $63.13 \times 1000/270000 = 0.234$ mm/year versus 0.235 mm/year subsosion rate for a post-Elsterian time period of 270 000 years).

This calculation is based on the condition that grain-in-grain gypsification of anhydrite to gypsum takes place to form the Geschichtetes Gips-, Anhydritgestein without any increase in volume associated with hydration. The validity of this assumption is supported by observations that sequences and structural features in the original evaporite rocks, for example, are completely preserved in the Geschichtetes Gips-, Anhydritgestein.

Figure 7 shows cores from different boreholes containing rock salt from various stratigraphic units occurring at the salt table plus the overlying Geschichtetes Gips-, Anhydritgestein.

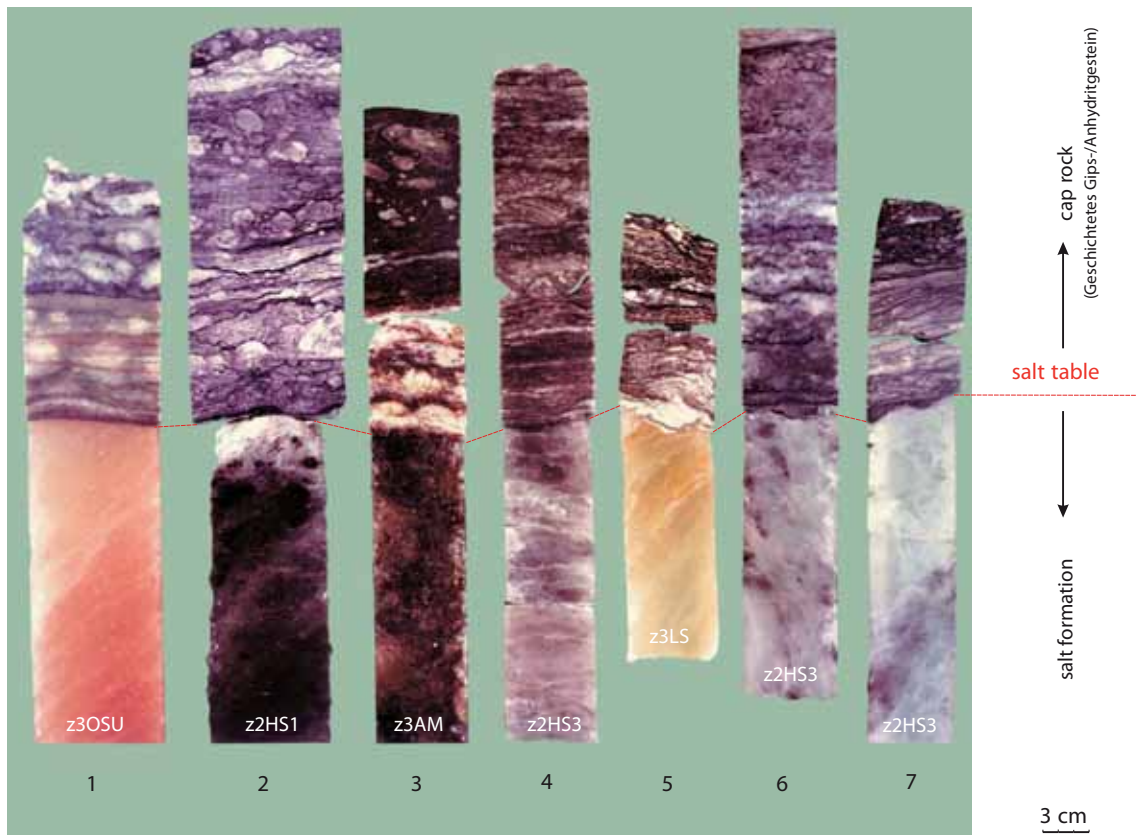


Figure 7: Genesis of Geschichtetes Gips-, Anhydritgestein, salt table and underlying salt formation in selected cores (1 to 7).

Unlike the semi-steep to steep bedding in the salt formation, the bedding in the Geschichtetes Gips-, Anhydritgestein is almost parallel and horizontally aligned to the salt table. Due to the dissolution of the halite, the residual sulphates are deposited with a strictly parallel orientation at the bottom of the Geschichtetes Gips-, Anhydritgestein, depending on the nature of the sulphates. Only then does partial gypsification and accretive crystallization take place, while the shape of the sulphates (nodules, pinstripes, flakes, etc.) remains roughly preserved. Given the solution conditions at the salt table, it is assumed that approx. 0.7 wt% of the sulphate in the original rock probably dissolves with the halite.

Table 3: Calculated subsrosion rates and amount of salt subroded from Geschichtetes Gips-, Anhydritgestein in selected exploration boreholes.

Borehole	Thickness of the Geschichtetes Gips-, Anhydritgestein [cm]	Stratigraphy at salt table	Anhydrite content of the salt rock [wt-%, averages]*	Subroded column of the salt rock, rounded off [m]	Subrosion rate since Elsterian Glacial Stage			
					270000°	330000°°	420000°°°	480000°°°°
					years ago			
					[mm/year]			
Go 5001	--	-- z2	--	--	--			
Go 5002	90	Oberes Orangesalz z3OSO	1.0	124	0.46	0.38	0.3	0.26
GoHy 15	130	Hauptsalz (1-3)** z2HS	2.8**	64	0.24	0.19	0.51	0.13
GoHy 65	45	Kristallbrockensalz z2HS3	1	62	0.23	0.19	0.15	0.13
GoHy 133	160	Hauptsalz (1-3)** z2HS	2.8**	78	0.29	0.24	0.19	0.16
GoHy 143	--	-- z2HS3	--	--	--			
GoHy 484	5	Liniensalz z3LS	3.8	2	0.007	0.005	0.004	0.004
GoHy 503/515	--	-- z3LS	--	--	--			
GoHy 515	--	-- z3LS	--	--	--			
GoHy 524	75	Kristallbrockensalz z2HS3	1	103	0.38	0.31	0.25	0.22
GoHy 555	30	Streifensalz z2HS2	1.5	27	0.1	0.08	0.07	0.06
GoHy 654	--	-- z3AM	--	--	--			
GoHy 841	--	-- z2HS2	--	--	--			
Go 1002	30	Knäuelsalz z2HS1	5.8#	7	0.03	0.02	0.017	0.015
Go 1003	--	-- z2HS2	--	--	--			
Go 1004	345	Knäuelsalz z2HS1	5.8#	81	0.3	0.25	0.19	0.16
Go 1005	190	Knäuelsalz z2HS1	5.8#	44	0.17	0.14	0.11	0.09
GoHy 1121	--	-- z3	--	--	--			
GoHy 1131	--	-- z3	--	--	--			
GoHy 1141	--	-- z2	--	--	--			
GoHy 1151	--	-- z2	--	--	--			
GoHy 1161	10	Kristallbrockensalz z2HS3	1	14	0.05	0.04	0.03	0.029
GoHy 1171	--	-- z2	--	--	--			
GoHy 1181	--	-- z2	--	--	--			
GoHy 1302	--	-- z2	--	--	--			

Table 3: (continued)

Borehole	Thickness of the Geschichtetes Gips-, Anhydritgestein [cm]	Stratigraphy at salt table	Anhydrite content of the salt rock [wt-%, averages]*	Subroded column of the salt rock, rounded off	Subsrosion rate since Elsterian Glacial Stage			
					270000°	330000°°	420000°°°	480000°°°°
					years ago			
					[mm/year]			
GoHy 1303	--	-- z2	--	--	--			
GoHy 1304	--	-- z2	--	--	--			
GoHy 1305	110	Hangendsalz z2HG	0.7	216	0.8	0.66	0.52	0.45
GoHy 3010	--	-- z4	--	--	--			
GoHy 3020	20	Mittleres Liniensalz z3LSM	5##	5	0.02	0.016	0.013	0.01
GoHy 3030	--	-- z2	--	--	--			
GoHy 3040	45	Kristallbrockensalz z2HS3	1	62	0.23	0.19	0.15	0.13
GoHy 3050	30	Hauptsalz (1-3)** z2HS	2.8**	15	0.05	0.04	0.035	0.031
GoHy 3060	20	Hauptsalz (1-3)** z2HS	2.8**	10	0.04	0.03	0.023	0.02
GoHy 3070	50	Hauptsalz (1-3)** z2HS	2.8**	24	0.09	0.07	0.06	0.05
GoHy 3080	30	Kristallbrockensalz z2HS3	1	41	0.15	0.13	0.1	0.09
GoHy 3090	50	Hauptsalz (1-3)** z2HS	2.8**	24	0.09	0.07	0.06	0.05
GoHy 3100	65	Tonmittelsalz z3TM	1	89	0.33	0.27	0.21	0.19
GoHy 3110	20	Bank-/Bändersalz z3BK/BD	0.3	92	0.34	0.28	0.22	0.19
GoHy 3120	3	Hauptsalz (1-3)** z2HS	2.8**	1	0.005	0.004	0.003	0.003
GoHy 3130	15	Anhydritmittelsalz z3AM	2.4	9	0.03	0.026	0.02	0.018
GoHy 3140	10	Hauptsalz (1-3)** z2HS	2.8**	5	0.018	0.015	0.012	0.01
GoHy 3150	30	Hauptsalz (1-3)** z2HS	2.8**	15	0.054	0.044	0.035	0.031
GoHy 3151	120	Oberes Orangesalz z3OSO	1.0	165	0.61	0.5	0.39	0.34
GoHy 3152	40	Bank-/Bändersalz z3BK/BD	0.3	184	0.68	0.56	0.44	0.38
GoHy 3153	25	Kristallbrockensalz z2HS3	1	34	0.13	0.1	0.08	0.07
GoHy 3154	40	Kristallbrockensalz z2HS3	1	55	0.2	0.17	0.13	0.12
GoHy 3155	93	Unteres Orangesalz z3OSU	0.5	256	0.95	0.78	0.61	0.53
Mean	--	--	--	--	0.236	0.193	0.152	0.133

* From chemistry database "Salzgeologie" (salt geology) of BGR.

** Hauptsalz (1-3): Mean of Hauptsalz z2HS1, z2HS2, and z2HS3, as exploration did not provide more precise data.

According to MÜLLER-SCHMITZ (1985: 29).

According to BORNEMANN & FISCHBECK (1987: 157).

° Lexikon der Geowissenschaften: Nord-Silb (2001).

°° According to JARITZ (1994: Table 1).

°°° According to SCHLAAK (1999: Fig. 27).

°°°° According to ZIRNGAST et al. (2003: Fig. 7.8-1).

Core 1 shows the steeply dipping outcrop of the Unteres Orangesalz (z3OSU) at the salt table (Fig. 7). The sulphate impurities consist of shadowy bands of flakes, scattered anhydrite and polyhalite, and haematite scales, which give the halite a red-orange colour. The subsrosion in the Geschichtetes Gips-, Anhydritgestein results in horizontally-bedded, fine-crystalline gypsum anhydrite rock interbedded with violet haematite flakes. In core 2, the salt table is underlain by Knäuelsalz (z2HS1). The characteristic impurities in the halite are scattered anhydrite knots and nodules as well as randomly scattered anhydrite flakes. The Geschichtetes Gips-, Anhydritgestein has a depositional texture of anhydrite knots floating in a fine-crystalline anhydrite matrix. In core 3, the salt table is underlain by a highly contaminated cloudy zone of the Anhydritmittelsalz (z3AM). The subsrosion residues in the Geschichtetes Gips-, Anhydritgestein consist of an alternating sequence of horizontally bedded pure gypsum horizons with layers enriched with clay flakes and haematite scales.

Cores 4, 6 and 7 show Kristallbrockensalz (z2HS3) beneath the salt table. The minor impurities consist of randomly scattered anhydrite flakes. Anhydrite knots are rare. In all three cores, the overlying gypsum anhydrite laminate consists of an almost identical, horizontally layered, laminated texture. Core 5 shows Liniensalz (z3LS) beneath the salt table. The anhydrite impurities primarily consist of anhydrite lines of a thickness of up to 5 mm spaced at regular intervals of 10 to 15 cm. Subsequent to the subsrosion of the halite, the lines were deposited horizontally directly on the Geschichtetes Gips-, Anhydritgestein to form layers as is clearly visible at the salt table (Fig. 7).

The cores described above confirm that the sulphatic impurities are deposited directly on the Geschichtetes Gips-, Anhydritgestein without any significant solution phase. The lithological features in the rock salt are transferred to characteristic recognisable textures in the growing gypsum anhydrite laminate.

For the deduction of the subsrosion rates, the time elapsed from the Elsterian Glacial to the present day is required. According to the Lexikon der Geowissenschaften (Dictionary of Geosciences 2001: Table Quartäres Eiszeitalter, Quaternary ice age) the time elapsed is approx. 270 000 years. ZIRNGAST et al. (2003) proposed an age of 480 000 years based on the latest findings in Quaternary literature. Additional references to Elsterian Glacial channel formation can be found in the literature. JARITZ (1994: Pl. 1) quotes an age of approx. 330 000 years for the formation of the Gorleben Channel and thus for the Hutgesteinsbrekzie. SCHLAAK (1999: Fig. 27) dated the formation of Elsterian deep channels at approx. 420 000 years ago. As these varying values affect the calculation of the subsrosion rates, they are compared in Table 3.

The time periods used for the calculations are possibly too long and the deduced subsidence rates too low, because subsidence during the youngest Weichselian Glacial period has not yet been unequivocally proven due to the sedimentation processes above the salt dome. Its absence would mean deducting approx. 100 000 years from the assumed values for the post-Elsterian period.

This simple calculation yields subsidence rates of a few hundredths to a few tenths of a millimetre per year for the period from the Elsterian Glacial to the present day (Table 3) and average rates of the order of 0.1 to 0.2 mm/year. If absence of subsidence during the youngest Weichselian Glacial is taken into account, the average values are between approx. 0.2 and 0.4 mm/year. ZIRNGAST et al. (2003: 222) estimated an average value of 0.22 mm/year (max. 0.43 mm/year) from an evaluation of the depositional patterns of sediments of the Holstein interglacial stage.

When the results are displayed in their spatial context (Fig. 8), it becomes obvious that the highest post-Elsterian Glacial subsidence rates occur in a narrow zone stretching parallel to the structural axis to the south of the exploration mine. Higher values generally occur in the SW central zone. The values decrease towards the edge of the salt dome.

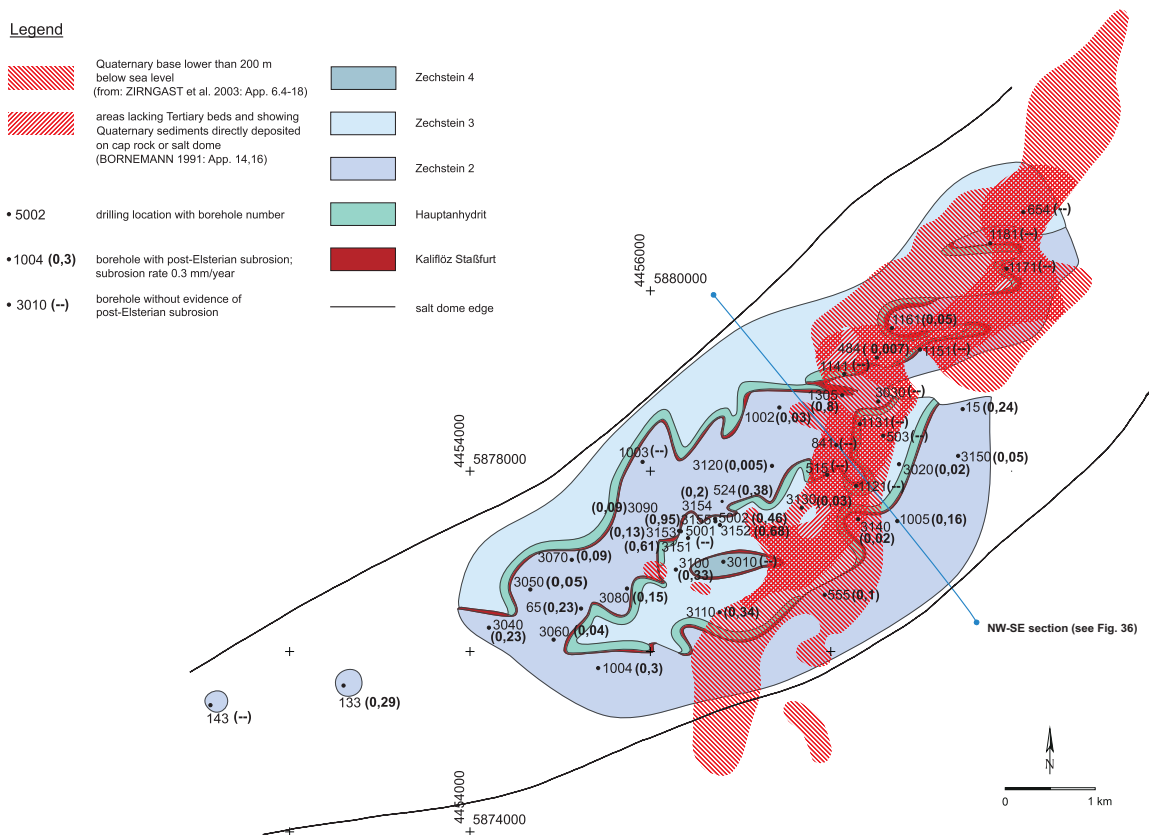


Figure 8: Geological map of the salt table (BORNEMANN 1991: App. 21) and post-Elsterian subsidence rates (Hauptanhydrit is simplified as a continuous band).

The subsrosion rates that can be identified underneath the Quaternary channel are extremely low. The location of the channel is shown in Figure 8 by the 200 m depth contour of the Quaternary base and the zone where Quaternary sediments directly overlie the rock salt. It appears that the development of the channel was followed by rapid saturation of the groundwater to form saturated brine. Groundwater conditions must have been mostly stagnant, preventing further extensive subsrosion of the rock salt exposed by the formation of the channel. An exception is the Kaliflöz Stassfurt outcrop at the salt table (GoHy 1305), which underwent more intense subsrosion and alteration as it contains easily soluble materials. Such zones of intense subsrosion are contained within inverted beds of the Kaliflöz Stassfurt and are confined to the NE part of the salt dome structure, far away from the planned repository (Fig. 8).

APPEL & HABLER (1998) chose a different approach to estimate Quaternary subsrosion rates in the area of the Gorleben salt dome based on the statistical analysis of drilling data. Their idea is based on the varying depths of the base of the Holstein sediments, which they attribute to subsrosion of the salt dome surface during the Saalian Glacial period.

They assume the following:

- The Gorleben Channel was filled up to a largely uniform level at the beginning of the Holstein interglacial period and that the different depths of the base are not attributable to differences in relief.
- The base of the Holstein sediments was not affected by glacio-tectonics during the younger glacials.
- There was no compaction of the deeper-lying older Elsterian clay layers.
- Boreholes with evidence of subsrosion can be statistically differentiated from boreholes with no subsrosion.
- The Saalian Glacial period lasted 100 000 years.

The different ages and the genesis (marine/limnetic) of the various Holsteinian sediments are not incorporated in this approach.

According to APPEL & HABLER (1998), the results of the statistical analysis of the drilling data indicated that the average subsrosion rates during the Saalian Glacial were between approx. 0.3 and 0.5 mm/year. The average values are thus slightly higher than the subsrosion rates calculated from the thickness differences of the Geschichtetes Gips-, Anhydritgestein. This is certainly also attributable to the short duration of 100 000 years assumed for the Saalian Glacial period. However, they are of the same order of magnitude as the subsrosion rates extrapolated for the central area of the western part of the salt dome.

Comparing the subsrosion rates calculated by the different methods, the most significant differences appear in the values for the Gorleben Channel. Whilst APPEL & HABLER (1998) assumed that considerable subsrosion took place during the post-Elsterian period, analysis of the thickness measurements of the Geschichtetes Gips-, Anhydritgestein shows only low subsrosion rates and only in a few places. If the channel had been affected by stronger post-Elsterian subsrosion, extensive young cap rock sequences of considerable thickness would have been found. As this is not the case, the true values are probably between the values determined by the two different methods.

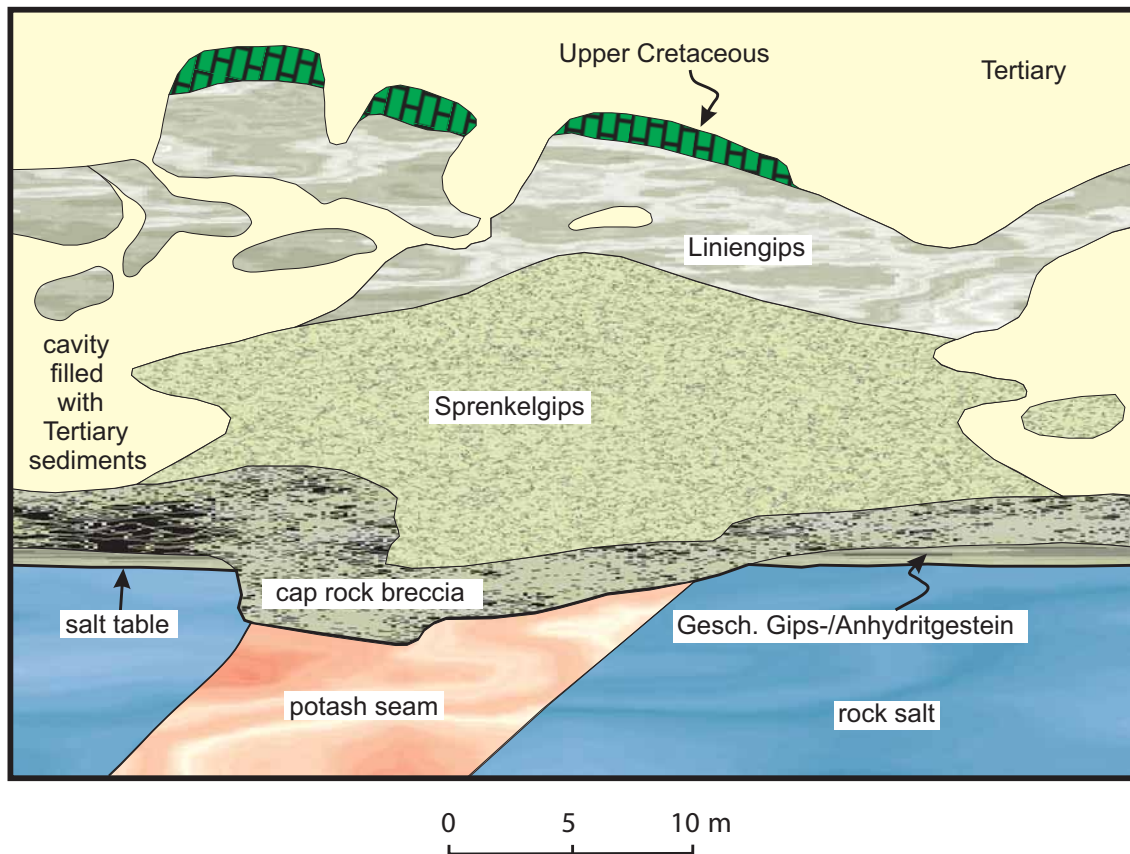
It is probably safe to assume that selective subsrosion took place underneath the channel, the extent of which was locally determined by the groundwater dynamics during the post-Elsterian Glacials and Interglacials, and by the hydrochemical conditions depending on the salt table relief and the type of salt rocks cropping out at the salt table. The selective subsrosion also seems to have involved several phases, as shown by the condition of the subroded Kaliflöz Stassfurt in the borehole series GoHy 1301 to 1305. In the sequences penetrated by these boreholes showing conversion of the potash seam into pure, partially gypsum-bearing rock salt, there was at least local reprocessing as indicated by the presence of embedded, in parts finely-laminated rock salt lumps containing haematite scales and boron minerals (MINGERZAHN 1987: 97 ff.). It may even be concluded that the subsrosion and the associated conversion of the potash seam took place long before the creation of the Gorleben Channel, and that the Quaternary material did not fill the space occupied by the former potash seam until later, during the Elsterian Glacial period.

Based on these considerations, it cannot be asserted that there were generally higher subsrosion rates in the channel in the period from the Elsterian Glacial to the present day. It is more likely that rates were lower in the channel than in other parts of the salt dome.

3.1.1.2 Cretaceous and Tertiary subsrosion

The dating of the cap rock sequence with the Flaser-, Knollengips, Liniengips and Sprenkelgips is discussed in detail by JARITZ (1994), who dates the cap rock units lying above the Hutgesteinsbrekzie as mainly Cretaceous on the basis of fossils and lithological analyses.

Figure 9 illustrates the situation on the basis of the sequence penetrated by Shaft Gorleben 1.



	Sequence of events	Time frame
1	subsidence and formation of the cap rock with Flaser-/Knollengips, Liniengips and Sprenkelgips	mainly Cretaceous
2	erosion of the Flaser-/Knollengips	Cretaceous
3	burial by Cretaceous sediments	e.g. Campanian
4	mainly erosion of the Cretaceous sediments	Late Cretaceous to Palaeocene
5	filling of karst cavities	Palaeocene to Eocene
6	formation of the cap rock breccia (Hutgesteinsbreckzie)	Elsterian Glacial Stage
7	formation of the Geschichtetes Gips-/Anhydritgestein	Late and Post Elsterian

Figure 9: Sediment history of the cap rock illustrated by the exposure in Shaft Gorleben 1 (schematic drawing after JARITZ 1994).

The thickness of the (Cretaceous) Tertiary sequence lying above the cap rock in the western central part of the salt dome can be determined by comparing the map of the Quaternary base (ZIRNGAST et al. 2003: Apps. 6.4-18) with the "Top cap rock" contour map (BORNEMANN 1991: App. 15). The thickness of the Tertiary in this area is approx. 20 to 100 m. The variation in thickness indicates Tertiary subsrosion processes at the salt table, assuming that these deposits are neither disturbed nor allochthonous nor that they have been thinned by Quaternary erosion. It is noticeable that the Tertiary is thicker (approx. 60 to 80 m) in areas where post-Elsterian subsrosion is at a maximum. This is shown particularly clearly when the isopach maps of specific Tertiary horizons are included in the analysis (see maps in ZIRNGAST et al. 2003).

Allowing for the exceptions referred to above, the maps support the conclusion that subsrosion to the south of the exploration mine had already begun in the Tertiary and continued after the Elsterian Glacial. The assumed stronger subsrosion to the south of the shafts could be explained by the elevated salt table determined in this area, because such elevations are preferential areas for increased subsrosion.

3.1.2 Middle Mesozoic cap rock formation

During the surface exploration programme, only salt dome exploration borehole Go 1005 penetrated cap rock formations on the flanks of the salt dome. At a depth of 1879.3 to 1894.5 m, the borehole penetrated the Anhydritmittelsalz of the Leine-Folge (BORNEMANN & FISCHBECK 1987 b), then broke through the edge of the salt dome at 1894.5 m, and encountered a sequence of rock salt, polyhalite and siltstones to fine sandstones of the Late Bunter with scattered inclusions of claystone breccia. The lower part of this sequence was primarily dominated by inclusions of anhydrite in rock salt.

Below 1906.3 m, strongly faulted beds consisting of Pegmatitanhydrit (z4PA) of the Aller-Folge were found down to 1907.3 m. The anhydrite had a dense jaspoid appearance whilst all bedding features of the Pegmatitanhydrit were still recognisable. However, no halitic components were present, for instance, filling the space between the skeletal crystals of the anhydrite pseudomorphs of gypsum. This indicates that the Pegmatitanhydrit in this zone has been affected by subsrosive processes. The strontium concentration of 1300 to 2300 ppm is, despite subsrosion, also in the range found in Pegmatitanhydrit deposits (z4PA) within the salt dome.

The fault at 1907.3 m is followed by grey, dark-grey and partially brown-red to red anhydrite rocks. Sulphur isotope analysis (approx. 10 to 13 ‰ $\delta^{34}\text{S}$ relative to the CDT standard) indicates that these are also derived from redeposited and recrystallized sulphate minerals

of Zechstein origin and can be interpreted as cap rock. The upper parts of the anhydrite rock also contain claystone breccia, claystone inclusions with coal fragments and sandy sediments which are dated using fossil spores as Valanginian and Barremian.

The last section of the borehole from approx. 1921 m to final depth at 1930 m mainly penetrated grey to light-grey sandstones. These contain a few dark-grey, rounded anhydrite nodules up to 5 cm in size and a few anhydrite layers with a thickness in the order of centimetres. In addition to irregularly scattered pyrite aggregates, the sandstones contain coal fragments of a length of up to 5 mm, which become more common with increasing depth. The fossil analysis dates the sandstones to be of Valanginian/Barremian origin as well.

It can be assumed from the drilling results and the history of salt dome formation that this deep-lying fossil cap rock was formed prior to the Valanginian/Barremian (Early Cretaceous), probably from Late Lias to Malm (Jurassic). The inclusions of rounded anhydrite nodules indicate that parts of this cap rock were apparently being altered when the sandstone was deposited in the Valanginian/Barremian age.

As the current depth of the cap rock is solely attributable to epirogenic subsidence and as it does not contain any sediments of the younger overburden, this cap rock does not appear to have moved very far from its location at the SE edge of the salt dome during the strong Cretaceous diapiric uplift and formation of the SE salt dome overhang. The situation at the NW edge of the salt dome at that time was quite different. This area was affected by erosion and truncation of the cap rock due to the strong salt uplift. "Conservation" of the cap rock at the SE edge of the salt dome was evidently due to the fact that it was located at a special position on the former Lower Cretaceous edge of the salt dome where no or only very minor upward movement of the salt took place in contrast to the central part and the NW flank of the salt dome. The formation over time of the older cap rock and an explanation for its location are shown in Figure 10.

Borehole Go 1004 also penetrated the SE flank of the salt dome at 1881.4 m and reached final depth in the Solling-Folge of the Middle Bunter (BORNEMANN & FISCHBECK 1988 n). No cap rock was encountered in this borehole. The cover of younger Triassic and Jurassic sediments, which were in place before the Early Cretaceous, was obviously sufficient to prevent the formation of cap rock.

Given the sequence of movements occurring during diapiric growth, no comparable old cap rocks are expected to be found at a similar position and depth on the NW flank of the salt dome, because any such cap rock would probably have been uplifted to a higher position along with the upward movement of the salt, and eroded in the Upper Jurassic

to Lower Cretaceous at the NW edge of the salt dome. This means that the cap rock at today's upper surface of the salt dome including its older sections, must be younger than the cap rock encountered by borehole Go 1005 because it could only have formed from the Lower Cretaceous onwards after the most mobile phase of salt movement was concluded (Fig. 10).

3.2 Salt table and selective subsrosion

Based on the data of the surface boreholes (see Fig. 2), a contour map of the salt table was created, which shows the surface relief of the salt dome (Fig. 11). Many salt table boreholes encountered the Hauptsalz of the Stassfurt-Folge at the salt table. The findings proved that water from the overburden caused no significant mineralogical changes in these rock salt strata. One exception was borehole GoHy 3080 (BORNEMANN & FISCHBECK 1988 j) which encountered only the youngest beds of the Hauptsalz (overturned Kristallbrockensalz) underlain by Hangendsalz. The presence of clay flakes, calcite and localised gypsification of sulphates revealed the influence of waters from the overburden all the way down to final depth at 28.7 m beneath the salt table. The alterations are attributable to the stratigraphic vicinity to the underlying and probably subroded Kaliflöz Stassfurt through which water from the overburden was able to affect the adjoining rock salt. Boreholes specifically targeted at the potash seam yielded similar findings and also showed alterations to the overlying rock salt (e.g. GoHy 1151, 3153: BORNEMANN & FISCHBECK 1988 c, k).

A series of boreholes (e.g. GoHy 1301 to 1305: BORNEMANN & FISCHBECK 1988 e to i; GoHy 3153: BORNEMANN & FISCHBECK 1988 k; GoHy 3155: BORNEMANN & FISCHBECK 1988 m) were drilled to investigate the assumed special alterations of the easily soluble potassium/magnesium minerals in the Kaliflöz Stassfurt at the salt table (MINGERZAHN 1987). The potash seam is completely subroded and impoverished, and is encountered in part as red-coloured rock salt containing varying quantities of gypsum crystals, polyhalite, haematite flakes (GoHy 3153) or even strong impregnation and layers of clastic material of the overburden. The presence of kainitite, for instance in borehole GoHy 1304, also shows the effect of groundwater on the potash seam, as it is produced by conversion of carnallitite. Overall, the boreholes revealed that the potash seam can be subroded or affected by groundwater to a depth of several tens of metres, and in extreme cases up to approx. 170 m (GoHy 1305) below the salt table. On the other hand, the potash seam encountered in borehole GoHy 3154 (BORNEMANN & FISCHBECK 1988 l) in the form of brecciated carnallitite facies lies only 26 m below the salt table and was not affected by groundwater and, like the surrounding Hauptsalz, shows no alteration products or other signs of alteration. This indicates that the depth of penetration of groundwater into the Kaliflöz Stassfurt and its subsrosion is subject to large local variation. Moreover, the

conditions can change significantly even over short distances. The Kaliflöz Stassfurt is in increased danger of subsrosion if the outcrop at the salt table is overturned, i.e. it is not protected from subsrosion by the Grauer Salzton that in the normal bedding sequence is usually above it.

The potash seam outcrop at the salt table was the subject of a special investigation during the sinking of shaft Gorleben 1. This involved drilling boreholes RB377 and RB061 from the shaft directly into the dipping potash seam. The boreholes and shaft exposures provided detailed information on how the seam was affected during the Quaternary (BORNEMANN 1991) and its features at the salt table (BORNEMANN et al. 2002 a). In both boreholes, the effect of the brine, which led to the impoverishment of the Kaliflöz Stassfurt, stops at a relatively horizontal level at around 325 m depth. This corresponds to a true vertical depth of 70 m below the salt table.

Both boreholes encountered the same facies sequence in the conversion zone, from top to bottom:

- Halite facies, potassium-free (gypsum, anhydrite)
- Halite facies, potassium-bearing (polyhalite, sylvite)
- Kainite facies (Kainite, sylvite)
- Brecciated carnallitite (Trümmercarnallitit).

Legend

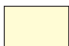
















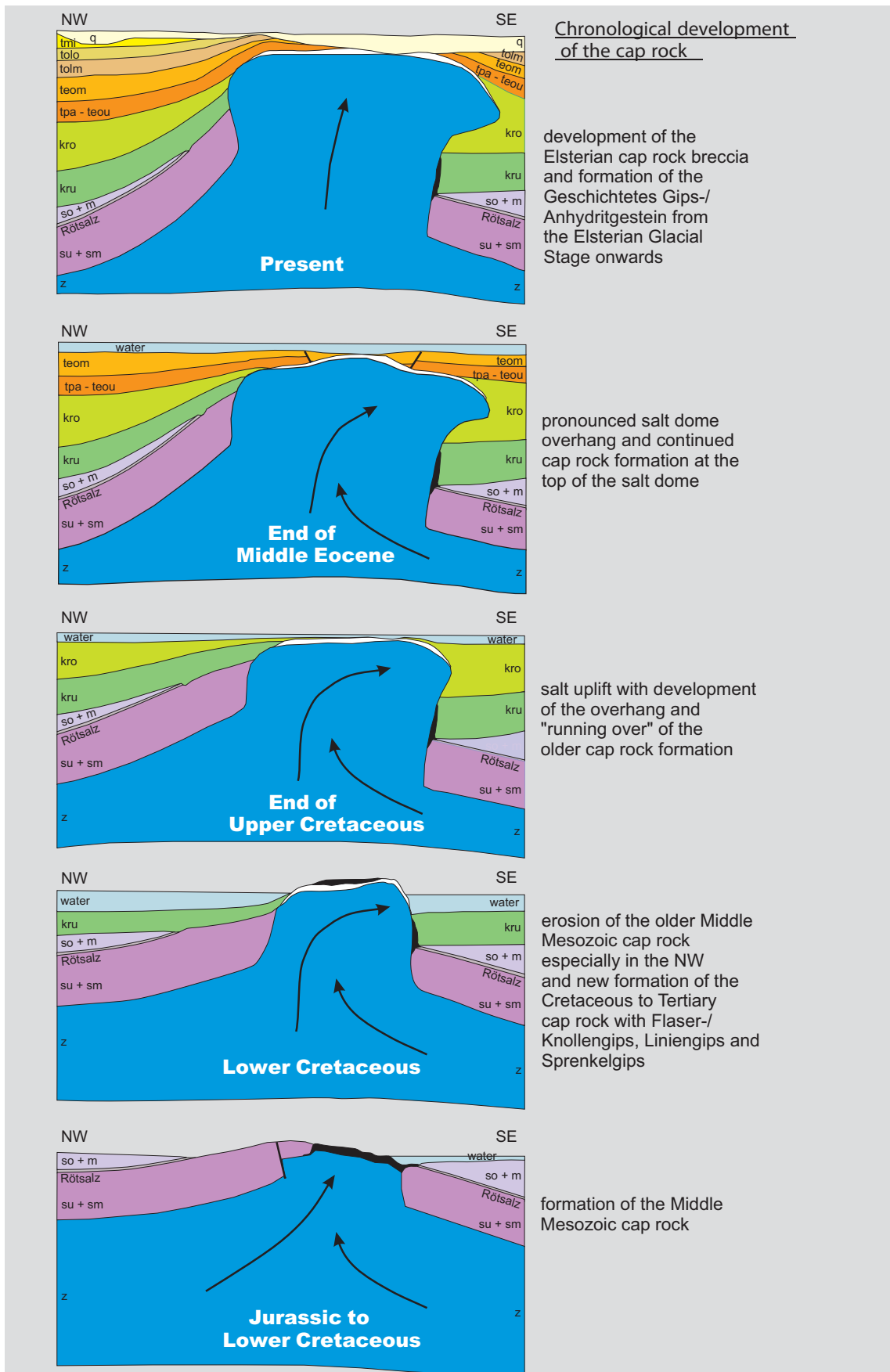
 q: Quaternary	 kro: Upper Cretaceous	 Cretaceous to Quaternary cap rock
 tmi: Miocene	 kru: Lower Cretaceous	 Middle Mesozoic cap rock
 tolo: Upper Oligocene	 so+m: Upper Bunter and Muschelkalk	 water
 tolm: Middle Oligocene	 Rötsalz	 preferential direction of the uplift of the Stassfurt rock salt (z2HS)
 teom: Middle Eocene	 su+sm: Lower and Middle Bunter	 assumed fault
 tpa-teou: Palaeocene to Lower Eocene	 z: Zechstein	thicknesses are schematic

Figure 10: Formation of the cap rock over time (see next page).



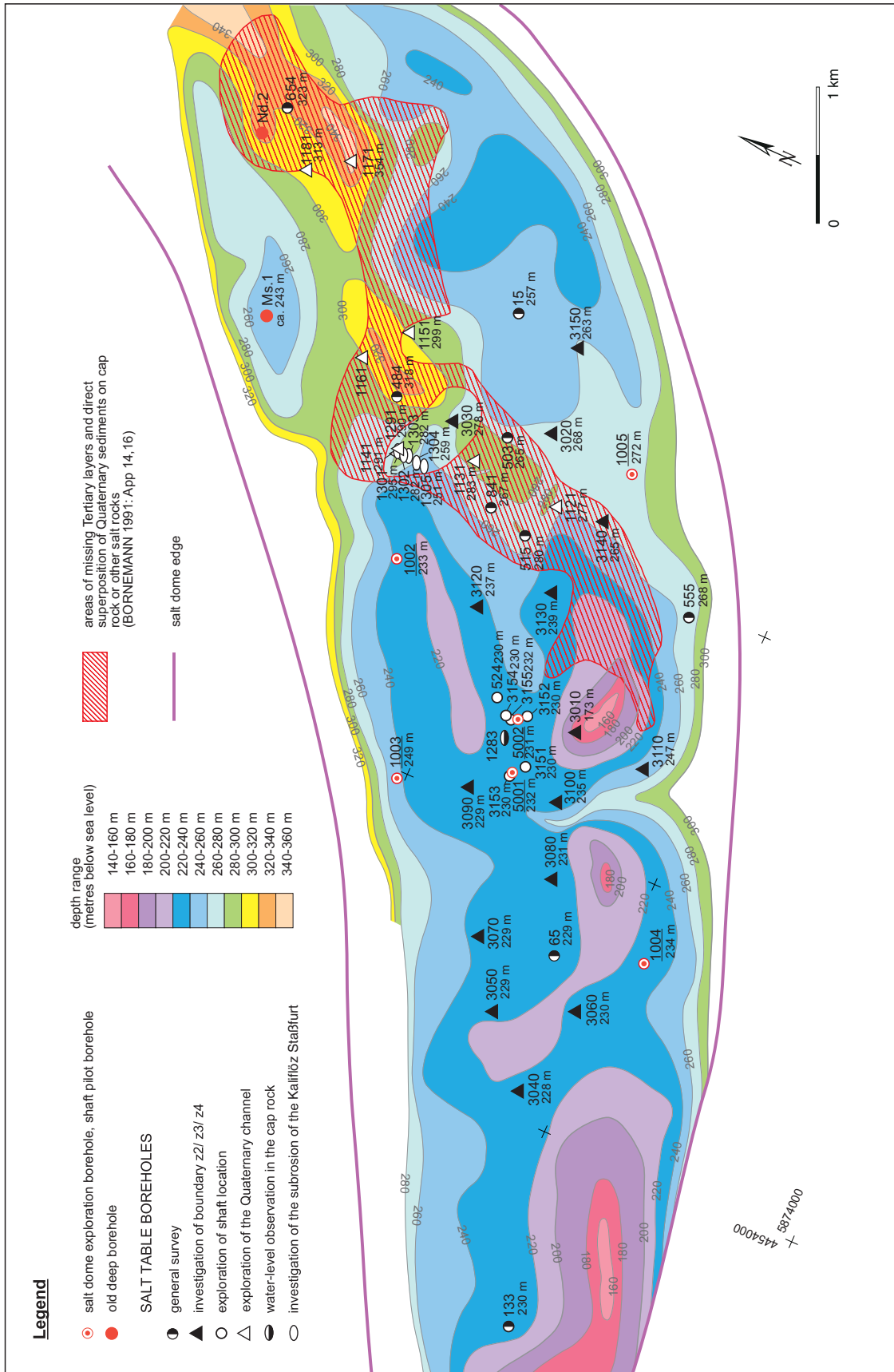


Figure 11: Contour map of the salt table of the Gorleben salt dome.

Although the conversion zones were continuously cored, no other mineral facies were observed. The transition from the halite facies to the kainite facies is very sharp. In contrast, the transition from the kainite facies to the brecciated carnallite extends over several metres. The individual facies zones are very inhomogeneous. This shows that the conversion process that took place in the seam was very complex and involved several recrystallization stages. This can be demonstrated using the conversion steps of the CaSO_4 component within the halite facies as an example: fine-grained polyhalite lies in interstices between crystalline salt, whilst occurrences of idiomorphic anhydrite blasts and idiomorphic gypsum blasts occur next to strongly corroded anhydrite crystals.

Evaporitic rocks from other stratigraphic zones, such as the sequence of Gebänderter Deckanhydrit (z2DA) to Grauer Salzton (z3GT) and Leine-Karbonat (z3LK) up to the Hauptanhydrit (z3HA), show the effect of groundwater at the salt table. This was confirmed in boreholes GoHy 1121, 1141, and 1291 (BORNEMANN & FISCHBECK 1988 a, b, d) on the basis of the fissure fillings found in these boreholes. In the upper parts close to the salt table, these fillings consist of clays of the overburden and halite, whilst the deeper-lying fissure fillings contain halite or sylvite and further down carnallite.

The findings described above show that the otherwise relatively flat salt table can have considerable subsidence relief where easily soluble salt minerals crop out at its surface (Fig. 11). Poorly soluble evaporites (Hauptanhydrit) at the salt table, however, are a frequent cause of cap rock thickening. The penetration depths of water from the overburden beneath the salt table mainly vary between some metres and 56 m. Only in regions where steeply dipping, overturned potash seams occur does the cap rock reach a maximum thickness of 170 m (see BORNEMANN (1991: Tables 2, 4).

3.3 *Composition and structure of the salt dome*

3.3.1 *Stratigraphy and petrography*

The stratigraphic sequence in the salt dome was penetrated and classified from the Hauptsalz of the Stassfurt-Folge (z2) to the Tonbrockensalz of the Aller-Folge (z4) by means of four salt dome exploration boreholes, 2 shaft pilot boreholes, and 44 salt table boreholes (BORNEMANN 1982; 1987 a, b; BORNEMANN & FISCHBECK 1987 a; 1988 a-n). The prior knowledge of the subdivision of the Zechstein sequence identified in the Gorleben salt dome was revised and refined (e.g. BORNEMANN 1991), which made the necessary detailed lithostratigraphic analysis within the stratigraphic sequence possible. Combined with the structural data, this allowed the exploration of the salt dome with as little damage to the safety barrier as possible.

Table 7 (see Appendices) contains a detailed summary of the Zechstein stratigraphic units with information on the lithology of the layers and their average thicknesses in the Gorleben salt dome. Considering the distance to the potash mining sites of Hanover and to the potash and salt mines in Saxony-Anhalt, the differences in stratigraphy are very minor. This indicates that sedimentation in the Zechstein Basin was relatively uniform.

The original thickness of the Stassfurt-Folge can only be estimated to be between 700 and 950 m because this sequence is intensely folded, marker horizons are missing, and the lower sequences (e.g. Basissalz of the Stassfurt-Folge) have not been penetrated. A true bedding thickness of approx. 320 m was calculated for the Leine-Folge. The thickness of the Aller-Folge is approx. 60 m. The thicknesses of the individual beds are given in Table 7 (see Appendices). These are reference values or average thicknesses. It should be kept in mind that these thicknesses can vary enormously depending on the halokinetic position.

The information on the structure and stratigraphy of the Zechstein sequence gained from surface exploration was largely confirmed when sinking the shafts and during underground exploration. Some details were refined or modified. Two different deformation regions in the salt dome can be discerned when describing the stratigraphy. One of them is the core of the salt dome represented by the beds of the Hauptsalz (z2HS). The second structural region consists of the younger sequences of the Leine-Folge and Aller-Folge (z3, z4) found up to the edge of the salt dome. The different movements of the two structural regions are compensated by the Kaliflöz Stassfurt on the interface of the Stassfurt-/Leine-Folge by extreme thinning or intense folding and accumulation. The general difference in the structure of the two regions is that the sedimentary character of the Hauptsalz is mostly destroyed due to the distance travelled during uplift. The Hauptsalz is largely homogenized and bears almost no gas or brine inclusions (see Chapter 3.3.4). In contrast to this, the younger beds of the Leine-Folge and Aller-Folge have not travelled far and are therefore only intensely folded. Their primary sedimentary features are mostly preserved.

The second geological report by BORNEMANN et al. (2002 a) provides an overview of the stratigraphy and structure of the salt dome by means of geological maps and cross sections. This report contains the general geological maps of the levels at 820 m, 840 m, 880 m, and 930 m as well as the geological vertical cross sections through both shafts and in the area of cross-cut 1 West and cross-cut 1 East (App. 4 and 5).

3.3.1.1 *Stassfurt-Folge (Zechstein 2)*

Due to the marked deformation during salt uplift, the evaporites of the Stassfurt-Folge now have the form of a halotectonic breccia. The original primary sedimentary (diagenetic) bedding sequence was destroyed and homogenized mainly by fracturing and re-healing during the uplift.

The rock now consists of several different components of different genesis (BORNEMANN et al. 2000):

- Halite crystal lumps:
With or without fine internal layering (inclusions of gas and brine), residues of primary crystal halite beds and banks
- Matrix:
Fine-crystalline to medium-crystalline halite with anhydritic impurities

The matrix composition is characterised by the following:

- Chevron crystals:
Clear crystals of 0.5 to 1 cm in size, deposited at residual anhydrite bands (PAPE et al. 2002; PAPE 1993)
- Residual anhydrite bands:
Clusters, nodules and streaks, residues of primary anhydrite bands
- Halite crystals:
0.5 to 2 cm, clear, broken remainders of primary halite crystal lumps
- Halite crystals:
Some millimetres to 2 cm, secondary halite from healing processes.

These findings apply mainly to the Hauptsalz (z2HS), which was particularly mobile during the formation of the salt dome and therefore subjected to high stresses.

The rock salts of the Stassfurt-Folge are divided into three stratigraphic units:

- The **Basissalz (z2BS)**
- The **Hauptsalz (z2HS)**
- The **Hangendsalz (z2HG)**

To date, only the Hauptsalz and Hangendsalz have been penetrated by drilling and exposed in the exploration mine. It is possible that in cross-cut 1 West some amounts of Basissalz (z2BS) are folded into the Knäuelsalz because very low bromide values of 25 to 52 µg/g halite were detected in some zones of borehole 02YER02 RB032 (SCHRAMM & BORNEMANN 2004: App. 4).

The **Hauptsalz (z2HS)** can be subdivided into three units based on the amount and character of the sulphate inclusions.

The oldest section is called the **Knäuelsalz (z2HS1)**. It consists of dark-grey to black medium-crystalline to coarse-crystalline rock salt, which contains a very large amount of impurities in the form of dispersed anhydrite as well as irregularly scattered anhydrite nodules and clusters. Local clusters of angular crystal halite lumps sized 1 to 12 cm and rounded rock salt eyes also occur. The halite crystal lumps are mainly clear but may also contain some fine internal layering formed by lines of fine brine and gas bubbles. Bedding is very difficult to identify in the Knäuelsalz as there are no major layers of pure halite and the anhydritic impurities only rarely reflect the primary sedimentary bedding due to the strong deformation. No minerals other than anhydrite occur in the halite of the Knäuelsalz.

The extreme deformation and homogenization explain why the Knäuelsalz contains no significant amounts of brine or gas. Large sections of this stratigraphic unit occur in the salt dome exploration boreholes Go 1002 (254 to 387 m) and Go 1005 (296 to 347 m) as well as in cross-cuts 1 West and 1 East at Exploration Area 1 (EB 1).

There is a gradual transition over a few metres from the Knäuelsalz into the overlying **Streifensalz (z2HS2)**. The Streifensalz consists of pure bands and stripes of up to 0.5 m thickness, regularly interbedded with halite banks of varying thickness containing impurities in the form of anhydrite shreds and streaks. Anhydrite clusters and nodules occur only to a lesser extent. The density of the anhydrite flakes and residual anhydrite bands also varies widely. The interbedding is also discernable by the change in colour of the banks and bands from dark-grey to light-grey. Crystal halite lumps occur more frequently towards the top of the sequence.

With the exception of anhydrite, the Streifensalz sequence usually does not contain any other minerals alongside halite. Exceptions occur, for instance, in strongly deformed zones with interbeds of a dual-layer, isoclinally folded potash seam (e.g. salt dome exploration borehole Go 1005). In this borehole, red carnallite clusters, sized up to approx. 1 cm, were observed in the upper Streifensalz located mainly in interstices of the crystal halite lumps. The same applies to the overlying Kristallbrockensalz. The carnallitic inclusions are evidence for highly concentrated solution fronts, which presumably entered the

Hangendsalz and Kristallbrockensalz as a result of the penetration of the neighbouring sequences by the Kaliflöz Stassfurt.

In the northern main drift (northern flank) of EB 1, a pinstriped Liniensalz-like facies occurs in the uppermost Streifensalz. This zone has an average thickness normal to bedding of approx. 35 m and is interstratified with pure salt banks that are irregularly spaced by 0.5 to 2 m and consist of fine-crystalline to medium-crystalline, rarely coarse-crystalline halite. These beds are largely free of anhydritic impurities, have thicknesses normal to the bedding of 20 to 30 cm, and have an unchanged lateral extension of several hundred metres.

A genetic interpretation of the pure salt banks based upon bromide analysis and the structural characteristics of the Streifensalz is at present not possible. The pure salt banks may either have a primary sedimentary origin or may have been the result of halotectonics. In the latter case, the pure salt banks would represent shear zones healed with secondary halite.

Larger exposures of the Streifensalz have been encountered in cross-cuts 1 West and 1 East in EB 1 as well as in salt dome exploration boreholes Go 1002 (387 to 531 m), Go 1003 (272 to 313 m), Go 1004 (259 to 477 m), and Go 1005 (347 to 389 m and 457 to 528 m).

The **Kristallbrockensalz (z2HS3)** is the youngest unit in the Hauptsalz and is characterised by an abundance of crystal halite lumps and eyes, which become more frequent from base to top (Fig. 12). The crystal lumps are very pure, display a fine internal stratigraphy of strings of small brine inclusions or anhydrite crystals, and their size can exceed 10 cm. They are no longer in their original sedimentary position but rotated, and often float with no particular orientation in a fine-crystalline to medium-crystalline halite matrix, contaminated by scattered anhydrite and occasional anhydrite streaks and bands, which decrease from base to top. Approx. 10 m below the top of the unit, the first polyhalite impurities are observed in addition to the anhydrite. The presence of polyhalite is often accompanied by a light-orange coloration of the halite. The polyhalite concentration increases rapidly upwards and replaces the anhydrite.

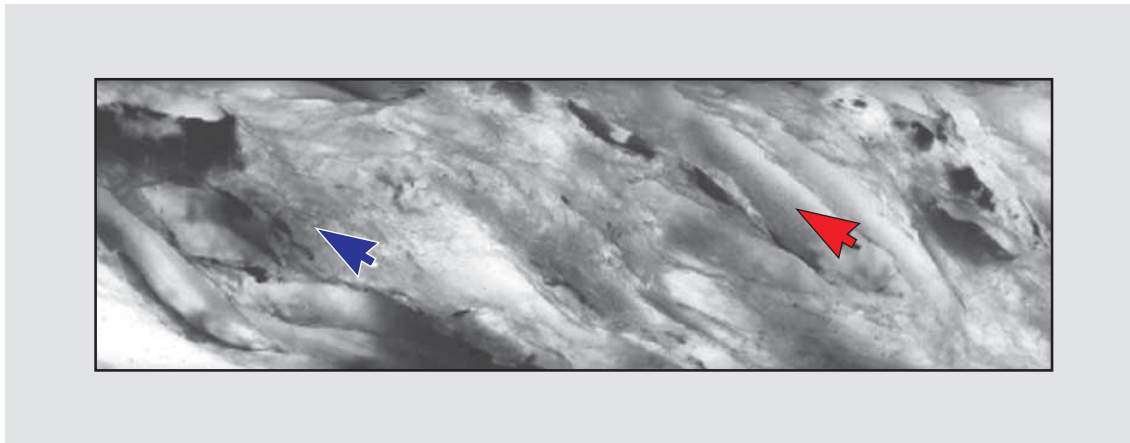


Figure 12: Core containing typical Kristallbrockensalz. The red arrow indicates crystal lumps, the blue arrow indicates matrix. The black areas represent anhydrite impurities. Height = approx. 5 cm.

In parts of the salt dome with less deformation, the Kristallbrockensalz resembles the Liniensalz (z3LS) and consists of slightly fractured halite crystal bands of varying thickness (some centimetres to decimetres), interstratified at regular intervals of 20 to 30 cm with anhydritic bands some millimetres thick. Within the Kristallbrockensalz, several of the underground exploration boreholes in EB 1 each encountered a single, dense, grey anhydrite lump at as yet undetermined stratigraphic positions. These anhydrite lumps must originate from a larger anhydrite bank broken up by halotectonics. This bank might be used as a marker horizon for stratigraphic classification in further investigations.

The average thickness of the Kristallbrockensalz is approx. 60 m. The main exposures are in the salt dome exploration boreholes Go 1002 (531 to 603 m and 1845 to 2000 m), Go 1003 (313 to 442 m, 515 to 685 m, and 736 to 784 m), Go 1004 (477 to 516 m), Go 1005 (389 to 414 m) as well as in the underground exploration boreholes 02YER02 RB032, 02YEQ01 RB427, 02YEQ01 RB118, 02YEQ01 RB119, 02YER20 RB254, and 02YER20 RB488 drilled on the northern flank of the main anticline in EB 1.

The relatively abrupt break-off of the crystal halite lumps and eyes marks the boundary to the **Hangendsalz (z2HG)**. The thickness of the Hangendsalz ranges from a few decimetres to 10 m maximum depending on its halokinetic position. The Hangendsalz is grey, with a light-grey, light-orange to brownish colour in transmitted light, and has a mainly fine-crystalline and in some sections medium-crystalline texture. There are no crystal halite lumps, round crystal halite eyes with a thickness of up to 3 cm do occur locally.

A typical feature of the Hangendsalz is the continuous, closely spaced, regular sequence of pure salt bands (approx. 2 to 10 cm thick) alternating with intermittent, dark-grey, anhydritic/polyhalitic bands of flakes with a thickness of one to a few centimetres. Powder samples taken in the upper part of the sequence contained scattered kieserite flakes. In

addition to the normally grey type of Hangendsalz, exploration borehole Go 1004 also penetrated a grey-brown sequence from 516 to 549 m. Orange to yellow-orange coloured bands are revealed in transmitted light, which are caused by bands of flakes enriched with scattered polyhalite.

The boundary between the Hangendsalz and the **Kieseritische Übergangsschichten (z2UE)** is defined by the first continuous kieserite band. The kieserite bands consist of grey, fine-crystalline halite with irregular interbedding of dark-grey to black anhydritic stripes and bands. The halite is only slightly translucent in transmitted light due to the kieserite content. The amount of white to light-grey kieserite increases rapidly towards the Kaliflöz Stassfurt. There is also a minor amount of polyhalite. In some exposures, the Kieseritische Übergangsschichten are interstratified with secondary sylvite occurring as large milky-opaque crystals, or also with secondary red and white carnallite, which makes it difficult to determine the boundary to the overlying Kaliflöz Stassfurt.

In some exposures, langbeinite was identified in clusters and bands. Boreholes Go 1002 and 1003 encountered kieserite pseudomorphs of idiomorphic langbeinite tetrahedra up to 2 cm in size. The thickness of the Kieseritische Übergangsschichten varies from 0 to 2.5 m depending on the halotectonic position.

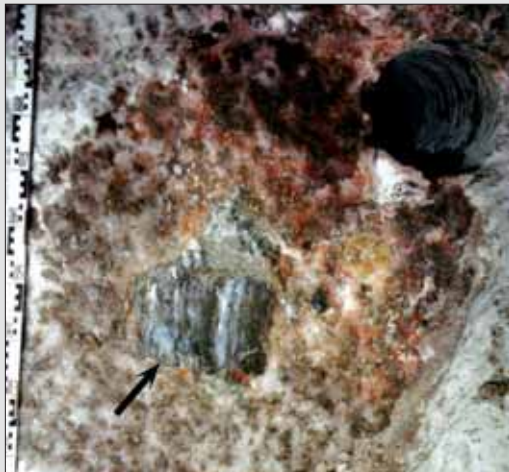
The boundary to the **Kaliflöz Stassfurt (z2SF)** is usually distinct and is defined by a marked increase in carnallite. In all salt dome exploration boreholes and salt table boreholes, the potash seam is present as a brecciated carnallite facies. This also applies to the underground exploration with the exception of localised special facies in the potash seam updoming between the shafts. The special facies will be described in more detail further below.

The potash seam consists of fractured beds and clusters of white to dark-grey kieserite and very small amounts of anhydrite. Fractured, light-grey, fine-crystalline halite banks float in a matrix of red, violet and white or clear carnallite. In some areas, the carnallite is rich in gas, forming crackling carnallite. The sedimentary bedding is only identifiable in a few thicker halite banks due to intense deformation.

In almost all drilled sections of the Kaliflöz Stassfurt, a fine-crystalline anhydrite bank of a thickness of approx. 5 to 10 cm or its residues were found at the base of the seam. Its precise stratigraphic position in the seam is impossible to determine due to the intense deformation. Exploration borehole Go 1003 encountered anhydrite pseudomorphs of gypsum in the anhydrite bank. Consequently, it can be assumed that it was deposited as gypsum and is of primary sedimentary origin.

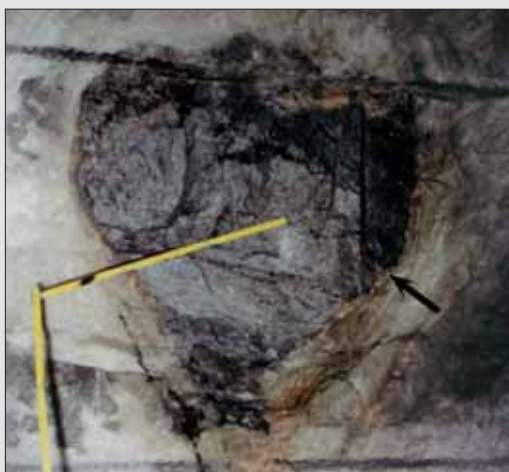
Due to the deformation, the potash seam can be divided into two sub-units.

The lower unit consists of a more or less distinctive alternating sequence of heavily fractured carnallite and halite banks where the sedimentary features of the bedding can still be recognised despite the strong degree of deformation. In the upper part of the seam (usually for several metres up to the overlying roof salt), the carnallite and halite beds have been turned into a homogeneous mixture as a result of a more intense deformation. The halite banks are completely broken into round nodules of a thickness of some centimetres to decimetres, floating with no identifiable orientation in a carnallite matrix. In some areas, the intense deformation has also incorporated fragments of the overlying beds (Gebänderter Deckanhydrit, Grauer Salzton and Hauptanhydrit) within this sub-unit. Thus, the upper part of the potash seam usually contains granules of clay and to a lesser extent granules of anhydrite from the overlying beds (Fig. 13).



Ventilation drift,
drift location 58.5 m,
roof.

(Photograph by Schubert, DBE)



Eastern access to workshops,
drift location 37 m,

(Photograph by Reiß, DBE)

Figure 13: Isolated and rotated blocks of Hauptanhydrit (arrows), surrounded by thinned Kaliflöz Stassfurt in a brecciated carnallite facies.

The thickness of the Kaliflöz Stassfurt varies widely with an average between 15 and 30 m. Depending on the tectonic position, it can be either completely pinched-off or attain a thickness of more than 70 m in case of intense folding.

Metamorphosis stages

Various stages of impoverishment or alteration of the potash seam can be identified in the core material. The normal facies for the Kaliflöz Stassfurt is brecciated carnallite (Trümmercarnallit). Increasing impoverishment (1. → 3.) is indicated by the following features:

1. Brecciated carnallite interspersed with sylvite, halite and kieserite
2. Sylvinite with halite and secondary anhydrite
3. Secondary anhydrite with halite

The Zechstein 2 updoming and the accumulation of the Kaliflöz Stassfurt are the main halokinetic structural characteristics in the infrastructure zone between shafts 1 and 2. They were identified by the underground exploration boreholes 02YEA04 RB021, 02YEA04 RB022, 02YEA04 RB029, 02YEA24 RB030, 01YEF20 RB059, 01YEF20 RB217, 02YEA12 RB218, as well as the geotechnical boreholes 02YEA06 RB170 and 02YEA06 RB171. Due to the formation of the Zechstein 2 updoming, the Kaliflöz Stassfurt has suffered impoverishment on the northern and eastern flanks of the updoming because of the effects of migrating brines from the pinched-off Hauptanhydrit (Fig. 14).

The transition from the Kaliflöz Stassfurt to the **Decksteinsalz (z2DS)** is distinct. The Decksteinsalz usually consists of red-brown or light-grey, mainly fine-crystalline halite with a thickness of 0.2 to 0.5 m. The bedding is characterised by colourless halite bands and dark-grey to black anhydrite layers some millimetres thick. The Decksteinsalz was absent in many of the boreholes where the Kaliflöz Stassfurt was directly overlain by the Gebänderter Deckanhydrit.

The **Gebänderter Deckanhydrit (z2DA)** has a thickness normal to bedding of approx. 1.5 m and is subdivided into the Unterer and Oberer Gebänderter Deckanhydrit. The Unterer Gebänderter Deckanhydrit consists of dark-grey to light-grey anhydrite rock with interbedded claystone and kieserite, which cause the banded structure. There are also some areas of mostly red-brown halite flakes and, to a lesser extent, isolated carnallite clusters. The Oberer Gebänderter Deckanhydrit consists of an alternation of grey anhydrite banks and black claystone banks with a thickness of up to 10 cm. The different banks display distinct boundaries. In some parts, the rock is streaked with fine fissures, which are mainly healed with red carnallite.

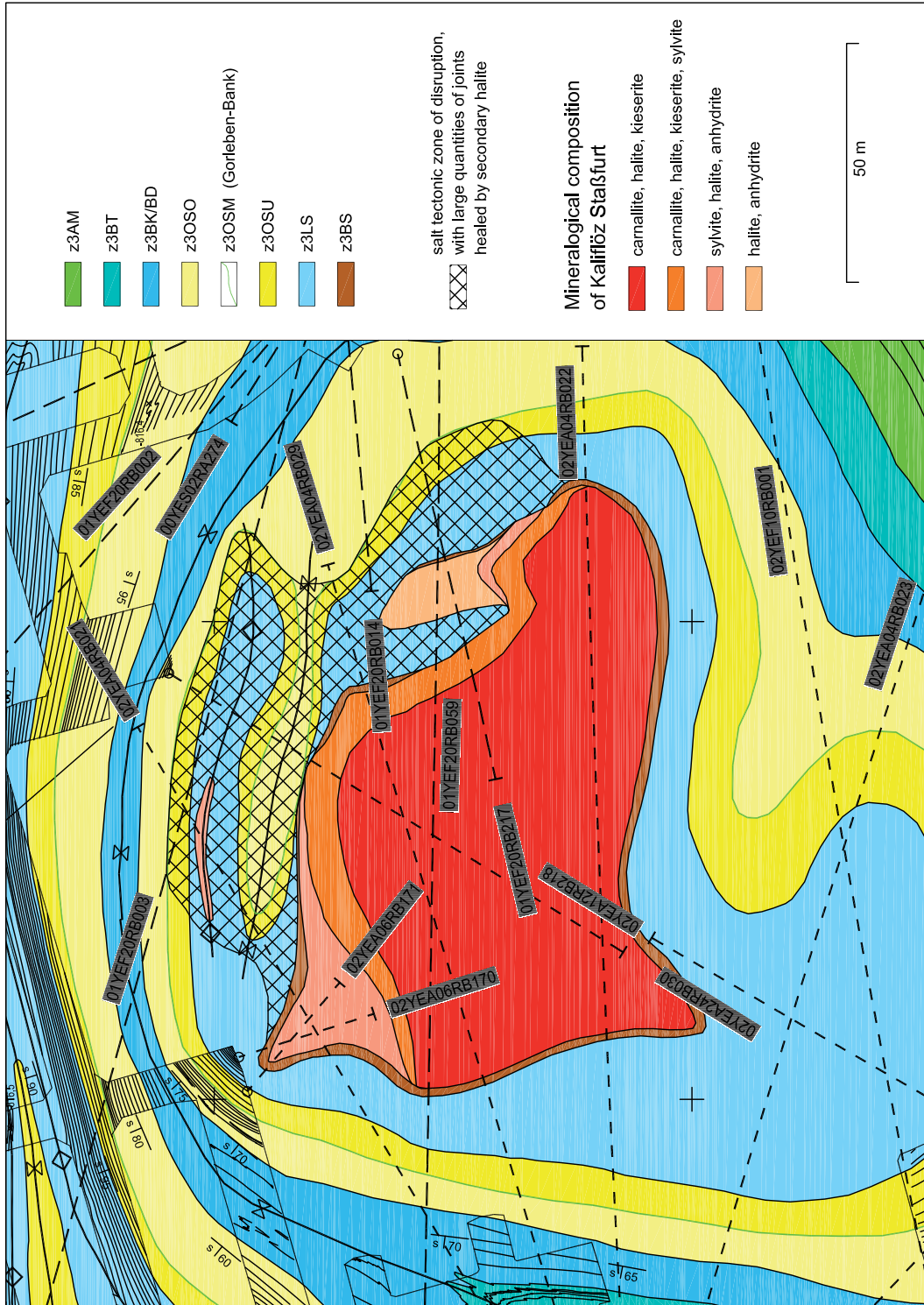


Figure 14: Metamorphosis stages of the Kalifjöz Stassfurt in the area of the upcoming between the shafts on the 840 m-level.

3.3.1.2 *Leine-Folge (Zechstein 3)*

A sharp change in lithology marks the boundary between the Gebänderter Deckanhydrit and the Grauer Salzton. The **Grauer Salzton (z3GT)** forms the base of the Leine-Folge. It can be subdivided into the Unterer and Oberer Grauer Salzton (z3GTU, z3GTO). In some parts, the sequence is strongly jointed. The joints appear mainly in the form of feather joints healed with fibrous halite or fibrous carnallite.

The **Unterer Grauer Salzton (z3GTU)** consists of homogeneous black claystone with irregular inclusions of anhydrite pseudomorphs of gypsum, which can aggregate to form structures resembling fir trees with a maximum length of 10 cm. The average anhydrite concentration is 55 wt.%. The other minerals are hydrotalcite, chlorite and quartz. To a lesser extent, magnesite, halite, illite and kaolinite are also present.

The **Oberer Grauer Salzton (z3GTO)** is characterised by black, thinly laminated (1 mm) and friable claystone. The anhydrite concentration is lower than in the Unterer Grauer Salzton and the sediment is of a finer grain. The main mineral components are illite and quartz. The amounts of halite and kaolinite are lower. The magnesite content increases towards the roof.

The Grauer Salzton was found in underground exploration boreholes and as relicts in the ventilation drift and in cross-cut 1 West. Subdivision into Unterer and Oberer Grauer Salzton was only possible in borehole 02YER02 RB033. The Grauer Salzton has an almost constant thickness of approx. 2.5 m in all exposures unaffected by halotectonics.

The boundary to the **Leine-Karbonat (z3LK)** is marked by the sharp change from black claystone to beige-grey anhydritic magnesite rock. The Leine-Karbonat consists of light-grey to beige-grey fine-crystalline, dense, rarely bedded hydrotalcite-bearing anhydritic magnesite rock which only locally contains bands of light-grey anhydrite shreds and thin anhydrite layers. Characteristic features particularly in the upper part of this sequence are the ooids and oncoids of max. 2 mm in size, which in some areas form rock and which indicate shallow marine conditions at the place of their deposition. In addition to the ooids, fossils of smooth-shelled ostracods, schizodont mussels and fusulina foraminifera were found. The ooids are mainly anhydritized. This reveals that the rock has been affected by numerous recrystallization processes.

The Leine-Karbonat has an almost constant thickness of approx. 1.5 m in all exposures that are not affected by halotectonics. Analyses of the boreholes and underground exposures generally reveal that the sequence from Gebänderter Deckanhydrit to Leine-Karbonat only occurs in the presence of Hauptanhydrit.

A sharp boundary separates the **Hauptanhydrit (z3HA)** from the Leine-Karbonat. It consists of blue-grey anhydrite changing to grey anhydrite towards the upper boundary, with interstratified beige-grey magnesitic flasers, streaks and lamellae, which represent structures of algae. The carbonate content, i.e. the proportion of algal structures, decreases upwards. This finding is supported by the gamma-ray log (slight decrease upwards) and by the density log (slight increase upwards) (Fig. 15).

The thickness of the Hauptanhydrit is generally between 40 and 80 m (Fig. 16).

KOSMAHL (1969) divides the Hauptanhydrit into 13 zones based on the magnesite inclusions, which reflect the sedimentary to diagenetically formed texture. This subdivision is also largely recognisable in the Gorleben salt dome. However, Zones 12 and 13 (black clay bank and anhydrite shell) were not recognised in the Hauptanhydrit sections penetrated by the salt dome exploration boreholes and the underground exploration. It is assumed that they were sheared off during diapirism. Cores from salt table borehole GoHy 3155, which penetrated a gypsified Hauptanhydrit block in the cap rock, revealed the presence of the black clay bank and finely laminated anhydrite shell in the block and thus confirmed that these zones are also present in the salt dome.

The **Lamellenanhydrit 1 (z3HA1)** consists of a dark-grey to blue-grey fine-crystalline anhydrite rock with numerous anhydrite pseudomorphs of gypsum with a size of up to 1 cm. The lower part of the sequence consists of several beige-grey magnesitic algal layers some millimetres thick, the frequency of which rapidly decreases upwards. They are replaced by magnesitic algal shreds some centimetres in size, lined up in the bedding. The laminate anhydrite has a thickness of approx. 0.5 to 1 m.

The **Flocken- und Flaseranhydrit (z3HA2)** is characterised by beige-grey algal carbonate shreds, flakes and flasers. The bedding features bands of magnesite shreds of up to 2 cm in size. These magnesite shreds have sharp boundaries in the upper part of the sequence and angular frayed boundaries in the lower part of the sequence. Some scattered layers of algal carbonate with a thickness of some millimetres occur in the upper part. The Flocken- und Flaseranhydrit has a thickness of approx. 1.5 to 3 m.

The **Lamellenanhydrit 2 (z3HA3)** is a bed of beige-grey algal carbonate consisting of magnesitic lamellae some millimetres thick. The distance between the lamellae decreases from bottom to top, and they terminate at the top with a sharp boundary. The thickness of this unit is a few cm to approx. 10 cm.

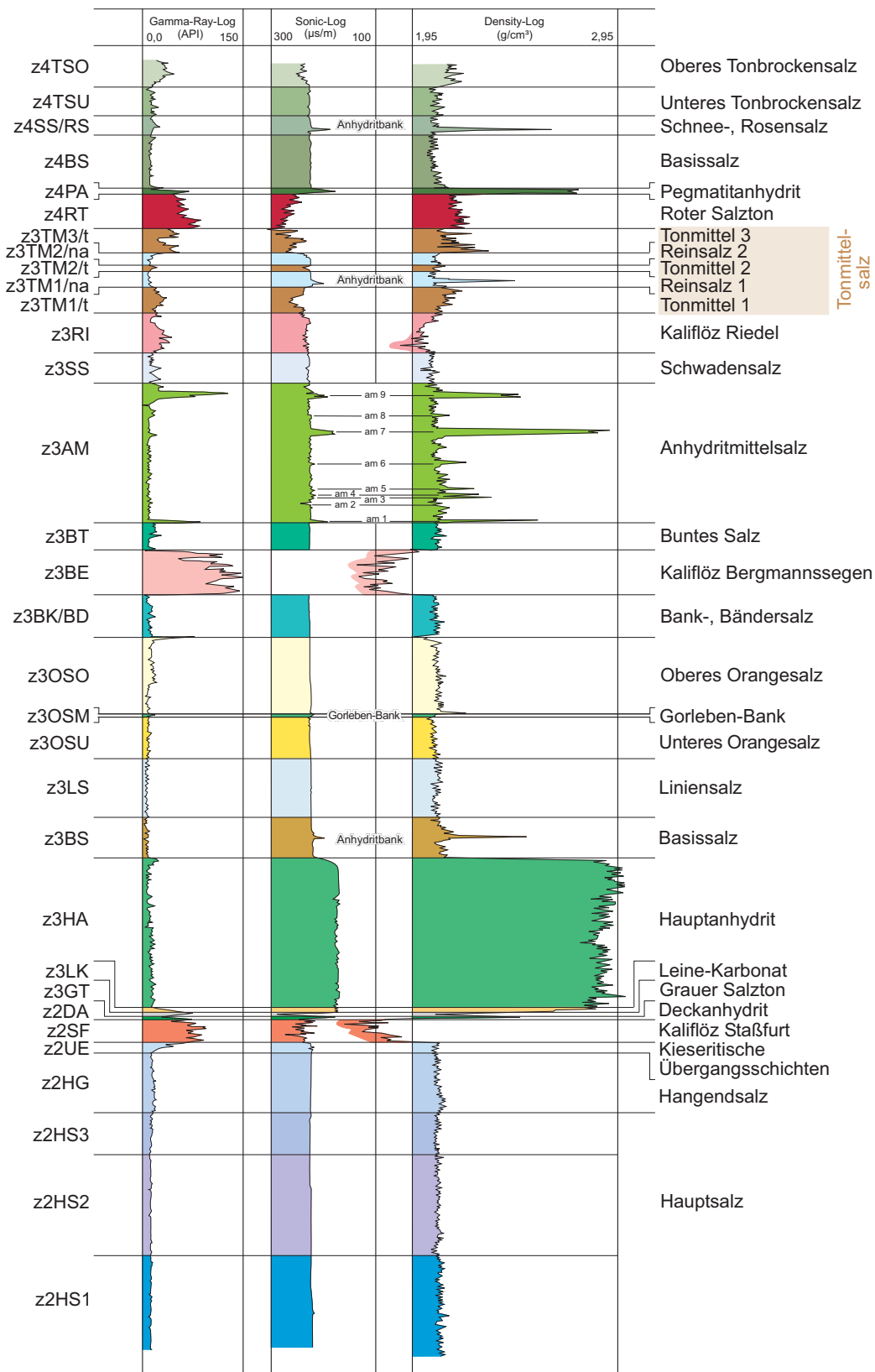


Figure 15: Synthetic profile of borehole logs within the beds of the Stassfurt-Folge, Leine-Folge und Aller-Folge.

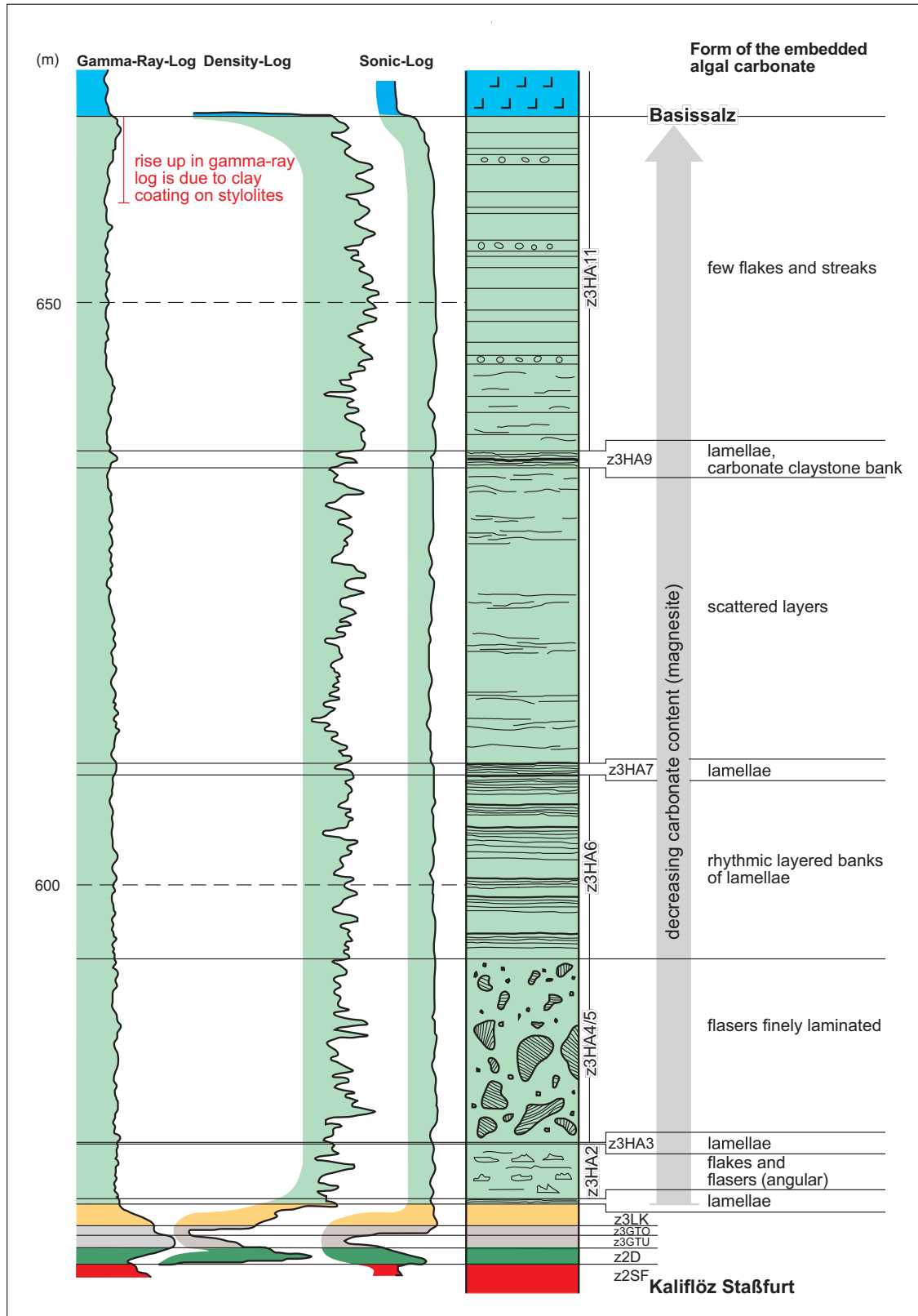


Figure 16: Stratigraphy and carbonate inclusions in the Hauptanhydrit illustrated by the Hauptanhydrit section in borehole Go 1005.

The **Flaseranhydrit (z3HA4)** is dominated by beige-grey magnesitic blobs of up to 10 cm and more in size with tight internal lamination which resemble stromatolites. They float mainly without orientation in a blue-grey anhydrite matrix, which complicates identification of the Hauptanhydrit bedding in this section. The thickness of this unit is approx. 1.5 to 3 m.

The sedimentary texture of the **Schlierenanhydrit (z3HA5)** is similar to that of the Flaseranhydrit. However, the magnesitic blobs are only up to a few centimetres in size. The bedding is again barely recognisable. Differentiating between Flaseranhydrit and Schlierenanhydrit is often impossible if no major magnesitic blobs are exposed in the Flaseranhydrit. The two beds are therefore often classified conjointly as Flaser- und Schlierenanhydrit (z3HA4/5). The thickness of the Flaser- und Schlierenanhydrit is approx. 6 to 11 m.

The fine-crystalline grey-blue **Bänderanhydrit (z3HA6)** is interspersed with millimetre-sized anhydrite blasts and lath-shaped anhydrite crystals. In this sequence, a continuous characteristic stratigraphy resumes in the form of rhythmic sedimentation, which is repeated several times. The cycles have differing thickness. Individual cycles start at the base with pure anhydrite containing a few magnesitic shreds. Further upwards magnesitic lamellae (algal carbonate) gradually begin to occur, becoming denser towards the top (spacing of some millimetres). These finish with a sharp upper boundary, marking the start of the next cycle. The Bänderanhydrit is approx. 5 to 8 m thick.

The uppermost lamella layer of the last sedimentary cycle in the upper part of the Bänderanhydrit is called the **Lamellenanhydrit 3 (z3HA7)**. It consists entirely of condensed algal carbonate lamellae. It has a thickness of up to approx. 0.1 m.

The overlying **Bündelanhydrit (z3HA8)** is characterised by the almost complete absence of macroscopic carbonates except for some scattered magnesite lamellae and shreds in the lowermost 2 m of the sequence. The Bündelanhydrit can be distinguished by its dark-grey anhydrite strings with a thickness of some millimetres to some centimetres, which often merge into 5 to 10 cm-thick bundles. The strings in the bundles are slightly branched and interlinked. The distance between the bundles varies widely and is usually in the order of metres. The total thickness of the Bündelanhydrit also varies widely. Nonetheless, it is found in all exposures. The thickness of this unit is approx. 10 to 34 m.

In the overlying **Flaser- und Bänderanhydrit (z3HA9)** magnesitic algal carbonate structures start anew. They are concentrated in an approx. 5 cm-thick dark-grey to black argillaceous carbonate bank, which contains centimetre-sized anhydrite pseudomorphs of gypsum as well as ooids. The carbonate bank is enclosed in anhydrite rock, which contains large to abundant amounts of algal carbonate lamellae. The Flaser- und Bänderanhydrit is not present in all exposures. It has a thickness of up to approx. 11 m.

Like the Bündelanhydrit (z3HA8), the overlying **Maseranhydrit (z3HA10)** is characterised by the absence of macroscopic carbonate inclusions. It consists of light-grey to blue-grey fine-crystalline to cryptocrystalline, structureless, almost unlayered anhydrite. A characteristic is the absence of almost any bedding features. The Maseranhydrit is not present in all exposures. The thickness of this unit is up to 19 m.

The **Bänderanhydrit (z3HA11)** is the uppermost sequence of the Hauptanhydrit in the drifts within the Gorleben salt dome and has a mineralogical composition and structure that completely differs from the other beds of the Hauptanhydrit. It is almost impossible to identify any macroscopic carbonate inclusions. According to BÄUERLE (1998), the Bänderanhydrit consists of an alternating sequence of anhydrite breccias, intercalated turbidites and the eponymous bedding-parallel bands, which display a cyclic structure with graded bedding. The alternating sequence indicates that the surface of the Hauptanhydrit showed relief before the deposition of the younger halitic beds of the Leine-Folge.

Another characteristic of this zone is the abundance of stylolites, which are only rarely found in the other layers of the Hauptanhydrit. In some areas (e.g. exploration borehole Go 1005 from 1318.2 to 1324.0 m), the formation of the stylolites caused extreme reductions in thickness with almost complete destruction of the sedimentary structure. These are vertical stylolites, which were formed very early (during the Zechstein period) due to the petrostatic pressure of the overlying halitic strata. Mass calculations based on the amplitudes of the stylolites indicate a dissolution of 19 to 26 % of the sulphate. According to BÄUERLE (1998), the exclusive occurrence of stylolites in the Bänderanhydrit indicates that the lower layers of the Hauptanhydrit had already been converted into anhydrite whilst the Bänderanhydrit was still in the form of gypsum. Only in this zone did the petrostatic pressure built up by high sedimentation rates of the overlying evaporite beds cause the formation of stylolites. The thickness of this unit is up to 19 m.

Figure 17 shows normally bedded sequences of Grauer Salzton to Hauptanhydrit penetrated by boreholes in the salt dome, using the Grauer Salzton as the reference horizon. With the exception of the disturbed sections in exploration borehole Go 1003, there are only minor variations in thickness in the Grauer Salzton and the Leine-Karbonat. The Hauptanhydrit, however, displays a variation in thickness of a maximum of 20 to 30 m over short distances due to primary sedimentary conditions. This is due to the absence or varying thickness of the sequences Bündelanhydrit (z3HA8) to Bänderanhydrit (z3HA11). The thickness variations in each of the units in the lower part of the Hauptanhydrit up to the Lamellenanhydrit 3 (z3HA7) are also large but the total thickness of the zones up to Lamellenanhydrit 3 only varies by approx. 7 m between exposures.

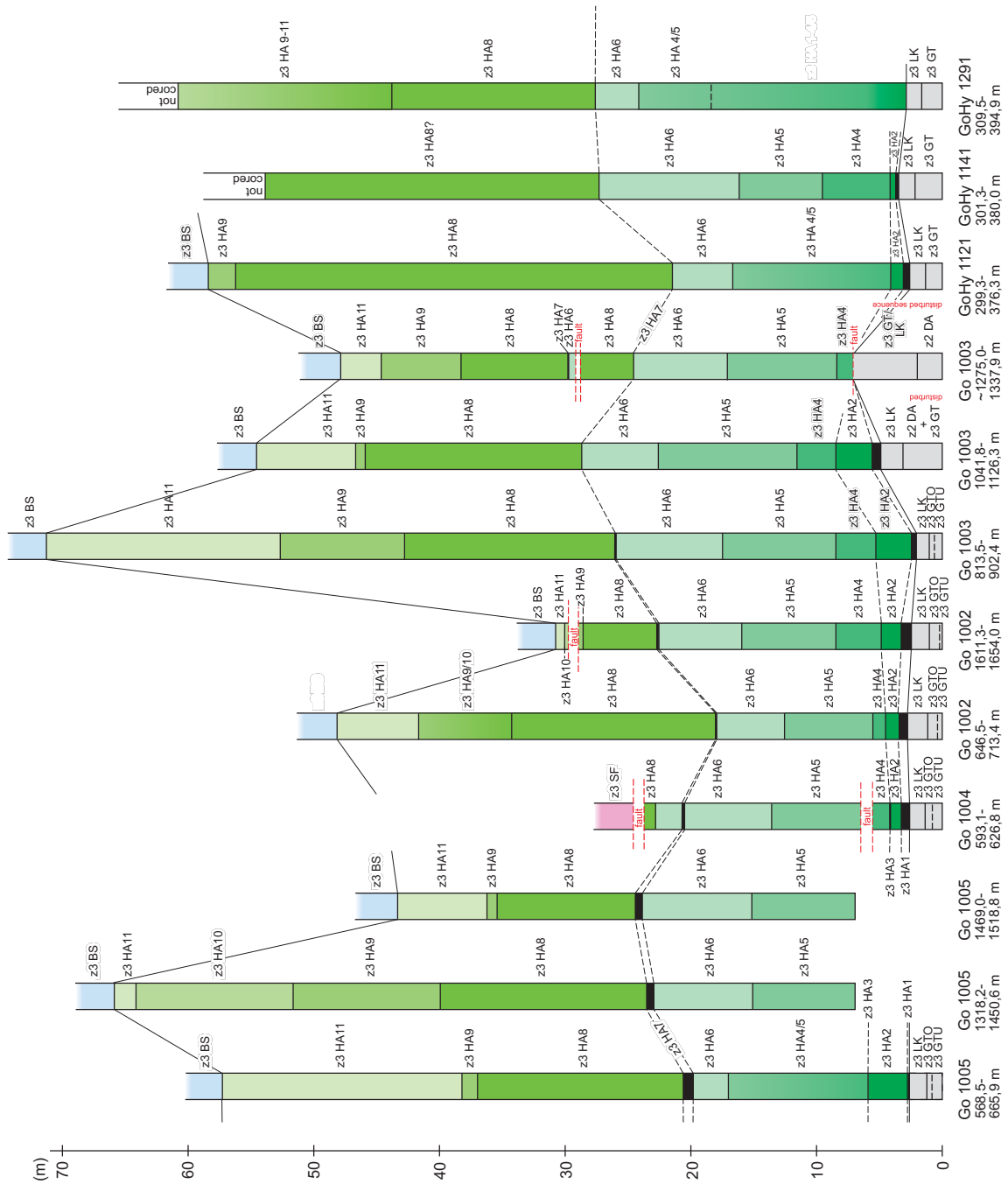


Figure 17: Stratigraphic sequence and true thickness of the layers of the Hauptanhydrit - comparison of several exposures.

The observed variations in thickness and absence of beds in the upper parts of the Hauptanhydrit, which led to extreme changes in thickness over short distances, are similar to those described by HEMMANN (1968) in the Sub-Hercynian Basin (see also BEHLAU & MINGERZAHN 2001). The exposures in mine workings in the Sub-Hercynian Basin reveal that these variations in thickness are caused by cliff formation in the Hauptanhydrit. FULDA (1929) coined the term “anhydrite cliff” for anhydrite protrusions of this kind. Corresponding sedimentary textures found during the exploration and analyses of the Hauptanhydrit facies confirmed the sedimentary origin of these formations in the Gorleben salt dome (BÄUERLE et al. 2000). This phenomenon had previously only been encountered at the edges of the Zechstein Basin. The exposures in the Gorleben salt dome and in the Harsefeld salt dome reveal, however, that Hauptanhydrit cliffs also formed in the central part of the Zechstein Basin. This means that similar sedimentary conditions must have existed throughout the Zechstein Basin at the time the Hauptanhydrit was deposited.

A notable feature is the presence of small clusters and tubules filled with red, clear carnallite, which permeate the lower and middle part of the Hauptanhydrit like small veins. This carnallite impregnation is not present in the upper beds of the Hauptanhydrit. Some areas of the Hauptanhydrit display intense shearing. The individual fissures are primarily healed with carnallite, sylvite or halite. Borates also occur as fissure fillings, though to a lesser extent.

In addition to numerous fissures, the Hauptanhydrit is also cut by larger faults. These are mostly normal faults and cause gaps in the sequence of strata of a few metres to 10 metres. However, a reverse fault (overthrusting) was also encountered in the deeper anhydrite sequence penetrated by borehole Go 1003. This reverse fault caused a doubling of the bedding of approx. 10 to 15 m. All fault zones have widths ranging from decimetres to a few metres and are healed with secondary carnallite or by the intruding Kaliflöz Stassfurt. These fillings are often highly impregnated with gas (crackling carnallite). In addition to carnallite, these fault zones also contain in some areas blocks of Grauer Salzton and Leine-Karbonat, which were dragged in during faulting.

In addition to the rupturing deformation of the Hauptanhydrit described above, underground exploration revealed that more intense deformation also led to the fracturing of the Hauptanhydrit into separate, sometimes rotated blocks of varying size which are lined up in the bedding to form layers resembling rows of cherry stones (boudinage). Every block is enveloped by the surrounding halite rocks (see Figs. 13 and 18) and insulated from the others so that no extensive links can form between the fissure networks of single blocks. Thus, each of the blocks with its internal fissure volume is also a preferential brine and gas reservoir under petrostatic pressure.

The halite precipitation phase in the Leine-Folge began with the **Basissalz (z3BS)**, which has a sharp boundary to the Hauptanhydrit. The light-grey to light-brown fine-crystalline halite rock is contaminated by a large number of light-grey anhydritic bands with a thickness of up to 1 cm. They have intervals of a few millimetres, increasing to a maximum of 10 cm towards the top (Fig. 18). Between these main bands 2 to 6 fine pinstripes of anhydrite occur. These separate crystal halite beds of up to 3 cm thickness are permeated by idiomorphic halite crystals approx. 1 to 2 cm in size. The Basissalz is usually only poorly translucent in transmitted light.

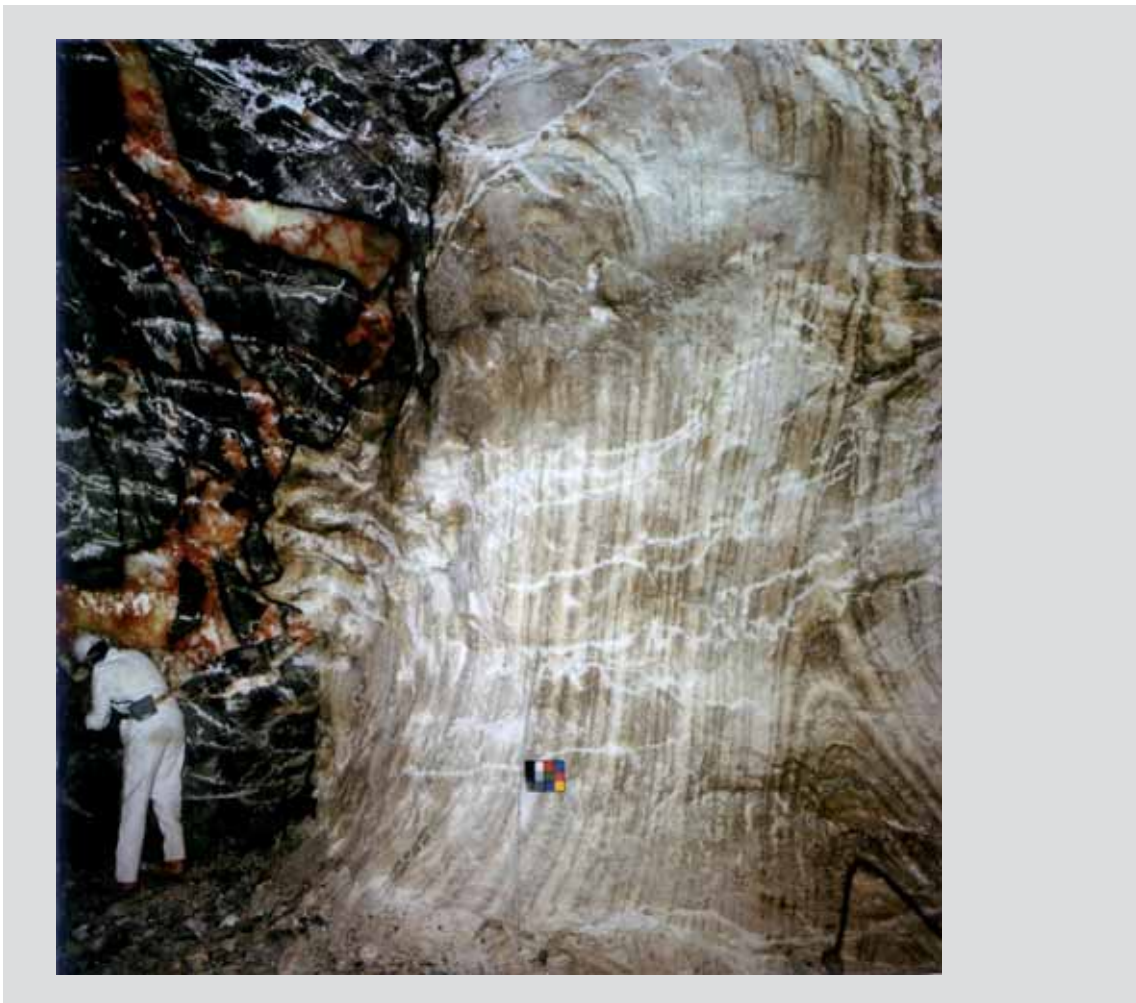


Figure 18: Hauptanhydrit block in combination with discordant layering and folding of the Basissalz. Cross-cut 1 West, 840 m-level, drift position 50 m, western wall. (Photograph: Bauer, DBE)

Normal banding of the Basissalz is locally interrupted by halite banks of up to 40 cm thickness, which contain inclusions of irregularly scattered light-grey anhydritic flakes and blobs. The sedimentary stratification is only poorly discernible in these sections. They were probably formed by submarine slumps because the relief built up by the Hauptanhydrit

had not at that time been levelled by sediments. In addition to this, the Basissalz is usually intensely folded. It is unclear whether these are submarine slump folds or halokinetic folds.

Approximately in the middle of the Basissalz, there is a fine-crystalline light-grey anhydrite bank the thickness of which ranges from 20 to 80 cm between exposures. The anhydrite bank is largely unstratified although in some places dark-grey flasers hint at stratification. Similar to the very much thicker Hauptanhydrit, this bank was also broken up into separate blocks as a result of diapirism, the blocks floating like a layer within the surrounding halite (Fig. 19). Excellent examples are shown in the exposures of the Basissalz in cross-cuts 1 West and 1 East. The anhydrite bank is clearly identifiable as a marker horizon in the geophysical borehole logs. The boundary between the Basissalz and Liniensalz salt (z3LS) is where the halite becomes purer because of the absence of anhydritic dust lines, the distances between the bands become more regular, and there is a change in colour from (light-) brown to light-grey. The total thickness of the Basissalz is approx. 15 m.



Figure 19: Boudinage of the anhydrite bank in the Basissalz. The anhydrite blocks are completely separated from each other and enveloped by Basissalz. In some sections white recrystallized halite fills the gaps. The anhydrite layer is outlined by black paint.
Ventilation drift, position 65 m, eastern wall.
(Photograph: Bauer, DBE)

The regular occurrence of up to 1 cm-thick, and occasionally up to 4 cm-thick light-grey, sometimes finely laminated anhydrite bands is typical of the approx. 30 m-thick **Liniensalz (z3LS)**. The normal distance between the bands is 15 to 20 cm close to the bottom and increases to 30 to 50 cm close to the roof. The band structure and the band separation basically depend on the tectonic fold position encountered in the salt dome, i.e. fold flank or fold core. On the fold flanks, the bands are ruptured into lines of separate segments whilst microfolds and overthrusting occur in the cores of the folds.

In the infrastructure zone of the mine, the distances between the bands become smaller approaching the Zechstein 2/Zechstein 3 boundary until the bands are only a few mm to 1 cm apart, at which stage the bands are no longer continuous but take on the appearance of rows of separate knots. The same features were observed in the shafts in the elongated isoclinal anticlines that stretch for several hundred metres from the shafts to the exploration level.

The bands were counted to help mapping and identification of the folds (anticlines, synclines). These band counts and the underground mapping revealed that the Linien-salz contains approx. 230 bands and that bands 82/83, 139/140, 177/178 and 199/200 are in the form of characteristic double bands. The **110. Linie** was also identified as a strong marker horizon (BORNEMANN et al. 2001: App. 1).

In its undeformed state, the 110. Linie can be divided into four zones from base to top according to BÄUERLE (2000):

- **Zone I:** Light-grey, fine-crystalline, mainly structureless, homogeneous anhydrite bed with a thickness normal to bedding of up to 2 cm in the analysed sections. Followed concordantly by Zone II of the 110. Linie.
- **Zone II:** This is a fine-crystalline to medium-crystalline, grey to grey-brown, sometimes translucent halite bed with a thickness normal to bedding of up to 2 cm. This bed is sometimes reduced to halite crystal eyes by strong halokinetic stress.
- **Zone III:** The halite layer is followed concordantly by a fine-crystalline, light-grey to grey stratified anhydrite bed. The stratification is caused by grey-black layers of a thickness of tenths of millimetres that occur at intervals of some millimetres.
- **Zone IV:** The top zone is formed by a concordantly overlying fine-crystalline halite bed only a few millimetres thick, which is bounded at the top by a 1 to 2 mm-thick fine-crystalline anhydrite band.

The 110. Linie has a thickness normal to bedding of 1.8 to 5 cm. In the west ventilation drift (820 m-level, 01YEA02), the 110. Linie even reaches a thickness normal to bedding of more than 10 cm (drilling location 1.8, 01YEA02 RB011). The spacing of the bands underlying the 110. Linie (widely spaced) and the overlying bands (closely spaced) helps to identify the orientation of the bedding (Fig. 20) and indicates changes in the sedimentary environment in the sequence overlying the 110. Linie. These changes involved a reduction in seawater salinity, which led to increased sulphate precipitation.



Figure 20: Anticline in the Liniensalz with marker horizon 110. Linie (see arrow).
The figure shows a significant change in the spacing of the bands: widely spaced in the lower section, closely spaced in the upper section.
840 m-level, landing drift of Shaft 2, drift position 135 m, eastern wall.
(Photograph: Bauer, DBE)

A special feature in the Liniensalz is a 30 x 60 cm anhydrite block found in the roof of cross-cut 1 West (infrastructure zone). The light-grey, fine-crystalline to cryptocrystalline anhydrite rock is unstratified and strongly permeated by light-grey halite. Similar anhydrite bodies were encountered in the Liniensalz in the Bartensleben/Marie mine (Morsleben). At Morsleben, they are interpreted as blocks from the Hauptanhydrit, which have slumped into the Liniensalz (BEHLAU & MINGERZAHN 2001; HEMMANN 1968).

The halite interbedded with the anhydrite bands is fine-crystalline to medium-crystalline, sometimes coarse-crystalline, usually colourless to grey and highly translucent in transmitted light. Between the Hauptanhydrit bands, 5 to 11 thin anhydrite dust layers are interstratified. These anhydrite dust layers separate clear or yellow translucent, sometimes finely laminated crystal salt beds with thicknesses varying between some centimetres and 10 cm.

Depending on the degree of deformation, these crystal salt beds are fractured to a varying degree. The joint surfaces (mini faults) are healed with secondary fine-crystalline halite. The crystal salt layers are often separated by very fine-crystalline, up to 1-cm-thick halite beds which contain higher proportions of insoluble impurities. These beds are probably shear surfaces that opened up parallel to bedding during the folding of the sequence and healed subsequently. In more strongly deformed areas, the halite has a sigmoidal texture in which the otherwise continuous crystal salt layers are sheared into lenticular bodies.

In the underground geological mapping, the boundary to the Unteres Orangesalz (z3OSU) is defined by the last continuous anhydrite band (band 131). In the surface exploration boreholes, the boundary is between bands 207 and 239, probably due to counting errors.

The Liniensalz is followed by the **Orangesalz (z3OS)**, which is divided into Unteres Orangesalz (z3OSU), Mittleres Orangesalz (z3OSM) and Oberes Orangesalz (z3OSO). This tripartite division is based on the presence of a bank consisting mainly of anhydrite found in the Orangesalz in the Gorleben salt dome. This bank is called the Mittleres Orangesalz or the Gorleben-Bank (BORNEMANN 1991). No marker horizon of this kind has been encountered in the Orangesalz in the Hanover potash area (HALTENHOF & HOFRICHTER 1972; SIEMEISTER 1969) or in the Sub-Hercynian Basin (HEMMANN 1968; LÖFFLER 1960). A horizon in a similar stratigraphic position in the Lübtheen salt dome (former name: Jessenitz) with petrographic features similar to the Gorleben-Bank is described by NETTEKOVEN & GEINITZ (1905) as a "black band". It is also known that the 110. Linie was found in the Liniensalz in a cavern exploration borehole in the Kraak salt dome. It is thus assumed that the Gorleben-Bank is also present there. The further spatial extent of the Gorleben-Bank in the Zechstein Basin is still unclear. It is probable that the occurrences that have already been identified represent a special sedimentary event that took place in a small separate sub-basin of the Zechstein Sea.

The fine-crystalline to medium-crystalline **Unteres Orangesalz (z3OSU)** is light-orange to orange-brown. Layers of crystal halite lumps occur only to a lesser extent. Millimetre-thin anhydritic/polyhalitic bands of flakes are a typical feature, which become increasingly indistinguishable towards the roof until they can almost only be recognised in transmitted light. A plainly visible colour change ranging from white, colourless to light-orange occurs between the bands of flakes. There are 275 bands in total. Between bands 259 and 260, there is a marked white halite bank and the anhydritic/polyhalitic bands of flakes here mostly have a centimetres-thick polyhalitic fringe.

In addition to the 110. Linie, the **Mittleres Orangesalz (z3OSM)**, i.e. the **Gorleben-Bank**, is an important marker horizon within the group of striped salts of the Leine-Folge. Without knowledge of these two marker horizons, the geological mapping of the shafts and the underground exploration with boreholes in the infrastructure zone would have produced only limited structural information.

BÄUERLE (2000) described the sediments, stratigraphy and geochemistry of the Gorleben-Bank in detail. The subdivision of the standard profile of the Gorleben-Bank is largely based on the exposures of the Gorleben-Bank from exploration borehole Go 1004 (depth: 721.90 to 722.65 m), the underground exploration borehole 02YEA04 RB025 (depth: 0.20 to 0.40 m), the exposure of the Gorleben-Bank in the conveyor drift at the 880 m-level (03YEA01, drift position 31 m) and BORNEMANN (1991).

A complete sequence of the Gorleben-Bank can be subdivided from base to top into the following seven zones (Fig. 21):

- **Zone I:** The first zone of the Gorleben-Bank consists of a contaminated halite horizon. It is 1 to 45 cm thick, fine-crystalline and tinted dark-orange to brown-orange. The halite differs from the underlying beds by having a higher proportion of partly stratified polyhalite and anhydrite flakes (on average < 1 to 2 mm) that are responsible for the colour of the bed. The bedding-parallel boundary to the underlying sequence can either be sharp and marked by a band of flakes, or gradual.
- **Zone II:** The boundary to Zone I is concordant and either sharply defined or in some cases gradual. This zone consists of Flaser- und Flockenanhydrit of light-grey to grey, fine-crystalline anhydrite rock with a thickness ranging from 0.2 to 2.5 cm. The anhydrite encloses light-grey to grey-brown halite flakes (on average < 1 to 2 mm) and to a lesser extent grey-black, anhydritic and clayey flakes (on average < 1 to 2 mm), as well as flasers (up to several millimetres in length). These inclusions sometimes form a diffuse to wavy stratification. A special facies of the Flaser- und Flockenanhydrit are anhydrite and clay flakes (on average < 1 to 2 mm) in a grey-brown, fine-crystalline halite matrix. At the top, the Flaser- und Flockenanhydrit is usually bounded by a continuous bedding-parallel shear surface with a clay filling, which frequently displays slickensides. The direction of the slickensides is imprinted on the Flaser- und Flockenanhydrit in the form of foliation that is easily identifiable when penetrated parallel to the shear surfaces.

- **Zone III:** Zone III consists of a grey-black clay bed with a maximum thickness of 2 mm, which lies concordantly on the Flaser- und Flockenanhydrit. If a zone of movement (see Zone IV) is present in the profile of Gorleben-Bank, then this clay layer is often divided into two parts (Zones III a and III b), representing the bottom and top shear surfaces of the zone of movement. If the filling of the shear surface consists of more than one layer, the individual layers are sometimes separated by a thin clay fringe formed by redeposition in the shear zone (e.g. western wall of connecting drift, vehicle/electrical workshop).
- **Zone IV:** This is a zone of shear movement that is always bedding-parallel, has opening widths of 0.1 to 34 cm, and is present in most exposures. The filling consists mainly of halite and/or carnallite. The halite is medium-crystalline to coarse-crystalline, rarely fine-crystalline, and milky-white to colourless. The carnallite is fine-crystalline to coarse-crystalline and tinted yellow to blood red (Fig. 22). Halite and carnallite may occur together or alone. If the matrix of the filling is formed by halite, then carnallite is only present in intercrystalline interstices within the halite. Anhydrite fragments from the anhydrite beds of the Gorleben-Bank, clay shreds, and in some cases polyhalite aggregates and sylvite crystals are often included in this zone. The shear zone in the Gorleben-Bank is often subdivided within the exposures in the underground workings. This finding is explained using the section exposed in the conveyor drift (03YEA01, drift position 31 m) at the 880 m-level as an example: the filling in this exposure has a five-fold structure consisting of two parallel halite layers and three parallel carnallite layers. The layers have a thickness normal to bedding of 1 to 12 cm and are separated by thin clay layers and/or secondary anhydrite and/or anhydrite beds torn from Zones V-VI of the Gorleben-Bank. The halite fillings are sometimes also made up of various parallel layers, each consisting of a crystal carpet. The halite beds also contain interstitial carnallite. The shear zone usually only has a single or two-fold structure in the underground workings.
- **Zone V:** This unit of the Gorleben-Bank consists of finely stratified anhydrite with a thickness normal to bedding of 0.2 to 1.5 cm, which lies concordantly on Zone IV with a sharp boundary. The anhydrite rock is fine-crystalline, dark-grey to grey-black, and divided by clayey layers into lamellae in the tenth of a millimetre range.
- **Zone VI:** Above a sharp boundary, Zone V is overlain concordantly by stratified anhydrite with a thickness normal to bedding of 0.3 to 34 cm. The light-grey to grey, fine-crystalline anhydrite rock is divided into millimetres-thick layers by dark-grey horizons. The spacing of the layers increases upwards.

- **Zone VII:** The last zone of the Gorleben-Bank is 1 to 5 cm thick and consists of four tightly spaced concordant anhydrite bands with interbedded halite. The 1 to 3 mm thick anhydrite bands are fine-crystalline, light-grey to grey and in some parts finely laminated. The halite interbeds are fine-crystalline and light-orange to orange. The halite crystals are often twisted parallel to bedding by halotectonics.

The thickness normal to bedding of the Gorleben-Bank in the infrastructure zone between the shafts south of Exploration Area 1 ranges from 3.5 to 70 cm. The Gorleben-Bank displays a variation in thickness which originated during sedimentation in all exposures within the salt dome, particularly in the stratified anhydrite beds (Zones V to VI). These anhydrite beds play a crucial role in the migration of brine and gases in the Gorleben-Bank. Thus, only these two zones within Gorleben-Bank are referred to when describing the spatial changes in thickness.

For this, the sections of the Gorleben-Bank penetrated by the exploration boreholes Go 1002, Go 1003, Go 1004, Go 1005, and the two shaft pilot boreholes Go 5001 and Go 5002 were considered. The analysis only included penetrations where the Gorleben-Bank was undamaged or showed only slight halokinetic stress. If no intact section of the Gorleben-Bank was encountered in a borehole (e.g. shaft pilot borehole Go 5001) a best possible intact section of the Gorleben-Bank was reconstructed by combining the sections of the thickest zones.

The following thickness variations of the stratified anhydrite beds in the Gorleben-Bank (Zones V to VI) were identified from the reconstruction, referring to the present-day positions of the beds:

- The thickest sections were found in exploration borehole Go 1002 (northern flank of the salt dome) where the thickness normal to bedding exceeds 14 cm, and in shaft pilot borehole Go 5001 (western central area) where the thickness is approx. 10 cm.
- The thinnest section of the stratified anhydrite beds of Gorleben-Bank occurs in shaft pilot borehole Go 5002 with a thickness normal to bedding of max. 3 cm. From this point, the thickness increases slightly towards the SE flank of the salt dome (Go 1005, approx. 4 cm).
- Compared to shaft pilot borehole Go 5001, where the thickness normal to the bedding is approx. 10 cm, the thickness decreases towards the south (Go 1004, approx. 5 cm) and towards the NW (exploration borehole Go 1003, approx. 5 cm).

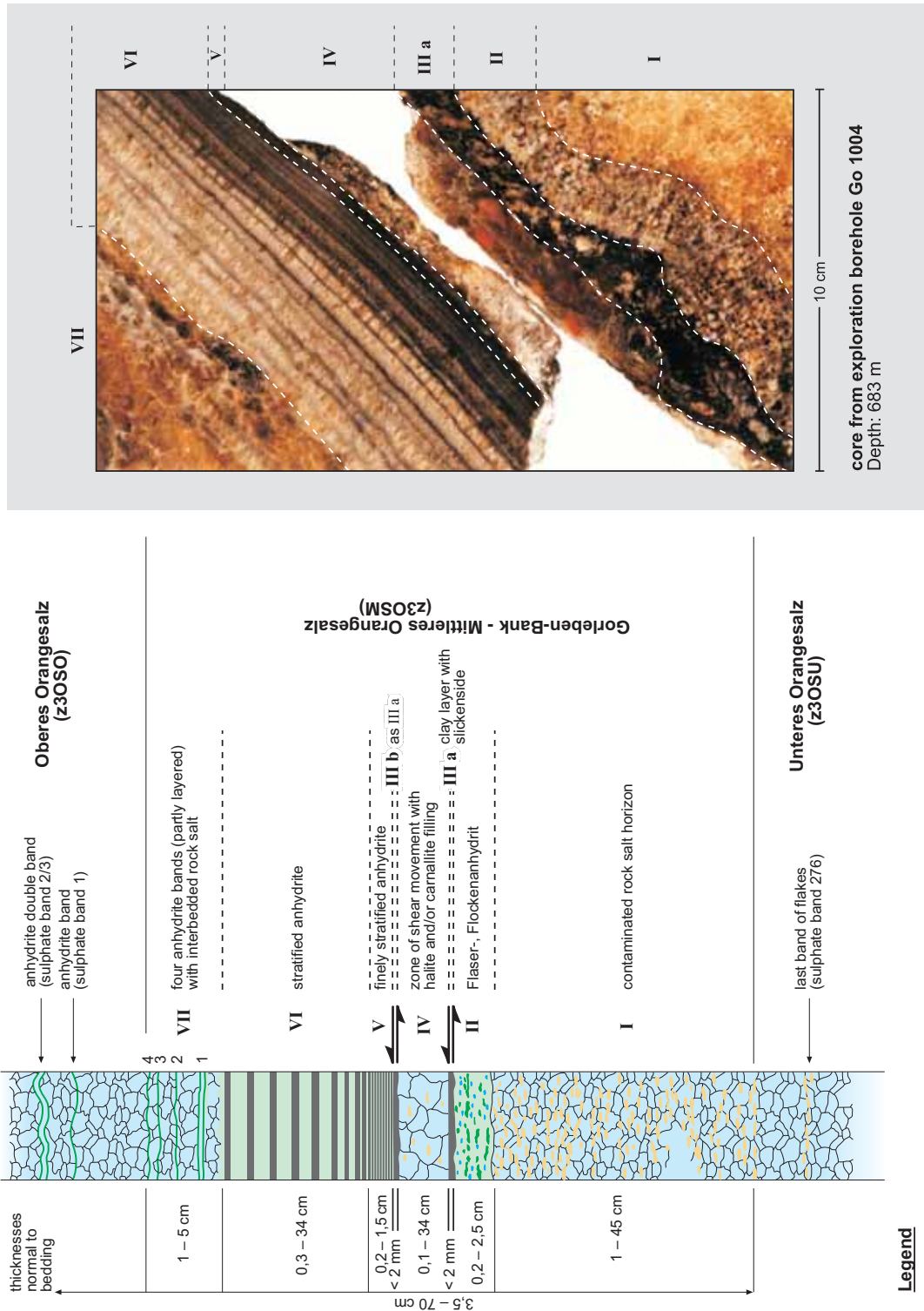


Figure 21: Stratigraphy and petrography of the Gorleben-Bank (z3OSM).

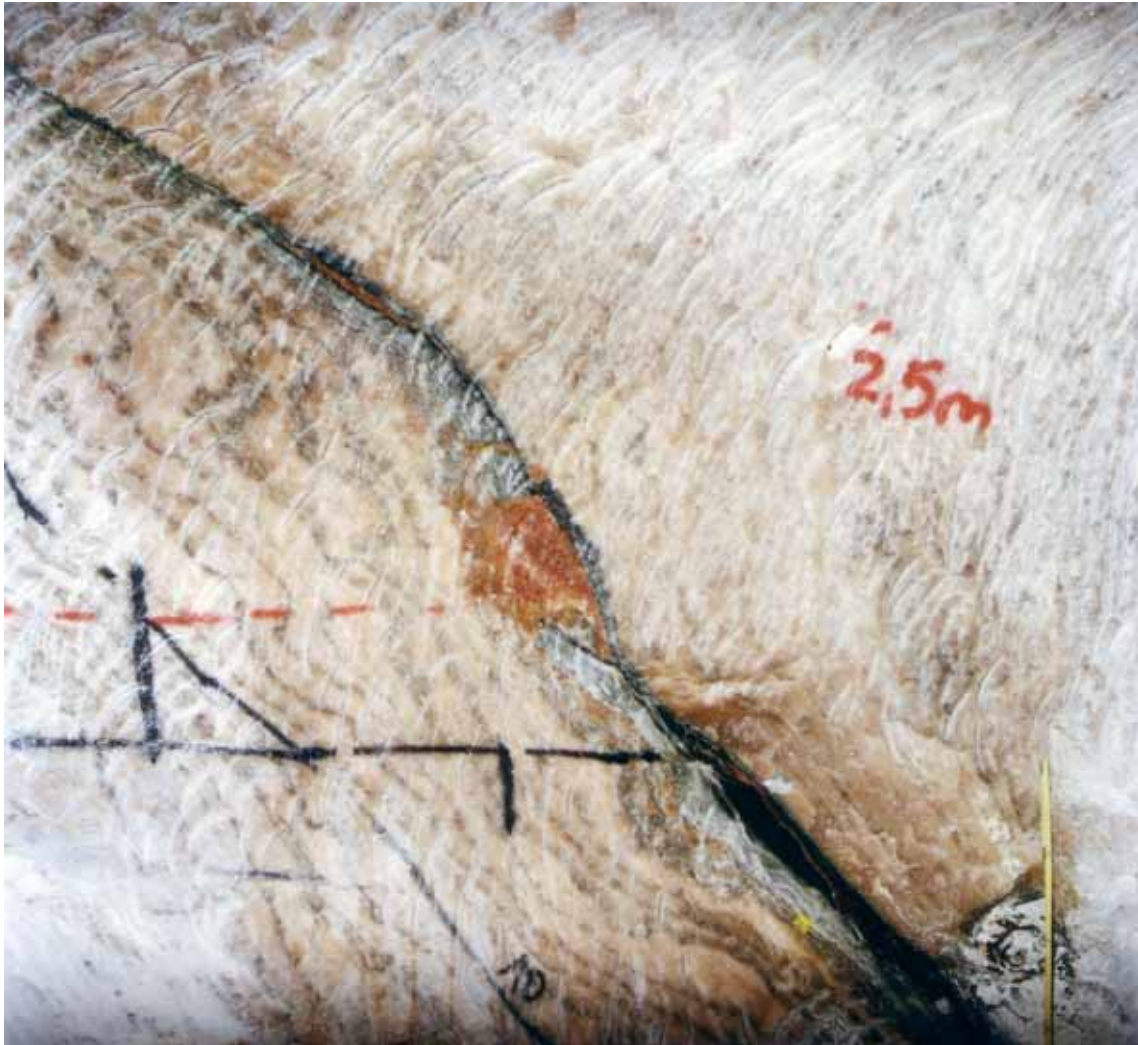


Figure 22: Gorleben-Bank, ruptured and overturned.

The ruptured sections and parts of the shear zone (black) are healed with secondary red and yellow carnallite. Access drift to vehicle workshop, 840 m-level, drift position 10 m, southern wall.

(Photograph: Bauer, DBE)

The determined thickness distribution provides only an approximate trend because the boreholes are more than 2 km apart in some cases. Moreover, the geological logs of the underground exploration boreholes and the geological maps of the drifts in the underground workings revealed that variations in thickness can occur over very short distances. The thickness variation in the two shafts serves as an example. In Shaft 2, the Gorleben-Bank shows low thickness values for all 8 penetrations. No solutions or gases were encountered in these sections. In Shaft 1, however, the thickness of the Gorleben-Bank increases significantly below 850 m (the Gorleben-Bank was also penetrated eight times) where, due to the thickening of the stratified anhydrite beds, it becomes a reservoir for brine and gases.

The reconstruction of the thicknesses indicates the existence of relief during the sedimentation of the Gorleben-Bank. This may be attributed to the Hauptanhydrit which lies stratigraphically below the Gorleben-Bank and which displays a highly variable top morphology in many parts of the Zechstein Basin where its base is undeformed (HEMMANN 1968; KOSMAHL 1969). The variation in thickness of the Gorleben-Bank is therefore caused by the relief of the Hauptanhydrit which is still weakly imprinted upon Gorleben-Bank even through the intervening halite beds of the Basissalz through to the Unteres Orangesalz.

The sulphate bands within the Oberes Orangesalz often display intense folding directly above the Gorleben-Bank (Fig. 23 and 24). The sulphate bands in the Unteres Orangesalz remain largely undisturbed, despite similar deformation in the overlying beds. This means that the zone of movement of the Gorleben-Bank acted as a shear horizon between the Unteres and Oberes Orangesalz during folding. If the folds in the Oberes Orangesalz were smoothed out, a difference in length on the order of tens of metres would result. Particularly in the Unteres Orangesalz but also occasionally in the Liniensalz and rarely in the Oberes Orangesalz, the Gorleben-Bank acted as a kind of “disruptive body” creating secondary structures during such halokinetic deformation. These are described as follows:

Fissures

Fissures are frequently associated with the area directly adjacent to Gorleben-Bank. In this case, fissures are defined as secondary structures which usually poke downwards like fingers from the Gorleben-Bank into the underlying beds, and which are sometimes branched and often penetrate the bedding normal to the strata (Figs. 25 and 26).

The structures can also run at a sharp angle to the bedding or parallel to the bedding without any visible connection to the Gorleben-Bank. They narrow at the ends and pinch out. Fillings of these fissures consist of secondary hypidiomorphic medium-crystalline to coarse-crystalline halite. Carnallite occurs occasionally as interstitial filling. Occasionally, cavities are also present. The fissure surfaces are usually covered by a secondary sulphate fringe, sometimes up to several millimetres thick, which marks the lower surface at the time the fissure was formed. No offsets are observed on the walls. The fissures occur only down to 1-3 m beneath the Gorleben-Bank and only rarely directly above the Gorleben-Bank. The origin of these fissures is closely associated with the special petrophysical properties of the Gorleben-Bank because it presented a mechanical disruptive body within the rock salt and had different rheological properties to the surrounding halite.



Figure 23: Intense folding of the beds in the Oberes Orangesalz. The beds of the Unteres Orangesalz remain untouched by the intense folding due to the Gorleben-Bank acting as a buffer horizon (Shaft 2, depth 595.3 to 606.0 m).



Figure 24: Seismogram-like folding of the Gorleben-Bank.

This type of folding is extremely rare and is probably due to the fact that the intense deformation affected the Zechstein 3/Zechstein 2 boundary. Most of the beds of the Gorleben-Bank are missing, only the shear zone (black) and the overlying stratified anhydrite (grey) are present.

Main drift, 840 m-level, drift position 280 m, northern wall.

(Photograph: Bauer, DBE)

Secondary recrystallization zones

Most secondary recrystallization zones occur beneath the Gorleben-Bank (in the Unteres Orangesalz and to a smaller extent in the Liniensalz), and only rarely in the Oberes Orangesalz. These structures are bedding-parallel or at sharp angles to the sulphate bands, typically have elongated, rectangular to slightly oval, sometimes irregular cross sections, and have lengths and widths in the order of tens of centimetres (Figs. 27, 28 and 29).



Figure 25: Fissure filled with red carnallite in the Unteres Orangesalz the bedding of which dips from upper left to lower right. The fissure strikes perpendicular to the bedding and is associated with the halokinetic pinch-off of the sequence of Grauer Salzton to Hauptanhydrit in the area of the updoming of the Kaliflöz Stassfurt between the shafts.

Landing drift Shaft 2, 820 m-level, drift position 38 m, southwestern wall.
(Photograph: Engelhardt, DBE)

The outline of these fissures or nodes resembles the form of a loaf of bread with a flat lower boundary and a domed upper boundary. The fillings consist of secondary coarse-crystalline hypidiomorphic halite with secondary medium-crystalline to coarse-crystalline carnallite in the interstices. One of the boundary surfaces of these structures usually has a secondary sulphate fringe sometimes several millimetres thick, which marks the original lower surface. No offsets or links between the individual structures are visible on the exposures.



Figure 26: Starting at the Gorleben-Bank, a secondary mineralization permeates the underlying Unteres Orangesalz, the sedimentary bedding of which is almost completely destroyed in this area. No fault-induced dislocation of the bedding is detectable. The mineralization consists mainly of white coarse-crystalline halite and red carnallite on the edges. Milling workshop, 840 m-level, drift position 65 m. (Photograph: Bauer, DBE)

The shape of these structures is atypical for fissures in the proper sense. Thus, these structures are regarded as secondary recrystallization zones. The three-dimensional model of the bedding, which is based on the digitization of the wall maps in Shaft 2, indicates that these recrystallization zones may be a result of shearing processes.



Figure 27: Gorleben-Bank, with underlying Unteres Orangesalz with secondarily crystallized, white coarse-crystalline halite zones, resembling the outline of loaves of bread. The lower boundary is flat and contains an anhydrite filling, the upper boundary is domed. Access to vehicle workshop, 840 m-level, drift position 5 m, southern wall. (Photograph: Bauer, DBE)

Shattered zones

Shattered zones are those areas in the rocks that consist of halite or anhydrite fragments floating in a secondary halite matrix. Zones of this kind occur in the case of strong halokinetic deformation primarily in the sequence from the Liniensalz up to and including the Unteres Orangesalz, e.g. in the eastern part of the potash seam updoming between the shafts.

The **Oberes Orangesalz (z3OSO)** is fine-crystalline to medium-crystalline and mainly yellow-orange to brown-orange. In normal profile, the colouring decreases from the base towards the top. Banks of crystal salt are rare. Local colouring from light orange to orange is observed.

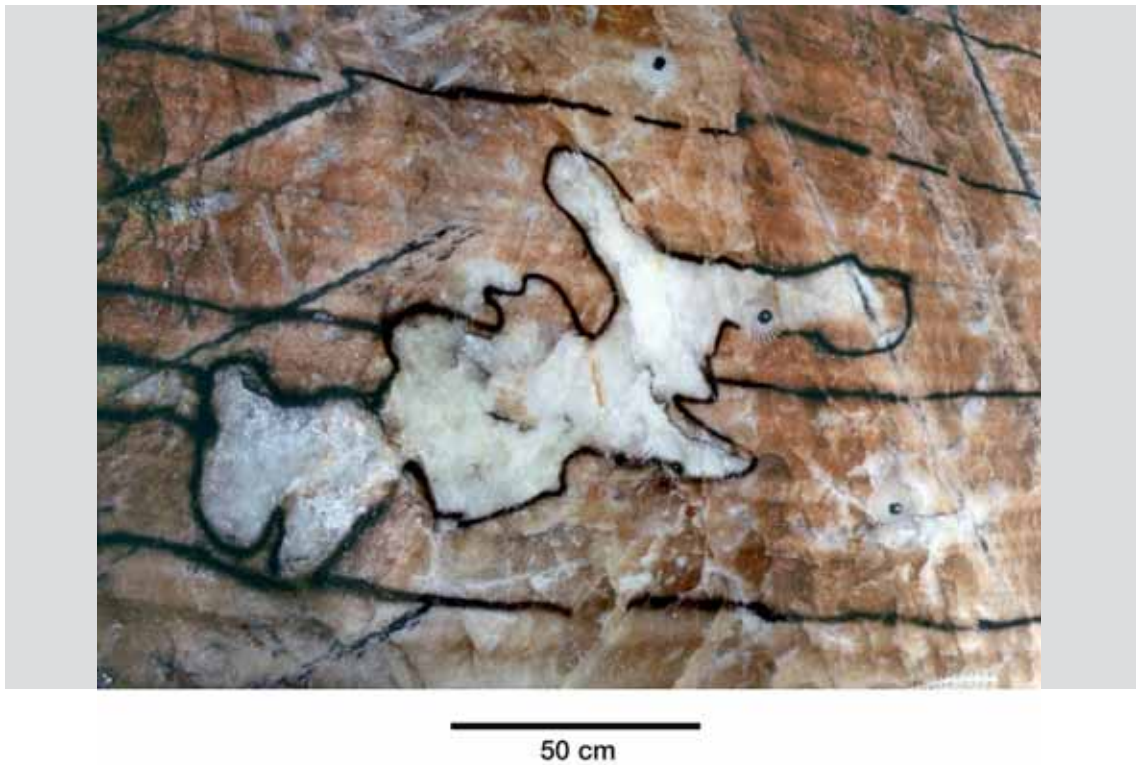


Figure 28: Zone of secondary recrystallization with uneven boundary in the Unteres Orangesalz, filled with white coarse-crystalline halite. The outline is enhanced with black paint. Store, 840 m-level, drift position 35 m, roof. (Photograph: Bauer, DBE)

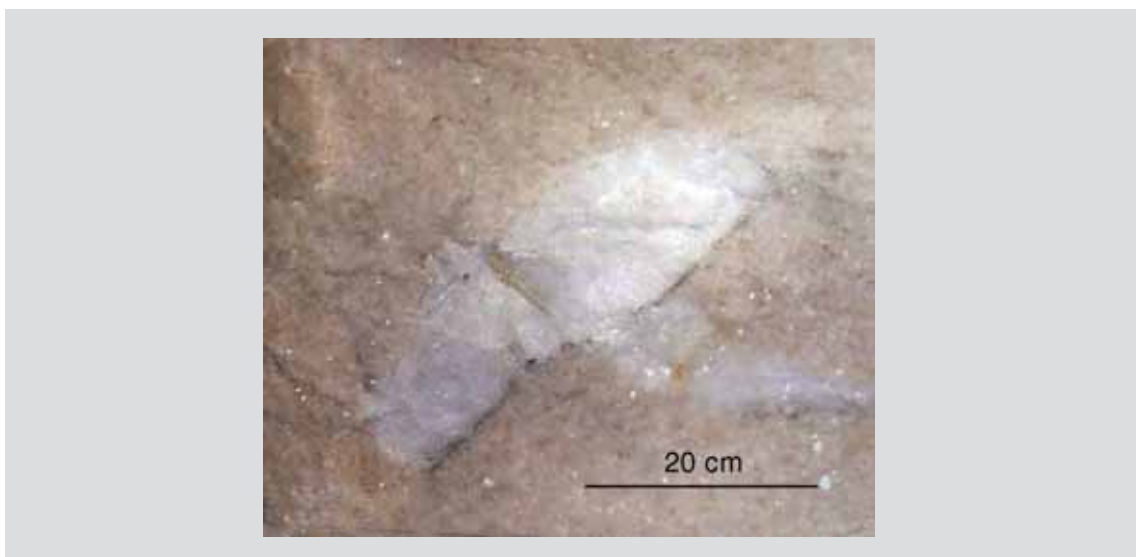


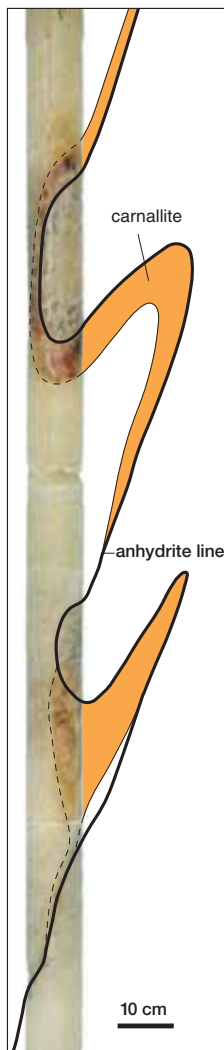
Figure 29: Filled cavity, resembling a loaf of bread, with secondarily crystallized white and clear coarse-crystalline halite, partly intersticed with carnallite or brine. The lower side is flat and coated with an anhydrite fringe. The upper side is domed like a loaf of bread. Shaft 2, approx. 835 m. (Photograph: Wiesch, DBE)

The halite above the Gorleben-Bank is clearly interstratified with up to 0.5-cm-thick grey anhydrite bands, which are usually intensely folded. Counting of the bands restarts above the Gorleben-Bank at 1. In places, up to and in excess of 130 bands could be counted altogether. Detailed stratigraphic analysis revealed that the double bands 2/3, 4/5, 12/13, 22/23, 37/38 and 51/52 are useful marker horizons in undisturbed sequences. From approx. band 70 upwards, the marked anhydrite bands give way to anhydritic/polyhalitic bands of flakes. The upward increase in polyhalite concentration is also visible in the gamma-ray log. The distance between the bands increases from 2 to 5 cm at the boundary of Gorleben-Bank to an average of 20 cm towards the top. The boundary between the Oberes Orangesalz and the Bank-/Bändersalz lies between bands 120 and 124 in the normal section. The Oberes Orangesalz in this region is very pure and the bands of sulphatic flakes are only just recognisable.

A facies differing from the standard sequence occurs in the vicinity of the shafts at the 840 m- and 820 m-levels. In these areas, formation of secondary polyhalite was found in the form of abundant, scattered as well as stratified polyhalite flakes in the middle and upper part of the Oberes Orangesalz accompanied by a red-orange coloration of the halite. Strongly polyhalitized sulphate bands as well as idiomorphic anhydrite crystals of up to 1 cm size are also present. This recrystallization was probably caused by a brine front released by the processes that formed the Zechstein 2 updoming of the Kaliflöz Stassfurt and pinched off the Hauptanhydrit. The pinch-off opened up fissures that allowed the brines to migrate into the adjacent rock. The criteria defining the boundaries in the standard sequence are blurred by the secondary polyhalite formation. As a consequence, the Oberes Orangesalz is assigned a greater thickness than would normally be the case, at the expense of the Bank-/Bändersalz.

It is remarkable that throughout the striped salt layers (z3LS and z3OS) clusters and layers of carnallite are irregularly scattered. This was particularly distinctive in the salt dome exploration boreholes Go 1003 and Go 1002 drilled on the NW flank of the salt dome, whilst in boreholes Go 1004 and Go 1005 (SE flank) and shaft pilot boreholes Go 5001 and Go 5002 clusters and layers of this kind were only rarely encountered. The same applies to the underground exposures in the infrastructure zone.

Mostly, the individual carnallite layers have an approximate thickness of 1 cm, though some are up to 10 cm thick, and are mainly oriented parallel to the bedding. If these beds are hit with a hammer, the carnallite crackles and gaseous hydrocarbons are released. Detailed mapping of the beds shows that these carnallite layers lie mostly above the sulphate bands. The two layers are usually separated by a thin halite layer. Another finding was that the carnallite layers follow the anhydritic bands even if the bands are intensely folded. Their structural position above the bands remains unchanged. These



carnallite layers are interpreted as carnallite-bearing crystals from brines, which must have intruded along the bedding planes before the beds were folded (Fig. 30).

The overlying **Bank-/Bändersalz (z3BK/BD)** is approx. 14 m thick and appears to be almost featureless at first glance. It is fine-crystalline to medium-crystalline, very pure and light-orange to white translucent in transmitted light. The only structural elements are discontinuous, usually strongly folded bands of anhydritic/polyhalitic flakes with a thickness of a few mm, and diffusely formed anhydrite bands. The bands cannot be counted.

The mineralogy and development of the beds from Basissalz to Bank-/Bändersalz can also be identified in the geophysical borehole logs (Fig. 15). The density log clearly shows the continuous decrease in rock density (decreasing sulphate concentration) from the top of the Hauptanhydrit to the Gorleben-Bank. Above this bed, the density abruptly increases again (sudden rise in sulphate concentration). The gamma-ray log, though, shows a slight increase due to the increasing polyhalite concentration until reaching the Gorleben-Bank. In the overlying sequence it drops at first and then rises again up to the Bank-/Bändersalz. This indicates that even when the Gorleben-Bank is absent (squeezed off halokinetically) it is still possible to clearly differentiate the beds using the geophysical borehole logs.

Figure 30: Core of Liniensalz (borehole Go 1002; depth 900.50 to 902.16 m) showing a recumbent fold of an anhydrite band, accompanied by a carnallite inclusion on top. This is accumulated in the “bow” or core of the folds and pinched off at the sides except for residues.

Despite the folding, the carnallite layer is always above the anhydrite band, so it can be assumed that it was deposited before folding and may be of sedimentary origin.

Only exploration borehole Go 1003 encountered a potash seam above the Bank-/Bändersalz. The seam consists of brecciated carnallitite, which resembles that of the Kaliflöz Stassfurt. This potash seam is only encountered on one other occasion, as a rock salt horizon in the lower part of salt dome exploration borehole Go 1005. Its stratigraphic position corresponds to the **Kaliflöz Bergmannsseggen (z3BE)**, which is restricted to the region of the Lehrte-Sehnde salt dome. At that location, the potash seam was deposited between the layers of the Banksalz and the Bändersalz. It is probable that the occurrence of the potash seam is restricted to the northern flank of the Gorleben salt dome because it was not encountered anywhere else (except in Go 1005) despite the penetration of the Bank-/Bändersalz sequence in other boreholes.

The boundary between the Bank-/Bändersalz and the overlying **Buntes Salz (z3BT)** is distinct and marked by the sudden appearance of abundant anhydrite flakes and bands. The Buntes Salz is divided into three swath salt zones and three pure salt zones (Fig. 31).

The first swath zone starts at the base, in some cases with three clearly developed anhydritic bands. The halite itself is fine-crystalline to medium-crystalline, dark-orange to orange-brown and is highly contaminated by irregularly scattered anhydrite flakes and streaks. In some areas, the transition to the first zone of pure salt is indistinct. The pure salt zone cannot always be clearly distinguished from the swath zones above and below. Where the pure salt zone can be distinguished, it is 20 to 30 cm thick. Anhydritic impurities are scattered like clouds.

The second swath zone resembles the first and contains anhydrite flakes, which show weak stratification. The second pure salt zone has sharp lower and upper boundaries to the adjacent swath zones 2 and 3. The fine-crystalline halite is light-orange and contains hardly any anhydritic impurities. The thickness of this unit is approx. 0.2 to 0.5 m.

The third swath zone is grey-orange and strongly contaminated by grey anhydritic streaks usually oriented parallel to the bedding. The transition from the third swath zone to the third pure salt zone is usually blurred. The third pure salt zone is marked by an irregular distribution of interstratified anhydritic flaky lines and bands.

The **Anhydritmittelsalz (z3AM)** starts with an anhydrite bank. Thus, the boundary to the underlying Buntes Salz is distinct. The Anhydritmittelsalz can reach an overall thickness of approx. 60 m. Nine Anhydritmittel have been identified in the Anhydritmittelsalz. Anhydritmittel 1 to 6 and 8 are less than 0.5 m thick and have no specific sedimentary structures which might facilitate their identification (Fig. 32). They are mostly unstratified and consist of fine-crystalline grey anhydrite, containing localised anhydrite pseudomorphs of gypsum, or strongly interstratified with halite and carnallite. In some cases, the Anhydritmittel have a weak clayey layer at the base. The Anhydritmittel 7 and 9 are up to 2.3 m thick. Anhydritmittel 7 consists of dense, fine-crystalline, grey to dark-grey anhydrite, in which a large number of anhydrite pseudomorphs of gypsum are embedded in banks. The pointed ends of the up to 10-cm-long crystals always point to the bottom so that this feature can be used to differentiate top from bottom. The Anhydritmittel 9 consists of a sylvinitic kieserite-anhydrite rock. Detailed mapping reveals a subdivision into five beds of varying structure and mineralogical composition (FISCHBECK 1990). The distances between the Anhydritmittel vary. The Anhydritmittel 2, 3 and 4 form a marked closely-spaced group of three bands.

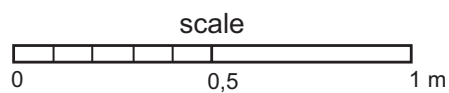
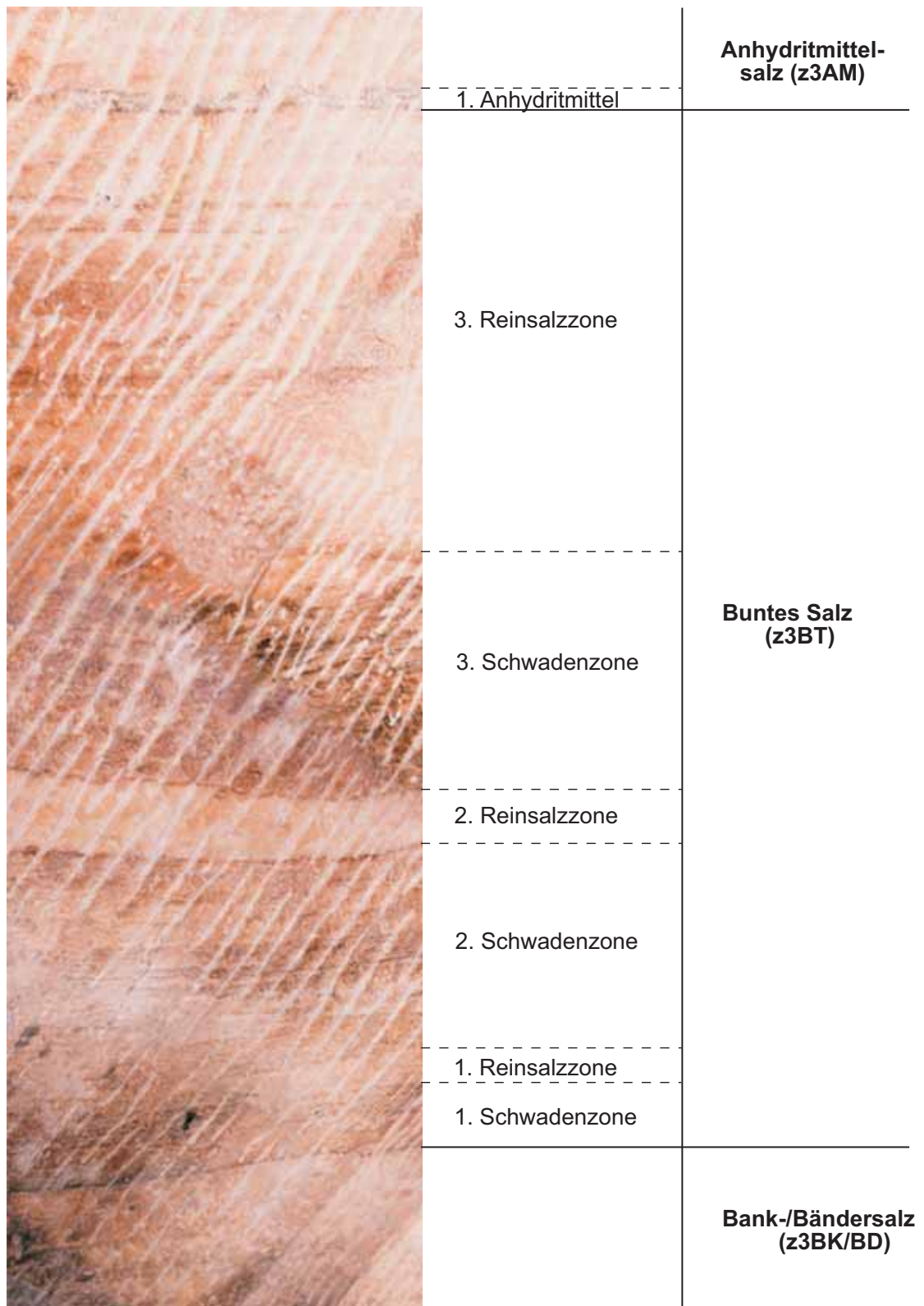


Figure 31: Stratigraphy of the Bunter Salz.

The fine-crystalline to coarse-crystalline halite interbedded with the Anhydritmittel contains a varying proportion of impurities in the form of anhydrite streaks, flasers and shreds, which reflect a repeated rhythmic structuring of the beds. Major cycles (thickness in the order of metres) and minor cycles (thickness in the order of decimetres) can be clearly differentiated. Each cycle (even the minor cycles) begins at the base with a pure salt zone, which gradually becomes more impure upwards as a result of anhydritic contamination. The cycles then end in a swath zone with a high proportion of impurities. A sharp boundary marks the next pure salt zone. The rhythmic structure of these beds can be used to differentiate top from bottom. Below the Anhydritmittel, the rhythmic structure of the beds is usually not developed. The swath zone is absent in these cases and thus the Anhydritmittel starts directly above the pure salt zone.

Polygonal structures are only encountered within Anhydritmittelsalz 1. They are arranged parallel to bedding and extend over several metres. HERDE (1953) interpreted these structures as desiccation cracks which were caused by the regression of the sea and desiccation of the sediments during sedimentation.

Almost every exposure of the Anhydritmittelsalz is marked by the presence of carnallite nodes as well as fissures healed with secondary carnallite and halite. This indicates that during diapirism the Anhydritmittelsalz were reservoirs for highly concentrated brines, which may still be present within the Anhydritmittel. The brines were partially released by the fracturing of the Anhydritmittel during deformation, which led to the impregnation of the neighbouring halites and the precipitation of secondary carnallites and halites. The conclusion that the Anhydritmittel are reservoirs for brines is confirmed by the finding that, from approx. 1762 to 1790 m in the salt dome exploration borehole Go 1005, the Anhydritmittel (z3AM7 to z3AM9) as well as the scattered anhydrite in the halite have been almost completely altered to polyhalite.

The overlying, approx. 12 m-thick **Schwadensalz (z3SS)** consists of a dirty-grey, fine-crystalline to medium-crystalline, occasionally coarse-crystalline halite sequence irregularly interstratified with anhydritic flakes forming stripes and bands. The subdivision by HERDE (1953) into five pure halite zones and five swath zones, all with cyclic structures, is not present in the Gorleben salt dome.

The approx. 10 m-thick horizon of the impoverished **Kaliflöz Riedel (z3RI/na)** consists of red-brown to dark-grey, fine-crystalline to medium-crystalline halite with dark-grey clayey-anhydritic flakes and streaks. The interstices are filled with irregularly scattered red and yellow carnallite. The halite is only poorly translucent in transmitted light. The Kaliflöz Riedel was penetrated several times by salt dome exploration borehole Go 1004, and is also present as a potash seam horizon in borehole Go 1005.

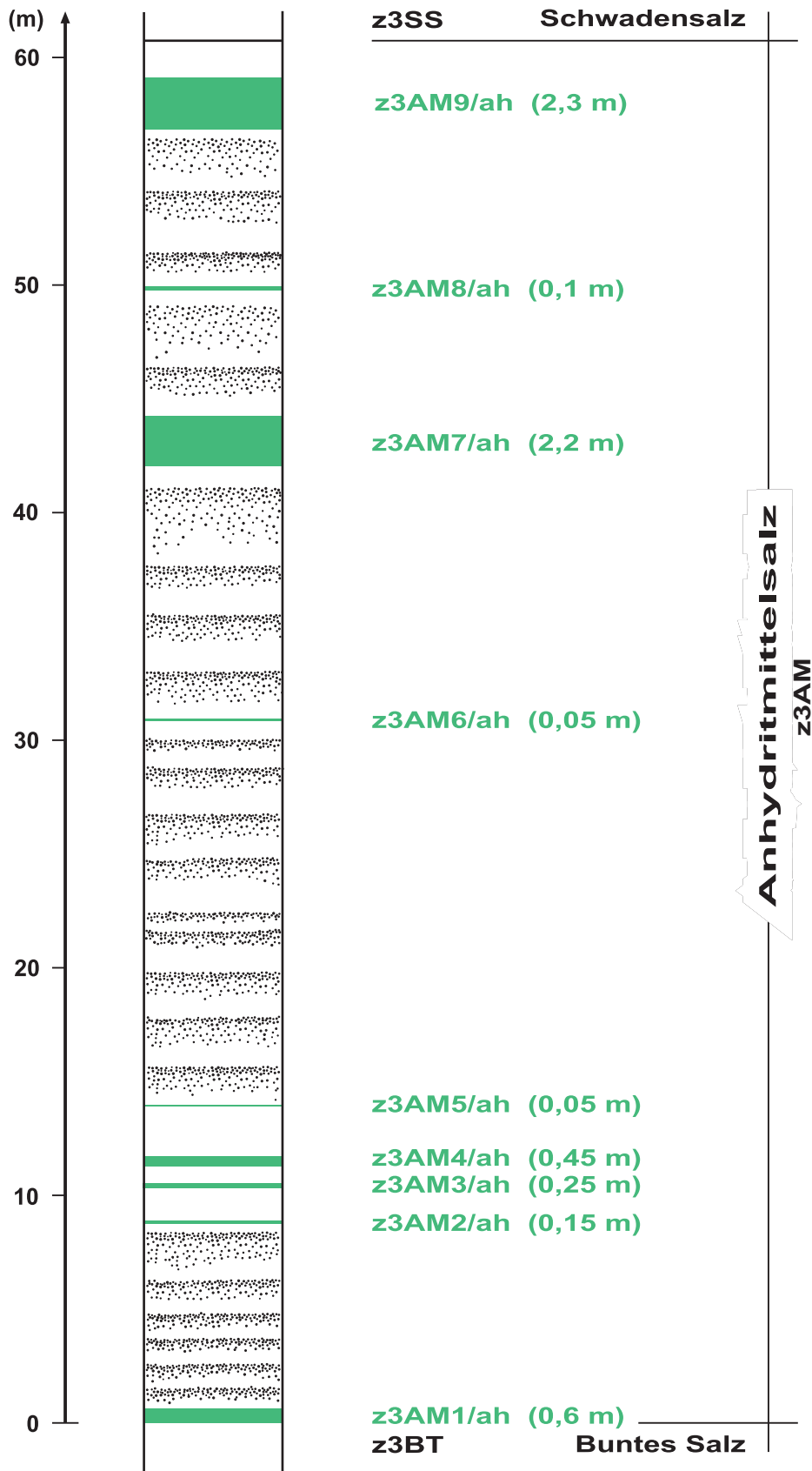


Figure 32: Schematic view of the sequence of strata in the Anhydritmittelsalz.

The boundary to the overlying approx. 36 m-thick **Tonmittelsalz (z3TM)** is located where red-brown clay clasts are embedded in the rock salt. The Tonmittelsalz is divided into five units consisting of three clay bands and 2 pure salt bands (Fig. 33). The clay bands consist of an alternating sequence of 1 to 5 cm thick halite layers and equally thick interbeds of clayey and to a lesser extent sandy texture and of grey, green or brown colour. These often contain stratiform deformed idiomorphic halite crystals of a size of up to 1 cm. The numerous fissures are healed with fibrous halite or fibrous carnallite. The clay content in the clay bands increases from base to top.

The upper boundaries of the first and second clay bands to the pure salt are distinct. The pure salt consists of orange-coloured, fine-crystalline to medium-crystalline halite with impurities of irregularly scattered layers of anhydrite flakes as well as occasional anhydritic bands of up to 1 cm thickness. The first pure salt is marked by several closely spaced anhydrite banks, with a maximum thickness of 20 cm.

3.3.1.3 Aller-Folge (Zechstein 4)

The **Roter Salzton (z4RT)** forms the pelitic base of the Aller-Folge. The boundary to the underlying Tonmittelsalz is blurred in the metre range. The Roter Salzton consists of red-brown claystone containing in some areas anhydritic fine-grained sandstone nodules up to 5 cm in size as well as deformed idiomorphic halite crystals up to 2 cm in size. The bedding is usually difficult to identify because of strong deformation. The numerous fissures are healed by fibrous halite. The top of the Roter Salzton is formed by a grey-green claystone bed, which is approx. 10 cm thick. The Roter Salzton has a thickness normal to bedding of up to 10 m.

A sharp boundary marks the base of the overlying **Pegmatitanhydrit (z4PA)**. The sedimentological structure of this bank that primarily consists of anhydrite and has a thickness normal to bedding of approx. 1.5 m can be divided into five sedimentary units (BORNEMANN 1991; KLÖCKER 2000). Using three cores from the areas of Hanover, Halle and Gorleben, KLÖCKER (2000) demonstrated that these five sedimentary units can be correlated even over long distances. This indicates that similar sedimentary environments existed over a large area of the Zechstein Basin during the sedimentation of the Pegmatitanhydrit.

Characteristic features are the locally abundant occurrences of anhydrite pseudomorphs to gypsum up to 15 cm in size, as well as beige-grey magnesian blobs and layers (Fig. 34).

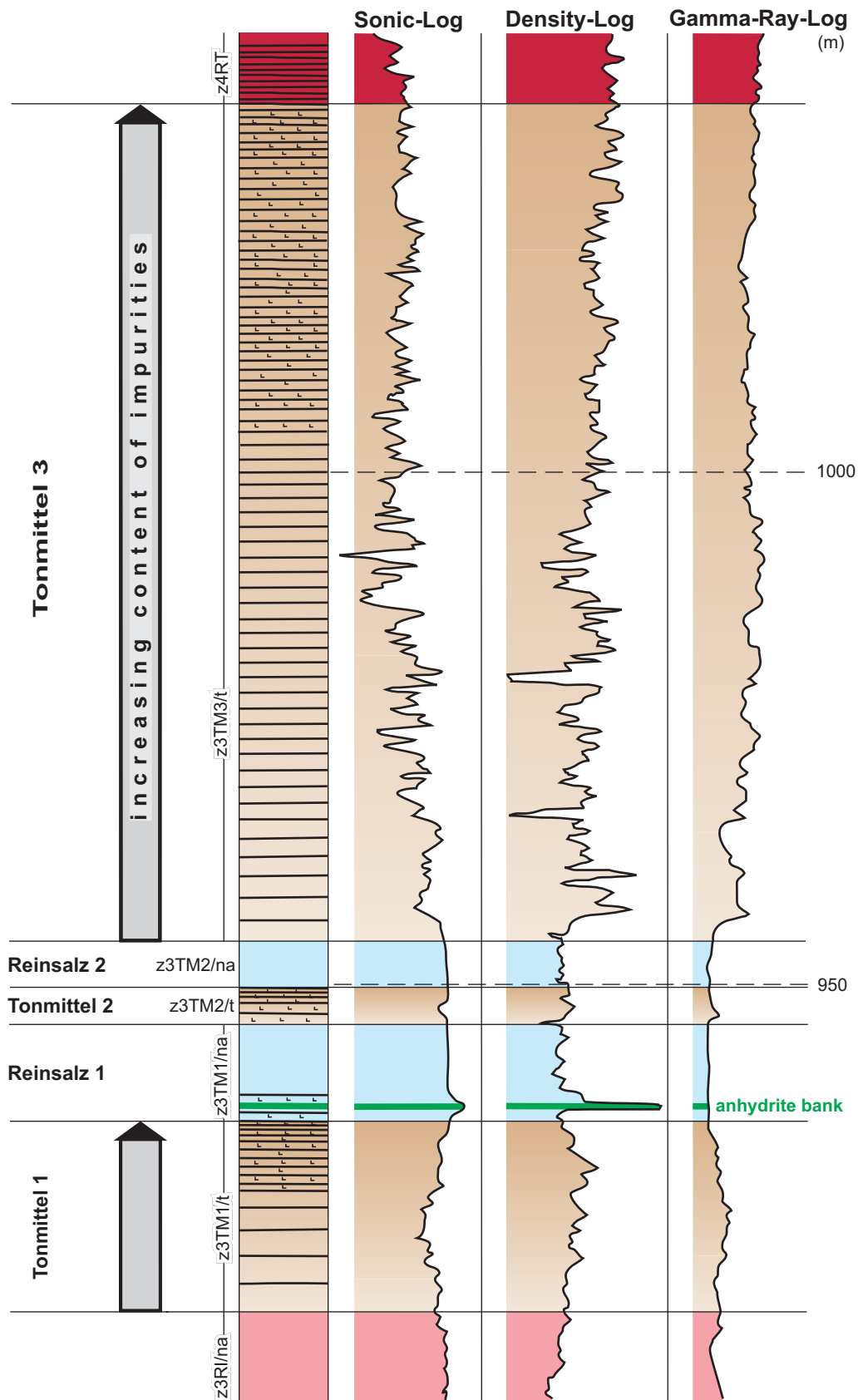


Figure 33: Borehole log and petrographic sequence of the Tonmittelsalz as encountered in salt dome exploration borehole Go 1004.

The Pegmatitanhydrit can be divided from base to top into the packages of beds detailed below. The Roter Salztön is superposed by the lowest bed of the Pegmatitanhydrit which consists of a grey, dense, jaspoid anhydrite bank several centimetres thick (**z4PA1**), interstratified at the base with beige-grey algal carbonate lamellae. Above lies brown-red anhydrite rock (**z4PA2**) interspersed with halite nodes. The base of z4PA2 contains stratiform, centimetre-sized, angular magnesian blobs. The upper part contains irregularly scattered anhydrite pseudomorphs of gypsum. The package **z4PA3** consists of magnesian algal-carbonate lamellae (1 to 2 cm thick) with local stromatolite-like structures.

The overlying **z4PA4** bed is characterised by beige-grey magnesian algal carbonate blobs and anhydrite pseudomorphs of gypsum with a size of up to 10 cm and more, which are irregularly scattered throughout the bed. Its bedding is indistinct or non-existent. The youngest stratigraphic bed (**z4PA5**) consists of an alternating sequence of anhydritic carbonate laminate layers and layers of anhydritic pseudomorphs of gypsum, the points of which have grown on the anhydritic-carbonatic lamellae. The pseudomorphs open towards the roof.

The **Basissalz (z4BS)** is tinted orange and is fine-crystalline. It is characterised by light-grey scattered anhydrite bands some millimetres to 2 cm thick. The anhydrite bands decrease towards the top and fade into thin polyhalitic bands and lines of flakes. Kieseritic blobs of up to 2 cm in size are irregularly scattered within the rock salt. The total thickness of the Basissalz is approx. 25 m.

The beds of the **Schneesalz** and **Rosensalz (z4SS, z4RS)** are indistinguishable from one another in some exposures in the salt dome. This rock salt is red-orange, mainly fine-crystalline and contains local inclusions of kieselite flakes. Typical features are thin polyhalitic bands with anhydrite occurring at intervals of 20 to 50 cm. Isolated carnallite nodes with a size of some millimetres to 1 cm are irregularly scattered within the sequence. The lower part of the sequence contains an approx. 50 cm-thick, fine-crystalline, grey anhydrite bank. The total thickness of both units is approx. 8 m.

The youngest stratigraphic member is the **Tonbrockensalz (z4TS)**. It was divided into the Unteres and Oberes Tonbrockensalz based on differences in the appearance of the claystone inclusions. The **Unteres Tonbrockensalz (z4TSU)** is grey-brown to brown-orange and contains thick stratiform layers of clay flakes, which in turn contain light-grey anhydrite blobs, shreds and clasts. These clay flake layers occur at intervals of 5 to 20 cm. In contrast to this, the **Oberes Tonbrockensalz (z4TSO)** has irregularly scattered clay flakes and lumps instead of stratiform layers. Bedding is very difficult to identify. Other impurities are light-grey, fine-crystalline anhydrite knots and flasers of some millimetres to 1 cm in size.

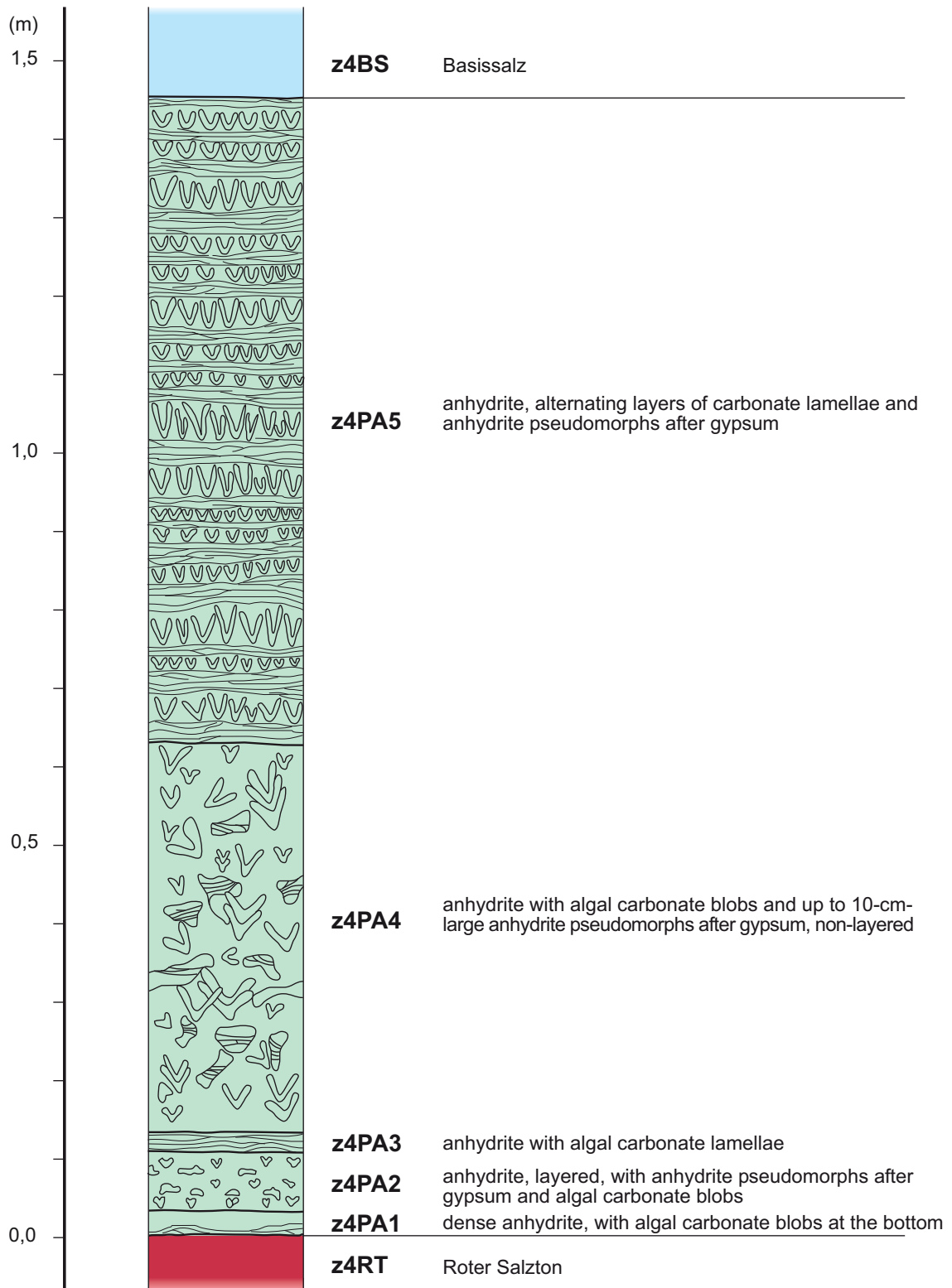


Figure 34: Schematic view of the stratigraphic sequence and petrographic structure of the Pegmatitanhydrit.

3.3.2 Structure of the Gorleben salt dome

3.3.2.1 Large-scale folding in the Gorleben salt dome

The internal structure of a salt dome is characterised by the extreme folding of the sequence of strata that form the structure. Principally, two deformation levels are differentiated within the salt domes formed by Zechstein sediments in Germany and adjacent countries: the first consists of rock salts of the Stassfurt-Folge (z2), and the second consists of the younger beds of the Leine-Folge and Aller-Folge (z3 and z4; see also Chapter 3.3.1).

With respect to the external shape of a salt structure, the type and arrangement of faults, and the large-scale folding of the two halotectonic units of the Zechstein 2 and Zechstein 3/4, it can be said that rounded and small oval salt domes have an extremely complicated internal structure whilst elongated oval diapirs have a less intense large-scale folding. Along the longitudinal axis of the elongated structures mostly coherent sections of homogeneous Zechstein 2 rock salt are found.

In Figure 35, the internal structure and size of the Gorleben salt dome, mapped as a geological outline of the 840 m-level, are compared to other salt domes, clearly demonstrating the finding mentioned above.

The internal structure of the Gorleben salt dome is shown in one vertical (Fig. 36) and one horizontal (see Fig. 8) geological cross section (see also BORNEMANN 1991: App. 21, 23). The construction is largely based on the results of the salt table boreholes, salt dome exploration boreholes and shaft pilot boreholes. The figures show the three stratigraphic units of the Stassfurt-Folge, Leine-Folge and Aller-Folge cropping out at the salt table as well as the mainly assumed outcrops of the Hauptanhydrit and the Kaliflöz Stassfurt. Additional vertical profiles and geological maps of individual levels are attached to this report in Appendices 4 and 5.

The vertical and horizontal cross sections show four tectonic/stratigraphic units from NW to SE, which are predominantly aligned with the axis of the salt dome, taking into account a cross fold that cannot be identified in more detail. These units are the NW flank of the salt dome with beds of the Leine-Folge and Aller-Folge followed in the SW by the core of the salt dome, which consists of the Hauptsalz of the Stassfurt-Folge. The third structural section is the SE flank of the salt dome, which forms an inverted syncline parallel to the axis of the salt dome in the well-explored central part of the salt dome. This structure contains the youngest beds cropping out at the salt table (see borehole GoHy 3010, Fig. 8). The fourth unit is the salt overhang to the SE, which primarily consists of an inverted section of the Hauptsalz that originated from the core zone. The structure in this

part of the salt dome can be explained as follows: during an earlier stage of salt dome formation, the faster flowing Hauptsalz overfolded the salts of the Leine-Folge and Aller-Folge, which then were formed into the present-day inverse syncline.

The series of cross sections in BORNEMANN (1991: App. 23) and in Appendices 4 and 5 give an idea of the extent and geometry of these four structural sections in the salt dome. The cross sections are mainly based on the results of the exploration and salt table boreholes. For the zones near the surface, the results of the salt table boreholes were integrated into the presentation.

The vertical geological cross section (Fig. 36), which is based on the results of salt dome exploration boreholes Go 1002 and Go 1005, shows an interpretation of the structure down to the base of the salt dome. This incorporates the drilling results of the deep borehole Gorleben Z1 drilled on the NW flank of the structure. These showed that the bottom of the salt structure is primarily made up of evaporites of the Leine-Folge and Aller-Folge. The Hauptsalz of the Stassfurt-Folge has largely migrated from the rim synclines on the flanks into the salt dome.

A horizontal geological cross section of the exploration level is given in BORNEMANN (1991: App. 22) and in App. 4. This cross section is based on the results of the exploration boreholes, shaft pilot boreholes and salt table boreholes and particularly on the analyses of the oriented cores extracted from these boreholes. When determining the horizontal extent of the core zone consisting of the Hauptsalz of the Stassfurt-Folge, it was assumed that wherever the Hauptsalz was found at the salt dome surface by salt table boreholes it also had to be present further below. However, it must generally be assumed, that the folding and stratigraphic boundaries depicted beyond the diameters around the boreholes specified above are not true representations but merely projections based on general halotectonic considerations.

Figure 35 outlines the complicated internal structure of salt domes. In addition to the projection of the 840 m-level within the Gorleben salt dome (BORNEMANN 1991), horizontal cross sections of four other salt structures are shown at the same scale to compare sizes (ESSAID & KLARR 1982; HERDE 1953; MIDDENDORF & KÜHN 1966; RICHTER-BERNBURG 1980; SCHACHL 1987). Unlike the Gorleben salt dome, the internal structure of the other four salt structures is well documented by exposures in mine workings and underground boreholes. The salt domes of Hänigsen-Wathlingen and Benthe are similar to the Gorleben salt dome in structural style and outline. However, the Benthe salt dome is marked by steep-axial tectonics, i.e. overlapping folds, and thus cannot be used for comparison. Like the Gorleben salt dome, the Hänigsen-Wathlingen salt dome has gently plunging fold axes

aligned to the longitudinal axis of the salt dome. These fold axes have a certain amount of cross-folding (DE BOER 1971). Thus, with respect to the underground exploration of the Gorleben salt dome, the Hänigsen-Wathlingen salt dome can be used as a model for the overall deformational style of the internal structure.

Folds of all sizes occur in the Gorleben salt dome with amplitudes in the order of centimetres to 100 m. Folding affects almost all stratigraphic sequences encountered in the salt dome with almost no fracturing. The only exception is the Hauptanhydrit, which fractures during folding and breaks up into separate segments that then float as isolated blocks lined up in the bedding of the surrounding rock salt (Fig 37).

The thicker anhydrite bands behave similarly (see Fig 19). They form boudin-type bodies lined up along the bedding like a string of pearls. The folding is mostly isoclinal, i.e. the bedding of both flanks of the fold is parallel, which means that it is often difficult to identify the core of the fold if marker banks are missing. To a lesser extent, symmetrical folds also occur. There is no apparent correlation between lithology and fold location and type. The type of folding is probably dependent on the degree of deformation. It is assumed that isoclinal folds always occur in a more strongly deformed zone.

Analysis of the core material and the underground exposures reveal that the majority of the fold axes plunge at relatively shallow angles up to a maximum of 30 °. Fold axes with steeper plunges are rare. This leads to the conclusion that the major folds in the salt dome also show more or less shallow axial plunges (DE BOER 1971; BORNEMANN 1979).

In the boreholes and the explored areas in the salt dome, there is no evidence of large-scale overlapping folds, which would require steep-axial tectonics. The hypothesis that there are no overlapping folds in the Gorleben salt dome, which had been formulated fairly early during the surface drilling programme, was fully confirmed by subsequent drilling and underground exploration.

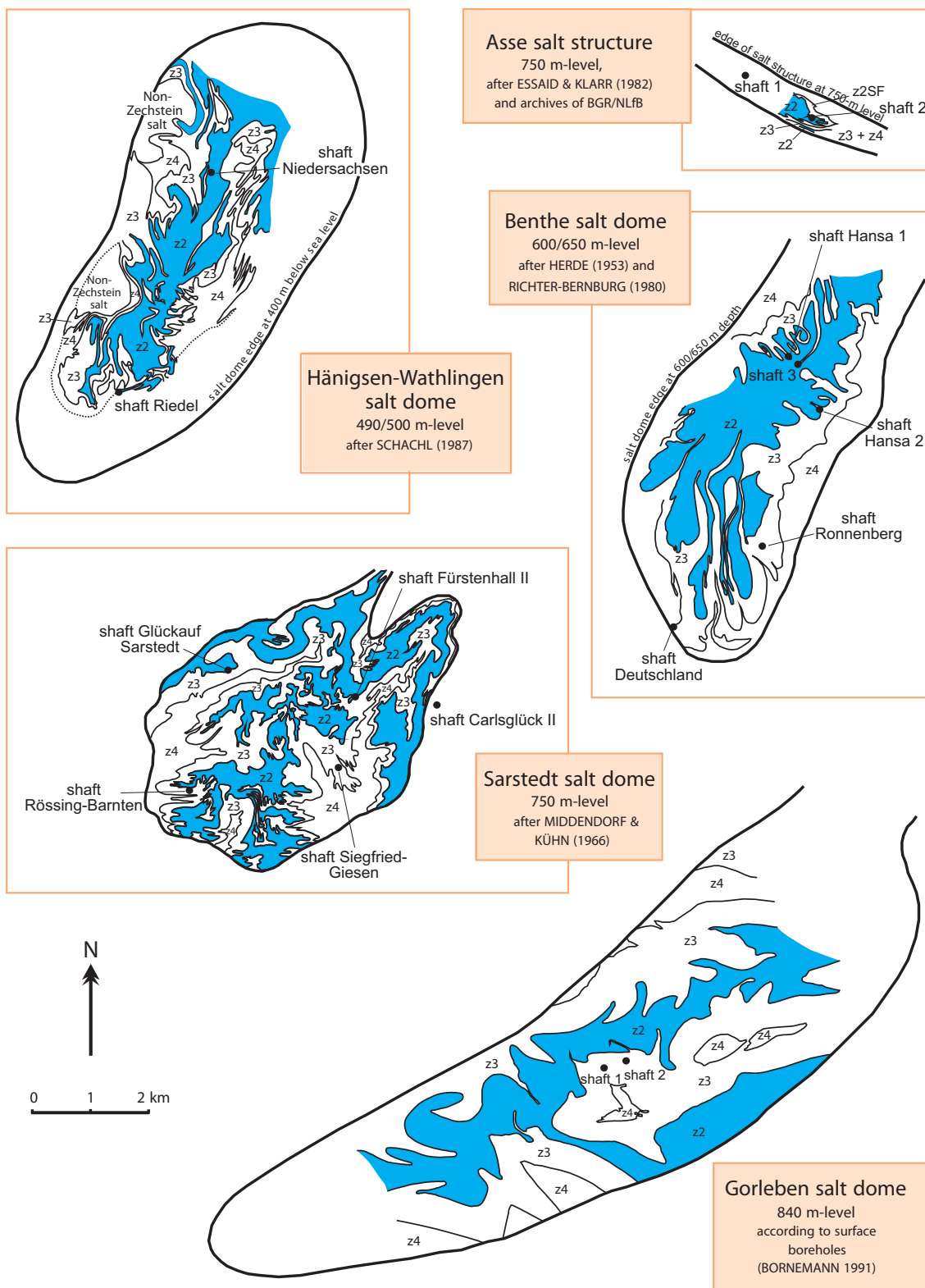


Figure 35: Geological outline of the Gorleben salt dome and comparison of the z2 extent with other salt structures.

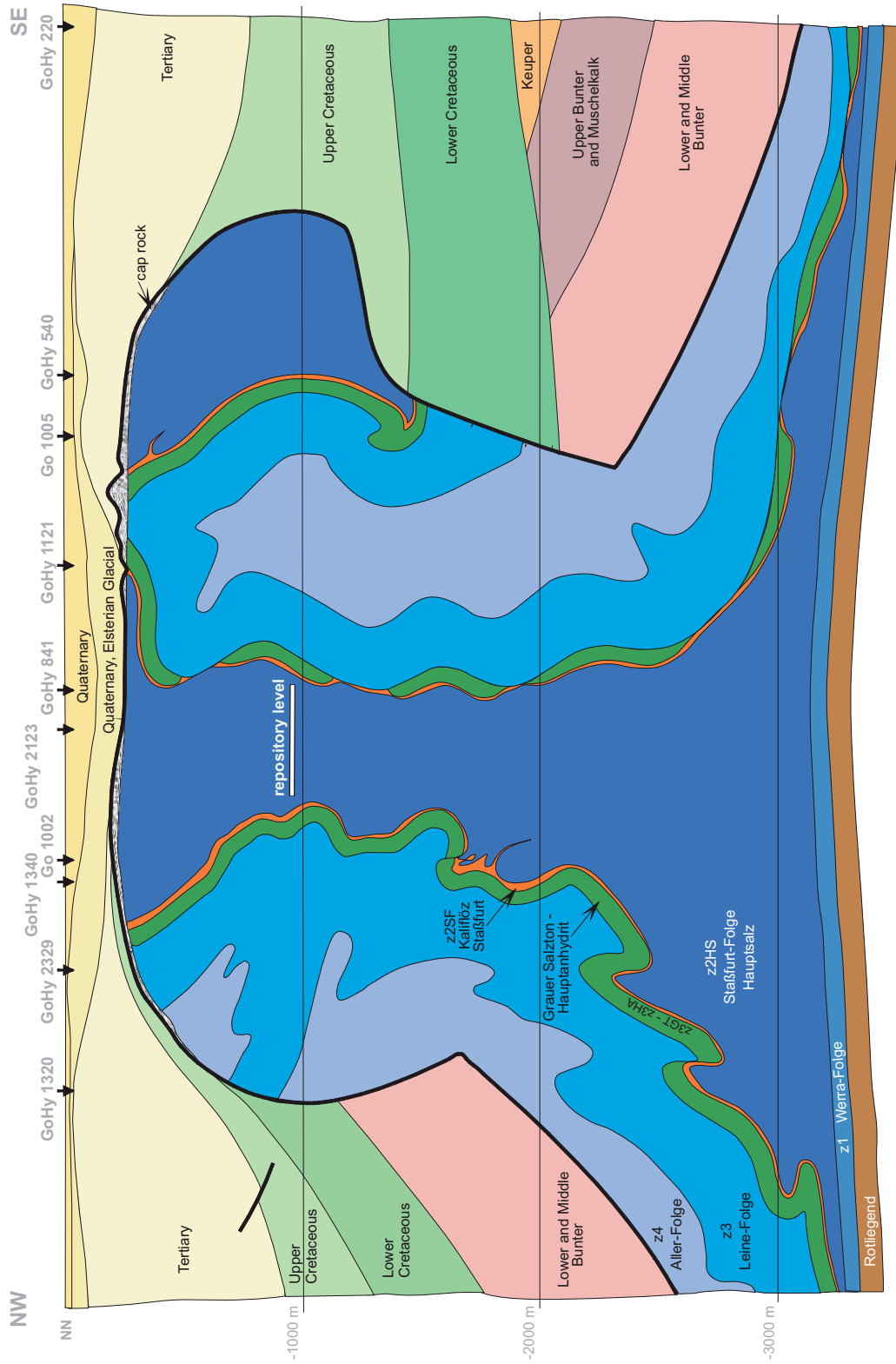


Figure 36: Simplified cross section of the Gorleben salt dome (cross section C-C); from BORNEMANN 1991, App. 23). The Hauptnhydrit is shown in a simplified form as a continuous band.

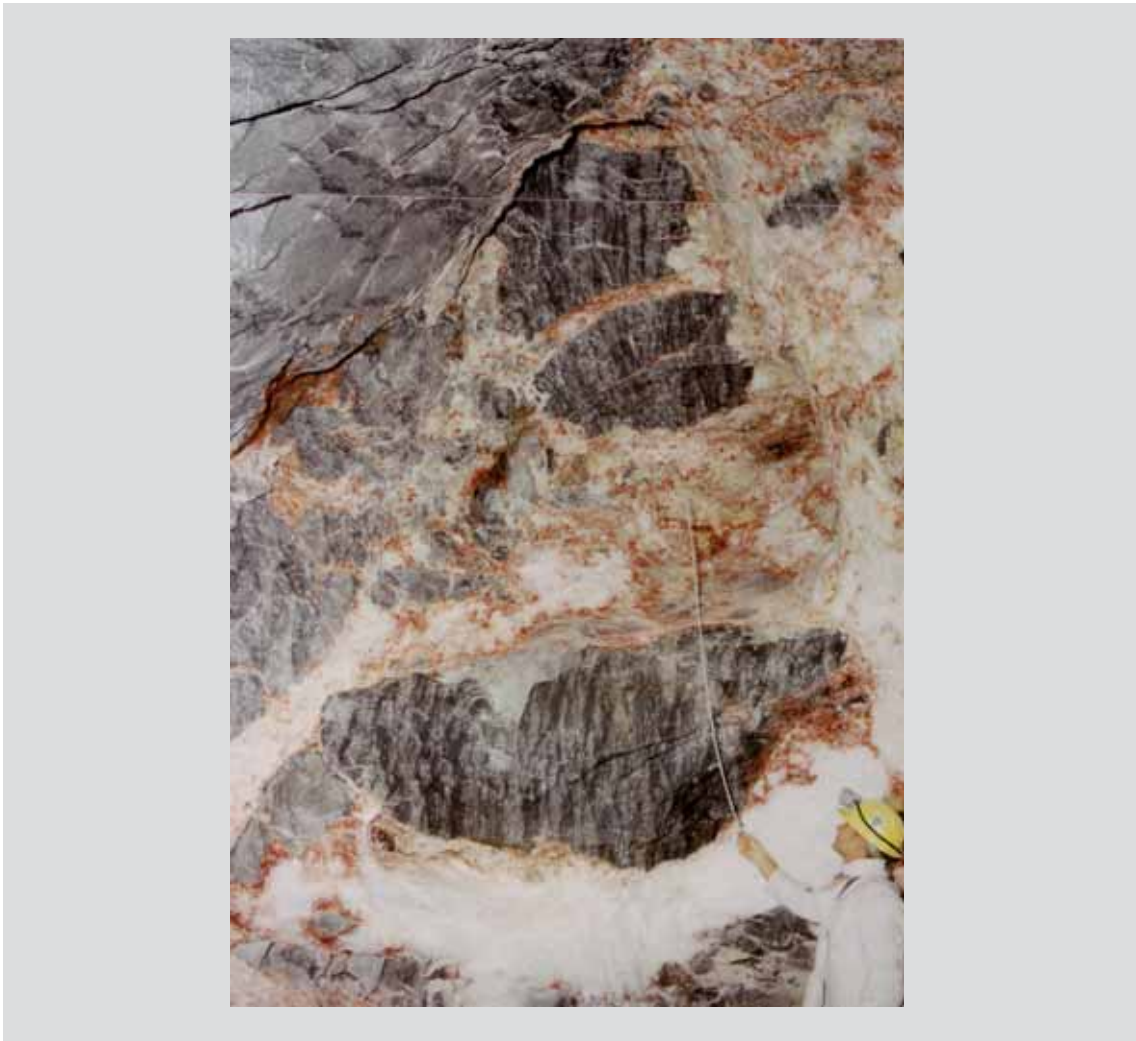


Figure 37: Lumps of Hauptanhydrit in secondary carnallite halite matrix.
The lumps have been sheared from a Hauptanhydrit block due to halotectonics.
Cross-cut 1 West, 840 m-level, drift location 40 m, former drift face.
(Photograph: Bauer, DBE)

3.3.2.2 Investigation of the structural geology in the shafts

The following is a summary of the investigation results on the structural geology in the shafts.

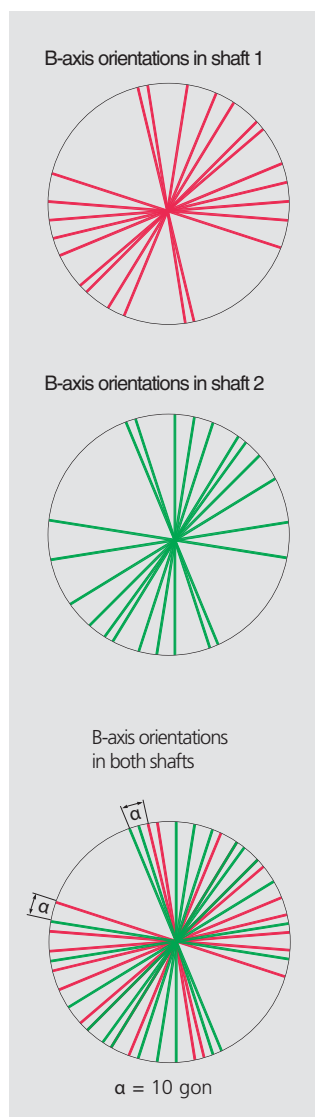
Fold inventory

The older stratigraphic units of the Leine-Folge were mapped in the upper section of Shaft Gorleben 1, whilst the younger stratigraphic units of the Leine-Folge were encountered in Shaft Gorleben 2. Due to the north-westerly dip of the beds in Shaft 1, the shaft is closer to the Zechstein z2/z3 boundary even though Anhydritmittelsalz was encountered in the lower part of the shaft.

Eight major folds were identified in both shafts. Due to their similar tectonic inventories, it was possible to correlate the major folds. The same applies to the zones with minor folds or subordinate folds.

Fold axes (B-axes)

If the direction of the B-axes alone is considered without taking into account the direction or the amount of plunge, it becomes clear that both shafts have the same B-axis inventory (Fig. 38). The axis spectrum ranges from N-NW to W-SW or S-SE to E-NE. It is noted that the directional spectrum of the B-axis inventory in Shaft 2 is rotated to the west by approx. 10 gon compared to the directional spectrum in Shaft 1.



If the depth dependency of the plunge direction of the B-axes is combined with the geological findings in the shafts and at the 840 m-level (BORNEMANN et al. 2001), it becomes evident that the different structural styles depend directly on depth (Fig. 39). Below 604 m (cyan-coloured in Fig. 39) the folding style is completely determined by the Zechstein 2 updoming. In the shafts, the B-axes are therefore perpendicular to the outline of the Zechstein 2 updoming.

The middle section between 490 and 604 m (coloured yellow-orange in Fig. 39) is also influenced by the Zechstein 2 updoming. However, here only the roof section of the Zechstein 2 updoming affects the structure. However, the first plunge directions that reflect the original plunge directions before the formation of the Zechstein 2 updoming also appear. This zone therefore represents the transition between the influence of the Zechstein 2 updoming and the primary large-scale structure of the salt dome. From 490 m to the salt table (coloured magenta in Fig. 39), the original large-scale structure is present with virtually no influence from the Zechstein 2 updoming.

Figure 38: Comparison of fold axis directions (B-axes) in Shafts 1 and 2.

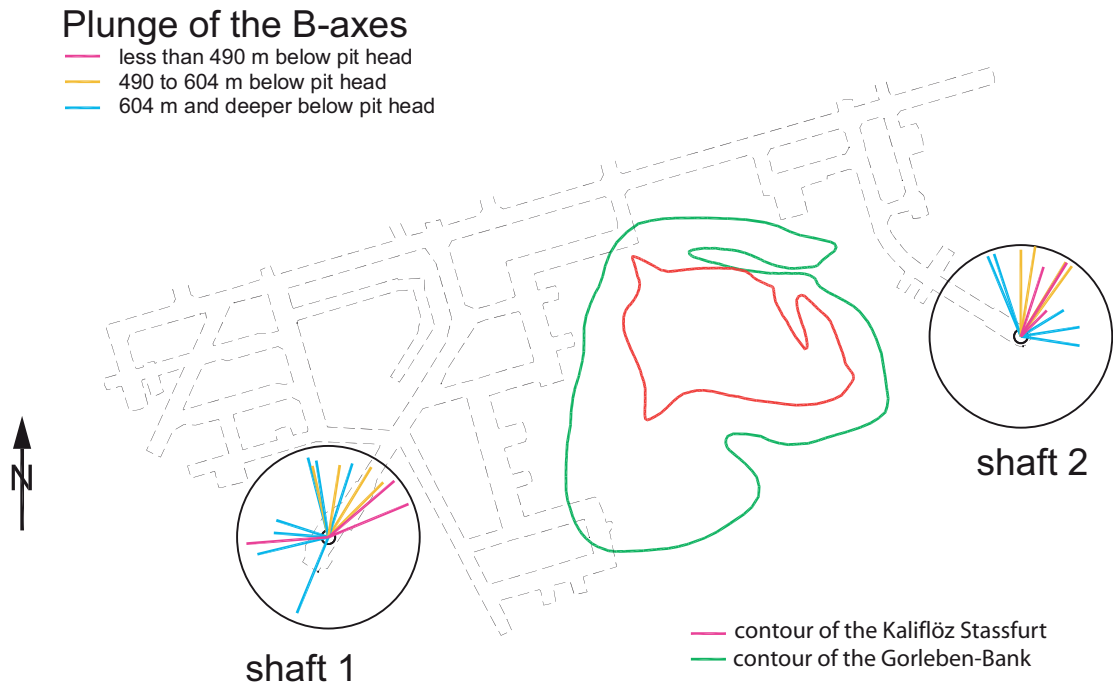


Figure 39: Plunge of the fold axes in the shafts.



Figure 40: Dip of the axial planes in the shafts (see also Fig. 39).

Axial planes

The dip directions of the axial planes also depend on depth. Accordingly, the Zechstein 2 updoming also affects the spatial arrangement of the axial planes. As the dip of the axial planes points orthogonally away from the outline of the Zechstein 2 updoming, the updoming is enclosed by the axial planes below 604 m (coloured cyan in Fig. 40). Of note is that the northern side of the roof section of the Zechstein updoming is encountered in the middle section of Shaft 1 from 490 to 604 m whilst the southern side is encountered in Shaft 2. The original large-scale structure of the salt dome resumes above 490 m.

Thicknesses of beds

The thickness of the beds in both shafts decreases considerably on the flanks of the folds while a considerable increase is observed in the hinge zones. Thinning on the flanks of the folds is more marked in Shaft 1, whilst thickening in the fold hinges is more dominant in Shaft 2.

3.3.2.3 Geological structure of the infrastructure section

The following summarizes the exploration results on the geological structure of the infrastructure area. Information gained from drilling in the area around the shafts revealed five different structural subzones:

- Zechstein 2 updoming between the shafts
- SE-verging folds in the area of Shaft 1
- SW-verging folds in the area of Shaft 2
- Fold zone north of the Zechstein 2 updoming
- “Shear” and fold zones at the boundary between Zechstein 3 and Zechstein 2

The Zechstein 2 updoming between the two shafts was identified very early in the exploration programme. A part of this updoming is formed by a very thick layer of the Kaliflöz Stassfurt, which was encountered at the 840 m- and 820 m-levels. In the roof of the Zechstein 2 updoming, the Kaliflöz Stassfurt has accumulated and has a thickness of approx. 70 to 80 m. From the 930 m-level downwards, the beds of the Hangendsalz and Kristallbrockensalz appear. The potash seam resumes its normal thickness on the flanks of the Zechstein 2 updoming. The sequence from the Hauptanhydrit (z3HA) to the Gebänderter Deckanhydrit (z2DA) (totalling a thickness normal to bedding of max. 100 m) was pinched off by halotectonics with the exception of a few isolated block fragments. The Basissalz (z3BS) is only present in the form of residues affected by tectonics. The

pinch-off of the potash seam and the associated missing bedding of approx. 100 m, led to major stress redistribution in this zone and local fragmentation of the Mittleres and Unteres Orangesalz. This process must also be the source of the fissures in the Bank-/Bändersalz in the pilot drift of Shaft 2 (820 m-level) and in Shaft 2 (from 802 m to 850 m in the Oberes Orangesalz to Bank-/Bändersalz).

To the NW (in the area of Shaft 1), the Zechstein 2 updoming is followed by a syncline, an anticline, and another syncline, followed by tightly folded Liniensalz down to the Zechstein 3/Zechstein 2 boundary. All the beds in this zone have a north-westerly dip. The folds are isoclinal and point to the SE, i.e. they lie on the Zechstein 2 updoming. The youngest sequence of strata found in the synclines is the Anhydritmittelsalz, while the syncline east of Shaft 1 only contains thin beds of the lower Anhydritmittel. The syncline west of Shaft 1, which was encountered during the sinking of the shaft and which contains only the Anhydritmittel 1 to 4, contains no Anhydritmittelsalz on the 840 m-level due to the varying axial plunge of the B-axes in the SE part of the syncline. The intersection of boreholes 01YEF20 RB059 and 02YEF11 RB013 is the deepest point of the synclinal axis. In addition to the lower Anhydritmittel of the Anhydritmittelsalz, these two boreholes also penetrated Anhydritmittel 7 and 9 which have a thickness normal to bedding of max. 2.2 and 2.3 m respectively.

As in the western part, the Zechstein 2 updoming (around Shaft 2) is followed in the E and NE by a syncline, an anticline, and another syncline. All beds in this zone dip to the NE and the folds lean to the SW, i.e. just like the folds around Shaft 1, they also lie on the Zechstein 2 updoming. Unlike the strictly isoclinal folds around Shaft 1, the folds to the NE of Shaft 2 appear to open, so that broad outcrops of the Liniensalz to Orangesalz beds occur. This trend also appears to continue to the east.

Analysis of borehole 01YEF20 RB003 confirms that the folds are linked by centroclinal strike of the axes around the Zechstein 2 updoming. From 72.45 to 112.6 m a symmetric anticline in the Liniensalz was encountered in this borehole. The anticline causes a parallel strike of the Unteres and Mittleres Orangesalz so the Liniensalz in the Zechstein 2 updoming is not structurally linked to the Liniensalz occurring further to the north.

Synopsis of the folding in the infrastructure area and in the vicinity of the shafts

Some of the folds encountered in the shafts reach as far downwards as the 840 m-level, at least to the north of the shafts. The results of drilling and drifting in the infrastructure zone (BORNEMANN et al. 1998) allowed detailed mapping of the horizontal geometry of the Zechstein 2 updoming between the shafts. By relating the large-scale folds identified in the shafts to those at the 840 m-level, the maximum height of the Kaliflöz Stassfurt in

this part of the salt dome could be estimated. This is at approx. 770 m depth and approx. 170 m west of Shaft 2. The northern and eastern flanks of the Zechstein 2 updoming dip steeply downwards whilst the western flank dips at a much shallower angle SE of Shaft 1.

The steeply dipping flanks of the Zechstein 2 updoming result in the large amplitudes of the major folds to the north of the shafts, which in some places exceed 250 m. These fold amplitudes are evidence of the upward penetration by the Zechstein 2 updoming several hundred metres into the large-scale Zechstein 3 syncline of the infrastructure/shaft zone. Thus, the Zechstein 2 updoming is responsible for the depth-dependent structural variation encountered in the shafts.

Folding kinematics

Folding in both shafts and in the infrastructure zone consists of bending shear folds. This type of folding is due to the collective folding of thick incompetent halite layers interbedded with thin competent anhydritic beds. As the competent anhydritic beds only form a small part of the total sequence, the proportion of shear movement is so large that in some parts there is a smooth transition to pure shear folding. The Gorleben-Bank as well as the thicker Anhydritmittel are the competent beds in this case whilst the surrounding beds, e.g. the sequence of Liniensalz to Unteres Orangesalz or the sequence of Oberes Orangesalz to Bank-/Bändersalz, are the incompetent beds.

The more competent beds envelop the less competent beds by forming large-scale folds. This causes typical disharmonic minor folding with strongly dipping axial surfaces in the less competent beds in the cores of the large-scale folds. Thus, the large-scale folds were used to determine the opening angle and the amplitude. It is of note that the isoclinal folding typical of salt domes is only found in Shaft 1, whilst Shaft 2 is characterised by tight folding.

Fold system development over time

Around the shafts, the large-scale folding of the salt dome is primarily marked by gently E-NE-plunging B-axes and semi-steep to gently dipping axial surfaces dipping N-NW. This is still preserved in the upper part of the shaft (magenta in Fig. 39 and 40). This folding of the Leine-Folge was penetrated secondarily from below by the evaporites of the Stassfurt-Folge sequence, which forced the primary large-scale folding upwards. The primary large-scale folds of the Leine-Folge were affected to such a degree that the B-axes were strongly shifted from their original direction and now show strong variations depending on the position of the exposure with respect to the large-scale fold. The Zechstein 2 updoming had only a minor influence on the plunge values, which remained gently dipping. However, the axial planes were subjected to extreme deformation and now have complex structures.

The remote effect of the Zechstein 2 updoming between 380 and 630 m caused the layers to lie horizontally between the shafts. This is why no EM reflections were registered in this part of the shaft; the alignment of the beds prevented reflections. EM reflections were only registered in the lower part of the area between the shafts where the beds again lie at a steep angle to the survey profile.

The secondary uplift of the evaporites of the Stassfurt-Folge into the Leine-Folge caused strong thinning by stretching of the beds on the flanks of the folds and compressional thickening in the former hinge zones causing an overall phacoidal pattern. This process may have been intensified by another Zechstein 2 updoming between approx. 350 and 750 m coming close to Shaft 2 from the N-NE. This would have compressed the isoclinal folds that were originally present in this section as well, causing today's tight folds. The combination of these two events led to the extreme increase in bedding thickness in the cores of the folds, the relatively low fold amplitudes, and the westerly rotation of the directional spectrum of the B-axes in Shaft 2.

In brief, the primary large-scale folds of the Leine-Folge were superimposed by two events: the Zechstein 2 updoming in the vicinity of the shafts and the exploration levels, and additionally, the Zechstein 2 evaporites intruding into the zone around Shaft 2 from N-NE. These two events led to today's multi-phase isoclinal folding of the beds of the Leine-Folge.

3.3.2.4 Structural geology of Exploration Area 1 (EB 1)

The following zones were identified in the structural geology of Exploration Area 1 (see Apps. 4 and 5).

Hauptsalz anticline

The Hauptsalz anticline is formed by z2HS beds with Knäuelsalz (z2HS1) in the anticline core. At the 840 m-level to the west of cross-cut 1 East, the z2HS anticline has a thickness normal to bedding of approx. 540 m. To the east of cross-cut 1 East, the thickness normal to bedding varies between 390 and 490 m. The variation in thickness is caused by the z3 drag fold, which is the result of the special folding on the northern flank at the 840 m-level.

The thickness normal to bedding in the NE is only a trend estimate because this area is marked by strong isoclinal internal folding and the fold inclusion of Streifensalz within the Knäuelsalz (e.g. the isoclinal Streifensalz syncline in driftway 2 East and the z3 drag fold in borehole 02YER20 RB254). In addition to this, there is a broadening of the outcrop of the Streifensalz and Kristallbrockensalz in the NE part of EB 1 in the area of boreholes 02YER20 RB254 and 02YER20 RB488 as a result of the gentle dip of the beds to N-NW.

The EMR surveys carried out in EB 1 revealed that the bedding thicknesses of z2HS encountered in the EB 1 exposures continue for at least 100 m above and below the 840 m-level. The core of the anticline consists of 165 m-thick Knäuelsalz to the SW and 230 m-thick Knäuelsalz to the NE. The position of the B-axis cannot be determined precisely because there is no longer any primary bedding in the Knäuelsalz. On the northern flank of the z2 main anticline, the Knäuelsalz is followed in the SW by Streifensalz with a thickness normal to bedding of 210 m. The thickness normal to bedding of the Streifensalz decreases to 80 m towards the NE.

The actual thickness of the Kristallbrockensalz remains largely constant at approx. 90 m over the whole northern flank. Only in the vicinity of the z3 drag fold penetrated by borehole 02YER20 RB254 does the Kristallbrockensalz thin out to approx. 60 m thickness normal to bedding. A bed of Hangendsalz 3 to 5 m thick was encountered along the whole northern flank, which in some parts contains isoclinally interfolded material of the Kaliflöz Stassfurt.

A meaningful statement of the thickness normal to bedding of the Streifensalz on the southern flank can only be given for the zone between drilling location 1.2 and borehole 02YER02 RB261. At this location the Streifensalz has a thickness of approx. 80 m. The Kristallbrockensalz is extremely thinned out or even wholly suppressed by halotectonics. The same applies to the Hangendsalz and the Kieseritische Übergangsschichten. To the E-NE of borehole 02YER02 RB261, the Streifensalz and Kristallbrockensalz are extremely isoclinally folded, along with interfoldings of z3 synclines, which structurally already belong to the southern z3/z2 boundary. The z2HS has a thickness ranging between 75 and 120 m along the whole southern flank of the Hauptsalz anticline (south of the anticlinal axis).

Southern flank of the Hauptsalz anticline

The southern flank dips at an angle of approx. 70 gon W-NW to NW in the western part of EB 1 to the NW of borehole 02YEF11 RB003. To the east, the dip turns to N-NW and becomes steeper with an angle of approx. 85 gon. Further on, the dip of the beds turns to the NW and abruptly switches to the west in the area of the ventilation drift and cross-cut 1 East. This change in dip along the flanks is interpreted as local displacement of the beds, as the drilling results of 02YER20 RB500 indicate a very steep dip towards S-SE. The southern flank on the whole is characterised by an overall W-SW to E-NE strike with steep dip.

The southern flank of the main anticline displays special folding due to strong lateral and vertical shear movements at the z2/z3 boundary. In some exposures single stratigraphic members are missing in the area of the z2/z3 boundary due to halotectonic pinch-off (Figs. 41 and 42). The shearing is associated with the uplift of the z2 rock salt. The main

uplift of the Zechstein 2 saliniferous formation occurred in the southern part of EB 1 and led to more intense folding on the southern flank than on the northern flank. This led to the formation of four z3 synclines at the 840 m-level (labelled synclines M 1 to 4 in Fig. 43) with widely differing dimensions. These are separated from one another by z2 anticlines and the Kaliflöz Stassfurt that marks the boundary to z3 in the infrastructure zone. These isoclinal folds are the result of shearing at the z2/z3 boundary and belong structurally to the southern flank. The transition from the Hauptsalz anticline to the main syncline of the infrastructure zone is to be interpreted as a complex shear zone (blue in Fig. 43). The two large-scale fold axes are not shown in their true positions and are only used to define the boundaries of the shear zone (black in Fig. 43).

The B-axes of the shear zone dip semi-steeply, sometimes steeply to the west. Anticline M1 therefore reaches farthest down in the area of cross-cut 1 West, extending down to approx. 200 m below the 840 m-level.



Figure 41: Boundary of Zechstein 2/Zechstein 3 with thinned-out Kaliflöz Stassfurt (centre) and halotectonic pinch-off of the sequence from Grauer Salzton to Hauptanhydrit (max. 100 m).

The Basissalz and remnants of the anhydrite bank (black circle in the Basissalz) of the Zechstein 3 sequence are on the right side and the thinned-out Hangendsalz and Kristallbrockensalz of Zechstein 2 can be seen on the left.

Cross-cut 1 East, drift position approx. 110 m, eastern wall.

(Photograph: Bauer, DBE)



Figure 42: Intensely deformed and folded Liniensalz with isoclinal interfolding of Orangesalz close to the Zechstein 3/Zechstein 2 boundary. The stripe intervals are in the centimetre range and the anhydrite stripes are torn into segments. Shaft undercut to the 880 m-level, drift position 369 to 374 m, western wall. (Photograph: Bauer, DBE)

The M1 syncline is the widest of the z3 synclines in the shear zone, being approx. 60 m wide, because large blocks of Hauptanhydrit occur on both flanks of the syncline. The depths and widths of the synclines depend on the distribution of the Hauptanhydrit. This is due to the lower mobility of the Hauptanhydrit blocks, which remained at depth whilst the rock salt rose upwards. They are therefore located in the hinge zones of the synclines. Extreme examples are synclines M 2 and M 3 penetrated by boreholes 02YER02 RB154 and 02YER02 RB261. The hinge zones, which lie approx. 140 m below the 840 m-level consist solely of Hauptanhydrit blocks with a thickness of a few tens of metres. At the 840 m-level, synclines M 2 and M 3 are only a few metres long and wide. Due to the westerly plunging B-axes, the z3 synclines taper off in the vicinity of cross-cut 1 East. Isoclinal shear folds in the Knäuelsalz and Streifensalz were encountered in the vicinity of cross-cut 1 East and to the north of syncline M 2.

The Kristallbrockensalz is significantly thinned out on the southern flank of the main anticline. The Hangendsalz and the Kieseritische Übergangsschichten are also almost completely absent due to halotectonics. At the contact between syncline M 1 and the infrastructure zone, the Kaliflöz Stassfurt occurs as two layers of brecciated carnallitite and forms the anticline separating syncline M 1 and the main syncline of the infrastructure zone. Blocks of Hauptanhydrit occur in the infrastructure zone only in boreholes 02YEF11 RB012 and 02YEF11 RB003. These boreholes are to the SW of cross-cut 1 West and are the

only ones which penetrated a completely stratiform sequence of the z2/z3 boundary. The presence of additional Hauptanhydrit blocks deeper down is expected only in the vicinity of the ventilation drift and cross-cut 1 East because here folded Basissalz was exposed which indicates the presence of Hauptanhydrit. Due to the extreme isoclinal folding of the Zechstein 3 sequence at the z3/z2 boundary in the infrastructure zone, major blocks of Hauptanhydrit are not expected at this location.

Northern flank of the Hauptsalz anticline

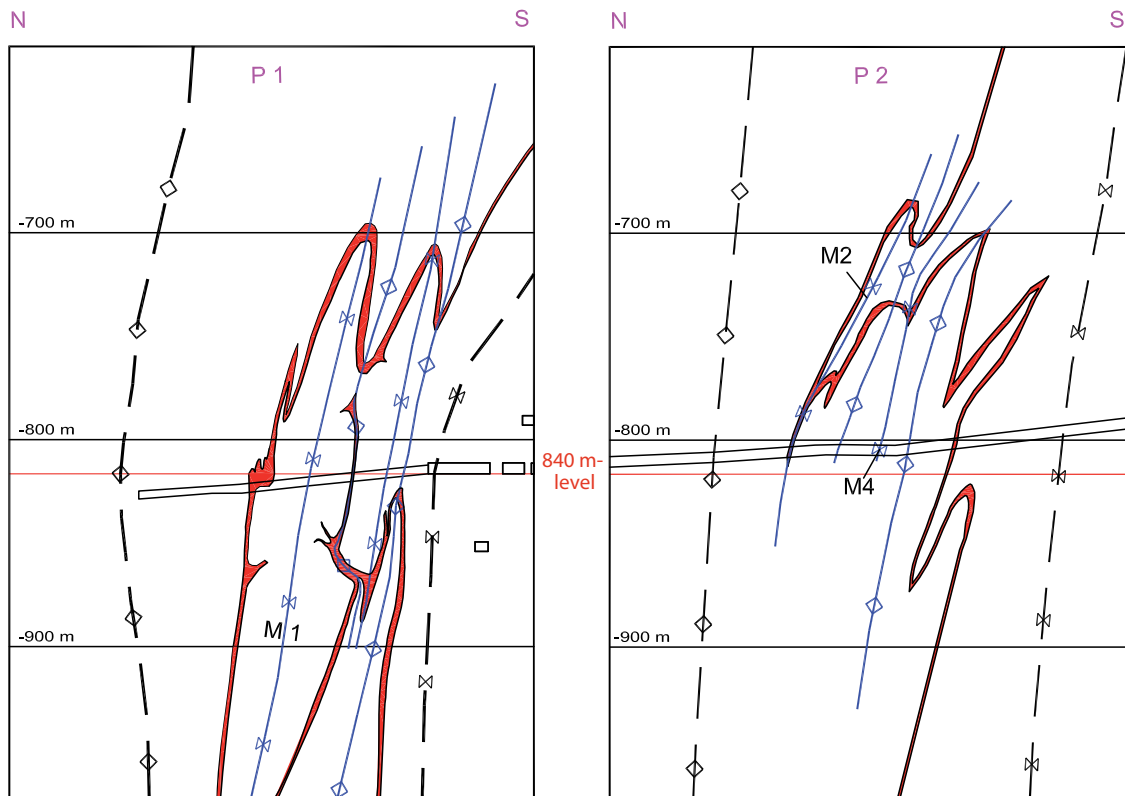
Analysis of the surface exploration boreholes Go 1002 and Go 1003 indicates that the northern flank has not suffered as severe shear movements as the southern flank and shows less special folding. Accordingly, a shear fold lying in front of the z2/z3 boundary was encountered only in the vicinity of borehole 02YER20 RB254.

Boundary z2/z3 in stratiform bedding

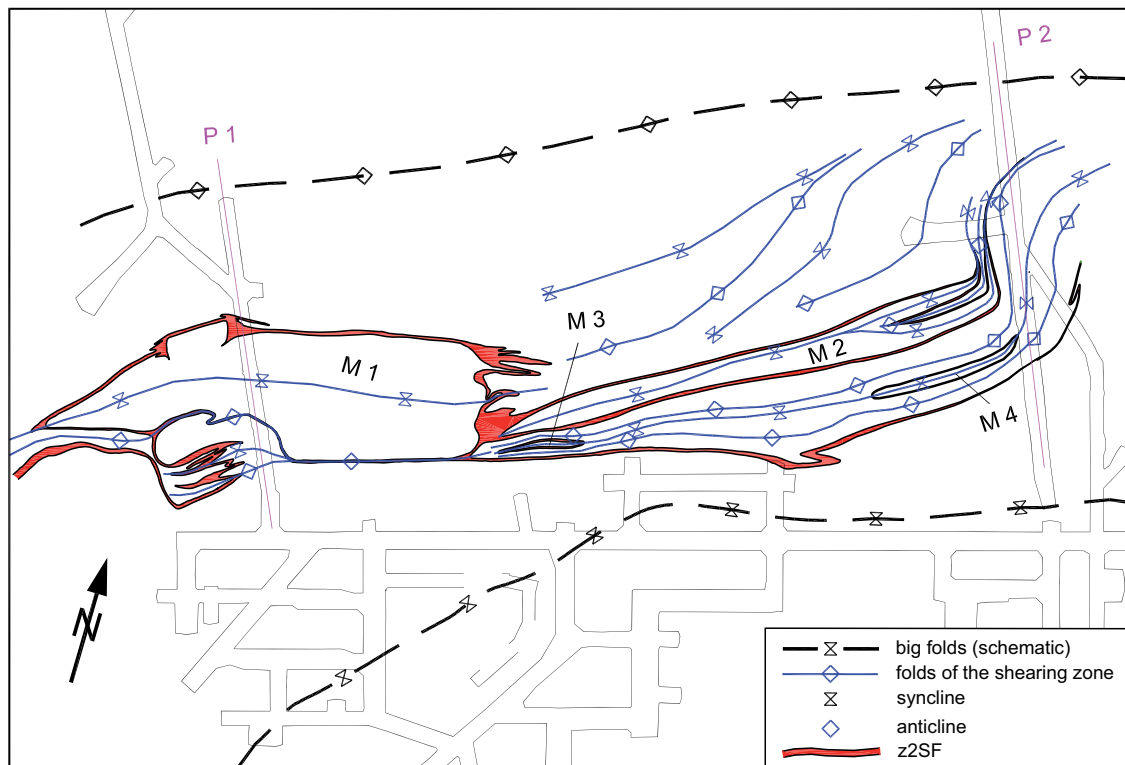
The z2/z3 boundary strikes W-SW to E-NE between drilling location 5.4 and borehole 02YER20 RB488. The beds dip steeply to the S-SE in the vicinity of deep borehole Go 1003 and drilling location 5.2. E-NE of drilling location 5.2, the dip of the beds changes to N-NW. Based on the drilling results and the results of the EMR surveys, the zone in which the dip direction changes can be narrowed down to the direct vicinity of drilling location 5.2. A fracture in the Hauptanhydrit to the NW of drilling location 5.2 can be clearly interpreted from the change in dip direction. Further on, towards borehole 02YER20 RB488, the dip oscillates between N-NW and NW. The dip of the beds at the z2/z3 boundary remains steep throughout the described zone. The angle of dip decreases to semi-steep only in the vicinity of borehole 02YER20 RB254.

A plausible projection towards depth can be made on the basis of the steeply dipping boreholes 02YER02 RB032 in the west and 02YEQ01 RB120 in the east, as well as the EMR surveys in boreholes 02YEQ01 RB427 and 02YER20 RB254 and the northern driftway. This projection still needs to be verified by drilling downwards. The continuation of the projection towards the east, incorporating the results of surface exploration borehole Go 1002 (BORNEMANN 1991), is to be considered an interpretation ahead of the face because of the large distance between the exposures. The dip of the beds appears to turn to the south and become steeper in the direction of exploration borehole Go 1002.

The strong changes in dip and strike of the beds indicate that the Hauptanhydrit is broken into individual blocks on the northern flank as well. Here, the Hauptanhydrit blocks are probably closer together than on the southern flank because the northern flank has been less affected by shearing.



Sketch of profiles P1 and P2



Sketch of 840 m-level

Figure 43: Sketch showing two profiles (P1 and P2), and an outline of the fold structure on the southern flank of the main anticline.

Boundary z2/z3 with z3 drag fold

The outcrop of the z3 drag fold at the 840 m-level is limited to the zone between drilling location 5 and borehole 02YER20 RB488. The drag fold continues downwards for a distance of 50 m maximum. The interface with the z2/z3 boundary is formed by a dual-layer potash seam. Towards the roof, the drag fold can no longer be distinguished from the z2/z3 boundary, i.e. the fold is only a local dragging of the z2/z3 boundary to the 840 m-level. The fold was caused by displacement of Hauptanhydrit blocks on the northern flank during diapirism.

The Hauptsalz beds dip to the NE, and this dip becomes shallower from the core zone towards the northern flank. This trend is confirmed by EM reflectors above and below the borehole. Due to the structuring on the northern flank, a connection between this drag fold and the apophysis of the Kaliflöz Stassfurt in borehole Go 1003 is unlikely.

3.3.3 Mineralogy and geochemistry of the salt rocks

3.3.3.1 Bromide standard profile of the Stassfurt-Folge (Zechstein 2)

To be able to assess the bromide distribution in the Zechstein 2 rock salt in the part of the Gorleben salt dome explored so far, the bromide profiles of boreholes Go 1002, 02YEQ01 RB119 and 02YER20 RB254 were presented in a diagram (Fig. 44). The diagram was created as follows:

- All profile sections with recognisable folding were cut from the individual profiles. The following profile sections were used:
 - Bromide profile Go 1002: drill metrage 572.35 to 616.29
 - Bromide profile 02YEQ01 RB119: drill metrage 0 to 38.85
 drill metrage 137.70 to 424.15
 drill metrage 565.20 to 574.65
 - Bromide profile 02YER20 RB254: drill metrage 0 to 52.83
 drill metrage 148.56 to 185.12
 drill metrage 265.34 to 340.65
 drill metrage 377.68 to 390.60
 drill metrage 398.53 to 407.30

- The longest core sequence of each stratigraphic unit of the profiles was used as the standard thickness, which was then used to normalize all other sections. The standard thickness was determined as:
 - 133.07 m for the Knäuelsalz (bromide profile Go 1002)
 - 144 m for the Streifensalz (bromide profile Go 1002)
 - 61.70 m for the Kristallbrockensalz (bromide profile 02YEQ01 RB119)
 - 2.97 m for the Hangendsalz (bromide profile 02YER20 RB254)
 - 3.66 m for the Kieseritische Übergangsschichten (bromide profile Go 1002)
- The bromide curves for each bromide profile shown in the diagram are derived from the running average calculated from 7 data points in each case. An additional bromide trend curve was generated from the running average of 9 data points.

Interpretation of the bromide distribution

The individual bromide profiles display an almost continuously rising trend. This corresponds to the bromide distribution of a progressive evaporation phase. This means that the primary bromide trend has been largely preserved despite halokinetic brecciation of the rock salt layers during diapirism. This interpretation is confirmed by a comparison with bromide profiles from the Zechstein 2 sequences of the Rossleben anticline, the Aschersleben anticline, the Stassfurt anticline and the Bernburg main anticline (SCHULZE 1960). Nevertheless, notable differences occur between individual bromide profiles, which are largest in the Streifensalz and Kristallbrockensalz (Fig. 44).

The following factors could have had an influence on or could be the cause of the measured deviations:

- The profiles are based on different methods of sampling (mixed samples or separation of halite crystal blocks from halite matrix). The bromide concentrations were also measured in different laboratories using different analytical methods (IC and XRF). However, a systematic error arising from this can be excluded because there is no continuous parallel shift over the whole length of the bromide curves (Fig. 44).
- Primary bromide distribution differences in the profiles established during sedimentation of the rock salt beds may have been caused by large differences in relief in the depositional area (SCHULZE 1960). Today's horizontal distances between the bromide profiles are 1.6 km at maximum, i.e. this would have required a highly variable and marked relief of the original depositional area during the sedimentation of the Zechstein 2 salt. However, there is no evidence for this assumption.

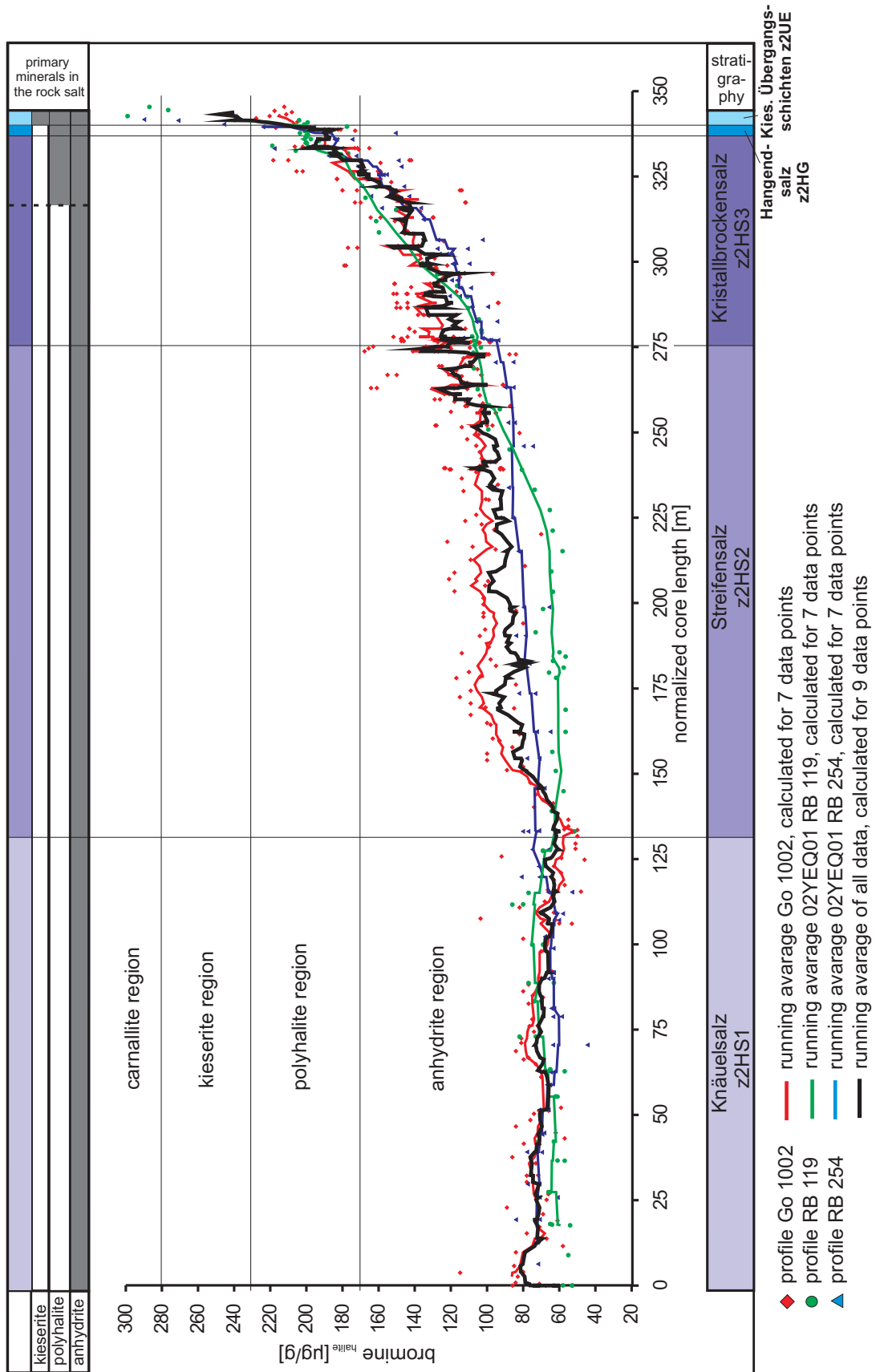


Figure 44: Bromide standard profile of the Zechstein 2.

- The differences in the bromide curves are caused by the halokinetic brecciation of the beds during diapirism.

This can be described by the following model:

The beds were initially folded during the first phase of diapirism. Further stress and compression led to the rupture of the sequence along the fold hinges. This was followed by the injection of bedding sequences from stratigraphically older zones of lower bromide concentrations into stratigraphically younger rock salt sequences of higher bromide concentrations, and vice versa. This led to imbrication of the sequences. Progressing diapirism led to intense brecciation and mixing of the bedding sequences, which created the present salt structures and caused the observed bromide variation depending on the degree of mixing of the younger and older halite beds. The lowest bromide concentrations are expected in the oldest rock salt layers deposited in a phase of progressive evaporation. SCHULZE (1960) measured bromide concentrations between approx. 30 and 60 µg/g in the Zechstein 2 rock salt directly above the Basalanhydrit. The bromide concentrations in the Knäuelsalz and Streifensalz in the Gorleben salt dome are between 40 and 50 µg/g, representing the stratigraphically oldest rock salt units in the Stassfurt-Folge.

Summarized results for Zechstein 2

The analysed bromide profiles are from different areas of the salt dome, which means that the results derived from the bromide profiles apply to the whole area of the salt dome explored so far. The results of the bromide analysis of the Zechstein 2 show that the northern German mineral regions formulated by KÜHN (1955) also apply to the Gorleben salt dome.

The following mineral regions and bromide concentrations were identified in the stratigraphic units:

- Knäuelsalz:
 - Bromide content: 44 to 115 µg/g
 - Mineral region: anhydrite region
- Streifensalz:
 - Bromide content: 50 to 168 µg/g
 - Mineral region: anhydrite region

- Kristallbrockensalz:
 - Bromide content: 94 to 219 µg/g
 - Mineral region: anhydrite region → polyhalite region
- Hangendsalz:
 - Bromide content: 177 to 245 µg/g
 - Mineral region: lower polyhalite region → lower kieserite region
- Kieseritische Übergangsschichten:
 - Bromide content: 203 to 299 µg/g
 - Mineral region: polyhalite region → lower carnallite region

The proportion of accessory constituents in the Zechstein 2 rock salt decreases from base to top up into the Hangendsalz. The geochemical data indicate trends while anhydrite concentrations between 4 and 8 wt% and insoluble residues of 0.5 wt% were found in the Knäuelsalz. The anhydrite concentration and the insoluble residues decrease upwards into the Kieseritische Übergangsschichten to less than 2 wt% and 0.2 wt% respectively. Polyhalite first appears in the youngest Kristallbrockensalz and reaches concentrations of over 4 wt% in the Kieseritische Übergangsschichten. The mineral distribution indicates an undisturbed progressive evaporation during sedimentation.

The difference in bromide distribution between halite matrix and adjacent halite crystal blocks, as well as the special structure of the rocks, indicate that the characteristic structure of the Hauptsalz was created by halokinetic brecciation during diapirism (BORNEMANN et al. 2000; SCHRAMM & BORNEMANN 2004). The brecciated salt formation was healed with secondary halite (see Fig. 44). Despite the halokinetic brecciation and mixing, the primary trend of bromide curves indicating progressive evaporation is still recognisable. Hence no brines from outside the salt dome were involved in this process. If external brines had been involved, the trend would be either distinctively steeper or shallower. The brines required for healing the fissures came from fluid inclusions as well as from solutions bound in intergranular spaces.

Despite the halokinetic brecciation, all analysed bromide distributions display bromide curves that largely rise continuously from base to top. This trend corresponds to a progressive evaporation during sedimentation and represents a largely intact primary bromide distribution in the rock salt of the Zechstein 2 sequence compared to other bromide profiles, e.g. of the Central German Zechstein (SCHULZE 1960).

The bromide distribution can be used to identify the folding of the beds. The bromide distribution of the rock salt matrix in particular reflects the geological structure. Based on the knowledge of the mineral regions and mineral parageneses, the bromide stratigraphy of the Zechstein 2 rock salt beds can be determined (SCHRAMM et al. 2002, 2005). Although the bromide profiles reveal differences in the bromide curves, especially in the Streifensalz and Kristallbrockensalz, these differences can be explained by different degrees of halokinetic brecciation and mixing of the beds during diapirism.

3.3.3.2 Bromide standard profile of the Leine-Folge (Zechstein 3)

The zone from the boundary of the Hauptanhydrit/Basissalz up to the Tonmittelsalz was analysed to create a bromide standard profile of the Leine-Folge. This work was based on the bromide standard profile of the Liniensalz sequence of the Gorleben salt dome created by BÄUERLE (2000), which was extended by new data (BORNEMANN et al. 2001).

The bromide standard profile was prepared using only bromide profiles from cores that were not significantly affected by halotectonics because this guaranteed finding the original bromide distribution prevalent during sedimentation of the rock salt. The bromide standard curve was derived from the bromide profiles of shaft pilot borehole Go 5001 (depth: 675.80 to 730.70 m), exploration boreholes Go 1003 (depth: 1337.91 to 1511.10 m), Go 1005 (depth: 1206.20 to 1270.95 m), and Go 1004 (depth: 713.41 to 1027.00 m). These partially overlapping bromide profiles are from different parts of the salt dome. This bromide standard profile is therefore applicable to the whole salt dome. The marker horizons anhydrite bank in the Basissalz, the 110. Linie in the Liniensalz and the Gorleben-Bank in the Orangesalz were used as reference points for elaborating the profile. The method of sulphate band counting in the rock salt beds established by BORNEMANN (1991) was also used for orientation.

The sequence penetrated by exploration borehole Go 1003 displayed the least halokinetic deformation. Therefore the thicknesses normal to bedding of the sections from the first band to the 110. Linie, from the 110. Linie to the Gorleben-Bank, and from the Gorleben-Bank to sulphate band 55 in the Oberes Orangesalz were used as standard thicknesses. Using this standard, the thicknesses normal to bedding of the corresponding sections in the other profiles were normalized. As the Go 1003 profile only reaches up to sulphate band 55 in the Oberes Orangesalz (BÄUERLE 2000), the higher profile sections in the Oberes Orangesalz were also normalized to this section. Only one bromide profile (from exploration borehole Go 1003) is available for determining the bromide distribution in the Zechstein 3 Basissalz. A thickness normal to bedding of the Basissalz of 16 m according to BORNEMANN (1991) was used in this case to normalize the Basissalz sequence penetrated by exploration borehole Go 1003.

Description of the bromide standard profile

The z3 standard bromide profile starts with bromide concentrations exceeding 300 µg/g halite at the base of the Basissalz (z3BS) at the interface with the Hauptanhydrit (Fig. 45). These very high bromide concentrations drop abruptly to 80 to 90 µg/g halite after the first few decimetres of the Basissalz. The bromide curve then climbs continuously to values between 120 and 135 µg/g halite towards the anhydrite bank marker in the Basissalz. Directly below the anhydrite bank, the bromide curve drops below 80 µg/g halite in the Basissalz.

Bromide values of 80 to 90 µg/g halite characterise the boundary between the Basissalz and the Liniensalz. The bromide curve then climbs continuously to over 200 µg/g halite within the Liniensalz (z3LS) just below the 110. Linie. The bromide values again drop abruptly immediately below the 110. Linie.

The falling bromide trend reaches concentrations of 94 to 175 µg/g halite directly above the 110. Linie. From this point on, the bromide curve rises continuously to a maximum of 245 µg/g halite at the Gorleben-Bank marker. Just as at the anhydrite bank in the Basissalz and the 110. Linie in the Liniensalz, there is a similar abrupt drop in the bromide curve upon reaching the Gorleben-Bank. It starts below the Gorleben-Bank and continues into the layer immediately above. Just as in the zones immediately above the other marker horizons, the bromide concentrations have a broad range at this level varying between 101 and 237 µg/g halite. From the drop in the bromide curve in the Oberes Orangesalz (z3OSO), the bromide curve again starts to climb slowly and passes with slightly varying bromide concentrations into the Bank-/Bändersalz (z3BK/BD) where the values are between 143 and 227 µg/g halite (Fig. 45). After reaching a maximum of approx. 215 µg/g halite, the bromide curve descends to 175 µg/g halite towards the transition to the Buntessalz (z3BT).

The bromide concentrations in the Buntessalz vary between 152 and 209 µg/g halite within the alternating swath and pure salt zones. This is followed by the Anhydritmittelsalz (z3AM) which has generally lower bromide concentrations with an average of 141 µg/g halite and considerable variation between 101 and 194 µg/g halite. The Schwadensalz follows in the next part of the profile, also with an average concentration of 141 µg/g halite. A trend towards higher average bromide concentrations begins in the overlying sequence at the base of the impoverished Kaliflöz Riedel (z3RI/na) followed by the Tonmittelsalz (z3TM).

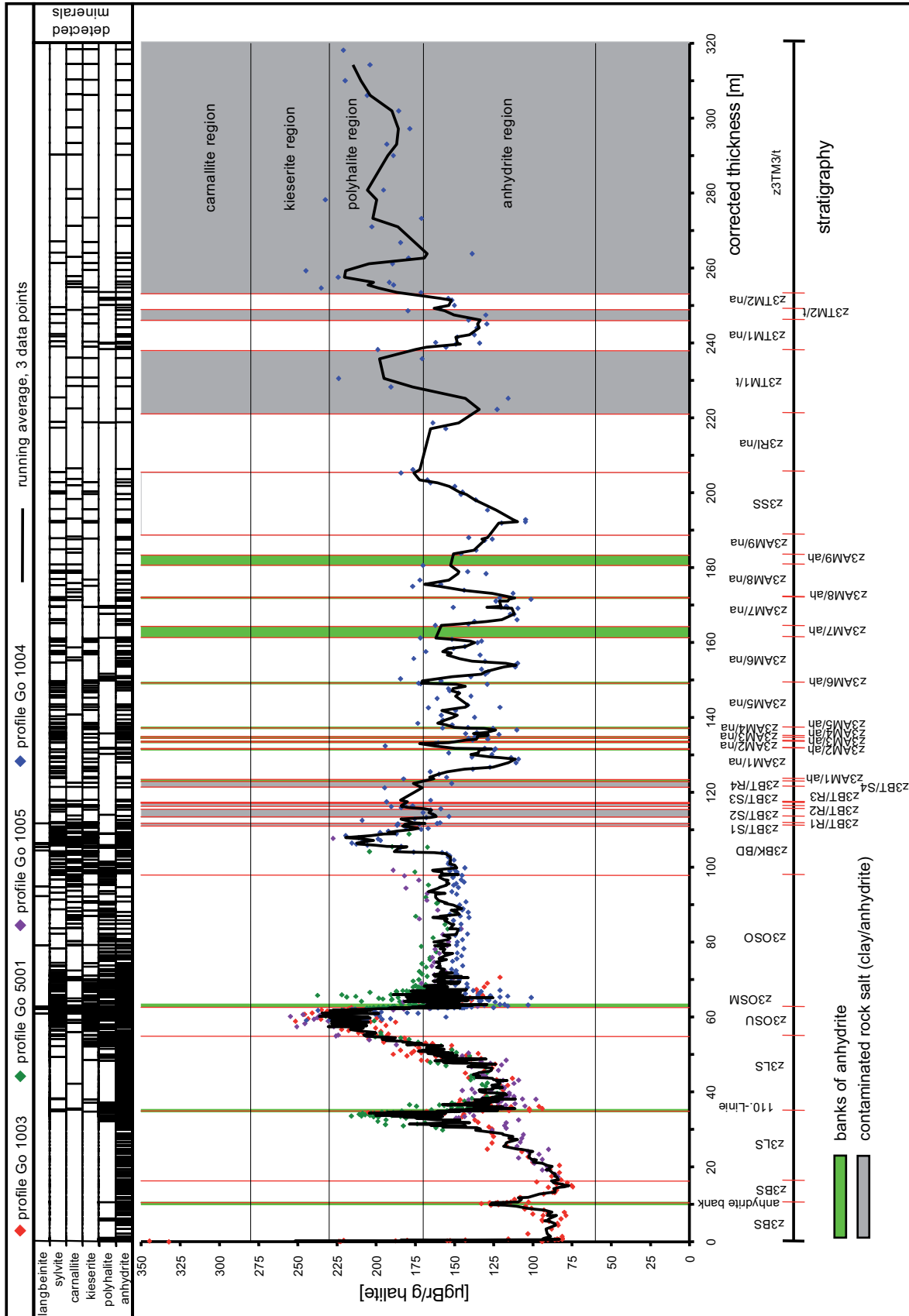


Figure 45: Bromide standard profile of the Zechstein 3 sequence.

Interpretation of the bromide standard profile

In general, the continuously rising bromide curve beneath the marker horizons reflects an undisturbed progressive evaporation phase in each case. The drop in the bromide curves at the marker horizons reflects the dilution of the brines during Zechstein evaporation as a result of the inflow of seawater. The sedimentological sequences of the marker horizons also indicate a dilution by pre-concentrated seawater because the marker horizons lack separate carbonate zones.

Immediately above the Hauptanhydrit, very high bromide concentrations (over 300 µg/g halite) were found in the Basissalz. The mineral paragenesis (halite, anhydrite ± polyhalite) does not correlate with the primary mineral association expected from bromide stratigraphy. The unusually high bromide values can be explained by synsedimentary to early diagenetic upwelling of very bromide-rich residual brines or pore fluids from the underlying beds, e.g. from the Kaliflöz Stassfurt. The ascending brines led to partial recrystallization of the halite causing the very high bromide contents.

Quite early studies reported a similar result from other parts of the Zechstein Basin (D'ANS & KÜHN 1944; SCHULZE 1959 a and b, 1960), also interpreting these results with the model of ascending bromide-rich brines. Highly variable bromide concentrations were also measured in the beds immediately overlying the marker horizons of the 110. Linie and the Gorleben-Bank. These are also attributable to bromide-rich solutions rising up from the underlying sequences as a result of compaction, leading to early diagenetic partial recrystallization of the halite beds (BÄUERLE 2000). Parts of the Bank-/Bändersalz, Buntessalz, Anhydritmittelsalz, Schwadensalz, impoverished Kaliflöz Riedel and Tonmittelsalz are also affected by ascending or circulating brines. In this zone too, the mineral parageneses do not correlate with the primary mineral associations expected from bromide stratigraphy.

Every profile displays major differences in bromide concentration directly at the base of the marker horizons. These variations are attributed to differences in relief during sedimentation and/or differences in migration paths. On the basis of sedimentary textures and core correlations, it was shown in the Gorleben salt dome that the Hauptanhydrit had a very distinctive sedimentary surface morphology varying by several tens of metres (BÄUERLE et al. 2000; BORNEMANN 1991). This relief affected all stratigraphic units till beyond the Gorleben-Bank and caused primary variations in thickness of the Gorleben-Bank. These findings led to the conclusion that, due to a density layering of the brine column in the sedimentary basin (BRAITSCH 1962; SONNENFELD 1984), deeper parts of the basin have more highly concentrated brines than shallower zones, and thus also higher bromide concentrations.

The crystallization of halite usually starts with the formation of hopper crystals at the surface of the seawater (LÖWENSTEIN & LAWRENCE 1985; PAPE 1993; SCHNEIDER 1995). Upon reaching a certain size, these crystals sink to the sea floor where they continue to grow in the presence of chevron crystals. Due to the higher bromide concentrations at the sea floor, halite crystals grown on the sea floor in a deeper part of the basin have higher average bromide concentrations than halite crystals grown on a shallower part of the sea floor. For the considered bromide profiles, this means that the differences in bromide concentration in the zones directly below the marker horizons reflect different water depths in the sedimentary basin. This model also explains the differences in bromide concentration in some profiles at the boundary between the Liniensalz and the Unteres Orangesalz. The continuous rise in the calculated bromide curves from the drops in the bromide curve at the anhydrite banks reflects the progressive degree of evaporation towards the marker horizons.

3.3.3.3 Mineralogical and geochemical investigations of the Kaliflöz Stassfurt

The Kaliflöz Stassfurt (z2SF) was encountered in various forms in a few exposures and many boreholes in the Gorleben salt dome. The objective of the investigations was to characterise the potash seam qualitatively and quantitatively in terms of its mineralogical and geochemical properties. To this end, the salt dome exploration boreholes Go 1002 and Go 1003 drilled on the NW flank of the salt dome, and the underground exploration boreholes within the Zechstein 2 updoming 02YEA06 RB170, 01YEF20 RB217, and 01YEF20 RB059 were selected and sampled in sections. The Kaliflöz Stassfurt (z2SF) was encountered repeatedly in the exploration boreholes. The colour and structure varied from section to section.

Analyses were carried out on whole rock samples as well as monomineralic samples where possible (pure halite and/or carnallite). It was possible to apply the genetic information derived from the analysis of the bromide concentrations in the pure minerals to the whole rock.

Kaliflöz Stassfurt (z2SF) on the NW flank

On the NW flank of the salt dome, the exploration boreholes Go 1002 and Go 1003 were analysed in detail.

Borehole Go 1002 penetrated two sections of the potash seam from 629 to 644 m and 1761 to 1779 m, which were continuously sampled, producing composite samples. The first (upper) section is inverted and can be divided into white carnallitite (629 to 634 m) and red carnallitite (635 to 644 m). The second section of the potash seam is normally bedded

and consists of white carnallite. The upper part of the first section of the potash seam from 629 to 634 m mainly consists of halite (52 wt%), carnallite (29 wt%) and kieserite (15 wt%). The carnallite and kieserite concentrations increase with depth (Fig. 46). Carnallite is the dominant mineral in the lower part of the first section of the potash seam at 45 wt% and in the second section at 46 wt%. The K_2O concentration increases from 5.2 wt% at the top to 8.1 wt% at the base (Table 4).

Table 4: Average mineral contents, bromide and rubidium contents of the carnallites, and K_2O contents of the Kaliflöz Stassfurt (z2SF) in the samples of the deep boreholes Go 1002 and Go 1003.

borehole	kaliflöz-section	whole rock										carnallite				
		depth from to		rock type	halite	anhydrite	polyhalite	kieserite	carnallite	syvaine	kainite	K_2O	depth	colour	Br Carnallite	Rb Carnallite
		[m]			[wt%]										[m]	
Go 1002	1	629	634	white carnallite	52	< 1	0	15	29	< 1	0	5,2	630,70	clear	3923	54
		635	644	red carnallite	32	< 1	< 1	20	45	< 1	0	7,7	638,14	red	4225	68
	2	1761	1779	white carnallite	29	< 1	< 1	22	46	< 1	0	8,1	1772,40	clear	4116	57
													1777,90	red	3507	83
Go 1003	1	452	470	colourless carnallite	46	< 1	n. n.	15	36	n. n.	2	6,1	<i>clear halites or carnallites were not extractable</i>			
	2	707	729	red carnallite	48	0	0	18	29	< 1	0	5,5				
	3	796	808	red carnallite	58	2	0	12	26	0	0	4,4				
		808	812	red carnallite (conglomerate)	40	< 1	1	15	40	< 1	0	7,3				

n.n. = below detection limit of quantitative XRD.

Pure carnallite (clear as well as red varieties) was extracted and analysed from depths 630.70, 638.14, 1772.40, and 1777.90 m. The red colour is probably due to very fine-grained haematite inclusions and isolated goethite inclusions (RICHTER 1962, 1964). The results of the bromide analyses show an increase from 3923 to 4225 $\mu\text{g}/\text{g}$ carnallite for the section between 629 and 644 m depth. This corresponds to progressive evaporation with the older zone in the upper part and the younger zone in the lower part (overturned bedding).

In the second potash seam section, the increase in bromide concentrations (Table 4) from base to top confirms normal bedding conditions. No correlation was found between colour and bromide concentration. There may be a potential correlation between colour and rubidium concentration where the lower rubidium concentrations are associated with the clear carnallite and the higher rubidium concentrations with the red carnallite. However, the data density is as yet too scarce to be conclusive.

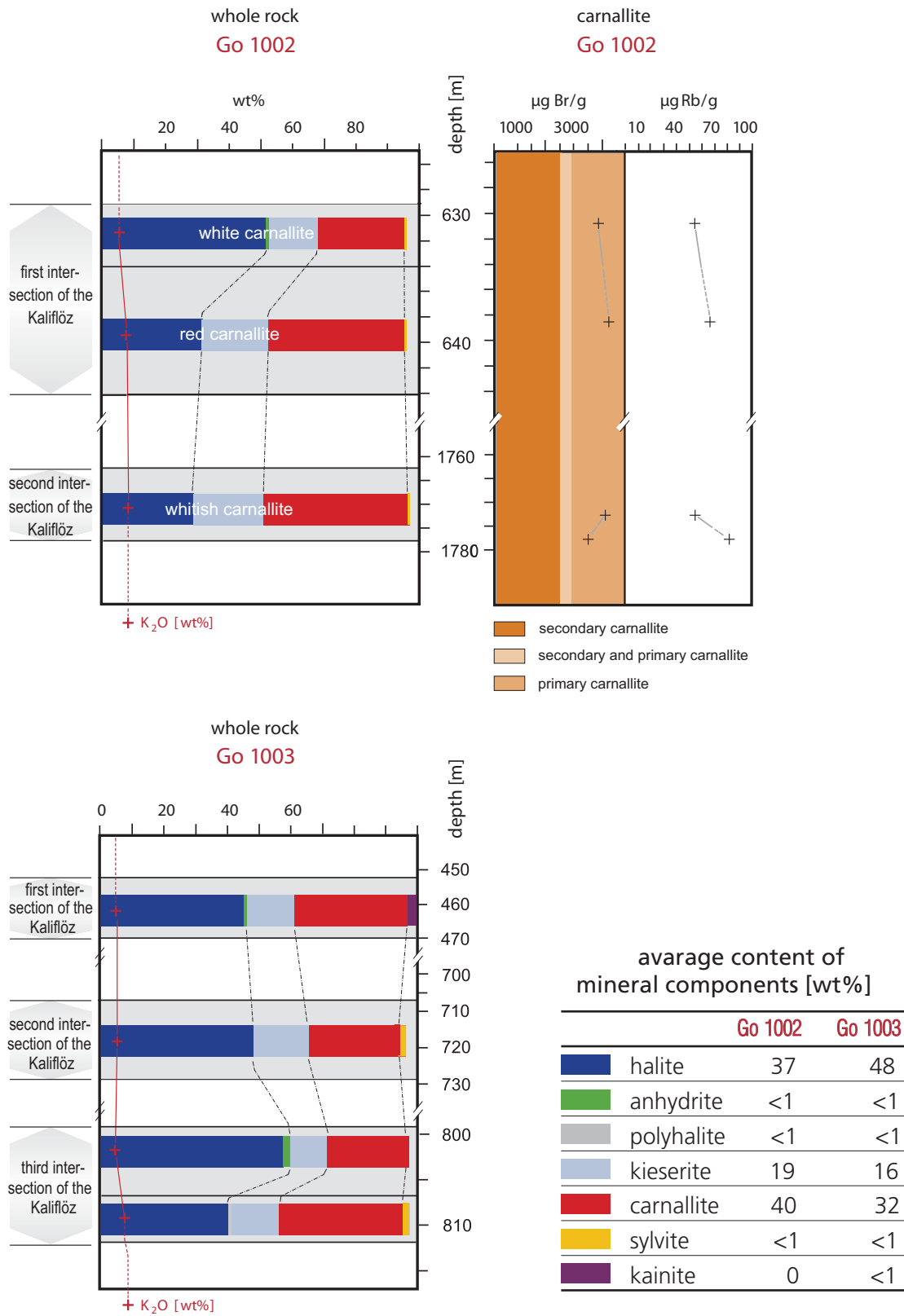


Figure 46: Quantitative mineral content of the Kaliflöz Stassfurt in the samples of deep boreholes Go 1002 and Go 1003, and bromide and rubidium content of the carnallite in the deep borehole Go 1002.

The bromide contents indicate no secondary alteration of the white and red carnallite in salt dome exploration borehole Go 1002. The mineralogical composition indicates a typical primary kieseritic carnallite. The bromide contents also indicate no secondary alteration because they exceed the maximum bromide content of 2400 or 2900 µg/g carnallite typical of secondary carnallite (MATTENKLOTT 1994). The rubidium analyses yield values in a range that could be interpreted either as primary or as secondary (MATTENKLOTT 1994).

Three sections of the potash seam penetrated by salt dome exploration **borehole Go 1003**, at depths of 452 to 470 m, 707 to 729 m, and 796 to 812 m, were analysed. The third section of the potash seam was divided into an upper and lower zone due to structural differences. The first potash seam section consists mostly of colourless carnallite. Halite dominates the mineral association at 46 wt%. In addition to 36 wt% carnallite and 15 wt% kieserite 2 wt% kainite were detected. Below this, the second section of the potash seam consists of red carnallite dominated by halite (48 wt%). At 29 wt%, the carnallite concentration is lower than in the first section, while the kieserite proportion of 18 wt% is slightly higher. The upper zone of the third section of the potash seam consists of red carnallite which is dominated by 58 wt% of halite. The conglomeratic red carnallite of the lower zone is characterised by equal proportions of halite and carnallite (40 wt% each). This section is inverted. The younger part (lower zone) with the higher carnallite concentration represents a later evaporation stage than the overlying zone from 796 to 808 m. The K₂O concentration varies between 4.4 and 7.3 wt% with no specific trend.

The Kaliflöz Stassfurt (z2SF) in the three sections encountered in the salt dome exploration borehole Go 1003 consists of kieseritic carnallite. Halite is consistently dominant in all sections and only in the lower zone of the deepest (third) section of the potash seam is an equal amount of carnallite to be found. The mineral composition does not indicate any secondary alteration. The mineral paragenesis of halite, carnallite, kieserite, ± anhydrite, ± polyhalite is typical of a primary formation at 25°C. The coexisting solution must have had a composition between points R and Z in the Jänecke projection. The mineral association with kainite can also be explained by primary deposition. During the progressive evaporation of the seawater, the already crystallized kainite probably reacted only incompletely with solution R to form carnallite and thus left behind kainite residues. An alteration of the carnallite to form kainite and sylvite can be ruled out because no sylvite was found in the samples.

Only traces of anhydrite and polyhalite are found in the potash seam sections of both boreholes and values of < 1 wt% are probably best considered as mathematical values (this applies particularly to sylvite). The minerals not identified by quantitative X-ray diffraction (XRD) are marked with "n.n." in Table 4.

Summary: NW flank

The Kaliflöz Stassfurt has an inhomogeneous composition on the NW flank of the salt dome. In borehole Go 1002, the average composition is 37 wt% halite, 40 wt% carnallite and 19 wt% kieserite. The Kaliflöz Stassfurt in borehole Go 1003 has larger amounts of halite with an average of 48 wt%, but less carnallite (32 wt%) and kieserite (16 wt%). Despite these minor differences, the potash seam can generally be considered as a kieseritic carnallitite. The highest carnallite concentrations in both boreholes are found in the deepest sections of the potash seam. No indication of any secondary alteration was found. The K_2O concentration in all analysed samples is below 10 wt%.

Kaliflöz Stassfurt (z2SF) in the area of the Zechstein 2 updoming

Exploration boreholes 02YEA06 RB170, 01YEF20 RB217, and 01YEF20 RB059 were selected as examples for the investigation of the Kaliflöz Stassfurt in the Zechstein 2 updoming. From borehole 02YEA06 RB170, one potash seam section was selected for analysis (only partially representative; the impoverished zone of the potash seam was ignored), from each of the other boreholes, 01YEF20 RB217 and 01YEF20 RB059, two sections of the potash seam were selected.

Four distinctively coloured zones were sampled in the potash seam section of borehole 02YEA06 RB170. A bulk sample was taken in each of the zones. These covered the following depths:

- 12.80 to 14.48 m white/clear rock
- 14.48 to 16.00 m red rock
- 23.34 to 24.07 m grey rock
- 29.25 to 30.00 m white rock

The mineralogical composition of the potash seam in **borehole RB170** is dominated by halite in the whole section sampled (51 to 59 wt%). Sylvite is the second most frequent mineral with an average of 31 wt%. The sylvite concentration drops from about 34 - 35 wt% to 20 wt% with increasing depth. Simultaneously the anhydrite content increases with increasing depth from initially 6 wt% to 20 or 21 wt%. The decreasing sylvite content indicates a progressive alteration by solution metamorphosis or impoverishment. This is also shown by the decrease in K_2O content from 22.2 wt% at the top to 12.5 wt% at the bottom. The K_2O content is relatively high. The rock type is a sylvinitic hard salt.

Two sections of the potash seam were sampled in **borehole RB217**. The upper section was continuously sampled from 64.61 to 87.00 m to produce a composite sample. The carnallite is grey-white coloured. Overall, this rock unit is characterised as hard salt. The second section of the potash seam was almost continuously sampled from 92.96 to 153.38 m. This section was divided into different zones based on colour, and each of the zones was analysed separately. Eight different coloured zones were analysed each zone representing a composite sample of the respective depth range:

- 92.96 to 93.36 m: grey, red, white
- 93.36 to 94.30 m: red
- 94.30 to 97.25 m: white, clear
- 97.25 to 135.50 m: red, white, clear
- 135.50 to 137.50 m: reddish, black-grey
- 137.50 to 146.75 m: red, black-grey
- 146.75 to 152.10 m: white, clear
- 152.10 to 153.38 m: white, orange

Parallel to the analyses of the bulk rock, some halite and carnallite spots in these sections were extracted and analysed separately.

The upper section of the potash seam has a grey-white colour. Halite dominates at 76 wt% followed by anhydrite at 18 wt% and carnallite at 1 wt% (Fig. 47). The K_2O content is very low at 0.2 wt%. Clear primary as well as clear secondary halite samples were extracted from the rock unit. The primary halites from the lower to middle part of the section revealed an increase in bromide content from 542 to 598 $\mu\text{g/g}$ from bottom to top. The secondary halites from the middle to the upper part displayed variable bromide contents between 92 to 130 $\mu\text{g Br/g}$ halite. Pure carnallite was also sampled. The consistently red carnallite had bromide contents of 3035 to 3763 $\mu\text{g/g}$ and rubidium contents of 174 to 391 $\mu\text{g/g}$. The increasing bromide content in the primary halites confirms the bedding conditions of the Kaliflöz Stassfurt established during the mapping. The older parts of the Kaliflöz Stassfurt with slightly lower bromide contents are in the lower part of the section while the higher bromide contents are in the upper part of the section (i.e. younger part of the Kaliflöz Stassfurt). However, interpretation on the basis of bromide content is of limited validity because only few data points are available (three analyses).

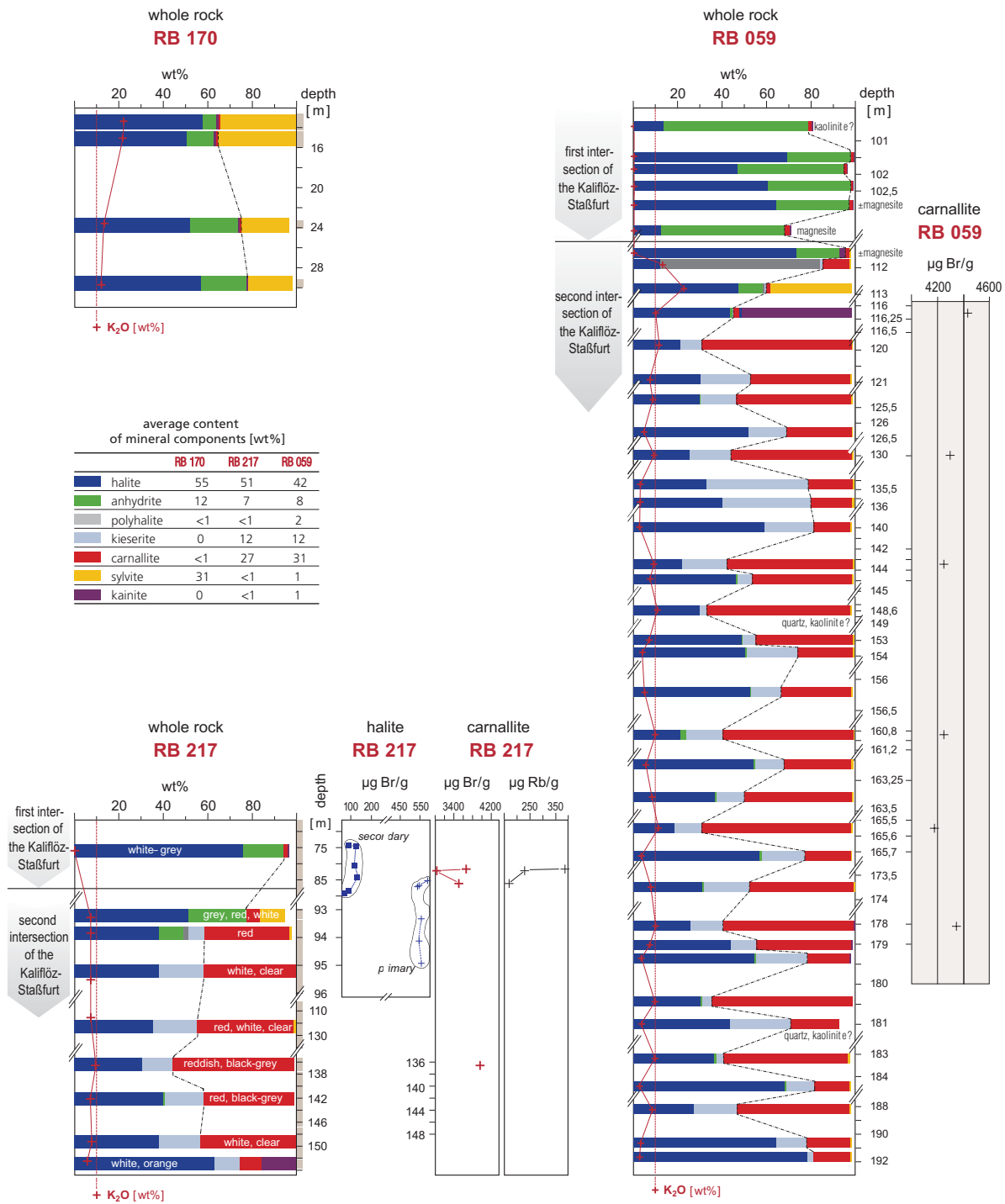


Figure 47: Quantitative mineral content of the Kaliflöz Stassfurt in the samples of boreholes RB170, RB059 and RB217 and bromide content of the halites and carnallites, and rubidium content of the carnallite. The bar widths give a symbolic representation of the mineral contents, using the same scale for all selected boreholes. In boreholes RB 170 and RB 217, the respective depth intervals are marked on the depth scales.

Analyses of the carnallites consistently showed bromide contents of over 2900 µg/g. Such values indicate primary deposition from evaporated seawater (at 35 °C, and over 2400 µg/g at 25 °C) based on a bromide concentration of 67 µg/g seawater (BRULAND 1983) at the beginning of evaporation. The ratio of bromide content in the primary halite to bromide content in the carnallite varies between 1:5 and 1:7, the latter corresponding to the theoretical primary paragenetic ratio. Halites with values of 92 to 130 µgBr/g were also found. This indicates a conversion caused by a metamorphic solution whose bromide concentration must have been between 657 and 1780 µg/g depending on the distribution coefficient (0.14 or 0.073).

The second section of the potash seam has a halite concentration of 52 wt% at the top. Other mineral contents are 25 wt% anhydrite, 10 wt% sylvite and 6 wt% carnallite. No trend was distinguishable in the quantitative mineral composition. A relatively high kainite content was noted in the lowest area sampled (17 wt%). The overall averages in the second potash seam section are: halite 42 wt%, carnallite 34 wt%, kieserite 13 wt%, anhydrite 5 wt%, kainite 2 wt% and sylvite 1 wt%. The K₂O content varies between 5.7 and 9.3 wt% with an average of 7.3 wt%. Three pure halites and one carnallite were also analysed. The clear halites display only slight variation in bromide content between 548 and 562 µg/g. A secondary alteration can be ruled out due to the high bromide values. The analysed carnallite was found to have a concentration of 4098 µgBr/g and therefore shows no sign of any metamorphic effects. The second section of the potash seam is a mainly kieseritic carnallitite with local sylvinitic or kainitic character.

Sampling in **borehole RB059** concentrated on two sections of the potash seam. The first section (99.8 to 103.9 m) is the eastern zone and was divided into six closely-spaced zones based on macroscopic differences. The second section was sampled from 111.08 to 191.65 m. This stretch of 80.57 m was divided into a total of 34 smaller zones based on colour differences (Fig. 47). One continuous sample was cut from each zone with an angle grinder.

The first section of the potash seam is characterised by halite and anhydrite (both averaging 45 wt%). In addition to carnallite with an average concentration of 1 wt%, XRD analysis also indicated the presence of magnesite and possibly kaolinite. The K₂O content is between 0.11 and 0.28 wt%. There is no recognisable trend. These findings do not necessarily indicate a potash seam. The presence of magnesite could potentially be a late-diagenetic reaction product or attributable to secondary alteration. In this case, already existing calcite/aragonite must have metamorphosed to dolomite and later metamorphosed completely into magnesite under the influence of MgCl₂-rich brines.

In some parts, the second section of the potash seam is very inhomogeneous (Fig. 47) with halite contents varying between 13 and 79 wt% and in one sample (RB059/8) polyhalite is the dominant mineral with 72 wt%. Some zones are even dominated by kieserite, carnallite and kainite. The average composition is 42 wt% halite, 36 wt% carnallite, 14 wt% kieserite, 2 wt% polyhalite and kainite, and 1 wt% anhydrite and sylvite. In some samples, quartz and possibly kaolinite were also identified, and magnesite was identified in one sample (Fig. 47). Magnesite with carnallite or sylvite as well as kainite with carnallite were found right at the beginning of the second section of the potash seam towards the west. The mineral association with sylvite contains no kieserite, and no sylvite was identified in the paragenesis of kainite with carnallite.

There is no doubt about the late-diagenetic alteration in the zones containing magnesite because calcite/aragonite and MgCl_2 -rich brines are required for the formation of magnesite. However, the subsequent zones with sylvite or kainite contain no definitive signs of secondary alteration. They can each be interpreted as primary mineral associations. The mineral paragenesis of carnallite and sylvite, with the simultaneous absence of kieserite, indicates that a seawater solution depleted of MgSO_4 must have prevailed (between points Q and E in the Jänecke projection). The solution could then have developed towards MgSO_4 enrichment and moved beyond point Q to the crystallization path between Q and R leading to the formation of kainite (plus carnallite). The solution could subsequently have moved beyond point R on the crystallization path towards Z, leading to the simultaneous formation of kieserite and carnallite. However, secondary conversion processes are also possible. The inflow of brines undersaturated with carnallite may lead to the formation of sylvite and the release of brines enriched in MgCl_2 . This brine in turn could then have been available for the formation of magnesite. The reaction of excess carnallite and kieserite with an NaCl-saturated brine would produce kainite, halite and fluid R in the presence of carnallite residues. A solution of 80.4 (25°C) or 80.8 mol MgCl_2 /1000 mol H_2O (at 35°C) would be sufficient to convert CaCO_3 to magnesite.

In the cores extracted west of the kainite and sylvite deposits, scatterings of pure carnallite could be sampled. Analysis showed little variation in bromide content – values being between 4175 and 4428 $\mu\text{g/g}$. They are therefore definitely of primary origin. The K_2O content in the bulk rock varies widely between 0.77 and 23.25 wt%. No trends were recognisable in the mineral content or in the bromide or K_2O content. Overall, the second section of the Kaliflöz Stassfurt (z2SF) penetrated by borehole 01YEF20 RB059 can be classified as a kieseritic carnallitite. Only the eastern zone close to the first section of the potash seam displayed a different mineralogical composition, which could be interpreted as a local secondary product.

Summary: Zechstein 2 updoming

Borehole 02YEA06 RB170 penetrated a completely metamorphosed sequence consisting of sylvinitic hard salt with increased K_2O contents in the sections of the potash seam in the vicinity of the z2 updoming.

The two sections of the potash seam penetrated by borehole 02YEA06 RB217 showed signs of primary deposition as well as traces of secondary alteration. The upper section consists of secondarily altered, halite-dominated hard salt with anhydrite and traces of carnallite. The lower section shows no secondary effects and mainly consists of kieseritic carnallite with local sylvite or kainite.

Borehole 01YEF20 RB059 is characterised by the impoverished hard salt zone of the first section of the potash seam penetrated in the east. After a partly sylvinitic or kainitic transition zone, the second section of the potash seam to the west consists primarily of a kieseritic carnallite with no secondary alteration. The borehole is locally characterised by higher K_2O contents than the other exposures.

Summary of the investigations of the Kaliflöz Stassfurt

On the NW flank of the Gorleben salt dome, the Kaliflöz Stassfurt (z2SF) consists of kieseritic carnallite, in the Zechstein 2 updoming it consists of kieseritic carnallite as well as hard salt. The zones of local secondary alteration are intensely impoverished in some parts, which largely explains the mineralogical and geochemical inhomogeneities. The mineralogical composition on the NW flank is marked by a slightly lower halite content (37 to 48 wt%) than in the Zechstein 2 updoming (42 to 55 wt%). There is a clear difference in anhydrite content between less than 1 wt% on the flank and up to 12 wt% in the Zechstein 2 updoming. Polyhalite and kainite only occur sporadically in both areas. Kieserite and carnallite are slightly more common on the NW flank, with averages of 16 to 19 wt% and 32 to 40 wt% respectively, than in the Zechstein 2 updoming (0 to 12 wt% and < 1 to 31 wt% respectively). Sylvite is virtually insignificant on the flank but ranges from less than 1 to 31 wt% in the Zechstein 2 updoming. From a genetic point of view, the flank displays no secondary effects and has a relatively uniform composition. If the metamorphically altered areas and the transition zones are ignored, it can be stated that the quantitative mineralogical composition and the K_2O content of the carnallites (5.24 to 8.13 wt%) of the Kaliflöz Stassfurt in the Zechstein 2 updoming are in the range of those on the flank.

3.3.4 Hydrocarbons, gases and brines in the Gorleben salt dome

3.3.4.1 Gaseous hydrocarbons and condensates

Occurrences

Hydrocarbons occur in many mines in the salt domes of Lower Saxony (GROPP 1919; EHRHARDT 1980; HERRMANN 1987; GERLING et al. 2002). The hydrocarbons occasionally encountered during the exploration of the Gorleben salt dome therefore came as no surprise. Liquid and gaseous hydrocarbons were encountered for instance during the sinking of the shaft pilot boreholes Go 5001 and Go 5002. Borehole Go 5001 in particular had gas inflows between 864.5 m and 872 m in the Bank-/Bändersalz (z3BK/BD) and between 960.0 m and 967.8 m in the Orangesalz (z3OS). Both boreholes were tested for inflows (GRÜBLER 1984). The total inflow of borehole Go 5001 amounted to almost 5 m³ condensate while the inflow into borehole Go 5002 was very low overall. The inflows were accompanied by gas in unquantified amounts. Another indication of the presence of gas is the occurrence of crackling salts, which crackle and release gas when cores are rubbed together or when dissolved in water. These crackling salts were encountered in various rock salt horizons and within the carnallite.

Other hydrocarbon occurrences were encountered during the excavation of the infrastructure zone and Exploration Area 1 (EB 1).

The occurrence of brines and gas inflows can originate from the following zones (BORNEMANN et al. 2001):

- Fissure reservoirs in anhydrite rocks or claystones.
These include the Gebänderter Deckanhydrit, Grauer Salzton, Leine-Karbonat, Hauptanhydrit, anhydrite bank in the Basissalz, Gorleben-Bank and Anhydritmittel in the Anhydritmittelsalz.
- Fault and fissure zones healed with secondary halite at the z2/z3 boundary and partially in the lower part of the Gorleben-Bank.
- Thinned-out and accumulated Kaliflöz Stassfurt at the z2/z3 boundary without the sequence from Gebänderter Deckanhydrit to Hauptanhydrit.

The outflow of the brine reservoirs previously under gas and petrostatic pressure occurring in some drifts in the Kaliflöz Stassfurt and in the vicinity of the Gorleben-Bank led to the formation of scattered flute-like cavities that quickly tapered away from the wall face (Fig. 48).



Figure 48: Gas flute in the Kaliflöz Stassfurt. It was formed when excavation work in the potash seam caused the release of gas that had been embedded under pressure in the brecciated carnallite (crackling carnallite). The flute is approx. 1.5 m long and has a diameter of approx. 30 cm. Cross-cut 1 West, 840 m-level, drift position 85 m, western wall. (Photograph: Bauer, DBE)

Releases of gases (usually together with brines) were only encountered during the drilling of boreholes 01YEF20 RB217 (Gorleben-Bank, fissure zone) and 02YEA12 RB218 (anhydrite bank in the Basissalz) and during the driving of the drifts (e.g. shaft undercut to the 930 m-level) in the vicinity of the Gorleben-Bank.

During the drilling of exploration boreholes 02YER02 RB032, 02YEQ01 RB119, 02YEQ01 RB120, and 02YER20 RB500 and the drifting of cross-cuts 1 East and 1 West, there were localised clusters of small-volume condensate inflows occurring almost exclusively in the oldest zone of the Hauptsalz (Knäuelsalz). These inflows were identified by the intense smell of hydrocarbons and slightly damp patches in the cores or on the roof and walls of the drifts. Many of these damp patches dried quickly and left brown stains on the walls and roof of the drifts. Convergence and loosening of the rocks around the drifts caused new condensate patches to develop even several months after drifting. Some of the damp patches were concentrated around anchor boreholes as well as cracks on pillar corners (Fig. 49).



Figure 49: Condensate occurrence in cross-cut 1 West at the pillar corner of drilling location 1.4 at approx. drift metre 325 under ultraviolet light (above) and artificial light (below). The two photographs show the same area. The visible condensate inflows are marked by brown stains on the sidewall. Weak lines of fluorescence can be seen under ultraviolet light in the upper part of the picture corresponding to convergence-induced cracks originating from the corner of the pillar. These cracks release intercrystalline-bound condensates.

With few exceptions, the occurrences are primarily in the Knäuelsalz (z2HS1) and at first glance, the occurrences seem to be symmetrically distributed in cross-cut 1 West with respect to the structural shape of the Hauptsalz anticline. The occurrences are concentrated near the boundary of Knäuelsalz to Streifensalz, whilst the core of the Hauptsalz anticline is free of condensates. However, this finding is not supported by the position of the occurrences in borehole 02YER02 RB032 as these are irregularly scattered throughout the Knäuelsalz. In the eastern part of EB 1 (cross-cut 1 East, 02YEQ01 RB119, 02YEQ01 RB120, and 02YER20 RB500), the occurrences are almost exclusively concentrated on the southern flank of the Knäuelsalz anticline, which means that there is no symmetry between the occurrences and the structure here either. No condensates were encountered in boreholes 02YER20 RB254 and 02YER20 RB488 (northern flank). Based on the available data, it can be stated that the occurrences are concentrated in the western part of EB 1 and that there is a strong decline towards the east (BORNEMANN et al. 2001: 45 ff.).

Other occurrences outside the Knäuelsalz are:

- one occurrence at drilling location 1.2 in the Streifensalz (southern flank of the Hauptsalz anticline)
- one occurrence in cross-cut 1 West in the younger Streifensalz (southern flank of the Hauptsalz anticline)
- two occurrences at drilling location 3 in the Streifensalz (southern flank of the Hauptsalz anticline)
- one occurrence in cross-cut 1 East in the Streifensalz (northern flank of the Hauptsalz anticline).

The four occurrences in the Streifensalz on the southern flank of the Hauptsalz anticline can be explained by the poorly definable boundary between the Knäuelsalz and the Streifensalz, and by the intense halokinetic alteration of the rock salt beds. Evidence of this includes the almost complete absence of Kristallbrockensalz in this section. The occurrence in cross-cut 1 East (Streifensalz) is probably also attributable to the poorly definable, halokinetically altered location of the boundary between the Knäuelsalz and the Streifensalz.

Analysis and genetic interpretation of the gaseous hydrocarbon occurrences

With respect to the sampling method, three types of gases are distinguished. Investigations were carried out on the following:

- **Inflows of free gases**
This is gas encountered during drilling or the driving of drifts. They were relatively easy to sample compared to the other types because of the large volumes involved.
- **Salt-bound gases**
These are sampled in salt blenders by dissolving 200 to 400 g crushed or uncrushed rock in previously degassed water and trapping the gas released in the pre-evacuated head space of the reaction vessel.
- **Headspace gases**
Unlike salt-bound gas in the rock salt, these gases have a limited migration capacity. As part of this gas in the salt is already released by changes in the underground in situ conditions, rock samples were sealed in acrylic containers during sampling. The gas accumulated in the headspace was analysed before further processing in the salt blender.

The results of the analysis are discussed in detail in GERLING & FABER (2001).

Due to their quantity and the resulting opportunities for analysis, the **free gas inflows** are very suitable for identification of the genesis of hydrocarbons (and of nitrogen) (GERLING et al. 2002). Most of the free gases are interpreted as autochthonous Zechstein products with thermal alteration and were probably produced from the organic matter in the Stassfurt-Karbonat (z2SK) (gas type 1). These gases also contain a small proportion of bacterial gas or gas from the early thermal alteration into methane, possibly also into ethane. This finding is explained by the special geological conditions. Unlike in clastic rock sequences, the products could not leave the system in this case because of the gas-tight evaporites above and below the host rock. Maturity estimates of the gases vary between 0.8 and 1.1 % vitrinite reflectance. The maximum value matches the current maturity at the base of the Zechstein sequence (Kupferschiefer in borehole Gorleben Z1). The lower maturity estimates can probably be attributed to the retained bacterial/early thermal products.

Another gas type occurs only in the Hauptanhydrit (gas type 2). This is a mixed gas dominated by Zechstein products (gas type 1) with approx. 40 to 45 % gas from the red beds of the Lower Permian. The mixing of the two gas types is only identifiable in the methane, on the basis of the $\delta^{13}\text{C}_{\text{H}_4}$ values and of the methane-enriched hydrocarbon composition, and in the isotopic composition of nitrogen. The ethane and propane definitely

originated only in the Zechstein. The migration of the red bed gas into the Hauptanhydrit took place during diapirism from the end of the Jurassic to the beginning of the Early Cretaceous. During this period, the greater part of the Hauptsalz had already moved from the rim syncline areas into the salt dome structure so that in some places the Hauptanhydrit already lay directly on the fissured beds of the lower Stassfurt-Folge and the Werra-Folge. The Hauptanhydrit was linked to the Lower Permian red beds via the fissures, which enabled the migration of gas from the red beds. The Hauptanhydrit was broken into separate blocks during the later stages of the salt dome development so that there is no longer any contact with the pre-Zechstein strata.

In addition to these two gas types, there is also a small group of free gas inflows, which represent a transition on the basis of their genetic classification. In one case – all gases from borehole 01YEF20 RB014 – the geological explanation is clear. The gas emanated from the Liniensalz at a point where the Hauptanhydrit was squeezed out. The other samples with the same isotopic signature – from boreholes 00YES01 RA044 and 00YES01 RA787 – originated from the Orangesalz.

A large number of rock samples from the surface salt dome exploration boreholes, the two shafts, and Exploration Area EB 1, were analysed for the presence of **salt-bound gases**. These usually contained very small amounts of gaseous hydrocarbons, whose molecular composition and carbon isotope ratio of methane could be analysed in almost all cases. However, only samples of sufficiently large gas volumes allowed the determination of the D/H-ratio of methane and the $^{13}\text{C}/^{12}\text{C}$ ratio of ethane and propane. Unlike the free gas inflows, the genetic classification of the salt-bound gases was in many areas equivocal or impossible. This is most probably due to uncontrolled partial gas losses prior to and during sampling. Many rock samples from EB 1, primarily samples from the Knäuelsalz (z2HS1), clearly contain gas type 1 hydrocarbons. Type 1 gases are also found in many rock samples from Shaft 1, as well as from Shaft 2, although in the latter with a composition richer in methane. This means that they are autochthonous Zechstein products of the organic matter of the Stassfurt-Karbonat (z2SK). Rock samples from the Streifensalz (z2HS2; EB 1) and from Shaft 1 contained salt-bound gases that were often isotopically heavier by approx. 5 ‰ and had a composition richer in methane. Thus, they can only be approximated as gas type 1. There is currently no plausible explanation for this difference to the gases encountered in the Knäuelsalz (z2HS1).

A special salt-bound gas occurs in the samples of the Kaliflöz Stassfurt (z2SF). It can be classified as a separate type (gas type 3). This gas is characterised by unusually positive carbon isotope ratios of methane, and in some cases also ethane. On the basis of field experiments in recent hypersaline systems, it is thought (GERLING et al. 2002: Chapter 3.3)

that this gas is of synsedimentary origin, i.e. it was generated and trapped in inclusions during the Zechstein period. Field tests revealed that organic matter, as well as gaseous hydrocarbons, assume very positive carbon isotope ratios at high salinities with almost constant D/H ratios. The main reason for this is the limited availability of carbon in the water and in the recent sediments as a result of high solar radiation (= high microbial activity = high production rates of organic matter from the CO_2 and/or HCO_3 in the water column), combined with reduced solubility of CO_2 in hypersaline brines (= reduced resupply of atmospheric CO_2 in the water body). Gas type 3 was found only rarely in other evaporites, e.g. in samples of Anhydritmittelsalz (z3AM).

Generally, the largest amounts of salt-bound gas were found underground in the Knäuelsalz (z2HS1). These gases were usually also significantly enriched in larger homologues (ethane, propane, etc.). This finding largely corresponds to the predominant distribution of condensate occurrences in the Knäuelsalz mapped under UV light (see BORNEMANN et al. 2001). A lack of correlation in individual cases is attributable to the selective information from the gas sampling compared to the UV mapping of the whole area. In addition to this, analysis of the samples from the surface exploration boreholes also revealed relatively large amounts of gas in the crackling carnallite, and occasionally in the Orangesalz, particularly in the Gorleben-Bank.

The interpretation of the **headspace gas** analysis results (GERLING et al. 2002) is based on sampling in EB 1 with improved containers from 1998 onwards. Despite careful sampling, it was not possible to completely avoid changes in gas composition during sampling. Most of the samples of headspace gas therefore give the impression that, although they are largely classified as gas type 1, most of them have positive methane $^{13}\text{C}/^{12}\text{C}$ ratios. In the latter samples, it is noticeable that the increase in ^{13}C content in the methane is paralleled by a decrease in methane in the gas composition. This trend clearly indicates the loss of ^{12}C -rich methane, an effect generally observed in all cases of gas loss whether by diffusion, oxidation or other means. The interpretation of the headspace gas suggests that the gas remaining in the salt has possibly undergone molecular and isotopic fractionation as a result of the gas loss. The headspace gases therefore provide qualitative evidence that the salt-bound gases represent only part of the gas inventory due to sampling losses.

Genetic interpretation of the condensate occurrences

For genetic reasons and, due to their molecular composition, for phenomenological reasons as well, condensates are considered to be transition products between oil and gas. They consist essentially of liquid hydrocarbons with low boiling points, roughly in the C_6/C_{16} range. Larger homologues occur in relatively small concentrations.

All investigation results of the unaltered or only slightly altered condensates in the Hauptsalz of the Gorleben salt dome indicate that they originated from an algal-rich carbonate source rock. These parameters, as well as the C-isotope ratios of the bulk samples and the fractions, are very similar to the analysis results from Zechstein oilfields in NE Germany and thus support the interpretation that they were generated from a Zechstein source rock. The main source substance is thought to be organic matter in the Stassfurt-Karbonat (z2SK), which is also the source of the gaseous hydrocarbons.

3.3.4.2 Other gas inclusions in the salt formation

In addition to gaseous hydrocarbons, probably even larger volumes of molecular nitrogen occur, as confirmed by analysis of the free gas inflows. The N_2 contents of the salt-bound gases, as well as the headspace gas, were not evaluated because of potential air contamination during sampling and during penetration of the gas occurrences. In addition to this, gases and gas mixtures are known from small, micrometre to millimetre-sized intra-crystalline fluid inclusions in the evaporites of the Gorleben salt dome.

Generally, there are two different groups of gases or gas mixtures in the inclusions: those containing nitrogen and those without nitrogen (SIEMANN & ELLENDORF 2001). The former can contain O_2 , whilst the latter are generally O_2 -free (see Fig. 50). In the case of the gas containing nitrogen and oxygen, it is assumed that they are inclusions of the Zechstein paleoatmosphere because they have a N_2/O_2 ratio similar to today's atmosphere. Pure nitrogen inclusions are always found in the direct vicinity of N_2 - O_2 -bearing inclusions. Combined occurrences of oxygen and nitrogen together with H_2 and H_2S were never encountered. Evaporite horizons with numerous inclusions of N_2 - O_2 or N_2 gases only rarely have inclusions of H_2 and H_2S and vice versa (Fig. 50). The most frequent gas mixtures in the nitrogen-bearing group consist of N_2 and CH_4 , or N_2 , CH_4 , and H_2 . These mixtures are generated by the decomposition of organic matter under anoxic conditions, which would apply for example to the Stassfurt-Karbonat. A corresponding explanation is also valid for the genesis of the gas group without nitrogen (N_2).

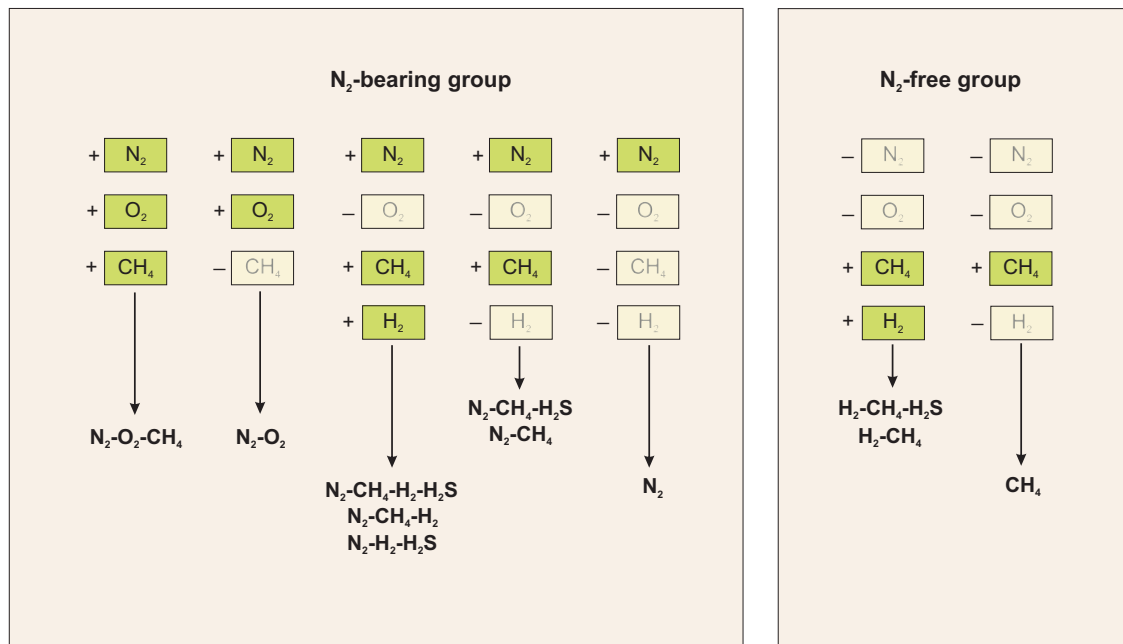


Figure 50: Gas composition of inclusions in evaporites in the Gorleben salt dome (according to SIEMANN & ELLENDORF 2001).

With respect to the nitrogen content, it cannot be excluded that at least some nitrogen was also produced by degassing processes in the underlying Early Permian or Carboniferous sedimentary rocks that contain a high proportion of organic matter. The migrating nitrogen must have become trapped in the inclusions of the evaporites during the early stage of halokinesis. Pure N₂ inclusions are frequent in the Knäuelsalz and Streifensalz (z2HS1, z2HS2). Inclusions with an N₂-CH₄ composition dominate in the Kristallbrockensalz (z2HS3) (ELLENDORF 1999).

Investigations carried out by PROHL (1998) revealed that in the case of the H₂-bearing inclusions, most of the samples had hydrogen contents below 15 vol%. This applies in particular to the Zechstein 2 samples. Zechstein 3 samples usually have lower H₂ contents of less than 3 vol% (ELLENDORF 1999: 73 ff.). It can be generally ruled out that the hydrogen formed within the inclusions. It is conceivable that the H₂ diffused from great depths or out of the rocks directly below the Zechstein evaporites. The H₂-bearing inclusions could also be explained by the decomposition of ammonium compounds. As N₂ is not found in all H₂-bearing inclusions, however CH₄ and H₂ are always encountered together, the most likely source of the hydrogen is considered to be the methanogenesis of organic molecules in a reducing environment rather than the aforementioned alternatives. From this, we may conclude that the hydrogen found in the inclusions has been there since they were originally formed, which suggests only a minor possibility of diffusive migration of hydrogen through the rock salt (see also SIEMANN & ELLENDORF 2001; PROHL 1998: 55).

The occurrence of H₂S in evaporites can be attributed to bacterial sulphate reduction. If sediments are buried at great depth, it is also possible that hydrogen sulphide is generated from organic sulphur compounds and reactions between hydrocarbons and sulphate minerals or dissolved sulphate at temperatures around 100 °C (HERRMANN 1988). This explains the co-occurrence of CH₄ and H₂S (ELLENDORF 1999: 74).

H₂O is by far the most frequently found gaseous phase in inclusions in the investigated evaporites. Gaseous H₂O occurs throughout, either alone or together with other gases (PROHL 1998: 20).

Unlike in other salt deposits, no CO₂ was found in the Gorleben salt dome. This is due to the absence of basaltic magmas, which have penetrated the saliferous formations in the Werra-Fulda Basin for example and are the source of intergranular CO₂ inclusions.

3.3.4.3 Brines

The inventory of an evaporite deposit also includes minor amounts of brines. Brines have been encountered in every salt dome in NW Germany explored from the surface or underground. This also applies to the Gorleben salt dome. The brines can either be of natural geological origin or solutions created by mining operations, or a mixture of natural and mining-associated solutions.

Theoretically, the following types of solutions can be present in salt domes:

- Natural solutions
 - Solutions penetrating the salt deposit from the surrounding rocks, such as surface water, groundwater or formation water, or fossil brines trapped in the salt deposit.
- Metamorphic solutions
 - are aqueous solutions affected by the interaction of migrating saline solutions from within the salt dome with the adjoining rock and/or altered by a temperature gradient. These solutions are trapped in the evaporitic rock and have reached chemical equilibrium with the evaporite.
- Mixed solutions
 - derive from the mixing of various saline solutions, originating from inside the salt dome. Conversion or crystallisation of the salt minerals may occur due to the resulting changes of chemism and the influence of rock temperature and solution temperature.

- Residual solutions from the depositional basin, i.e. the remains of fossil, evaporated and diagenetically altered seawater of the Zechstein period trapped in the saliniferous formation since deposition.

- Technical/Anthropogenic solutions

Ventilation solutions, drilling mud, cement water and other salt solutions created or altered by anthropogenic activities.

The underground exploration of the Gorleben salt dome revealed that occurrences of solutions (and gases) are not scattered throughout the salt dome but associated with specific stratigraphic horizons. The volumes of the solution (and gas) reservoirs encountered so far are between a few cubic centimetres and several 100 cubic metres (NOWAK et al. 2002).

The sedimentary or diagenetic association of the saliniferous rocks has been preserved despite halokinetic deformation and the existence of brine and gas reservoirs in certain rock types is made possible by their petrographic structure. It was therefore possible to make predictions for the underground boreholes as to whether the geological horizons being explored would permit solution or gas inflows. Such prediction requires adequate information on the geological structure from e.g. 3D models or EMR surveys. The chances of accidentally drilling into a reservoir close to the drilling location can be ruled out if these conditions are met. The following description of the reservoir horizons is restricted to the Zechstein 2 and Zechstein 3 sequences up to the Anhydritmittelsalz because no younger Zechstein beds were exposed by boreholes or by drifts during the underground exploration, nor will they be exposed in the future.

Solutions (and gases) in the Zechstein 3 sequence

Inflows of solutions (and gases) are expected only in those Zechstein 3 beds that primarily consist of anhydrite and can form bedding-parallel fissure reservoirs. These are as follows:

- Anhydritmittel 1, 7 and 9 in the Anhydritmittelsalz
- Gorleben-Bank (Mittleres Orangesalz)
- Hauptanhydrit with the accompanying Gebänderter Deckanhydrit (z2) to Leine-Karbonat

The **Anhydritmittel 1, 7, and 9** consist of anhydrite layers with a thickness of 0.2 m to 2.3 m. Taking into account that these beds are not continuous but have been formed into boudins to varying degrees depending on the extent of halotectonics, i.e. they have been cut into individual sections a few metres long that are not interconnected (see Chapter 3.3), the associated volumes of joint reservoirs amount to only a few litres. Examples of inflows from the Anhydritmittel are damp patches in the electrical workshop, the vehicle workshop, the connecting drift between the vehicle and the electrical workshop (840 m-level) and three locations in the southward air drift of the 820 m-level.

The **Gorleben-Bank** mainly consists of a tightly laminated anhydrite bank with a thickness that varies locally in the salt dome from a few millimetres to approx. 0.4 m. There is a correlation between brine (and gas) content and thickness insofar as thin zones of less than 10 cm thickness display no brine (or gas) content (e.g. Shaft 2 and surroundings). The inflows are exclusively restricted to the western flank of an anticline that runs approx. parallel to the drift landing in Shaft 1 (840 m-level), and is also exposed in Shaft 1 from 858 to 863 m and in the conveyor drift at the 880 m-level. The Gorleben-Bank is up to approx. 40 cm thick in these areas.

The reservoirs in the Gorleben-Bank can take various forms and be associated with:

- A bedding-parallel fault running through the Gorleben-Bank with slickensides on its top and bottom surfaces which is partially healed with secondary halite and secondary carnallite,
- Fissures in the Gorleben-Bank
- Secondary carnallite fillings in fold cores beneath Gorleben-Bank
- Reservoirs in the fanning-out, bedding-parallel anhydrite lamellae in the Gorleben-Bank

The reservoirs can range from a few cubic metres to 10 cubic metres in size. Connections between separate reservoirs are possible via the bedding-parallel fault in the Gorleben-Bank. Examples of inflows from the Gorleben-Bank are several damp patches and inflows at the landing and in the landing drift of Shaft 1 (840 m-level, with a max. volume of 4 m³), in Shaft 1 from 858 to 863 m (estimated inflow 1 m³ max.) and in the pilot boreholes for the conveyor drift at the 880 m-level (3.8 m³ inflow).

The underground exploration carried out so far proved that the **Hauptanhydrit** on the southern flank of the Hauptsalz anticline of the salt dome occurs as separate, mostly isolated blocks with no significant hydraulic connections with one another (BORNEMANN

et al. 2001; BORNEMANN et al. 1998). Pressure measurements confirmed that there is no connection with the salt table (NOWAK & WEBER 2002; NOWAK et al. 2002). Brines (and gases) are confined to fissures, which are scattered irregularly in the Hauptanhydrit blocks and are due to multiple repeated deformations from various directions during diapirism. The fissures are mostly healed with secondary halite and secondary carnallite. In some cases, healing was not complete. In some areas, drusy cavities of some centimetres in size were encountered. Open fissures some millimetres wide were rarely observed. The size of a reservoir in the Hauptanhydrit depends on the size and the degree of fissuring of the hosting Hauptanhydrit block.

Solutions (and gases) at the boundary of Zechstein 2 to Zechstein 3

Inflows of brines (and gases) are possible at the z2/z3 boundary if the Hauptanhydrit has been squeezed off as a result of halokinetic deformation and the Kaliflöz Stassfurt is either thickened or significantly thinned.

Two different types of occurrence can be distinguished:

1. Drusy cavities that are mostly healed with secondary halite and secondary carnallite. The brines occupy non-healed interstices between the crystals. Such drusy cavities can reach sizes of up to 1 m³. A connection between the occurrences does not exist. The volume of brines or gases released by drilling is in the order of a few litres. Examples of inflows are from cross-cut 1 West and the work rooms on the 840 m-level where pilot boreholes encountered brines (and gases) with inflows of 27 l and 21 l, and 15.8 l and 7.9 l respectively.
2. Faults and fissures resulting from strong deformation of the sequence of Unteres Orangesalz and Liniensalz which occur from the Gorleben-Bank (Mittleres Orangesalz) up to the Zechstein 3 / Zechstein 2 boundary. The sedimentary sequence of strata is totally destroyed in such areas by intercalated fissures and faults some metres in width. The fissures and faults are largely healed with secondary, clear coarse-crystalline halite (crystals up to and more than 10 cm). Secondary carnallite occurs in interstices to a lesser extent. The solutions and gases are trapped in non-healed interstices between the coarse-crystalline halite sections. Only a very rough estimate can be made of the total extent of the hydraulically interlinked zones. It is in the order of > 10 m. Examples of inflow volumes are those from boreholes 01YEF20 RB014 (80 m³) and 02YEA04 RB023 (24 m³).

Brines (and gases) in the Zechstein 2 sequence

The Hauptsalz of the Stassfurt-Folge (z2HS) is a “halokinetic breccia” and therefore does not have the properties described above which facilitated the formation of brine reservoirs in the past. Consequently, no significant amounts of brines (and gases) were encountered in this sequence during the underground exploration.

The original fabric of the Hauptsalz resembled that of the Liniensalz. During diapiric movement (approx. 2 to 5 km lateral and 3 km vertical) the sequence was mixed and homogenized by repeated fracturing and healing of the rock salt. The present-day result of these processes is a typical breccia. The remains of the former sedimentary or diagenetic fabric consist of halite crystal lumps as well as clustered shredded fragments of anhydrite bands which, depending on the bedding type of the Hauptsalz and on the degree of stress exerted on the rock, can either be concentrated in zones of varying width, or scattered in the halite matrix. The matrix primarily consists of recrystallized halite.

Most of the brines (and gases) of sedimentary and diagenetic origin previously contained in the Hauptsalz have either been squeezed out towards the salt table or into anhydrite fissure reservoirs of the Leine-Folge (e.g. Hauptanhydrit) due to the deformation of the salt formation. No occurrences of brines (and gases) were encountered during the underground exploration of the Hauptsalz in the Gorleben salt dome. This is particularly highlighted by the absence of brines in the area of the western and eastern cross-cuts as well as in three approx. 600 m-long exploration boreholes drilled laterally through the core zone in the Hauptsalz.

Only in the Knäuelsalz (z2HS1), which is the oldest sequence in the Hauptsalz and contains in some parts 10 to 20 % anhydritic intercalations, were minor inflows of condensates and gases encountered. These are residual condensates and gases bound to crystal boundaries, which were not squeezed out because of the higher anhydrite content. The small occurrences are clustered and limited to zones of rock salt one to several cubic metres in size. Examples of such occurrences in the Hauptsalz were encountered in cross-cut 1 East/drilling location 3.1 (inflow of a few litres), in borehole 02YEQ01 RB119 at 177 m (damp patch, unquantifiable amount), in borehole 02YEQ01 RB120 at 127.3 m (damp patch – condensate, unquantifiable amount) and in borehole 02YER02 RB032 at 303 m (damp patch – condensate, unquantifiable amount).

Brines in Shaft 1 and Shaft 2

In both shafts, between the salt table and a depth of approx. 320 m in Shaft 1 and approx. 290 m in Shaft 2, NaCl solutions were encountered in boreholes drilled from the shafts as well as on the shaft wall (BORNEMANN et al. 2002). These also contained minor amounts of the (calculated) components $MgCl_2$ and KCl as well as traces of $CaSO_4$ and $CaCl_2$. The bromide content ranged between 60 and 519 $\mu g/g$ (Shaft 1) and between 460 and 5100 $\mu g/g$ (Shaft 2).

HERRMANN & KNIPPING (1993 a) examined whether the composition of these NaCl solutions could be derived from the mineral components of the rock in which they were found or of the rock formations that were identified as migration paths for these solutions. Based on the bromide balance, they calculated that the bromide contents of the solutions could not originate only from the dissolution of the rock salt surrounding the shafts. But if small amounts of carnallite (1 to 5 wt%), as found in fissures and cavity fillings in this rock salt zone, are added to the generated solution, the resulting bromide contents are the same as in the encountered NaCl solutions in the shaft. This finding also applies to the concentrations of the main components.

According to HERRMANN & KNIPPING (1993 b) these solutions developed according to the following model: *“The solutions were created by dissolution of rock salt by water from the overburden of the salt dome in so called pot-shaped cracks. The pot-shaped cracks were caused by contraction of the evaporitic rocks as a result of the freeze sinking of the shafts.”* However, it cannot be completely ruled out that in some parts minor amounts of solutions from within the salt dome (e.g. solutions with bromide concentrations well above 250 $\mu g/g$ bromide) or small amounts of anthropogenic solutions (e.g. solutions with $CaCl_2$ components) were involved.

After reaching a depth of 350.2 m beneath the pit head in Shaft 1, an approx. 0.7-m-thick concrete floor was set on the shaft bottom, whilst the foundations and the shaft lining were being installed. Aqueous solutions were observed in one observation shaft and later on in control boreholes fitted with packers, which were drilled through this concrete floor. The aqueous solutions were observed from August 1993 until the concrete floor was removed. HERRMANN & KNIPPING (1994) interpreted these solutions as follows: *“The composition of the saturated NaCl solutions at the bottom of Shaft 1 in Gorleben can mainly be attributed to the dissolution of halite by unsaturated water. Chemical analysis alone cannot determine in which manner migration paths were formed. Moreover, the area around the sampling sites has been strongly contaminated by human activity. Given the volume of condensation water present at some times, the volumes of solution in the packers are relatively low.”*

From time to time, solutions entered both shafts from joints of the supporting rings as well as from rock salt immediately below the supporting rings. Analysis of the salt solutions during the observation period revealed that they were primarily of type 5 A after HERRMANN et al. (1978), i.e. strongly concentrated NaCl solutions with lesser amounts of MgCl_2 , MgSO_4 and KCl. There was major variation in the composition of the main components during the whole period in which this solution was sampled, and the variation is probably due to the sampling conditions. According to KNIPPING & SIEMANN (1996), it was only possible to collect samples that were possibly very strongly affected by evaporation and contamination with salt dust and ventilation solutions. Due to these unfavourable conditions during sampling, it is only possible to make the following limited interpretation of the origin and genesis of the solution: *“The chemical composition of the solution can be explained by the dissolution of rock salt by unsaturated aqueous solutions.”*

Generally, only two types of natural solution occur in Shaft 1, which can be distinguished by their main components:

- **Type 1:**
Highly concentrated MgCl_2 -bearing solutions, also containing MgSO_4 but no CaCl_2 . This corresponds to solution type 5 C according to the classification by HERRMANN et al. (1978).
- **Type 2:**
Highly concentrated MgCl_2 -bearing solutions, also containing CaCl_2 but no MgSO_4 . This corresponds to solution type 5 D according to the classification by HERRMANN et al. (1978).

Inflowing solutions were also registered during the sinking of Shaft 2 (BORNEMANN et al. 2002 b). These were anthropogenically influenced salt solutions which occurred at the supporting rings, or natural solutions such as those entering boreholes drilled from the shaft from 400 m depth downwards. The anthropogenically influenced salt solutions differ from the other shaft inflows by having much higher CaCl_2 contents. Two boreholes (00YES02 RA235 and 00YES02 RA236) were drilled from Shaft 2 into the Unteres Orangesalz and Gorleben-Bank (approx. 480 m beneath the pit head). These two boreholes encountered highly concentrated MgCl_2 -bearing salt solutions without CaCl_2 . The solutions encountered in both boreholes only differ in their trace element composition. The former (00YES02 RA 235) showed bromide contents of approx. 3000 $\mu\text{g/g}$ and lithium contents of 150 $\mu\text{g/g}$. The latter (00YES02 RA236) showed bromide contents of approx. 4000 $\mu\text{g/g}$ and lithium contents of approx. 400 $\mu\text{g/g}$.

KNIPPING (1995) explains the genesis of these solutions based on the geochemical analyses: *“After crystallization of the K-Mg mineral associations of the Stassfurt-Folge, concentrated $MgCl_2$ solutions existed at the bottom of the Zechstein Basin. After formation of the Leine rock salt which stratigraphically followed the Stassfurt-Folge, residues of the strong $MgCl_2$ -bearing solutions at the bottom of the Zechstein Basin entered gaps and fissures in other evaporitic beds as ‘free’ formation fluids via temporary local migration paths. They mixed with small amounts of metamorphic solutions generated by the dissolution of carnallite in an $MgSO_4$ -depleted carnallite rock by a saturated NaCl solution.”* This explains the increased Rb content and the slightly decreased bromide content compared to solution sample 236.001 for example. It is not possible to identify the point in time when this metamorphism took place. It may have been either shortly after formation of the carnallite or e.g. when the Zechstein 2 beds were uplifted and formed the salt dome. The important fact is that only solutions from within the salt dome were necessary for these processes and that the participation of formation water was not required. This is indicated by the high bromide contents in the solutions of $> 4000 \mu\text{g/g}$ solution. The salt solutions in Shaft 2 are therefore to be interpreted as the remains of fossil seawater, which were altered within the salt dome. Thus, neither water from the overburden nor formation water has entered the Gorleben salt dome in the sampled area 250 m below the salt table during geological time periods.

Salt solutions at Exploration Area 1 (EB 1)

Prognoses based on earlier investigation results (BORNEMANN et al. 1998) allowed the determination of areas where inflows of salt solutions were to be expected when exploring EB 1:

- Fissure reservoirs in anhydrite rocks or claystones
These include the Gebänderter Deckanhydrit, Grauer Salzton, Leine-Karbonat, Hauptanhydrit, anhydrite bank in the Basissalz, Gorleben-Bank and Anhydritmittel in the Anhydritmittelsalz.
- Fault or fissure zones healed by secondary halite at the z2/z3 boundary and in some of the lower parts of the Gorleben-Bank
- Thinned or thickened Kaliflöz Stassfurt at the z2/z3 boundary without the sequence from Gebänderter Deckanhydrit to Hauptanhydrit

No significant or unpredicted inflows of gases or solutions were encountered during the exploration of EB 1, particularly in the Hauptsalz. Solutions (and gases) were registered during the drilling of boreholes 01YEF20 RB217 (fissure zone in the Gorleben-Bank) and 02YEA12 RB218 (anhydrite bank in the Basissalz) and during the driving of the drifts (shaft undercut to the 930 m-level) in the vicinity of the Gorleben-Bank.

Almost all major inflows of gases and solutions were sampled. The results of the solution inflow analyses are summarized in HERRMANN & KNIPPING (1993 b), SIEMANN (1996), KNIPPING & SIEMANN (1996), HERBERT & SANDER (1997), SIEMANN & MENGEL (1998), HERBERT & SANDER (1998 a, b, c, d) and HERBERT & SANDER (2000).

3.3.4.4 Pressures in solution and gas reservoirs

In salt domes solutions and gases occur in isolated reservoirs. The pressures in such isolated reservoirs adapt to the petrostatic pressure in the surrounding rock due to the creep of the ductile rock salt over a long period of time. The pressure in an undamaged reservoir is therefore the same as the petrostatic pressure. The petrostatic pressure at a depth of 840 m for instance is 18 MPa at an average rock density of 2.2 g/cm³.

The pressures measured in the reservoirs encountered in the Gorleben salt dome were petrostatic as expected, i.e. they were initially higher than the hydrostatic pressure. These measurement results are sufficient proof that the reservoirs are isolated and that no link exists to the aquifer outside the salt dome. The petrostatic pressure inside the reservoirs could not be measured because the conductor pipes of the boreholes were not designed for such high pressures (NOWAK et al. 2002).

3.3.4.5 Permeabilities of the rock salt in the vicinity of solution and gas reservoirs

When a reservoir is penetrated, the pressurised fluids are pressed out of the reservoir into the borehole. As the flow continues, fluids from increasingly distant parts of the reservoir have to be conducted towards the borehole. Apart from the ambient pressure, the key factors determining the flow rate are the geometrical conditions and the viscosities of the fluids as well as the permeability of the rock through which the fluids flow.

Away from areas of solutions and gas occurrences, the ductile rock salt and the Hauptanhydrit have no permeabilities larger than 10⁻²¹ m² and can be considered to be impermeable. In areas of solutions and gas occurrences, the rock has permeabilities that are dependent on the structure of the pore space. The largest permeabilities can occur in fissured reservoirs, which may exist in the Hauptanhydrit and at the Zechstein 2 to Zechstein 3 boundary. The maximum permeability in a fissure reservoir is limited by the mutually supporting fissure surfaces required to transmit the pressure of the surrounding rock. Fissure widths in the order of a few millimetres can be found between the load-bearing points. Hauptanhydrit, which is to be considered impermeable in its compact state, can have permeabilities of more than 10⁻¹⁵ m² in fissured areas for instance (NOWAK et al. 2002).

The hydrocarbons occasionally encountered in the Hauptsalz were small-volume intercrystalline accumulations, which cause negligible (RB032) or very low flow rates (cross-cut 1 West). The permeabilities in these zones are well below 10^{-15} m². Fluids in cavernous fissure zones that can move almost independently of the reservoir rock are an exception. The volume of such zones is very small and has a maximum of only a few hundred cubic centimetres.

3.3.5 Water content of the rock salt

Between 0.1 and 2 vol.% H₂O is usually found in the thick rock salt beds of the Hauptsalz (z2HS) in North German salt domes (HERRMANN & KNIPPING 1993 a; JOCKWER 1981). The solutions occupy grain boundaries or form fluid inclusions.

Occasionally, inclusions are found which can contain up to 1000 m³ (HERRMANN & KNIPPING 1993 a; WEBER et al. 1998). However, these occurrences are isolated. Such solutions remain immobile as long as the almost isotropic stress state existing in the rock salt due to its capability to creep is not disturbed, e.g. by drifting (SCHULZE 2002).

Investigations of the fluid inclusions in the rock salt have so far provided no evidence regarding composition and origin of the solutions that would indicate inflows from outside the salt dome. HERRMANN et al. (1997) reported that the composition of the intercrystalline fluid inclusions reflects the source solutions available during seawater evaporation and early metamorphic processes.

Measurements of the water content in the Hauptsalz of EB 1 (SANDER & HERBERT 2000) produced very low values (Knäuelsalz: 0.014 wt%, Streifensalz: 0.017 wt% and Kristallbrockensalz: 0.012 wt%). In contrast, the water content of rock salt samples from the Asse structure, for instance, has a maximum of 0.04 wt% (GIES et al. 1990).

The low water content in the Hauptsalz in the Gorleben salt dome is due to the strong brecciation and homogenization of the rock salt beds during diapirism, which released, mobilized and squeezed out solutions originally trapped within the salt formation. In structures resembling salt pillows, the rock salt beds of the Hauptsalz were exposed to less halokinetic stress so the solutions trapped within the rock salt have not been squeezed out to the same degree.

4 Evaluation of the results

4.1 Size of the Hauptsalz as the host medium for a potential repository

In order to estimate the extent of the Hauptsalz as the potential host medium for high-level radioactive waste, the exposures of the Hauptsalz at the 840 m-level and 150 m below the 840 m-level were determined for Exploration Area 1 (BORNEMANN et al. 2001: 44). The northern and southern boundaries were defined by the first penetrated sections of the Kaliflöz Stassfurt nearest to the core zone. The western boundary is identical with the safety margin of the claim boundary. According to the geological prognosis, the eastern boundary runs approx. 150 m east of cross-cut 1 East.

The resulting area of the Hauptsalz is shown in Table 5. The dimensions of the repository area in EB 1 indicated in the table are only preliminary because the geological exploration of EB 1 has not yet been completed. This is particularly true for the shape of the northern and southern boundaries deeper down in EB 1.

If the repository planning and safety evaluations result in the selection of a repository concept that provides for the emplacement of high-activity waste in boreholes, then the northern and southern boundary of EB 1 will have to be explored well below the exploration level so that the boreholes for HAW can be precisely positioned in the Hauptsalz.

Table 5: Dimensions of the Hauptsalz in Exploration Area 1.

Section	without safety pillar	10 m safety pillar	50 m safety pillar
840 m-level	370 700 m ²	357 700 m ²	305 700 m ²
150 m below 840 m-level	390 900 m ²	377 800 m ²	325 700 m ²

To ensure that no artificial migration paths for solutions and gases are created during the geological exploration, no exploration boreholes are drilled downwards in the central part of the Hauptsalz. Due to the genesis of the salt dome, which involved the upward movement of salt, it can be assumed that if the margins are firmly established then the Hauptsalz must also be present in the central part.

The results of the investigations carried out so far regarding the dimensions of the Hauptsalz support the earlier prediction that the Gorleben salt dome contains a sufficient volume of salt suitable for the final disposal of high-activity, heat-generating waste. During the concluding exploration work, the boundaries of the Hauptsalz will have to be precisely defined in order to prove the long-term safety and to permit precise volume calculations.

4.2 Fissures and potential migration paths for saline solutions and gases

An assessment of the long-term geological safety of a planned repository in the Gorleben salt dome must also assess potential migration paths for fluids that might allow the migration of radionuclides from the repository into the overburden. Potential migration paths are fissures and faults. This report does not cover potential new artificial fissures created by the disposal of radioactive waste and the associated cutting of drifts etc., because these will be evaluated as part of the safety analysis.

Naturally formed fissures and faults are generally encountered in salt rocks but they are usually healed and closed by the formation of new salt minerals (see FISCHBECK & BORNEMANN 1993; FISCHBECK & MINGERZAHN 1997). Thus, they are no longer available for the migration of radionuclides. Hence, only fissures within the salt dome that may act as potential migration paths are described below. Open fissures (meaning filled with solution) were either encountered directly during the exploration work, i.e. during the sinking of shafts and cutting of drifts, or indirectly interpreted from the inflow of salt solutions into boreholes. It must be concluded that the fissure systems are of limited extent because the flow volumes of the salt solutions recorded in the Gorleben salt dome were low and either greatly diminished over time or ran dry completely. An estimate of the inflow volumes shows that the largest inflows of up to 100 m³ occur in the fragmented Hauptanhydrit and the secondary halite in fissure and fault zones at the z2/z3 boundary. All other occurrences of solutions mentioned in Chapter 3.3.4.3 involved only a few litres to a few cubic metres at most (BORNEMANN et al. 1998: 34). Similar observations apply for the gases co-occurring with the solutions, for instance in the fissures in the Hauptanhydrit or in other salt rocks. The gas volumes were similarly limited.

The fissures in the salt dome run either parallel to the bedding or at an angle. The fissure geometries (angle, width, length) depend on the material properties and stress loading of the evaporites. The widths of the fissures in the Hauptanhydrit, which are usually healed, range from millimetres to metres whilst the fissure lengths range from decimetres to tens of metres. No correlation between fissure spacing and e.g. lithology, banking structure or texture of the evaporite beds could be identified. The fissures are irregularly spaced. The occurrence of fissures is mainly restricted to the Hangendsalz (z2HG), Kristallbrockensalz (z2HS3), Hauptanhydrit (z3HA), parts of the Basissalz/Unteres Liniensalz (z3BS/z3LSU), Orangesalz (z3OS), Anhydritmittelsalz (z3AM), Tonmittelsalz (z3TM) and the Tonbrockensalz (z4TS). No fissures were encountered in the core region of the Hauptsalz (z2HS) and thus in the area of the planned repository.

The fissures in the Gorleben salt dome apparently occur always in the same stratigraphic and tectonic positions, e.g. near the boundary of the Stassfurt-Folge and Leine-Folge in the beds of the Hangendsalz of the Stassfurt-Folge. However, this rule applies at this boundary only if larger sequences are missing in this zone due to halotectonics or where the Kaliflöz Stassfurt has been thinned out by local impoverishment. As the Kaliflöz Stassfurt is not affected by solutions at other locations, despite being in the vicinity of brine-filled fissures in the Hangendsalz, it is found that the fissure occurrences are usually isolated and of restricted extent.

The Hauptanhydrit (z3HA) is generally characterised as a stratigraphic zone that is likely to contain fissures. This is probably due to its brittle petrophysical properties and its competent behaviour during halokinesis. However, since findings show that the Hauptanhydrit in the Gorleben salt dome has been broken into isolated blocks, it cannot be concluded that a major interconnected fissure system has formed. This applies particularly to the central Hauptanhydrit, which forms the southern flank of the Hauptsalz core zone of Exploration Area 1 (see BORNEMANN 1991: App. 23; BORNEMANN et al. 2000).

The main causes of fissure generating processes in salt rocks are generally:

- Climate change (only at the salt table)
- Salt movement/tectonics
- Metamorphosis

The fissures occurring in salt table borehole GoHy 1151 close to the salt table are thought to be of glacial origin. However, unlike the fissures of glacial origin found at the top of other salt domes (BAUER 1991), they have a shallow dip and, similar to the fissure pattern on the roof of granitic plutons, they are therefore interpreted as results of stress release, in this particular case after the retreat of the glacier.

Another source of fissures is the subsrosion of the Kaliflöz Stassfurt near the surface of the salt dome. The removal of potassium and magnesium minerals causes a reduction in the volume of the potash horizon, which then can cause rupturing of the adjacent rock salt. Fissures can also arise in beds that have different mechanical properties and are subjected to strong halokinetic stress. This is due to the differential mobility that exists e.g. in the carnallitic Kaliflöz Stassfurt and the neighbouring Hangendsalz which has poorer flow properties. This also occurs in some zones between the Hauptanhydrit and the neighbouring Basissalz, Liniensalz, and rarely also the Orangesalz. Fissures in salt structures can theoretically also have a tectonic origin that can be traced to the regional stress field. Ruptures of this kind as well as joints resulting from the cooling of the rock during the last glacials have not been identified in the Gorleben salt dome so far.

In the near “geological” future, two causes of natural fissuring due to a potential climate change could in principle affect the planned repository. The first is associated with the postulated re-advance of an inland glacier in 60 000 years or more (e.g. BOULTON & PAYNE 1992), which could cause fissures in the overburden and the salt dome by mechanical compressive stress. A second cause of fissuring may be the assumed development of permafrost in approx. 10 000 to 20 000 years time where joints might form as a result of differential cooling of the salt dome and the adjoining rocks.

In the case of a new ice age, the formation of fissures in the salt dome depends particularly on the depth of the salt table. As geological investigations have revealed that the mechanical depth impact of an advancing glacier only reached a maximum depth of approx. 200 to 300 m (EISSMANN 1987; HANNEMANN 1995), no such fracturing of the saliniferous formation in the Gorleben salt dome is expected based on the present depth of the salt dome.

The formation of fissures from differential cooling of the salt and the adjoining rock as a result of permafrost has so far only been described and discussed in the case of a shallow salt dome in the Hanover area (BAUER 1991). The maximum depth of permafrost during an assumed future ice age of Weichselian type is approx. 200 m (KELLER 1996: Table 3), which would not affect the Gorleben salt dome, so no fissuring of the salt rock is expected to occur as a result of ground cooling.

In millions of years, natural fissures could also occur due to further salt uplift. This would depend on an appropriate compressive stress field in a tectonically mobile crust as well as sufficient thickness of Hauptsalz in the rim synclines (to supply continued diapirism). Present-day knowledge on the structural development of the North German Basin indicates no tendency towards a compressive stress field. Besides, only small amounts of Hauptsalz remain in the rim synclines.

4.3 Consequences of subsidence for the long-term safety of a repository

Safe isolation of the hazardous materials from the biosphere is required for the post-operational phase of a repository. This aspect is the subject of safety analyses covering time periods “for which changes to the geological barriers and the human environment, particularly as a result of climate change, can still be forecast with a sufficient degree of reliability” (EHRlich et al. 1986: 2). With respect to the development of quantitative criteria in the search for repository locations with favourable overall geological conditions, AkEnd (2002: 30) determined that the period of isolation to be considered in long-term safety analyses of the respective repository sites should be in the order of 1 million years.

Regarding proof of the long-term safety of a repository at the Gorleben site, a reliable prognosis for this period with respect to subsidence appears feasible based on present-day knowledge (ZIRNGAST et al. 2003: 237 ff.). It has to be concluded that favourable geological conditions with no significant changes will prevail at this site during the required isolation period. This conclusion is based on the following considerations and applies to a safety analysis that takes the subsidence aspect into account.

The boundary surface between the cap rock and the saliniferous formation of the Gorleben salt dome, i.e. the salt table, is at an average depth of 250 m (see Fig. 36 and App. 5). At some locations on the NE part of the salt dome, i.e. at a distance of approx. 3 km from the planned repository area, it reaches a depth of 350 m. If the emplacement level of the planned repository was to be located at a depth of approx. 880 m, the thickness of the rock salt between the emplacement area and the salt table would be between 500 and 600 m. This thickness of the overlying rock salt is a safety-relevant component of the effective radioactive waste isolation in the salt rock formation.

The average subsidence rate derived from the long-term development of the salt dome is approx. 0.01 mm/year (EHRlich et al. 1986; KELLER 1990: Fig. 16). This corresponds to a lowering of the salt table by 10 m in one million years. If the extremely high average subsidence rate of approx. 0.2 mm/year determined for the post-Elsterian period is used in the calculations for an isolation period of 1 million years (see Table 3), then 200 m of the effective rock barrier would be affected by subsidence (see also Chapter 3.2).

During extreme events like glacial channel formation, easily soluble salt horizons may be locally affected by a deeper progressive subsidence than the rock salt. An example for such salt horizons is a potash seam cropping out at the salt table as an inverted bed, which is thus not overlaid by a protective clay layer. As shown by the drilling results, such "dissolution cavities" are rapidly healed by the recrystallization of halite. In addition to this, such extreme subsidence of the potash seam only occurs if the seam is overturned. When normally bedded, younger argillaceous layers prevent more intense subsidence. The model of the salt dome genesis indicates no inverted bedding of the Kaliflöz Stassfurt above the planned repository area of the Gorleben salt dome (see also Fig. 36).

If a new glacial period caused subsidence of a potash seam exposed at the salt table, no widespread reduction in thickness of the effective rock barrier would result. The particular subsidence of the potash seam would occur only locally and would be rapidly healed by crystallization or recrystallization and even during extreme ice ages like the Elsterian Glacial the effects would never affect the salt dome deeper than 200 m. However, a potential repository mine will not be set up beneath such an area, which is potentially

endangered by subsrosion, and a sufficient distance between the mine and this specific inverted potash deposit would thus be ensured.

In this context, it should be noted again that continuous subsrosion only takes place under specific conditions. The most important of these is that the salt table always has to be in zones in which subsrosion is facilitated by the hydrogeological situation, i.e. that subroded salt is transported away so that no saturated stagnant brines accumulate above the salt dome to impede the subsrosion process. This removal can only take place consistently if there is continued salt uplift or an epirogenic uplift with erosion of the overburden. Presently, this is only taking place to a very limited degree. JARITZ (1994: 196 ff.) calculated that the maximum and current rates of salt uplift are 0.07 to 0.08 mm/year and 0.01 mm/year respectively, i.e. in one million years the salt table may (in the absence of subsrosion) theoretically have risen by only 70 to 80 m or 10 m respectively. Based on the epirogenic events in the Tertiary, JARITZ (1994) postulated changes in height of 10 m over a period of one million years due to future uplift/subsidence. In the case of uplift, these 10 m would have to be added to the halokinetic uplift of the salt, or subtracted if epirogenic subsidence took place in order to calculate the theoretical elevation of the salt dome in one million years. The difference between present and future depth would thus be 80 to 90 m (60 to 70 m) or 20 m (0 m) respectively.

More recent findings on the geological evolution of the region have been presented by FRISCHBUTTER (2001) and LUDWIG (2001) who assume that the exploration area has subsided by more than 300 m since the Rupelian stage (Early Oligocene) and that the area is subsiding at a rate of up to 1 mm/year. Even if this rate is probably very high (it means 1 km subsidence in one million years) and may contain sources of error like sedimentary compaction, extrapolation, etc. (see FRISCHBUTTER 2001), both findings indicate a trend of increased future subsidence of the area. This means the salt table will subside, which will decrease groundwater dynamics with increasing depth and will provide better protection against erosion during future glacials due to reduced subsrosion rates as a result of increasing sedimentary beds overlying the salt dome.

Further conclusions on subsrosion can be drawn, at least for the SE edge of the salt dome, from the investigation of the Anhydritmittelsalz in borehole Go 1005. Unlike the other Anhydritmittel in the Anhydritmittelsalz, which consist of anhydrite rock, the Anhydritmittel 9 usually consists of a sylvinitic kieserite-anhydrite rock which is interpreted to have formed in several phases of metamorphism after consolidation and folding of the beds (FISCHBECK 1985). The Anhydritmittel 9 encountered in borehole Go 1005 was almost completely altered to polyhalite (ALBRECHT et al. 1991: 283). This alteration took place at a later stage and is locally restricted. This is thought to be due to the special position of

the Anhydritmittel 9 in this area close to the edge of the salt dome (located approx. 120 m below the edge and approx. 30 to 50 m horizontally from the edge), a position reached as a result of diapirism and movement of the salt rocks. This indicates that water penetrated the salt dome from the surrounding rock at least for a certain period and was responsible for the alteration of the salt rocks. This alteration of the Anhydritmittel 9 encountered in borehole Go 1005 proves old cap rock formation of the Middle Mesozoic. This means that by analogy with the time at which the older cap rock was formed, it is possible to restrict the time period for the polyhalitic alteration and penetration of the salt dome by water to the most dynamic period of diapirism during the Jurassic to Early Cretaceous. As this process is completed, there are no further migration paths from the flanks into the salt dome.

These considerations and calculations lead to the conclusion that the subsidence at the surface of the salt dome has no significance for a quantitative safety analysis. The safety-relevant component of the effective rock barrier remains sufficiently large with a thickness of 300 to 400 m to prevent the release of radionuclides from the repository into the biosphere in one million years even if extreme (improbably high) subsidence rates are assumed.

5 Summary

The exploration of the Gorleben salt dome in the district of Lüchow-Dannenberg in Lower Saxony began in 1979 and continued until the politically decreed moratorium on October 1, 2000, which involved the suspension of all site investigations. The investigation programme comprised the surface and underground geological and mining exploration of the site, as well as the elaboration and assessment of all issues required for a future suitability and safety assessment.

This report describes the procedures and the currently available results of the surface and underground investigation up to October 2000. As the underground exploration was interrupted, and work on Exploration Area 1 (EB 1) could not be completed, this report must be considered as incomplete with regard to an assessment of the salt dome and an associated geoscientific evaluation of its suitability.

The exploration of the salt dome from the surface began with deep salt dome exploration boreholes drilled from the surface, as well as seismic surveys and geochemical-petrographic analysis of the drilling samples. In the course of this work a new fine-stratigraphic subdivision of the Zechstein sequence was developed for certain stratigraphic horizons, which can be applied with limitations to the whole Zechstein Basin.

This detailed stratigraphic subdivision is necessary to ensure that the planned exploration and repository drifts can be driven while conserving the geological barrier. Additional detailed knowledge about the structure and character of the stratigraphic sequence was gained from the sinking of the shafts and the underground drifting and geophysical logging. In addition to the mapping and drilling results, the EMR survey results and the conversion of the exploration results into a 3D deposit model were particularly useful in determining the structure of the salt dome. The bromide concentration analysis of rock salt samples was also helpful in the stratigraphic identification of the beds.

The special bromide analyses and the other mineralogical and geochemical methods also provided valuable information on the genesis and metamorphosis of the evaporites. They revealed that the distribution of mineral contents and bromide indicates progressive evaporation during sedimentation and that the primary bromide distribution within the rock salt is still largely preserved despite diapirism. The differences in bromide concentration between halite in crystal lumps and in the matrix also provide evidence that the characteristic Hauptsalz fabric is a result of halokinetic brecciation. The geochemical analyses of the salts revealed no reactions with solutions from outside the salt dome.

A high priority was given to the issues of subsrosion at the salt table, of dissolution processes within the salt dome itself, and the occurrence of gases and particularly hydrocarbons. These investigations revealed that the salt table has been affected by average subsrosion rates of a few hundredths of a millimetre per year over long geological time periods. Subsrosion rates only rose to a few tenths of a millimetre per year for a “short time” in the post-Elsterian period. The subsrosion rates were derived from the chronologic classification of the Hutgesteinsbrekzie and especially from the genetic interpretation of the Geschichtetes Gips-, Anhydritgestein. In the area of the Gorleben Channel at one of the explored locations, the particularly soluble Kaliflöz Stassfurt has been subroded and altered down to a maximum depth of 170 m below the salt table. This section is approx. 3 km away from the planned repository area and is restricted to an inverted bedding of the potash seam that does not exist above the planned repository.

Assessments on the significance of subsrosion for the long-term safety of the planned repository showed that the thickness of the Hauptsalz, as the most important safety-relevant component of an effective rock barrier, will be still large enough to permanently prevent radionuclide transport from the repository into the biosphere even after one million years. The assessments are based on the calculated subsrosion rates, the probable regional epirogenic development, and the only minor remaining tendency of the salt to move upwards. The same applies to the situation at the sides of the salt dome, where subsrosion has not reached a safety-relevant extent for millions of years.

The solutions encountered in some boreholes and during drifting were restricted to specific stratigraphic horizons such as the Hauptanhydrit or the boundary between the Stassfurt-Folge and the Leine-Folge. The solution inflows occurred only for a limited period of time. Analyses revealed that these are associated with isolated cavities or fissure systems that emptied after penetration by the exploration activity. Similar exploration results apply to occurrences of hydrocarbons, which partially co-occurred with the inflows of solutions, and which were also of limited volume and duration.

The hydrocarbons were often simple gaseous compounds (methane, ethane, etc.) or condensates. Most of the free gases are interpreted as autochthonous Zechstein products with indicators of thermal alteration, which originated from the organic matter of the Stassfurt-Karbonat. Some of the gas probably originated from the red beds of the Lower Permian, and then migrated into the structure during diapirism. In addition to the hydrocarbons, other gases such as N₂, CO₂, O₂, H₂ and H₂S were identified.

The dimensions of the repository host rock (Hauptsalz) at the 840 m-level and 150 m below the 840 m-level can be estimated on the basis of the exploration results gathered to date in Exploration Area 1. With specification of a 50 m-wide safety pillar to the Kaliflöz Stassfurt and the Hauptanhydrit, at least 306 000 m² of the Hauptsalz are available for a potential repository in Exploration Area EB 1.

An assessment of the geological long-term safety of the planned repository must also take into consideration potential migration paths for radionuclides. Potential migration paths in evaporites are fissures and faults. Due to the creep properties of the rock salt as well as the diminishing or completely exhausted brine inflows and their minor volume, it must be assumed that the fissure systems are mostly healed and spatially limited. Thus, based on the present findings, there is no continuous migration path from inside the salt dome to the overburden or the surface.

Despite the still incomplete exploration of Exploration Area 1, it can be concluded from the present state of exploration of the saliniferous formation that there is no geoscientific evidence against the long-term safety of the Gorleben salt dome, and that the Hauptsalz of the Stassfurt-Folge is available in sufficiently large amounts to act as a potential host rock for the final disposal of high-activity waste.

Acknowledgments

The results of the surface and underground exploration of the Gorleben salt dome presented in this paper were mostly obtained through years of intense, constructive and fruitful cooperation with the experts of the DBE (Deutsche Gesellschaft zum Bau und Betrieb von Endlagern für Abfallstoffe mbH, Peine; German Company for the Construction and Operation of Waste Repositories Ltd.) and in close coordination with the Federal Office for Radiation Protection (BfS), Salzgitter.

The authors would like to thank the geologists (in particular J. Kutowski), mine surveyors and miners (in particular F. H. Koch) of the DBE who proved to be knowledgeable and meticulous and have always been reliable partners in the exploration effort as well as in the interpretation and evaluation of the exploration results. We would also like to thank the geoscientists of the BfS led by Dr. B. Thomauske and Dr. G. Stier-Friedland who have aided the investigations necessary for the suitability assessment of the salt dome through in-depth discussions of the exploration results and by uncomplicated organizational support.

Geological exploration of the Gorleben salt dome began almost 30 years ago. Numerous employees of the Federal Institute for Geosciences and Natural Resources (BGR) were involved either directly or indirectly in the exploration during this relatively long period and have contributed to the success of the exploration carried out so far with great personal effort and expertise. We would especially like to thank our former colleague Dr. M. Zirngast for his productive cooperation and numerous fertile discussions.

Experts of other institutions also provided advice and an intensive exchange of ideas leading to a better understanding of existing exploration results. We especially appreciate the fruitful discussions with Prof. Dr. A. G. Herrmann.

We would like to thank R. Götze, A. Hofmann, and M. Gern for their support in the sometimes very elaborate technical preparation of the core documentation and the mineralogical and geochemical analyses. Mrs S. Rose helped to create the diagrams for a clear presentation of the Gorleben exploration results.

References

- AkEnd (2002): Auswahlverfahren für Endlagerstandorte. Empfehlungen des AkEnd.-- Arbeitskreis Auswahlverfahren Endlagerstandorte (AkEnd): 260 pp., 30 Fig., 14 Tab., 3 Apps.; Berlin.
- ALBRECHT, H., BOEHME, J., BORNEMANN, O., DELISLE, G., EISENBURGER, D., FABER, E., FIELITZ, K., FISCHBECK, R., FRITSCH, J., GERLING, P., GIESEL, W., HOLLMANN, A., HUNSCHE, U., JARITZ, W., KOPIETZ, J., LEYDECKER, G., LUDWIG, R., NICKEL, H., NIPP, H.-K., PLISCHKE, I., SCHELKES, K., SCHMIDT, G., SCHULZE, O., STREBEL, O., TITTEL, G. & ZIRNGAST, M. (1991): Übertägige geowissenschaftliche Erkundung des Standortes Gorleben. Zusammenfassender Bericht, Stand: 01.01.1990.-- BGR, unpubl. report, Archiv-Nr. 108 880: 369 pp., 118 Fig., 62 Tab., 39 Apps.; Hannover.
- AMELUNG, P. (1998): Projekt Gorleben, 22. Zwischenbericht Geologie Salinar Schacht Gorleben 1, 2. Halbjahr 1997.-- DBE-Bericht, unpubl.: 22 pp., 1 Tab., 8 Apps., 1 Att.; Peine.
- AMELUNG, P. (1999a): Projekt Gorleben, 25. Zwischenbericht Geologie Salinar Gorleben Schacht 2, 1. Halbjahr 1999.-- DBE-Bericht, unpubl.: 14 pp., 1 App.; Peine.
- AMELUNG, P. (1999b): Projekt Gorleben, Schacht Gorleben 1, Endbericht Teil IV, Geologie des Salinars.-- DBE-Bericht, unpubl.: 56 pp., 11 Tab., 6 Apps., 3 Att.; Peine.
- AMELUNG, P. (2001): Projekt Gorleben, Bericht zur geologischen Feldaufnahme im Erkundungsbereich 1, 1995-2000.-- DBE-Bericht, unpubl.: 40 pp., 1 Tab., 8 Apps., 6 Att.; Peine.
- AMELUNG, P. & SCHUBERT, J. (2000): Projekt Gorleben: Dokumentation der Kondensatvorkommen im Hauptsalz.-- DBE-Bericht, unpubl.: 16 pp., 5 Tab., 1 Diagr., 9 Apps.; Peine.
- AMELUNG, P. & ZBRANCA, L. (1996a): Projekt Gorleben, 18. Zwischenbericht Geologie Salinar Schacht Gorleben 1, 2. Halbjahr 1995.-- DBE-Bericht, unpubl., 2 Tab., 7 Apps., 2 Att.; Peine.
- AMELUNG, P. & ZBRANCA, L. (1996b): Projekt Gorleben, 18. Zwischenbericht Geologie Salinar Schacht Gorleben 2, 2. Halbjahr 1995.-- DBE-Bericht, unpubl.: 21 pp., 2 Tab., 8 Apps., 2 Att.; Peine.

- AMELUNG, P. & ZBRANCA, L. (1996c): Projekt Gorleben, 19. Zwischenbericht Geologie Salinar Schacht Gorleben 1, 1. Halbjahr 1996.-- DBE-Bericht, unpubl., 6 Apps., 1 Att.; Peine.
- AMELUNG, P. & ZBRANCA, L. (1996d): Projekt Gorleben, 19. Zwischenbericht Geologie Salinar Schacht Gorleben 2, 1. Halbjahr 1996.-- DBE-Bericht, unpubl.: 19 pp., 2 Tab., 7 Apps., 2 Att.; Peine.
- AMELUNG, P. & ZBRANCA, L. (1997a): Projekt Gorleben, 20. Zwischenbericht Geologie Salinar Schacht Gorleben 1, 2. Halbjahr 1996.-- DBE-Bericht, unpubl.: 23 pp., 2 Tab., 7 Apps., 2 Att.; Peine.
- AMELUNG, P. & ZBRANCA, L. (1997b): Projekt Gorleben, 20. Zwischenbericht Geologie Salinar Schacht Gorleben 2, 2. Halbjahr 1996.-- DBE-Bericht, unpubl.; Peine.
- AMELUNG, P. & ZBRANCA, L. (1997c): Projekt Gorleben, 21. Zwischenbericht Geologie Salinar Gorleben Schacht 2, 1. Halbjahr 1997.-- DBE-Bericht, unpubl.: 13 pp., 6 Apps., 1 Att.; Peine.
- AMELUNG, P. & ZBRANCA, L. (1997d): Projekt Gorleben, 21. Zwischenbericht Geologie Salinar Schacht Gorleben 1, 1. Halbjahr 1997.-- DBE-Bericht, unpubl., 1 Tab., 8 Apps., 1 Att.; Peine.
- AMELUNG, P. & ZBRANCA, L. (1998): Projekt Gorleben, 22. Zwischenbericht Geologie Salinar Schacht Gorleben 2, 2. Halbjahr 1997.-- DBE-Bericht, unpubl.: 13 pp., 6 Apps., 1 Att.; Peine.
- APPEL, D. & HABLER, W. (1998): Quantifizierung postholsteinzeitlicher Subrosion am Salzstock Gorleben durch statistische Auswertung von Bohrerergebnissen.-- Mitt. geol. Inst. Univ. Hannover, 38: 7-30, 5 Fig., 3 Tab.; Hannover.
- BAUER, G. (1991): Kryogene Klüfte in norddeutschen Salzdiapiren?-- Zbl. Geol. Paläont., I/4: 1247-1261; Stuttgart.
- BAUER, P. (2001a): Projekt Gorleben, Schacht Gorleben 1, Endbericht Teil I; Zusammenfassung der geologischen Dokumentationseinheiten.-- DBE-Bericht, unpubl.: 26 pp., 5 Tab., 12 Apps.; Peine.
- BAUER, P. (2001b): Projekt Gorleben, Schacht Gorleben 2, Endbericht Teil I, Zusammenfassung der geologischen Dokumentationseinheiten.-- DBE-Bericht, unpubl.: 27 pp., 5 Tab., 11 Apps.; Peine.

- BÄUERLE, G. (1998): Sedimentäre Texturen und Stylolithen am Top des Hauptanhydrits (Zechstein 3) im Salzstock Gorleben.-- Univ. Hannover, Dipl.-Arb.: 97 pp., 67 Fig., 6 Tab., 11 Apps.; Hannover.
- BÄUERLE, G. (2000): Geochemisch-mineralogische Untersuchungen zur Genese, Lösungs- und Gasführung der Gorleben-Bank (Zechstein 3) im Salzstock Gorleben.-- Univ. Clausthal, Diss.: 237 pp., 32 Fig., 27 Tab., 27 Apps., 24 Att.; Clausthal-Zellerfeld.
- BÄUERLE, G., BORNEMANN, O., MAUTHE, F. & MICHALZIK, D. (2000): Turbidite, Breccien und Kristallrasen am Top des Hauptanhydrits (Zechstein 3) des Salzstocks Gorleben.-- Z. dt. geol. Ges., 151/1-2: 99-125, 12 Fig., 3 Att.; Hannover.
- BEHLAU, J. & MINGERZAHN, G. (2001): Geological and tectonic investigations in the former Morsleben salt mine (Germany) as a basis for the safety assessment of a radioactive waste repository.-- Engineering Geol., 61, 83-97, 4 Fig., 2 Tab.; Amsterdam.
- BfS (1990): Fortschreibung des zusammenfassenden Zwischenberichtes über bisherige Ergebnisse der Standortuntersuchung Gorleben vom Mai 1983.-- Bundesamt f. Strahlenschutz (BfS): 289 pp., 70 Fig., 18 Tab.; Salzgitter.
- BOEHME, J., FIELITZ, K., V. HOYER, M., KLINGE, H., KOPIETZ, J., LUDWIG, R., OCHMANN, N., SCHELKES, K., SOFNER, B. & WERNICKE, W. (1995): Projekt Gorleben. Standortbeschreibung Gorleben-Süd, Hydrogeologie des Deckgebirges, Kenntnisstand 1994.-- BGR, unpubl. report, Archiv-Nr. 112 693: 202 pp., 74 Fig., 18 Tab.; Hannover.
- BORNEMANN, O. (1979): Das Gefügeinventar nordwestdeutscher Salzstrukturen in Abhängigkeit von ihrer halokinetischen Stellung.-- Univ. Braunschweig, Diss.: 119 pp., 31 Fig., 5 Tab., 9 Att.; Braunschweig.
- BORNEMANN, O. (1982): Stratigraphie und Tektonik des Zechsteins im Salzstock Gorleben.-- Z. dt. geol. Ges., 133: 119-134, 4 Fig.; Hannover.
- BORNEMANN, O. (1987a): Die geologische Erkundung des Salzstocks Gorleben.-- Kerntechnik, 50/2: 138-142, 4 Fig., 1 Tab.; München (Hanser).
- BORNEMANN, O. (1987b): Geology and Mineralogy of the Gorleben Salt Dome. (In: MUHOPADHYAY, B. & KIRCHER, J. F. (Eds.): Proc. of Joint USA/FRG Salt Near-Field Geochemistry Workshop, Albuquerque, NM.)-- Batelle Mem. Inst.: 10 pp., 13 Fig.; Albuquerque/New Mexico/USA.

- BORNEMANN, O. (1991): Zur Geologie des Salzstocks Gorleben nach den Bohrergebnissen.-- BfS-Schriften, 4/91: 67 pp., 13 Fig., 5 Tab., 24 Apps.; Salzgitter.
- BORNEMANN, O., BÄUERLE, G., BEHLAU, J. & MINGERZAHN, G. (2001): Endlagerprojekt Gorleben - Geologische Bearbeitung der Erkundungssohle (Geologie, Mineralogie, Geochemie) -1. Geologischer Ergebnisbericht EB1.-- BGR, unpubl. report, Archiv-Nr. 0120767: 111 pp., 22 Fig., 5 Tab., 6 Apps.; Hannover.
- BORNEMANN, O., BEHLAU, J. & MINGERZAHN, G. (2002): Endlagerprojekt Gorleben - Geologische Bearbeitung der Erkundungssohle. 2. Geologischer Fachbericht (Geologische Schnitte zur untertägigen Erkundung).-- BGR, unpubl. report: 19 pp., 32 Apps.; Hannover.
- BORNEMANN, O., BEHLAU, J., MINGERZAHN, G. & SCHRAMM, M. (2002): Projekt Gorleben - Geologische Bearbeitung der Schächte Gorleben 1 und 2 (Hutgestein und Salinar). Abschlussbericht.-- BGR, unpubl. report: 159 pp., 17 Fig., 12 Tab., 28 Apps., 16 Att.; Hannover.
- BORNEMANN, O. & FISCHBECK, R. (1986): Ablaugung und Hutgesteinsbildung am Salzstock Gorleben.-- Z. dt. geol. Ges., 137: 71-83, 4 Fig., 1 Tab., 2 Att.; Hannover.
- BORNEMANN, O. & FISCHBECK, R. (1987a): Salzstockuntersuchungsbohrung Gorleben 1005. Schichtenverzeichnis ab Oberfläche des Salzstocks.-- BGR, unpubl. report, Archiv-Nr. 103623: 112 pp., 3 Tab.; Hannover.
- BORNEMANN, O. & FISCHBECK, R. (1987b): Zechstein 2 - 4 des Salzstocks Gorleben.-- Int. Symp. Zechstein 1987, Kassel, Exkursionsführer I: 145-160, 8 Fig., 1 Tab.; Wiesbaden.
- BORNEMANN, O. & FISCHBECK, R. (1988a): Salzspiegelbohrung GoHy 1121. Schichtenverzeichnis ab Oberfläche des Salzstocks (Stand: Oktober 1985).-- BGR, unpubl. report, Archiv-Nr. 103637: 16 pp., 3 Tab.; Hannover.
- BORNEMANN, O. & FISCHBECK, R. (1988b): Salzspiegelbohrung GoHy 1141. Schichtenverzeichnis ab Oberfläche des Salzstocks (Stand: Oktober 1985).-- BGR, unpubl. report, Archiv-Nr. 103639: 13 pp., 3 Tab.; Hannover.
- BORNEMANN, O. & FISCHBECK, R. (1988c): Salzspiegelbohrung GoHy 1151. Schichtenverzeichnis ab Oberfläche des Salzstocks (Stand: Oktober 1985).-- BGR, unpubl. report, Archiv-Nr. 103640: 28 pp., 3 Tab.; Hannover.

- BORNEMANN, O. & FISCHBECK, R. (1988d): Salzspiegelbohrung GoHy 1291. Schichtenverzeichnis ab Oberfläche des Salzstocks (Stand: Oktober 1985).-- BGR, unpubl. report, Archiv-Nr. 103645: 11 pp., 3 Tab.; Hannover.
- BORNEMANN, O. & FISCHBECK, R. (1988e): Salzspiegelbohrung GoHy 1301. Schichtenverzeichnis ab Oberfläche des Salzstocks (Stand: Oktober 1985).-- BGR, unpubl. report, Archiv-Nr. 103646: 7 pp., 3 Tab.; Hannover.
- BORNEMANN, O. & FISCHBECK, R. (1988f): Salzspiegelbohrung GoHy 1302. Schichtenverzeichnis ab Oberfläche des Salzstocks (Stand: Oktober 1985).-- BGR, unpubl. report, Archiv-Nr. 103647: 20 pp., 3 Tab.; Hannover.
- BORNEMANN, O. & FISCHBECK, R. (1988g): Salzspiegelbohrung GoHy 1303. Schichtenverzeichnis ab Oberfläche des Salzstocks (Stand: Oktober 1985).-- BGR, unpubl. report, Archiv-Nr. 103648: 31 pp., 3 Tab.; Hannover.
- BORNEMANN, O. & FISCHBECK, R. (1988h): Salzspiegelbohrung GoHy 1304. Schichtenverzeichnis ab Oberfläche des Salzstocks (Stand: Oktober 1985).-- BGR, unpubl. report, Archiv-Nr. 103649: 28 pp., 3 Tab.; Hannover.
- BORNEMANN, O. & FISCHBECK, R. (1988i): Salzspiegelbohrung GoHy 1305. Schichtenverzeichnis ab Oberfläche des Salzstocks (Stand: Oktober 1985).-- BGR, unpubl. report, Archiv-Nr. 103650: 28 pp., 3 Tab.; Hannover.
- BORNEMANN, O. & FISCHBECK, R. (1988j): Salzspiegelbohrung GoHy 3080. Schichtenverzeichnis ab Oberfläche des Salzstocks (Stand: Oktober 1985).-- BGR, unpubl. report, Archiv-Nr. 103658: 13 pp., 3 Tab.; Hannover.
- BORNEMANN, O. & FISCHBECK, R. (1988k): Salzspiegelbohrung GoHy 3153. Schichtenverzeichnis ab Oberfläche des Salzstocks (Stand: Oktober 1985).-- BGR, unpubl. report, Archiv-Nr. 103668: 15 pp., 3 Tab.; Hannover.
- BORNEMANN, O. & FISCHBECK, R. (1988l): Salzspiegelbohrung GoHy 3154. Schichtenverzeichnis ab Oberfläche des Salzstocks (Stand: Oktober 1985).-- BGR, unpubl. report, Archiv-Nr. 103669: 14 pp., 3 Tab.; Hannover.
- BORNEMANN, O. & FISCHBECK, R. (1988m): Salzspiegelbohrung GoHy 3155. Schichtenverzeichnis ab Oberfläche des Salzstocks (Stand: Oktober 1985).-- BGR, unpubl. report, Archiv-Nr. 103670: 22 pp., 3 Tab.; Hannover.

- BORNEMANN, O. & FISCHBECK, R. (1988n): Salzstockuntersuchungsbohrung Gorleben 1004. Schichtenverzeichnis ab Oberfläche des Salzstocks.-- BGR, unpubl. report, Archiv-Nr. 103622: 119 pp., 3 Tab.; Hannover.
- BORNEMANN, O. & FISCHBECK, R. (1991): Geologische Bearbeitung der Schächte 1 und 2 (Hutgestein und Salinar). 3. Zwischenbericht zum AP 9G 411210.-- BGR, unpubl. report, Archiv-Nr. 109625: 31 pp., 14 Fig., 11 Apps.; Hannover.
- BORNEMANN, O., FISCHBECK, R. & BÄUERLE, G. (2000): Investigation of deformation textures of salt rock from various Zechstein units and their relationship to the formation of the salt diapirs in NW Germany. (In: GEERTMANN, R. M. (Hrsg.): SALT 2000).- - Proc. 8th World Salt Symposium, Vol. 1: 89-94, 5 Fig., 1 Tab.; Amsterdam (Elsevier) - ISBN 0 444 50065 0.
- BORNEMANN, O., JARITZ, W. & WITTRUCK, J. (1988): Geologisches und geotechnisches Erkundungsprogramm, Teilprojekt I. BGR-Abschlußbericht zum Forschungsvorhaben KWA 85049.-- BGR, unpubl. report, Archiv-Nr. 103750: 33 pp., 5 Fig., 52 Apps.; Hannover.
- BORNEMANN, O., MINGERZAHN, G. & BEHLAU, J. (1998): Projekt Gorleben- Geologische Bearbeitung der Erkundungssohle (Stratigraphie und Tektonik). 1. Zwischenbericht zum Arbeitspaket 9G 4121100000.-- BGR, unpubl. report, Archiv-Nr. 117663: 36 pp., 2 Tab., 31 Apps.; Hannover.
- BOULTON, G. S. & PAYNE, A. (1992): Reconstructing the past and predicting the future regional components of global change: The case of glaciation in Europe.-- Proc. Workshop WC-1 (Waste Disposal and Geology Scientific Perspectives), 29th Int. Geol. Congr.: 51-134, 37 Fig.; Tokyo/Japan.
- BRAITSCH, O. (1962): Entstehung und Stoffbestand der Salzlagerstätten. (In: ENGELHARDT, W. v. & ZEMANN, J. (Hrsg.): Mineralogie und Petrographie in Einzeldarstellungen)-- 1. Edit., Band III: 232 pp., 47 Fig., 36 Tab.; Berlin (Springer).
- BRAITSCH, O. & HERRMANN, A. G. (1963): Zur Geochemie des Broms in salinaren Sedimenten. Teil I: Experimentelle Bestimmung der Br-Verteilung in verschiedenen natürlichen Salzsystemen.-- Geochim. Cosmochim. Acta, 27: 361-391, 5 Fig., 15 Tab.; New York.
- BRULAND, K. W. (1983): Trace Elements in Sea-water.-- Chem. Oceanography, 8, 45: 157-222; London.

- D'ANS, J. & KÜHN, R. (1944): Über den Bromgehalt von Salzgesteinen der Kalisalz-lagerstätten VI.-- Kali, verw. Salze und Erdöl, 34: 42-46, 59-64, 77-83; Hannover.
- D'ANS, J. & LAX, E. (1949): Taschenbuch für Chemiker und Physiker.-- 2. Edit: 1896 pp.; Berlin (Springer).
- DBE (1985a): Bergwerk zur Erkundung des Salzstockes Gorleben - Schacht 1 - Geologische Bearbeitung der Gefrier- und Temperaturmesslochbohrungen.-- DBE, unpubl. report, DBE-Archiv-Nr. 277693/9G/YES01/RB/H/BN/1/0/U: 11 pp., 2 Tab., 5 Apps.; Peine.
- DBE (1985b): Bergwerk zur Erkundung des Salzstockes Gorleben - Schacht 2 - Geologische Bearbeitung der Gefrier- und Temperaturmesslochbohrungen.-- DBE, unpubl. report, DBE-Archiv-Nr. 277725/9G/YES02/RB/H/BN/1/0/U: 15 pp., 3 Tab., 5 Apps.; Peine.
- DE BOER, H. V. (1971): Gefügeregelung in Salzstöcken und Hüllgesteinen.-- Kali und Steinsalz, 5: 403-425, 16 Fig.; Essen.
- EHLERS, J., MEYER, K.-D. & STEPHAN, H.-J. (1984): Pre-Weichselian Glaciations of North-West Europe.-- Quaternary Science Review, Vol. 3, No. 1: 1-40, 11 Fig., 1 Tabl., 3 Pl.; Oxford/U.K. (Pergamon).
- EHRHARDT, K. (1980): Exploration eines neuen Baufeldes im Grubenbetrieb des Steinsalzwerkes Braunschweig-Lüneburg der Kali und Salz AG. (In: COOGAN, A. H. & HAUBER, L. (Eds.): Fifth Symposium on Salt).-- The Northern Ohio Geol. Soc., Vol. 1: 231-238, 9 Fig.; Cleveland/Ohio/USA.
- EHRlich, D., RÖTHEMEYER, H., STIER-FRIEDLAND, G. & THOMASKE, B. (1986): Langzeitsicherheit von Endlagern. Zeitrahmen für Sicherheitsbetrachtungen - Bewertung der Subrosion des Salzstocks Gorleben.-- Atomwirtschaft, XXXI (5): 231-236, 4 Fig., 2 Tab.; Düsseldorf.
- EISENBURGER, D. & GUNDELACH, V. (1995a): Elektromagnetische Hochfrequenz-Reflexionsmessungen (EMR-Messungen) im Salinarteil der Schächte Gorleben. Ergebnisbericht I, AP 9G 4137000000.-- BGR, unpubl. report, Archiv-Nr. 113429: 7 pp., 13 Fig.; Hannover.

- EISENBURGER, D. & GUNDELACH, V. (1995b): Elektromagnetische Hochfrequenz-Reflexionsmessungen (EMR-Messungen) im Salinarteil der Schächte Gorleben. Ergebnisbericht II , AP 9G 4137000000.-- BGR, unpubl. report, Archiv-Nr. 113555: 7 pp., 13 Fig.; Hannover.
- EISENBURGER, D. & GUNDELACH, V. (1995c): Elektromagnetische Hochfrequenz-Reflexionsmessungen (EMR-Messungen) im Salinarteil der Schächte Gorleben. Ergebnisbericht III , AP 9G 4137000000.-- BGR, unpubl. report, Archiv-Nr. 113801: 7 pp., 13 Fig.; Hannover.
- EISENBURGER, D. & GUNDELACH, V. (1995d): Elektromagnetische Hochfrequenz-Reflexionsmessungen (EMR-Messungen) im Salinarteil der Schächte Gorleben. Ergebnisbericht IV, AP 9G 4137000000.-- BGR, unpubl. report, Archiv-Nr. 114091: 7 pp., 13 Fig.; Hannover.
- EISENBURGER, D. & GUNDELACH, V. (1995e): Elektromagnetische Hochfrequenz-Reflexionsmessungen (EMR-Messungen) im Salinarteil der Schächte. 4. Zwischenbericht, AP 9G 4137000000.-- BGR, unpubl. report, Archiv-Nr. 113088: 11 pp., 29 Fig., 1 Tab.; Hannover.
- EISENBURGER, D. & GUNDELACH, V. (1996): Elektromagnetische Hochfrequenz-Reflexionsmessungen (EMR-Messungen) im Erkundungsbereich der Füllorte von Schacht 1 und 2 in Gorleben. Ergebnisbericht I, AP 9G 4142100000.-- BGR, unpubl. report, Archiv-Nr. 115473: 15 pp., 33 Fig., 1 Tab.; Hannover.
- EISENBURGER, D. & GUNDELACH, V. (1999): Elektromagnetische Hochfrequenz-Reflexionsmessungen (EMR) in der Bohrung 02YEQ01 RB427 im Erkundungsbergwerk Gorleben. Ergebnisbericht, AP 9G 4142100000.-- BGR, unpubl. report, Archiv-Nr. 119467: 14 pp., 4 Fig., 11 Apps., 4 Radargr.; Hannover.
- EISENBURGER, D. & GUNDELACH, V. (2000a): Elektromagnetische Hochfrequenz-Reflexionsmessungen (EMR) in der Bohrung 02YEF20 RB217 im Erkundungsbergwerk Gorleben. Ergebnisbericht, AP 9G 4142100000.-- BGR, unpubl. report, Archiv-Nr. 119771: 14 pp., 4 Fig., 7 Apps., 2 Radargr.; Hannover.
- EISENBURGER, D. & GUNDELACH, V. (2000b): Elektromagnetische Hochfrequenz-Reflexionsmessungen (EMR) in der Bohrung 02YEQ01 RB194 im Erkundungsbergwerk Gorleben. Ergebnisbericht, AP 9G 4142100000.-- BGR, unpubl. report, Archiv-Nr. 119466: 13 pp., 3 Fig., 7 Apps., 2 Radargr.; Hannover.

- EISENBURGER, D. & GUNDELACH, V. (2000c): Elektromagnetische Hochfrequenz-Reflexionsmessungen (EMR) in der Bohrung 02YER20 RB254 im Erkundungsbergwerk Gorleben. Ergebnisbericht, AP 9G 4142100000.-- BGR, unpubl. report, Archiv-Nr. 119465: 14 pp., 3 Fig., 7 Apps., 7 Radagr.; Hannover.
- EISENBURGER, D. & GUNDELACH, V. (2000d): Elektromagnetische Hochfrequenz-Reflexionsmessungen (EMR) in der Bohrung 02YER20 RB488 im Erkundungsbergwerk Gorleben. Ergebnisbericht, AP 9G 4142100000.-- BGR, unpubl. report: 14 pp., 3 Fig., 7 Apps., 2 Radagr.; Hannover.
- EISENBURGER, D. & GUNDELACH, V. (2000e): Elektromagnetische Hochfrequenz-Reflexionsmessungen (EMR) in der Bohrung 02YER20 RB500 im Erkundungsbergwerk Gorleben. Ergebnisbericht, AP 9G 4142100000.-- BGR, unpubl. report, Archiv-Nr. 120310: 13 pp., 3 Fig., 7 Apps., 2 Radagr.; Hannover.
- EISENBURGER, D. & GUNDELACH, V. (2000f): Elektromagnetische Hochfrequenz-Reflexionsmessungen (EMR) in der Bohrung 04YEA01 RB480 im Erkundungsbergwerk Gorleben. Ergebnisbericht, AP 9G 4142100000.-- BGR, unpubl. report, Archiv-Nr. 119772: 12 pp., 3 Fig., 7 Apps., 2 Radagr.; Hannover.
- EISENBURGER, D. & GUNDELACH, V. (2001): EMR-Testmessungen zur Überprüfung der Bohrlochsonde DHU Exemplar „slave“ in der Bohrung RB238 im Erkundungsbergwerk Gorleben. Stellungnahme, AP 9G 4142100000.-- BGR, unpubl. report: 14 pp., 26 Apps.; Hannover.
- EISENBURGER, D. & GUNDELACH, V. (2002a): Elektromagnetische Hochfrequenz-Reflexionsmessungen (EMR) im Bereich der Infrastrukturräume (EB1) im Erkundungsbergwerk Gorleben. Ergebnisbericht II, AP 9G 4142100000.-- BGR, unpubl. report, Archiv-Nr. 118615: 142 pp., 35 Fig., 91 Apps., 515 Radagr.; Hannover.
- EISENBURGER, D. & GUNDELACH, V. (2002b): Elektromagnetische Hochfrequenz-Reflexionsmessungen (EMR) in der Bohrung 02YEA12 RB218 im Erkundungsbergwerk Gorleben. Ergebnisbericht, AP 9G 4142100000.-- BGR, unpubl. report: 14 pp., 4 Fig., 7 Apps., 2 Radagr.; Hannover.
- EISENBURGER, D. & GUNDELACH, V. (2002c): Elektromagnetische Hochfrequenz-Reflexionsmessungen (EMR) in der Bohrung 02YEQ02R RB264 im Erkundungsbergwerk Gorleben. Ergebnisbericht, AP 9G 4142100000.-- BGR, unpubl. report: 14 pp., 4 Fig., 7 Apps., 2 Radagr.; Hannover.

- EISENBURGER, D. & GUNDELACH, V. (2002d): Elektromagnetische Hochfrequenz-Reflexionsmessungen (EMR) in der Bohrung 02YER20 RB488 im Erkundungsbergwerk Gorleben - Fortsetzung -. Ergebnisbericht, AP 9G 4142100000.-- BGR, unpubl. report: 15 pp., 4 Fig., 7 Apps., 2 Radargr.; Hannover.
- EISENBURGER, D. & GUNDELACH, V. (2002e): EMR-Testmessungen zur Überprüfung der Bohrlochsonden DHU in der Bohrung RB238 im Erkundungsbergwerk Gorleben vom 21.9.2000-7.5.2001. Stellungnahme, AP 9G 4142100000.-- BGR, unpubl. report: 14 pp., 26 Apps.; Hannover.
- EISENBURGER, D., GUNDELACH, V. & KAHNT, W. (2000): Projekt Gorleben - Elektromagnetische Hochfrequenzmessungen (EMR) im Salinarteil der Schächte des Erkundungsbergwerks Gorleben; Abschlussbericht AP 9G4137000000.-- BGR, unpubl. report, Archiv-Nr. 0119493: 126 pp., 3 Fig., 2 Tab., 13 Apps., 78 Radargr.; Hannover.
- EISSMANN, L. (1987): Lagerungsstörungen im Lockergebirge. Exogene und endogene Tektonik im Lockergebirge des nördlichen Mitteleuropa.-- Geophys. u. Geol., Veröff. der KMU Leipzig, Bd. III, 4: 7-77; Berlin.
- ELLENDORF, B. (1999): Geochemische Untersuchungen an einzelnen Fluid Inclusions in Zechsteinevaporiten mittels Laser-Ramanspektrometrie, Ionenchromatographie und Laser-Ablation-ICP-Massenspektrometrie.-- Univ. Clausthal-Zellefeld, Diss.: 93 pp., 47 Fig., 15 Tab.; Clausthal-Zellerfeld.
- ENKE, F. (1982a): Bericht über die Verfüllung der Tiefbohrung Gorleben 1004.-- DBE-Bericht, unpubl.: 20 pp., 3 Apps.; Peine.
- ENKE, F. (1982b): Bericht über die Verfüllung der Tiefbohrung Gorleben 1005.-- DBE-Bericht, unpubl.: 20 pp., 3. Apps.; Peine.
- ENKE, F. (1983a): Bericht über die Verfüllung der Tiefbohrung Gorleben 1002.-- DBE-Bericht, unpubl.: 18 pp., 3 Apps.; Peine.
- ENKE, F. (1983b): Bericht über die Verfüllung der Tiefbohrung Gorleben 1003.-- DBE-Bericht, unpubl.: 13 pp., 3 Apps.; Peine.
- ENSTE, G. (1990): Projekt Gorleben, 8. Zwischenbericht Geologie salzspiegelnahes Salinar, Schacht Gorleben 1, 2. Halbjahr 1990.-- DBE-Bericht, unpubl.: 24 pp., 5 Apps., 1 Att.; Peine.

- ENSTE, G. & GÖBEL, V. (1989): Projekt Gorleben, 6. Zwischenbericht Geologie Deckgebirge Schacht Gorleben 1, 2. Halbjahr 1989.-- DBE-Bericht, unpubl.: 14 pp., 8 Apps.; Peine.
- ENSTE, G. & GÖBEL, V. (1990): Projekt Gorleben, 7. Zwischenbericht Geologie Hutgestein Schacht Gorleben 1, 1. Halbjahr 1990.-- DBE-Bericht, unpubl.: 20 pp., 2 Tab., 8 Apps., 1 Att.; Peine.
- ESSAID, S. & KLARR, K. (1982): Zum Innenbau der Salzstruktur Asse.-- Z. dt. geol. Ges., 133/2: 135-154, 2 Fig., 1 Tab.; Hannover.
- FISCHBECK, R. (1984): Umwandlungen von Kalisalzgesteinen aus der Ronnenberggruppe (z3) im Salzstock Gorleben.-- Kali und Steinsalz, 9: 61-65, 8 Fig., 1 Tab.; Essen.
- FISCHBECK, R. (1985): Mineralogische und petrographische Untersuchungen am 9. Anhydritmittel (z3AM9) aus der Bohrung Gorleben 1004. Laborbericht.-- BGR, unpubl. report, Archiv-Nr. 95709: 17 pp., 13 Fig.; Hannover.
- FISCHBECK, R. (1990): Mineralogical and Petrographic Studies on the Anhydritmittelsalz (Leine Cycle z3) in the Salt Dome Gorleben. (In: HELING et al. (Eds.): Sediments and Environmental Geochemistry. Selected Aspects and Case Histories)-- 1. Edit.: 210-219, 4 Fig.; Berlin (Springer) - 3-540-51735-9.
- FISCHBECK, R. & BORNEMANN, O. (1988): Genetische Überlegungen aufgrund von Brom-Bestimmungen in Salzgesteinen des Salzstocks Gorleben, Niedersachsen.-- Fortschr. Miner., Beih. 66/1: pp. 35; Stuttgart.
- FISCHBECK, R. & BORNEMANN, O. (1993): Hinweise auf Stofftransporte im Salzstock Gorleben aufgrund von kleintektonischen Untersuchungen und Brombestimmungen an halitischen Kluffüllungen.-- Geol. Jb., A 142: 233-256, 5 Fig., 9 Tab., 1 Att.; Hannover.
- FISCHBECK, R. & MINGERZAHN, G. (1997): Geochemische, mineralogische und petrographische Untersuchungen an Salzgesteinen und Kluffüllungen aus Schacht 2, Gorleben ab Teufe 349,0 m (Fundament) bis Teufe 843,2 m (vorläufige Endteufe). 5. Zwischenbericht zum Arbeitspaket 9G 411210.-- BGR, unpubl. report, Archiv-Nr. 116787: 64 pp., 20 Fig., 18 Tab., 2 Apps.; Hannover.

- FLECKENSTEIN, L. (1993a): Projekt Gorleben, 11. Zwischenbericht Geologie Hutgestein/Salinar Schacht Gorleben 2, 1. Halbjahr 1992.-- DBE-Bericht, unpubl.: 33 pp., 4 Tab., 12 Apps., 1 Att.; Peine.
- FLECKENSTEIN, L. (1993b): Projekt Gorleben, 12. Zwischenbericht Geologie Salinar Schacht Gorleben 1, 2. Halbjahr 1992.-- DBE-Bericht, unpubl.: 29 pp., 4 Tab., 8 Apps., 1 Att.; Peine.
- FLECKENSTEIN, L. (1993c): Projekt Gorleben, 12. Zwischenbericht Geologie Salinar Schacht Gorleben 2, 2. Halbjahr 1992.-- DBE-Bericht, unpubl.: 23 pp., 6 Apps., 1 Att., 4 Tab.; Peine.
- FRIEDRICH, A. J. (2000): Selbstdiffusion von Wasser im intergranularen Raum von Steinsalz.-- Univ. Heidelberg, Inst. f. Umweltphysik, Dipl.-Arb.: 78 pp., 13 Fig., 4 Tab., 1 App.; Heidelberg.
- FRISCHBUTTER, A. (2001): Recent vertical movements (map 4). (In: GARETSKY, R. G. et al. (Hrsg.): Neogeodynamics of the Baltic Sea Depression and Adjacent Areas. Results of IGCP Project 346).-- Brandenburgische Geowiss. Beitr., 8, 1: 27-31, 1 Tab.; Kleinmachnow.
- FULDA, E. (1929): Über „Anhydrit-Klippen“.-- Kali und verwandte Salze, 23: 129-133; Halle.
- GERLING, P. & FABER, E. (2001): Geologische Bearbeitung der Erkundungssohle (Geologie, Mineralogie, Geochemie): Dokumentation der chemischen Analysen von gasförmigen und flüssigen Kohlenwasserstoffen.-- BGR, unpubl. report: 20 pp., 4 Fig., 2 Tab., 5 Apps.; Hannover.
- GERLING, P., FABER, E. & WEHNER, H. (2002): Projekt Gorleben. Geologische Bearbeitung der Erkundungssohle (Geologie, Mineralogie, Geochemie). Interpretation der chemischen Analysen von gasförmigen und flüssigen Kohlenwasserstoffen (einschließlich der Daten aus der obertägigen Erkundung und der Schächte).-- BGR, unpubl. report, 84 pp., 31 Fig., 5 Tab., 2 Apps.; Hannover.
- GIES, H., HERBERT, H.-J. & JOCKWER, N. (1990): Zur Bedeutung der Wassergehalte für die Lithostratigraphie in Steinsalzhorizonten des Zechsteins.-- Kali und Steinsalz, Bd. 10, H. 7/8: 265-271, 18 Fig., 2 Tab.; Essen.

- GÖBEL, V. (1991): Projekt Gorleben, 9. Zwischenbericht Geologie Salinar Schacht Gorleben1, 1. Halbjahr 1991.-- DBE-Bericht, unpubl.: 22 pp., 1 Att., 6 Apps.; Peine.
- GROPP, H. (1919): Gasvorkommen in Kalisalzbergwerken in den Jahren 1907 bis 1917.-- Kali, 3: 33-42, 1 Tab.; Halle.
- GROTE, H. (1996): Projekt Gorleben, Schacht Gorleben 1, Endbericht Teil III, Geologie des Hutgesteins.-- DBE-Bericht, unpubl.: 35 pp., 6 Tab., 6 Apps., 1 Att.; Peine.
- GROTE, H. (1997): Projekt Gorleben: Schacht Gorleben 2 - Endbericht Teil III: Geologie des Hutgesteins, Teufe 199,2 m RHB - 258,1 m RHB.-- DBE-Bericht, unpubl.: 80 pp., 30 Fig., 9 Tab., 1 App.; Peine.
- GRÜBLER, G. (1984): Gasvorkommen in den Schachtvorbohrungen Go 5001 und Go 5002. (In: Bundesministerium für Forschung und Technologie, BMFT (Hrsg.): Bericht von einer Informationsveranstaltung des Bundes vor dem Schachtabteufen, Salzstock Gorleben).-- Entsorgung, Bd. 3: 165-181, 6 present.; Bonn.
- GRÜBLER, G. & REPERT, D. (1983): Bericht über die in den Schachtvorbohrungen Go 5001 und Go 5002 angetroffenen KW-Kondensate/-Gase und deren Untersuchungsergebnisse.-- DBE-Bericht, unpubl.: 56 pp., 14 Tab., 26 Apps.; Peine.
- GRÜBLER, G. & REPERT, D. (1985): Bericht über die durchgeführten Testarbeiten in der Bohrung Gorleben 1002.-- DBE-Bericht, unpubl.: 56 pp., 11 Apps.; Peine.
- HALTENHOF, M. & HOFRICHTER, E. (1972): Feinstratigraphie, Fazies und Bromgehalte isochroner Schichten des Liniensalzes (Zechstein 3) im zentralen Teil des Zechsteinbeckens (Raum Hannover).-- Geol. Jb., 90: 1-66, 15 Fig., 13 Tab., 3 Att.; Hannover.
- HAMPE, M. & KUTOWSKI, J. (2002): Projekt Gorleben: Durchführung geologischer Aufnahmen.-- DBE-Bericht, unpubl.: 17 pp., 1 Fig., 4 Apps., 3 Att.; Peine.
- HANNEMANN, M. (1995): Intensität und Verbreitung glazigener Lagerungsstörungen im tieferen Quartär und Tertiär.-- Brandenburgische Geowiss. Beitr., 2: 51-59; Kleinmachnow.

- HEMMANN, M. (1968): Zur Ausbildung und Genese des Leinesteinsalzes und Hauptanhydrits (Zechstein 3) im Ostteil des Subherzynen Beckens.-- Bergakad. Freiberg, Diss.: 214 pp., 52 Fig., 1 Tab., 17 Apps., 19 Att.; Freiberg.
- HERBERT, H.-J., BORNEMANN, O. & FISCHBECK, R. (1990): Die Isotopenzusammensetzung des Gipskristallwassers im Hutgestein des Salzstocks Gorleben - ein Nachweis für die elsterzeitliche Bildung der Hutgesteinsbrekzie.-- Kali und Steinsalz, Bd. 10, H. 7/8: 215-226, 7 Fig., 4 Tab.; Essen.
- HERBERT, H.-J. & SANDER, W. (1997): Chemische Analysen von Lösungen im Salzgebirge (Erkundungssohle), Berichtszeitraum 09/1995-12/1996.-- Ges. f. Anl.- u. Reaktorsicherheit mbH, unpubl. report: 65 pp., 1 Tab, 1 App.; Braunschweig.
- HERBERT, H.-J. & SANDER, W. (1998a): Chemische Analysen von Lösungen im Salzgebirge (Erkundungssohle), Berichtszeitraum 01.01.1997-30.04.1997.-- Ges. f. Anl.- u. Reaktorsicherheit mbH, unpubl. report: 54 pp., 13 Fig., 5 Tab, 8 Apps.; Braunschweig.
- HERBERT, H.-J. & SANDER, W. (1998b): Chemische Analysen von Lösungen im Salzgebirge (Erkundungssohle), Berichtszeitraum 01.05.1997-30.11.1997.-- Ges. f. Anl.- u. Reaktorsicherheit mbH, unpubl. report: 43 pp., 9 Fig., 5 Tab, 11 Apps.; Braunschweig.
- HERBERT, H.-J. & SANDER, W. (1998c): Chemische Analysen von Lösungen im Salzgebirge (Erkundungssohle), Berichtszeitraum 01.12.1997-29.05.1998.-- Ges. f. Anl.- u. Reaktorsicherheit mbH, unpubl. report: 44 pp., 10 Fig., 5 Tab, 10 Apps.; Braunschweig.
- HERBERT, H.-J. & SANDER, W. (1998d): Chemische Analysen von Lösungen im Salzgebirge (Erkundungssohle), Berichtszeitraum 30.05.1998-30.11.1998.-- Ges. f. Anl.- u. Reaktorsicherheit mbH, unpubl. report: 42 pp., 9 Fig., 5 Tab, 9 Apps.; Braunschweig.
- HERBERT, H.-J. & SANDER, W. (2000): Chemische Analysen von Lösungen im Salzgebirge (Erkundungssohle), Berichtszeitraum 01.12.1998-30.09.2000.-- Ges. f. Anl.- u. Reaktorsicherheit mbH, unpubl. report: 47 pp., 13 Fig., 5 Tab, 7 Apps.; Braunschweig.

- HERDE, W. (1953): Die Riedel-Gruppe im zentralen Teil des nordwestdeutschen Zechsteingebietes.-- Univ. Göttingen, Diss.: 127 pp., 16 Fig., 3 Tab., 30 Att.; Göttingen.
- HERRMANN, A. G. (1987): Gase in marinen Evaporiten.-- Univ. Clausthal-Zellerfeld, Inst. f. Miner. und mineral. Rohst., unpubl. report: 137 pp., 2 Fig., 3 Tab.; Clausthal-Zellerfeld.
- HERRMANN, A. G. & KNIPPING, B. (1993a): Fluide Komponenten als Teile des Stoffbestandes der Evaporite im Salzstock Gorleben. Vorkommen, Herkunft, Entstehung und Wechselwirkungen mit den Salzgesteinen.-- Tech. Univ. Clausthal, Inst. f. Miner. u. mineral. Rohst.: 140 pp., 32 Fig., 21 Tab.; Clausthal-Zellerfeld.
- HERRMANN, A. G. & KNIPPING, B. (1993b): Sicherstellung der Datenbasis zum Stoffbestand des Salzstocks Gorleben. Zwischenbericht zum PSE-Element 9G-261310. Berichtszeitraum 1.1.93-30.6.93 (Ergebnisse bis einschl. 31.7.93).-- Tech. Univ. Clausthal, Inst. f. Miner. u. mineral. Rohst., Zwischenbericht: 13 pp., 3 Fig., 2 Tab., 1 App.; Clausthal-Zellerfeld.
- HERRMANN, A. G. & KNIPPING, B. (1994): Sicherstellung der Datenbasis zum Stoffbestand des Salzstocks Gorleben. Zwischenbericht zum PSE-Element 9G-261310. Berichtszeitraum 30.6.93-31.12.93 (Ergebnisse bis einschl. 20.2.94).-- Tech. Univ. Clausthal, Inst. f. Miner. u. mineral. Rohst., Zwischenbericht: 23 pp., 4 Fig., 16 Tab.; Clausthal-Zellerfeld.
- HERRMANN, A. G., RUHE, S. & USDOWSKI, E. (1997): Fluid inclusions: Neue Erkenntnisse über den Stoffbestand NaCl-gesättigter Meerwasserlösungen im Zechstein 3.-- Kali u. Steinsalz, Bd. 12, H. 4: 115-124, 3 Fig., 5 Tab.; Essen.
- HERRMANN, A. G., SIEBRASSE, G. & KÖNNECKE, K. (1978): Computerprogramme zur Berechnung von Mineral- und Gesteinsumbildungen bei der Einwirkung von Lösungen auf Kali- und Steinsalzlagerstätten (Lösungsmetamorphose).-- Kali und Steinsalz, 7: 288-299; Essen.
- ISLINGER, C. (1992a): Projekt Gorleben, 10. Zwischenbericht Geologie Hutgestein Schacht Gorleben 2, 2. Halbjahr 1991.-- DBE-Bericht, unpubl.: 28 pp., 4 Tab., 5 Apps., 1 Att.; Peine.
- ISLINGER, C. (1992b): Projekt Gorleben, 10. Zwischenbericht Geologie Salinar Schacht Gorleben 1, 2. Halbjahr 1991.-- DBE-Bericht, unpubl.: 22 pp., 4 Apps.; Peine.

- JARITZ, W. (1980): Bemerkungen zur Geologie des quartären Untergrundes in der Umgebung von Gorleben.-- Z. dt. geol. Ges., 131: 522-529, 2 Fig.; Hannover.
- JARITZ, W. (1983): Das Konzept der Erkundung des Salzstocks Gorleben von Übertage und die Festlegung von Schachtstandorten.-- N. Jb. Geol. Paläont. Abh., 166/1: 19-33, 5 Fig.; Stuttgart.
- JARITZ, W. (1993): Die geowissenschaftliche Untersuchung des Salzstocks Gorleben auf seine Eignung für ein Endlager für radioaktive Abfälle.-- Geol. Jb., A 142: 295-304, 1 Fig.; Hannover.
- JARITZ, W. (1994): Die Entwicklungsgeschichte des Standortes Gorleben als natürliches Analogon für das Langzeitverhalten eines Barrierensystems.-- Z. dt. geol. Ges., 145/1: 192-206, 3 Fig., 1 Att.; Hannover.
- JOCKWER, N. (1981): Untersuchungen zu Art und Menge des im Steinsalz des Zechsteins enthaltenen Wassers sowie dessen Freisetzung und Migration im Temperaturfeld endgelagerter radioaktiver Abfälle.-- GSF, Inst. f. Tieflagerung, Wiss. Abt., GSF-Bericht T 119: 134 pp.; Braunschweig.
- KELLER, S. (1990): Das Ablaugungsverhalten der Salzstöcke in NW-Deutschland (Abschl.-Ber. des BMFT-Förderungsvorhabens KWA 5801 9 „Langzeitsicherheit der Barriere Salzstock“, Teilprojekt III).-- BGR, unpubl. report, Archiv-Nr. 106570: 87 pp., 17 Fig., 9 Tab., 3 Apps.; Hannover.
- KELLER, S. (1996): Beschreibung der paläohydrogeologischen Verhältnisse seit Ende der Saale-Kaltzeit und Langzeitprognose der hydrogeologischen Entwicklung für den Elbe-Raum zwischen Burg und Boizenburg. Teil I: Klimatische Entwicklung und Auftreten von Permafrost.-- BGR, unpubl. report, Archiv-Nr. 114499: 42 pp., 10 Fig., 3 Tab.; Hannover.
- KLINGE, H. (1994): Zusammenfassende Bearbeitung der chemischen und isotope-geochemischen Zusammensetzung der Grundwässer im Deckgebirge des Salzstocks Gorleben und seiner Randsenken. Projektgebiet Gorleben-Süd.-- BGR, unpubl. report, Archiv-Nr. 111699: 234 pp., 76 Fig., 6 Tab., 7 Apps. with 27 Fig.; Hannover.

- KLINGE, H., BOEHME, J., GRISSEMANN, C., HOUBEN, G., LUDWIG, R. R., SCHELKES, K., SCHILDKNECHT, F., CZORA, C., FRIEBE, J., GERSDORF, U. & KOSENKO, M. (2003): Projekt Gorleben, Standortbeschreibung, Teil II: Deckgebirge Hydrogeologie. Abschlussbericht zum Arbeitspaket 9G3411800000.-- BGR, unpubl. report, 283 pp., 12 Apps.; Hannover.
- KLINGE, H., BOEHME, J., GRISSEMANN, C., HOUBEN, G., LUDWIG, R.-L., RÜBEL, A., SCHELKES, K., SCHILDKNECHT, F. & SUCKOW, A. (2007): Die Hydrogeologie des Deckgebirges des Salzstocks Gorleben.-- Geol. Jahrbuch, Reihe C, 71: 147 pp., 59 Fig., 4 Tab., 1 Apps., 64 cit., Hannover.
- KLINGE, H., MARGANE, A., MRUGALLA, S., SCHELKES, K. & SOFNER, B. (2001): Hydrogeologie des Untersuchungsgebietes Dömitz-Lenzen. Ergebnisbericht.-- BGR, unpubl. report: 344 pp., 105 Fig., 27 Tab., 3 Apps.; Hannover.
- KLÖCKER, R. (2000): Petrologische, sedimentologische und mikrofazielle Untersuchungen des Pegmatitanhydrits (Zechstein 4) in NW- und Mitteldeutschland.-- Univ. Bochum, Dipl.-Arbeit: 69 pp., 40 Fig., 8 Apps.; Bochum.
- KNIPPING, B. (1995): Sicherstellung der Datenbasis zum Stoffbestand des Salzstocks Gorleben. Zwischenbericht zum PSE-Element 9G-261310. Berichtszeitraum 1.1.94-31.12.94.-- Tech. Univ. Clausthal, Inst. f. Miner. u. mineral. Rohst., Zwischenbericht: 47 pp.; Clausthal-Zellerfeld.
- KNIPPING, B. & SIEMANN, M. G. (1996): Sicherstellung der Datenbasis zum Stoffbestand des Salzstocks Gorleben. Zusammenfassender Zwischenbericht zum PSE-Element 9G-261310. Berichtszeitraum 01.07.95-31.12.95.-- Tech. Univ. Clausthal, Inst. f. Miner. u. mineral. Rohst., Zwischenbericht: 31 pp., 9 Fig., 3 Tab., 1 App.; Clausthal-Zellerfeld.
- KOSMAHL, W. (1969): Zur Stratigraphie, Petrographie, Paläogeographie, Genese und Sedimentation des Gebänderten Anhydrits (Zechstein 2), Grauen Salztone und Hauptanhydrits (Zechstein 3) in Nordwestdeutschland.-- Beih. Geol. Jb., 71: 129 pp., 1 Fig., 1 Tab., 29 Att.; Hannover.
- KÖTHE, A., ZIRNGAST, M. & ZWIRNER, R. (2003): Projekt Gorleben, Standortbeschreibung, Teil I: Deckgebirge Geologie. Abschlussbericht zum Arbeitspaket 9G3411900000.-- BGR, unpubl. report: 255 pp., 43 Fig., 20 Tab.; Hannover.

- KÖTHE, A., HOFFMANN, N., KRULL, P., ZIRNGAST, M. & ZWIRNER, R. (2007): Die Geologie des Deckgebirges und Strukturgeologie des Salzstocks Gorleben.-- Geol. Jahrbuch, Reihe C, 72: 201 pp., 42 Fig., 19 Tab., 3 Apps., 148 cit., Hannover.
- KÜHN, R. (1955): Mineralogische Fragen der in Kalisalzlagerstätten vorkommenden Salze.-- Kalium-Symposium 1955: 51-105, 6 Fig., 3 Tab., 13 Att.; Bern.
- KUSTER, H. & MEYER, K.-D. (1979): Glaziäre Rinnen im mittleren und nordöstlichen Niedersachsen.-- Eiszeitalter u. Gegenwart, 29: 135-156, 5 Fig., 3 Tab., 1 Att.; Hannover.
- KUTOWSKI, J. (2002): Projekt Gorleben: Handbuch Bohrkernbearbeitung.-- DBE-Bericht, unpubl.: 30 pp., 10 Apps.; Peine.
- KUTOWSKI, J., ISLINGER, C. & MEYER, T. (1996): Projekt Gorleben, Schacht Gorleben 1, Endbericht Teil II, Geologie des Deckgebirges und der Hohlraumfüllungen im Hutgestein.-- DBE-Bericht, unpubl.: 171 pp., 38 Tab., 6 Apps., 4 Att.; Peine.
- Lexikon der Geowissenschaften: Nord-Silb.-- Bd. 4, (2001); Berlin (Spektrum Akad. Verl. Heidelberg).
- LÖFFLER, J. (1960): Die Carnallitgesteine des Raumes Aschersleben-Schierstedt.-- Freib. Forsch.-H., C 87: 63 pp., 27 Fig., 7 Tab.; Berlin.
- LÖWENSTEIN, T. K. & LAWRENCE, A. H. (1985): Criteria for the recognition of salt-pan evaporites.-- Sedimentology, 32: 627-644, 23 Fig.; Oxford.
- LUDWIG, A. O. (2001): Vertical movements since the beginning of Rupelian stage (map 1). (In: GARETSKY, R. G. et al. (Hrsg.): Neogeodynamics of the Baltic Sea Depression and Adjacent Areas. Results of IGCP Project 346)-- Brandenburgische Geowiss. Beitr., 8, 1: 5-12, 4 Fig.; Kleinmachnow.
- MARTIN, M. (1995a): Projekt Gorleben, 16. Zwischenbericht Geologie Salinar Schacht Gorleben 1, 2. Halbjahr 1994.-- DBE-Bericht, unpubl.: 33 pp., 3 Tab., 8 Apps., 1 Att.; Peine.
- MARTIN, M. (1995b): Projekt Gorleben, 16. Zwischenbericht Geologie Salinar Schacht Gorleben 2, 2. Halbjahr 1994.-- DBE-Bericht, unpubl.: 28 pp., 3 Tab., 7 Apps., 1 Att.; Peine.

- MATTENKLOTT, M. (1994): Die Bromid- und Rubidiumverteilung in Carnallitgesteinen.-- Univ. Clausthal-Zellerfeld, Diss.: 214 pp., 49 Fig., 56 Tab.; Clausthal-Zellerfeld.
- MEYER, T. (1993a): Projekt Gorleben, 11. Zwischenbericht Geologie Salinar Schacht Gorleben 1, 1. Halbjahr 1992.-- DBE-Bericht, unpubl.: 29 pp., 3 Tab., 9 Apps., 5 Att.; Peine.
- MEYER, T. (1993b): Projekt Gorleben, 13. Zwischenbericht Geologie Salinar Schacht Gorleben 2, 1. Halbjahr 1993.-- DBE-Bericht, unpubl.: 27 pp., 5 Tab., 14 Apps., 1 Att.; Peine.
- MEYER, T. (1994a): Projekt Gorleben, 14. Zwischenbericht Geologie Salinar Schacht Gorleben 1, 2. Halbjahr 1993.-- DBE-Bericht, unpubl.: 15 pp., 7 Apps.; Peine.
- MEYER, T. (1994b): Projekt Gorleben, 14. Zwischenbericht Geologie Salinar Schacht Gorleben 2, 2. Halbjahr 1993.-- DBE-Bericht, unpubl.: 19 pp., 8 Apps.; Peine.
- MEYER, T. (1994c): Projekt Gorleben, 15. Zwischenbericht Geologie Salinar Schacht Gorleben 1, 1. Halbjahr 1994.-- DBE-Bericht, unpubl.: 20 pp., 1 Tab., 7 Apps.; Peine.
- MEYER, T. (1994d): Projekt Gorleben, 15. Zwischenbericht Geologie Salinar Schacht Gorleben 2, 1. Halbjahr 1994.-- DBE-Bericht, unpubl.: 20 pp., 1 Tab., 7 Apps.; Peine.
- MEYER, T. & ISLINGER, C. (1993): Projekt Gorleben, 13. Zwischenbericht Geologie Salinar Schacht Gorleben 1, 1. Halbjahr 1993.-- DBE-Bericht, unpubl.: 18 pp., 1 Tab., 8 Apps.; Peine.
- MIDDENDORF, E. & KÜHN, R. (1966): Befahrung des Kalibergwerks Siegfried -Giesen, Groß-Giesen bei Hildesheim, 8. September 1965.-- Fortschr. Miner., 43/2: 145-187, 24 Fig., 4 Tab.; Stuttgart.
- MINGERZAHN, G. (1987): Klastische Sedimente im subrodierten Kaliflöz Staßfurt (Zechstein 2) des Salzstocks Gorleben.-- Techn. Univ. Braunschweig, Dipl.-Arbeit: 120 pp., 61 Fig., 9 Tab.; Braunschweig.
- MÜLLER-SCHMITZ, S. (1985): Mineralogisch-petrographische und geochemische Untersuchungen an Salzgesteinen der Staßfurt-, Leine- und Aller-Serie im Salzstock Gorleben (Niedersachsen, B. R. Deutschland).-- Univ. Heidelberg, Diss.: 156 pp., 39 Fig., 24 Tab., 12 Att.; Heidelberg.

- MUNDRY, E., THIERBACH, R., WEICHART, H. & ZIEKUR, R. (1985): Erkundung unerschlossener Bereiche von Salzlagerstätten durch hochfrequente elektromagnetische Bohrlochmeßverfahren. F & E-Vorhaben KWA 5113. Schlußbericht.-- BGR, unpubl. report, Archiv-Nr. 98: 152 pp.; Hannover.
- NETTEKOVEN, A. & GEINITZ, E. (1905): Die Salzlagerstätte von Jessenitz in Mecklenburg.-- Mitt. Großherzogl. Mecklenburg. Geol. Landesanstalt, XVIII: 1-17, 2 Att.; Rostock.
- NOWAK, T. & WEBER, J. R. (2002): Hydraulische Charakterisierung der Salzbarriere Gorleben, Abschlussbericht.-- BGR, unpubl. report: 122 pp., 57 Fig., 16 Tab.; Hannover.
- NOWAK, T., WEBER, J. R. & BORNEMANN, O. (2002): Gas- und Lösungsreservoir im Salzstock Gorleben.-- BGR, unpubl. report: 71 pp., 44 Fig., 11 Tab.; Hannover.
- PAPE, T. (1993): Beobachtungen zum Gefüge des Kristallbrockensalzes (z2HS3) in Bohrkernen aus dem Salzstock Gorleben.-- Univ. Hannover, Dipl.-Arbeit: 73 pp., 28 Fig., 12 Apps.; Hannover.
- PAPE, T., MICHALZIK, D. & BORNEMANN, O. (2002): Chevronkristalle im Kristallbrockensalz (Zechstein 2) des Salzstocks Gorleben - Primärgefüge salinärer Flachwassersedimentation im Zechsteinbecken.-- Z. dt. geol. Ges., 153/1: 115-129, 6 Fig., 2 Att.; Stuttgart.
- POHL, W. (1992): W. & W. E. Petrascheck's Lagerstättenlehre. - Eine Einführung in die Wissenschaft von mineralischen Bodenschätzen.-- 4. Edit.: 504 pp., 246 Fig.; Stuttgart (Schweizerbart).
- PREUSS, H., VINKEN, R. & VOSS, H.H. (1991): Symbolschlüssel Geologie – Symbole für die Dokumentation und automatische Datenverarbeitung geologischer Feld- und Aufschlusdaten.--Niedersächs. Landesamt für Bodenforschung, 328 pp., Hannover.
- PROHL, H. (1998): Raman-spektroskopische Untersuchungen zur Zusammensetzung gasförmiger Einschlüsse in Gesteinen des Salzstocks Gorleben.-- Univ. Clausthal-Zellerfeld, Diss.: 62 pp., 34 Fig., 16 Tab., 1 Att.; Clausthal-Zellerfeld.
- REPPERT, D. (1982a): Bericht über die durchgeführten Testarbeiten in der Bohrung Gorleben 1005.-- DBE-Bericht, unpubl.: 22 pp., 5 Apps.; Peine.

- REPPERT, D. (1982b): Bericht über die Testarbeiten in der Bohrung Gorleben 1004.-- DBE-Bericht, unpubl.: 12 pp., 5 Apps.; Peine.
- REPPERT, D. (1983a): Bericht über die durchgeführten Packer-Tests in der Schachtvorbereitung Gorleben 5002.-- DBE-Bericht, unpubl.: 14 pp., 6 Tab., 5 Apps.; Peine.
- REPPERT, D. (1983b): Bericht über die durchgeführten Single-Packer-Tests in der Schachtvorbereitung Gorleben 5001.-- DBE-Bericht, unpubl.: 23 pp., 10 Tab., 8 Apps.; Peine.
- REPPERT, D. (1983c): Bericht über die durchgeführten Testarbeiten in der Bohrung Gorleben 1003.-- DBE-Bericht, unpubl.: 36 pp., 7 Apps.; Peine.
- RICHTER, A. (1962): Die Rotfärbung in den Salzen der deutschen Zechsteinlagerstätten. 1. Teil.-- Chemie der Erde, Bd. 22: 508-546, 22 Fig., 6 Tab., 2 Att.; Jena (VEB Gustav Fischer).
- RICHTER, A. (1964): Die Rotfärbung in den Salzen der deutschen Zechsteinlagerstätten. 2. Teil.-- Chemie der Erde, Bd. 23: 179-203, 10 Fig., 2 Att.; Jena (VEB Gustav Fischer).
- RICHTER-BERNBURG, G. (1980): Salt tectonics. Interior structures of salt bodies.-- Bull. Cent. Rech. Explor.-Prod. Elf-Aquitaine, 4, 1: 373-396, 24 Fig., 2 pl.; Pau.
- SANDER, W. & HERBERT, H.-J. (2000): Wassergehaltsbestimmung am Steinsalz (Erkundungssohle). Zwischenbericht für den Zeitraum 01.01.1998 - 31.12.1999. PSP Element 9G 412210-00.-- Ges. f. Anl.- u. Reaktorsicherheit mbH (GRS): 10 pp., 6 Tab.; Braunschweig.
- SCHACHL, E. (1987): Kali- und Steinsalzbergwerk Niedersachsen - Riedel der Kali und Salz AG, Schachtanlage Riedel. Zechsteinstratigraphie und Innenbau des Salzstocks von Wathlingen-Hänigsen.-- Int. Symp. Zechstein 1987, Kassel, Exkursionsführer G: 69-100, 18 Fig., 3 Tab.; Wiesbaden.
- SCHLAAK, N. (1999): Nordostbrandenburg - Entstehungsgeschichte einer Landschaft. (In: Entdeckungen entlang der Märkischen Eiszeitstraße).-- Gesellschaft zur Erforschung und Förderung der Märkischen Eiszeitstraße e.V.: 48 pp., 27 Fig.; Eberswalde.

- SCHRAMM, M. & BORNEMANN, O. (2004): Deformationsgrade bzw. -mechanismus des Steinsalzes im Rahmen der Salzstockbildung – Stand der Bearbeitung der Bromidprofile -, Tätigkeitsbericht 2003.-- BGR, unpubl. report, 9Y3215020000: 28 p., 1 Fig., 1 Tab., 14 Apps.; Hannover.
- SCHRAMM, M., BORNEMANN, O., WILKE, F., SIEMANN, M. & DIJK, H. L. (2002): Bromine Analysis - A Powerfull Tool to solve Stratigraphical Problems in Exploration Boreholes for Salt Caverns. (In: Techn. Meeting Papers, SMRI, Fall 2002 Meeting, Bad Ischl/ Austria).-- Solution Mining Research Inst. (Californien): 12 pp., 4 Fig.; Encinitas/ USA.
- SCHRAMM, M., BORNEMANN, O., SIEMANN, M., WILKE, F. & GELUK, M. (2005): Correlation between bromine concentrations in halites and their stratigraphical position in Zechstein 2 salt deposits of North-West Europe. -- Geophysical Research Abstracts, Vol. 7, 04552 (CD); European Geosciences Union 2005.
- SCHNEIDER, J. (1995): Eindunstung von Meerwasser und Salzbildung in Salinen.-- Kali und Steinsalz, 11: 325-330, 6 Fig.; Essen.
- SCHUBERT, J. (1996): Projekt Gorleben, Schacht Gorleben 2, Endbericht Teil II, Geologie des Deckgebirges und der Hohlräumfüllungen im Hutgestein.-- DBE-Bericht, unpubl.: 120 pp., 28 Tab., 6 Apps., 4 Att.; Peine.
- SCHUBERT, J. (2001): Projekt Gorleben, Schacht Gorleben 2, Endbericht Teil IV, Geologie des Salinars.-- DBE-Bericht, unpubl.: 42 pp., 9 Tab., 5 Apps., 5 Att.; Peine.
- SCHULZE, G. (1959a): Beitrag zur Stratigraphie und Genese der Steinsalzserien I-IV des mitteldeutschen Zechsteins unter besonderer Berücksichtigung der Bromverteilung.-- Freib.-Forsch.-H., A 123: 175-196, 17 Fig., 3 Tab.; Berlin.
- SCHULZE, G. (1959b): Stratigraphische und genetische Deutung der Bromverteilung in den mitteldeutschen Steinsalzlagern des Zechsteins - Abschlußbericht.-- Staatl. geol. Kommission der DDR, Zentr. geol. Dienst Halle (unpubl. report): 84 pp., 19 Fig., 35 Apps., 1 Att.; Halle.
- SCHULZE, G. (1960): Stratigraphische und genetische Deutung der Bromverteilung in den mitteldeutschen Steinsalzlagern des Zechsteins.-- Freib. Forsch.-H., C 83: 116 pp., 25 Fig., 4 Tab., 35 Apps.; Berlin.

- SCHULZE, O. (2002): Auswirkung der Gasentwicklung auf die Integrität geringdurchlässiger Barrieregesteine.-- BGR, unpubl. report: 142 pp., 27 Fig., 4 Tab., Att. A-G; Hannover.
- SIEMANN, M. G. (1996): Sicherstellung der Datenbasis zum Stoffbestand des Salzstocks Gorleben. Zwischenbericht zum PSE-Element 9G-261310. Berichtszeitraum 01.01.96-30.06.96.-- Tech. Univ. Clausthal, Inst. f. Miner. u. mineral. Rohst., Zwischenbericht: 18 pp., 8 Tab.; Clausthal-Zellerfeld.
- SIEMANN, M. G. & ELLENDORF, B. (2001): The composition of gases in fluid inclusions of late Permian (Zechstein) marine evaporites in Northern Germany.-- *Chemical Geology*, 173 (1-3): 31-44, 9 Fig., 5 Tab.; Amsterdam (Elsevier).
- SIEMANN, M. G. & MENGEL, K. (1998): Sicherstellung der Datenbasis zum Stoffbestand des Salzstocks Gorleben. Zwischenbericht zum PSE-Element 9G-261310. Berichtszeitraum 01.01.97-31.012.97.-- Tech. Univ. Clausthal, Inst. f. Miner. u. mineral. Rohst., Zwischenbericht: 17 pp., 5 Tab.; Clausthal-Zellerfeld.
- SIEMEISTER, G. (1969): Primärparagenese und Metamorphose des Ronnenberglagers nach Untersuchungen im Grubenfeld Salzdetfurth.-- *Beih. Geol. Jb.*, 62: 122 pp., 17 Fig., 16 Att.; Hannover.
- SONNENFELD, P. (1984): Brines and Evaporites.-- 613 pp., 135 Fig., 8 Tab.; Orlando/USA.
- WEBER, J. R., BORNEMANN, O. & MINGERZAHN, G. (1998): Lösung und Gase in Salzstrukturen - Beurteilung der Bedeutung für Untertagedeponien.-- *Geotechnik*, 21: 229-234, 5 Fig., 3 Tab.; Bochum.
- ZBRANCA, L. (1998): Projekt Gorleben, 23. Zwischenbericht Geologie Salinar Schacht Gorleben 2, 1. Halbjahr 1998.-- DBE-Bericht, unpubl.: 13 pp., 6 Apps., 1 Att.; Peine.
- ZBRANCA, L. (1999): Projekt Gorleben, 24. Zwischenbericht Geologie Salinar Schacht Gorleben 2, 2. Halbjahr 1998.-- DBE-Bericht, unpubl.: 13 pp., 6 Apps., 1 Att.; Peine.
- ZBRANCA, L. & PETZOLD, B. (1995a): Projekt Gorleben, 17. Zwischenbericht Geologie Salinar Schacht Gorleben 1, 1. Halbjahr 1995.-- DBE-Bericht, unpubl.: 29 pp., 2 Tab., 7 Apps., 2 Att.; Peine.

- ZBRANCA, L. & PETZOLD, B. (1995b): Projekt Gorleben, 17. Zwischenbericht Geologie Salinar Schacht Gorleben 2, 1. Halbjahr 1995.-- DBE-Bericht, unpubl.: 27 pp., 2 Tab., 7 Apps., 2 Att.; Peine.
- ZBRANCA, L. (1997a): Bohrrakte der Kernbohrung 01YEF20 RB001.-- DBE-Bericht, unpubl.: 4 pp., 10 Apps.; Peine.
- ZBRANCA, L. (1997b): Bohrrakte der Kernbohrung 01YEF20 RB002.-- DBE-Bericht, unpubl.: 4 pp., 10 Apps.; Peine.
- ZBRANCA, L. (1997c): Bohrrakte der Kernbohrung 01YEF20 RB003.-- DBE-Bericht, unpubl.: 4 pp., 10 Apps.; Peine.
- ZBRANCA, L. (1997d): Bohrrakte der Kernbohrung 01YEF20 RB014.-- DBE-Bericht, unpubl.: 4 pp., 14 Apps.; Peine.
- ZBRANCA, L. (1997e): Bohrrakte der Kernbohrung 01YEF20 RB015.-- DBE-Bericht, unpubl.: 4 pp., 10 Apps.; Peine.
- ZBRANCA, L. (1997f): Bohrrakte der Kernbohrung 01YEF20 RB059.-- DBE-Bericht, unpubl.: 4 pp., 10 Apps.; Peine.
- ZBRANCA, L. (1997g): Bohrrakte der Kernbohrung 02YEA04 RB021.-- DBE-Bericht, unpubl.: 4 pp., 10 Apps.; Peine.
- ZBRANCA, L. (1997h): Bohrrakte der Kernbohrung 02YEA04 RB022.-- DBE-Bericht, unpubl.: 4 pp., 10 Apps.; Peine.
- ZBRANCA, L. (1997i): Bohrrakte der Kernbohrung 02YEA04 RB024.-- DBE-Bericht, unpubl.: 4 pp., 10 Apps.; Peine.
- ZBRANCA, L. (1997j): Bohrrakte der Kernbohrung 02YEA04 RB025.-- DBE-Bericht, unpubl.: 4 pp., 10 Apps.; Peine.
- ZBRANCA, L. (1997k): Bohrrakte der Kernbohrung 02YEA04 RB029.-- DBE-Bericht, unpubl.: 4 pp., 10 Apps.; Peine.
- ZBRANCA, L. (1997l): Bohrrakte der Kernbohrung 02YEA24 RB030.-- DBE-Bericht, unpubl.: 4 pp., 10 Apps.; Peine.

- ZBRANCA, L. (1997m): Bohrake der Kernbohrung 02YEF10 RB001.-- DBE-Bericht, unpubl.: 4 pp., 10 Apps.; Peine.
- ZBRANCA, L. (1997n): Bohrake der Kernbohrung 02YEF11 RB001.-- DBE-Bericht, unpubl.: 4 pp., 10 Apps.; Peine.
- ZBRANCA, L. (1997o): Bohrake der Kernbohrung 02YEF11 RB003.-- DBE-Bericht, unpubl.: 4 pp., 10 Apps.; Peine.
- ZBRANCA, L. (1997p): Bohrake der Kernbohrung 02YEF11 RB004.-- DBE-Bericht, unpubl.: 4 pp., 10 Apps.; Peine.
- ZBRANCA, L. (1997q): Bohrake der Kernbohrung 02YEF11 RB012.-- DBE-Bericht, unpubl.: 4 pp., 14 Apps.; Peine.
- ZBRANCA, L. (1997r): Bohrake der Kernbohrung 02YEF11 RB013.-- DBE-Bericht, unpubl.: 4 pp., 14 Apps.; Peine.
- ZBRANCA, L. (1997s): Bohrake der Kernbohrung 02YEF11 RB058.-- DBE-Bericht, unpubl.: 4 pp., 10 Apps.; Peine.
- ZBRANCA, L. (1997t): Bohrake der Kernbohrung 02YEF20 RB004.-- DBE-Bericht, unpubl.: 4 pp., 10 Apps.; Peine.
- ZBRANCA, L. (1997u): Bohrake der Kernbohrung 02YER02 RB026.-- DBE-Bericht, unpubl.: 4 pp., 10 Apps.; Peine.
- ZBRANCA, L. (1998a): Bohrake der Kernbohrung 02YEA04 RB023.-- DBE-Bericht, unpubl.: 4 pp., 14 Apps.; Peine.
- ZBRANCA, L. (1998b): Bohrake der Kernbohrung 02YEQ01 RB119.-- DBE-Bericht, unpubl.: 4 pp., 12 Apps.; Peine.
- ZBRANCA, L. (1998c): Bohrake der Kernbohrung 02YEQ01 RB120.-- DBE-Bericht, unpubl.: 4 pp., 10 Apps.; Peine.
- ZBRANCA, L. (1998d): Bohrake der Kernbohrung 02YER02 RB033.-- DBE-Bericht, unpubl.: 4 pp., 10 Apps.; Peine.
- ZBRANCA, L. (1998e): Bohrake der Kernbohrung 02YER02 RB154.-- DBE-Bericht, unpubl.: 4 pp., 10 Apps.; Peine.

- ZBRANCA, L. (1998f): Bohrrakte der Kernbohrung 02YER02 RB233.-- DBE-Bericht, unpubl.: 4 pp., 13 Apps.; Peine.
- ZBRANCA, L. (1999): Bohrrakte der Kernbohrung 02YER02 RB261.-- DBE-Bericht, unpubl.: 4 pp., 14 Apps.; Peine.
- ZBRANCA, L. (2000a): Bohrrakte der Kernbohrung 02YEQ01 RB248.-- DBE-Bericht, unpubl.: 4 pp., 8 Apps.; Peine.
- ZBRANCA, L. (2000b): Bohrrakte der Kernbohrung 02YEQ01 RB427.-- DBE-Bericht, unpubl.: 4 pp., 13 Apps.; Peine.
- ZBRANCA, L. (2000c): Bohrrakte der Kernbohrung 02YER20 RB254.-- DBE-Bericht, unpubl.: 4 pp., 13 Apps.; Peine.
- ZBRANCA, L. (2001a): Bohrrakte der Kernbohrung 02YEQ01 RB194.-- DBE-Bericht, unpubl.: 4 pp., 12 Apps.; Peine.
- ZBRANCA, L. (2001b): Bohrrakte der Kernbohrung 02YER02 RB032.-- DBE-Bericht, unpubl.: 4 pp., 14 Apps.; Peine.
- ZIRNGAST, M. (1985): Dynamik des Salzstocks Gorleben.-- BGR, unpubl. report, Archiv-Nr. 97673: 53 pp., 10 Fig., 29 Apps.; Hannover.
- ZIRNGAST, M. (1990): Begrenzung und Volumen des Salzstocks Gorleben.-- BGR, unpubl. report, Archiv-Nr. 106565: 8 pp., 8 Fig., 5 Apps.; Hannover.
- ZIRNGAST, M. (1991): Die Entwicklungsgeschichte des Salzstocks Gorleben - Ergebnisse einer strukturgeologischen Bearbeitung.-- Geol. Jb., A 132: 3-31, 17 Fig., 2 Tab., 1 Att.; Hannover.
- ZIRNGAST, M. (1996): The development of the Gorleben salt dome (northwest Germany) based on quantitative analysis of peripheral sinks. (In: ALSOP, G. I. et al. (Eds.): Salt Tectonics).-- Geol. Soc. Sp. Publ., No. 100: 203-226, 16 Fig., 2 Tab.; London.
- ZIRNGAST, M., ZWIRNER, R., BORNEMANN, O., FLEIG, S., HOFFMANN, N., KÖTHER, A., KRULL, P. & WEISS, W. (2003): Projekt Gorleben. Schichtenfolge und Strukturbaue des Deck- u. Nebengebirges. Abschlussbericht.-- BGR, unpubl. report, 565 pp., 42 Fig., 32 Tab., 195 Apps.; Hannover.

Abbreviations

AAS	atomic absorption spectrometry
BfS	Federal Office for Radiation Protection (Bundesamt für Strahlenschutz)
BGR	Federal Institute for Geosciences and Natural Resources (Bundesanstalt für Geowissenschaften und Rohstoffe)
BMFT	Federal Ministry of Research and Technology (Bundesministerium für Forschung und Technologie)
BMU	Federal Ministry for the Environment, Nature Conservation and Nuclear Safety (Bundesministerium für Umwelt, Naturschutz und Reaktorsicherheit)
CDT	sulphur isotope standard (Canon Diabolo Troilit)
¹³ C	Carbon-13 isotope
¹⁴ C	Carbon-14 isotope
DBE	German Company for the Construction and Operation of Waste Repositories Ltd. (Deutsche Gesellschaft zum Bau und Betrieb von Endlagern für Abfallstoffe mbH)
DIN	German Standard (Deutsche Industrie-Norm)
EB 1	Exploration Area 1 (Erkundungsbereich 1)
EL 4	Exploration Location 4 (Erkundungslokation 4)
EMR	electromagnetic reflection
EN	European Standard
Go	name prefix of shaft pilot boreholes and salt dome exploration boreholes
GoHy	name prefix of salt table boreholes and boreholes belonging to the hydrogeological investigation programme (Gorleben Hydrogeologie)
HAW	Highly Active Waste
HFA	high-frequency absorption
IC	ion chromatography
ICP-OES	atomic emission spectrography with microwave-induced plasma excitement (optische Emissionsspektralanalyse mit induktiv gekoppelter Plasmaanregung)
ISO	International Organization for Standardization
KW	hydrocarbons (Kohlenwasserstoffe)
NN	sea level (Normal Null)
NW	northwest
¹⁸ O	oxygen-18 isotope
¹⁶ O	oxygen-16 isotope
ppm	parts per million (10 ⁻⁴ %)

XRD	X-ray diffraction (Röntgendiffraktometeranalyse)
XRF	X-ray fluorescence spectroscopy (Röntgenfluoreszenzanalyse)
SE	southeast
SMOW	standard mean ocean water, standard for oxygen isotope analysis
UV light	ultraviolet light
vol-%	volume percent
wt-%	weight percent
$\delta^{18}\text{O}$	deviation of the isotope ratio $^{18}\text{O}/^{16}\text{O}$ of a sample compared to standard mean ocean water
$\delta^{13}\text{C}$	deviation of the isotope ratio $^{13}\text{C}/^{12}\text{C}$ of a sample compared to (Pee Dee Belemnite limestone) PDB-Standard
$\delta^{34}\text{S}$	deviation of the isotope ratio $^{34}\text{S}/^{32}\text{S}$ of a sample compared to the sulphur isotope standard (Canon Diabolo Troilit)
δD	deviation of the isotope ratio D/H of a sample compared to ocean water

Note:

Stratigraphical and petrographical abbreviations correspond to the "Geological Symbol Key" (PREUSS et al. 1991) and the stratigraphic table of the Zechstein Folge 1 to 4 (Fig. 4 and Table 7). Common abbreviations, measurement units, and chemical symbols are not included.

List of tables

Table 1:	Salt table boreholes and associated exploration boreholes nearby.	35
Table 2:	Penetration depth of water from the overburden below the salt table and lithological changes in the adjacent formations caused by subsrosion.	38
Table 3:	Calculated subsrosion rates and amount of salt subroded from Geschichtetes Gips-, Anhydritgestein in selected exploration boreholes.	66
Table 4:	Average mineral contents, bromide and rubidium contents of the carnallites, and K ₂ O contents of the Kaliflöz Stassfurt (z2SF) in the samples of the deep boreholes Go 1002 and Go 1003.	151
Table 5:	Dimensions of the Hauptsalz in Exploration Area 1.	179
Table 6:	Simple derivation of post Elsterian time leaching rates based on the anhydrite contents in salt rocks at salt table and the thickness of Geschichtetes Gips-/Anhydritgestein	see App.
Table 7:	Stratigraphic table of the Zechstein beds, with information to the lithology and mean thickness	see App.

List of figures

Figure 1:	Geochronological scheme of the salt dome formation at the Gorleben site shown as a cross section (after JARITZ 1980; ZIRNGAST 1985, 1991).	10
Figure 2:	Borehole map – surface boreholes with exposures in the salt formation (abbreviations used for surface boreholes: GoHy - salt table boreholes, Go - pilot shaft boreholes and exploration boreholes).	17
Figure 3:	Subrosion of the Kaliflöz Stassfurt in the area of the Gorleben Channel as found in the salt table boreholes GoHy 1301 to 1305 and GoHy 1141.	40
Figure 4:	Overview of the stratigraphic position, thickness and lithological composition of the Zechstein layers encountered in the infrastructure area and in Exploration Area 1.	44
Figure 5:	Simplified calculation template of the ZECHMIN-7 software to quantify the mineralogical composition.	56
Figure 6:	Non-scale illustration of the sequence of strata in the cap rock (according to BORNEMANN & FISCHBECK 1986).	62
Figure 7:	Genesis of Geschichtetes Gips-, Anhydritgestein, salt table and underlying salt formation in selected cores (1 to 7).	65
Figure 8:	Geological map of the salt table (BORNEMANN 1991: App. 21) and post-Elsterian subrosion rates (Hauptanhydrit is simplified as a continuous band).	69
Figure 9:	Sediment history of the cap rock illustrated by the exposure in Shaft Gorleben 1 (schematic drawing after JARITZ 1994).	72
Figure 10:	Formation of the cap rock over time (see next page).	76
Figure 11:	Contour map of the salt table of the Gorleben salt dome.	78
Figure 12:	Core containing typical Kristallbrockensalz. The red arrow indicates crystal lumps, the blue arrow indicates matrix. The black areas represent anhydrite impurities. Height = approx. 5 cm.	84
Figure 13:	Isolated and rotated blocks of Hauptanhydrit (arrows), surrounded by thinned Kaliflöz Stassfurt in a brecciated carnallite facies.	86
Figure 14:	Metamorphosis stages of the Kaliflöz Stassfurt in the area of the updoming between the shafts on the 840 m-level.	88
Figure 15:	Synthetic profile of borehole logs within the beds of the Stassfurt-Folge, Leine-Folge und Aller-Folge.	91
Figure 16:	Stratigraphy and carbonate inclusions in the Hauptanhydrit illustrated by the Hauptanhydrit section in borehole Go 1005.	92
Figure 17:	Stratigraphic sequence and true thickness of the layers of the Hauptanhydrit - comparison of several exposures.	95

- Figure 18: Hauptanhydrit block in combination with discordant layering and folding of the Basissalz. Cross-cut 1 West, 840 m-level, drift position 50 m, western wall. (Photograph: Bauer, DBE) 97
- Figure 19: Boudinage of the anhydrite bank in the Basissalz. The anhydrite blocks are completely separated from each other and enveloped by Basissalz. In some sections white recrystallized halite fills the gaps. The anhydrite layer is outlined by black paint. Ventilation drift, position 65 m, eastern wall. (Photograph: Bauer, DBE) 98
- Figure 20: Anticline in the Liniensalz with marker horizon 110. Linie (see arrow). The figure shows a significant change in the spacing of the bands: widely spaced in the lower section, closely spaced in the upper section. 840 m-level, landing drift of Shaft 2, drift position 135 m, eastern wall. (Photograph: Bauer, DBE) 100
- Figure 21: Stratigraphy and petrography of the Gorleben-Bank (z3OSM). 105
- Figure 22: Gorleben-Bank, ruptured and overturned. The ruptured sections and parts of the shear zone (black) are healed with secondary red and yellow carnallite. Access drift to vehicle workshop, 840 m-level, drift position 10 m, southern wall. (Photograph: Bauer, DBE) 106
- Figure 23: Intense folding of the beds in the Oberes Orangesalz. The beds of the Unteres Orangesalz remain untouched by the intense folding due to the Gorleben-Bank acting as a buffer horizon (Shaft 2, depth 595.3 to 606.0 m). 108
- Figure 24: Seismogram-like folding of the Gorleben-Bank. This type of folding is extremely rare and is probably due to the fact that the intense deformation affected the Zechstein 3/Zechstein 2 boundary. Most of the beds of the Gorleben-Bank are missing, only the shear zone (black) and the overlying stratified anhydrite (grey) are present. Main drift, 840 m-level, drift position 280 m, northern wall. (Photograph: Bauer, DBE) 109
- Figure 25: Fissure filled with red carnallite in the Unteres Orangesalz the bedding of which dips from upper left to lower right. The fissure strikes perpendicular to the bedding and is associated with the halokinetic pinch-off of the sequence of Grauer Salzton to Hauptanhydrit in the area of the updoming of the Kaliflöz Stassfurt between the shafts. Landing drift Shaft 2, 820 m-level, drift position 38 m, southwestern wall. (Photograph: Engelhardt, DBE) 110

- Figure 26: Starting at the Gorleben-Bank, a secondary mineralization permeates the underlying Unteres Orangesalz, the sedimentary bedding of which is almost completely destroyed in this area. No fault-induced dislocation of the bedding is detectable. The mineralization consists mainly of white coarse-crystalline halite and red carnallite on the edges. Milling workshop, 840 m-level, drift position 65 m. (Photograph: Bauer, DBE) 111
- Figure 27: Gorleben-Bank, with underlying Unteres Orangesalz with secondarily crystallized, white coarse-crystalline halite zones, resembling the outline of loaves of bread. The lower boundary is flat and contains an anhydrite filling, the upper boundary is domed. Access to vehicle workshop, 840 m-level, drift position 5 m, southern wall. (Photograph: Bauer, DBE) 112
- Figure 28: Zone of secondary recrystallization with uneven boundary in the Unteres Orangesalz, filled with white coarse-crystalline halite. The outline is enhanced with black paint. Store, 840 m-level, drift position 35 m, roof. (Photograph: Bauer, DBE) 113
- Figure 29: Filled cavity, resembling a loaf of bread, with secondarily crystallized white and clear coarse-crystalline halite, partly intersticed with carnallite or brine. The lower side is flat and coated with an anhydrite fringe. The upper side is domed like a loaf of bread. Shaft 2, approx. 835 m. (Photograph: Wiesch, DBE) 113
- Figure 30: Core of Liniensalz (borehole Go 1002; depth 900.50 to 902.16 m) showing a recumbent fold of an anhydrite band, accompanied by a carnallite inclusion on top. This is accumulated in the “bow” or core of the folds and pinched off at the sides except for residues. Despite the folding, the carnallite layer is always above the anhydrite band, so it can be assumed that it was deposited before folding and may be of sedimentary origin. 115
- Figure 31: Stratigraphy of the Buntessalz. 117
- Figure 32: Schematic view of the sequence of strata in the Anhydritmittelsalz. 119
- Figure 33: Borehole log and petrographic sequence of the Tonmittelsalz as encountered in salt dome exploration borehole Go 1004. 121
- Figure 34: Schematic view of the stratigraphic sequence and petrographic structure of the Pegmatitanhydrit. 123
- Figure 35: Geological outline of the Gorleben salt dome and comparison of the z2 extent with other salt structures. 127
- Figure 36: Simplified cross section of the Gorleben salt dome (cross section C-C'; from BORNEMANN 1991, App. 23). The Hauptanhydrit is shown in a simplified form as a continuous band. 128

- Figure 37: Lumps of Hauptanhydrit in secondary carnallite halite matrix.
The lumps have been sheared from a Hauptanhydrit block due to halotectonics. Cross-cut 1 West, 840 m-level, drift location 40 m, former drift face. (Photograph: Bauer, DBE) 129
- Figure 38: Comparison of fold axis directions (B-axes) in Shafts 1 and 2. 130
- Figure 39: Plunge of the fold axes in the shafts. 131
- Figure 40: Dip of the axial planes in the shafts (see also Fig. 39). 131
- Figure 41: Boundary of Zechstein 2/Zechstein 3 with thinned-out Kaliflöz Stassfurt (centre) and halotectonic pinch-off of the sequence from Grauer Salzton to Hauptanhydrit (max. 100 m). The Basissalz and remnants of the anhydrite bank (black circle in the Basissalz) of the Zechstein 3 sequence are on the right side and the thinned-out Hangendsalz and Kristallbrockensalz of Zechstein 2 can be seen on the left. Cross-cut 1 East, drift position approx. 110 m, eastern wall. (Photograph: Bauer, DBE) 137
- Figure 42: Intensely deformed and folded Liniensalz with isoclinal interfolding of Orangesalz close to the Zechstein 3/Zechstein 2 boundary. The stripe intervals are in the centimetre range and the anhydrite stripes are torn into segments. Shaft undercut to the 880 m-level, drift position 369 to 374 m, western wall. (Photograph: Bauer, DBE) 138
- Figure 43: Sketch showing two profiles (P1 and P2), and an outline of the fold structure on the southern flank of the main anticline. 140
- Figure 44: Bromide standard profile of the Zechstein 2. 143
- Figure 45: Bromide standard profile of the Zechstein 3 sequence. 148
- Figure 46: Quantitative mineral content of the Kaliflöz Stassfurt in the samples of deep boreholes Go 1002 and Go 1003, and bromide and rubidium content of the carnallite in the deep borehole Go 1002. 152
- Figure 47: Quantitative mineral content of the Kaliflöz Stassfurt in the samples of boreholes RB170, RB059 and RB217 and bromide content of the halites and carnallites, and rubidium content of the carnallite.
The bar widths give a symbolic representation of the mineral contents, using the same scale for all selected boreholes.
In boreholes RB 170 and RB 217, the respective depth intervals are marked on the depth scales. 156
- Figure 48: Gas flute in the Kaliflöz Stassfurt. It was formed when excavation work in the potash seam caused the release of gas that had been embedded under pressure in the brecciated carnallite (crackling carnallite). The flute is approx. 1.5 m long and has a diameter of approx. 30 cm. Cross-cut 1 West, 840 m-level, drift position 85 m, western wall. (Photograph: Bauer, DBE) 161

Figure 49: Condensate occurrence in cross-cut 1 West at the pillar corner of drilling location 1.4 at approx. drift metre 325 under ultraviolet light (above) and artificial light (below). The two photographs show the same area. The visible condensate inflows are marked by brown stains on the sidewall.

Weak lines of fluorescence can be seen under ultraviolet light in the upper part of the picture corresponding to convergence-induced cracks originating from the corner of the pillar. These cracks release intercrystalline-bound condensates.

162

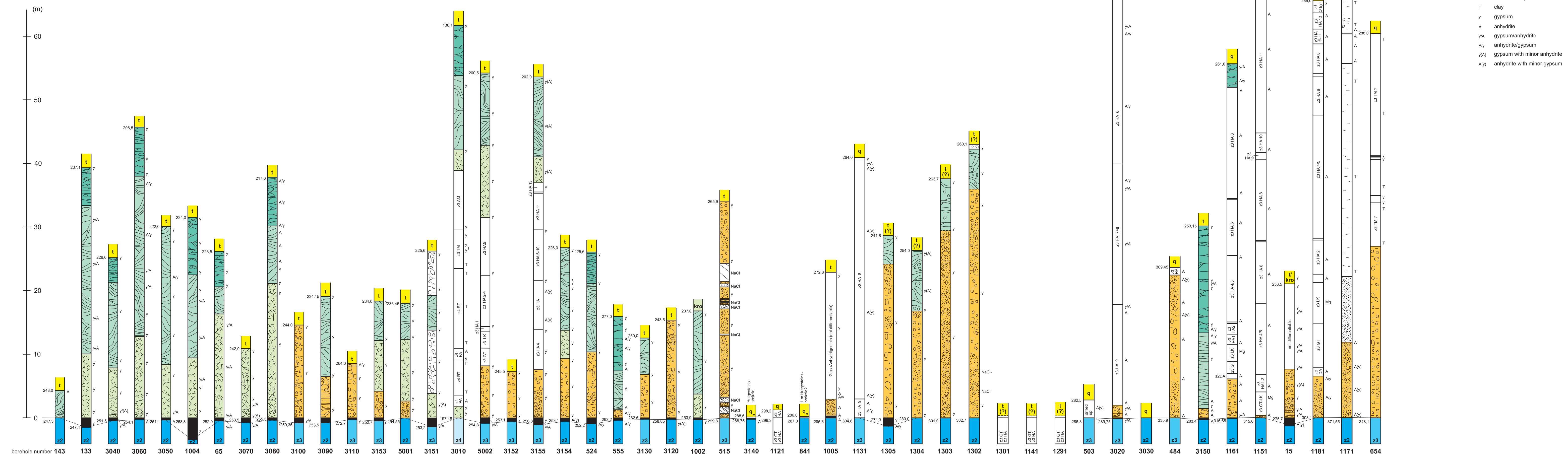
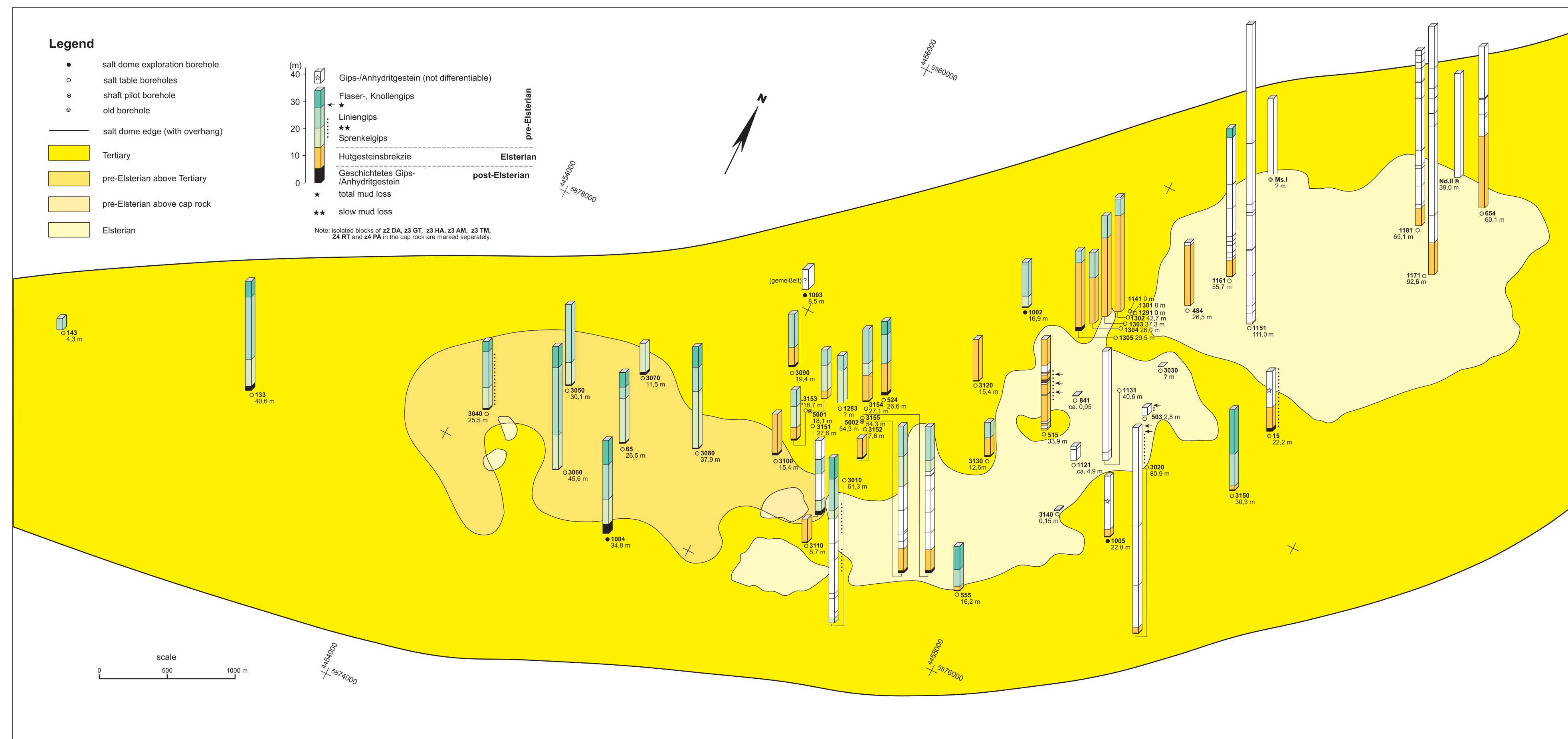
Figure 50: Gas composition of inclusions in evaporites in the Gorleben salt dome (according to SIEMANN & ELLENDORF 2001).

168

List of appendices

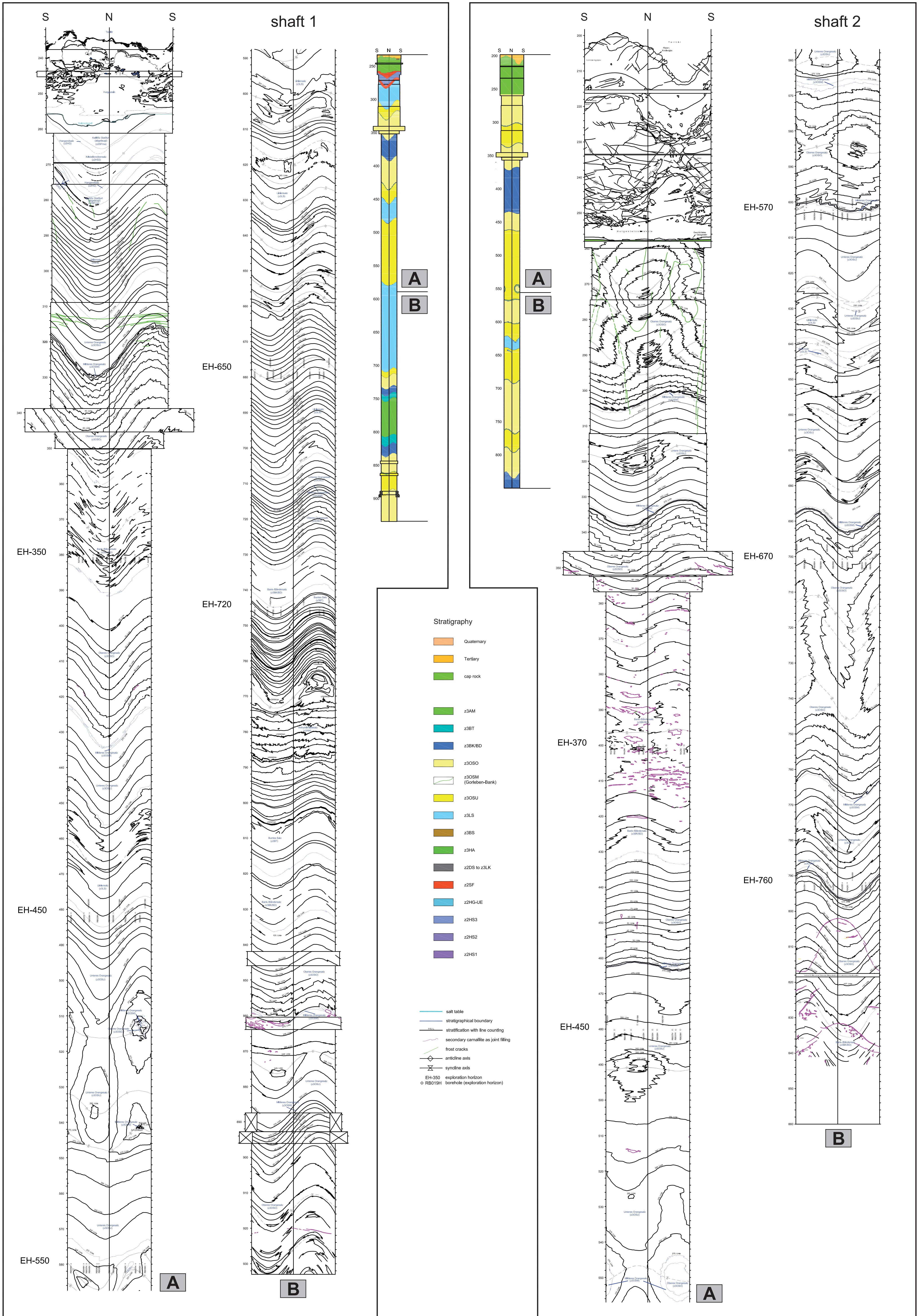
- Appendix 1: Spatial distribution, thickness, and petrography of the cap rock in the exploration, salt table and shaft pilot boreholes
- Appendix 2: Geology of shaft wall
- Appendix 3: Map of underground exploration boreholes
- Appendix 4: Geological maps
- Appendix 5: Geological cross sections
- Table 6: Simple derivation of post Elsterian time leaching rates based on the anhydrite contents in salt rocks at salt table and the thickness of Geschichtetes Gips-/Anhydritgestein
- Table 7: Stratigraphic table of the Zechstein beds, with information to the lithology and mean thickness

Spatial distribution, thickness, and petrography of the cap rock in the exploration, salt table and shaft pilot boreholes

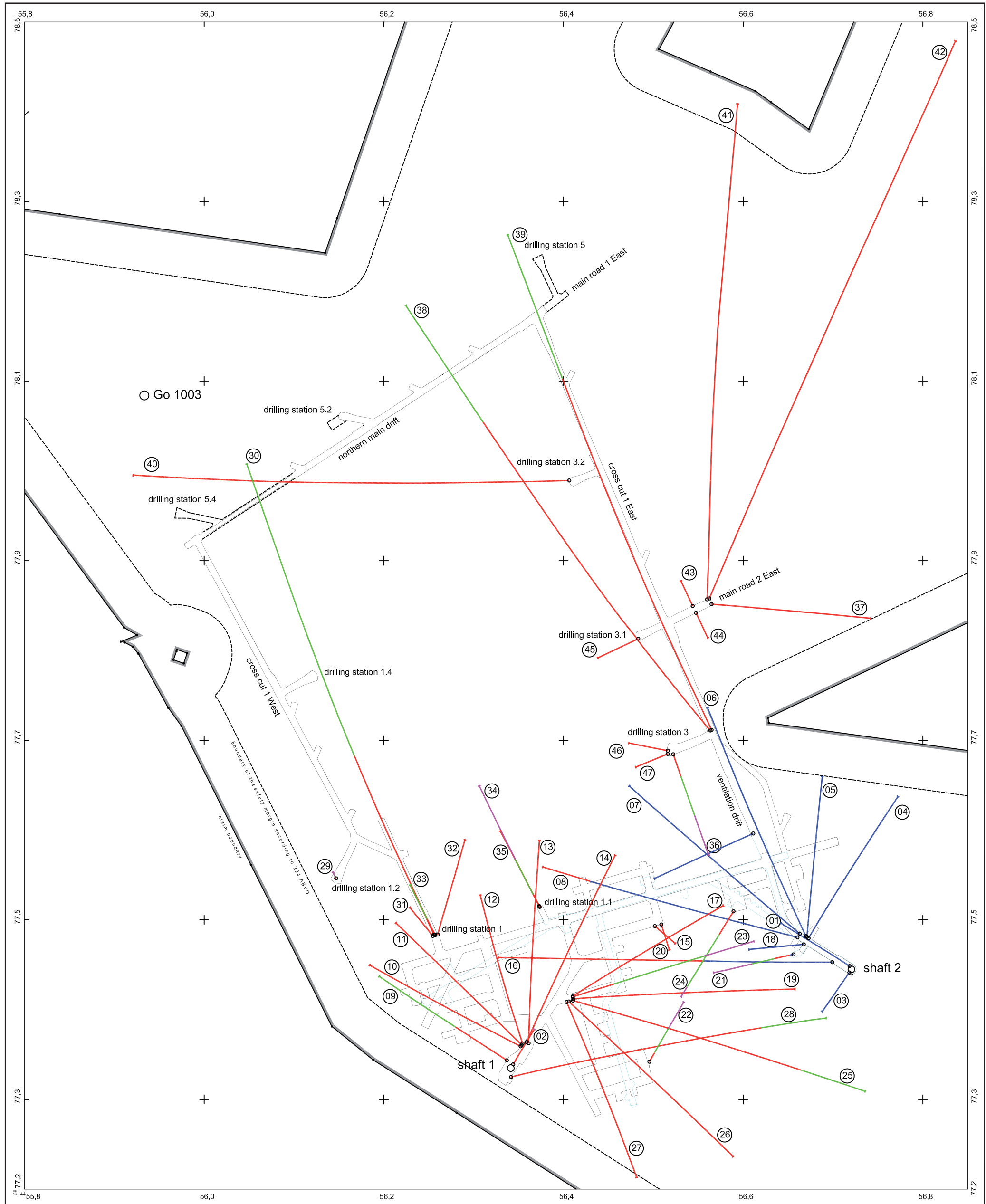


- Legend**
- q Quaternary
 - t Tertiary
 - kro Upper Cretaceous
 - z4 Allen-Folge
 - z3 Leine-Folge
 - z2 Stassfurt-Folge
 - z4 PA Pegmatitanhydrit
 - z4 RT Roter Salzion
 - z3 TM Tonmittelsalz
 - z3 AM Anhydritmittelsalz
 - z3 HA Hauptanhydrit
 - z3 LK Leine-Karbonat
 - z3 GT Grauer Salzion
-
- insoluble residue
- Flaser-, Knollengips
 - Liniengips
 - Sprenkelgips
-
- Elsterian
- Hulgesteinsbrekzie
 - Geschichtetes Gips-/Anhydritgestein
-
- post-Elsterian
- NaCl rock salt lump
 - T clay
 - y gypsum
 - A anhydrite
 - yA gypsum/anhydrite
 - Ay anhydrite/gypsum
 - y(A) gypsum with minor anhydrite
 - Ay(Anhydrite with minor gypsum

Geology of shaft wall



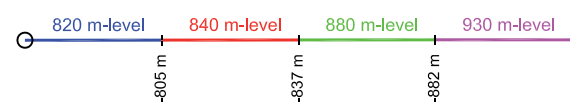
Map of underground exploration boreholes



Mine layout

- 820 m-level
- 840 m-level

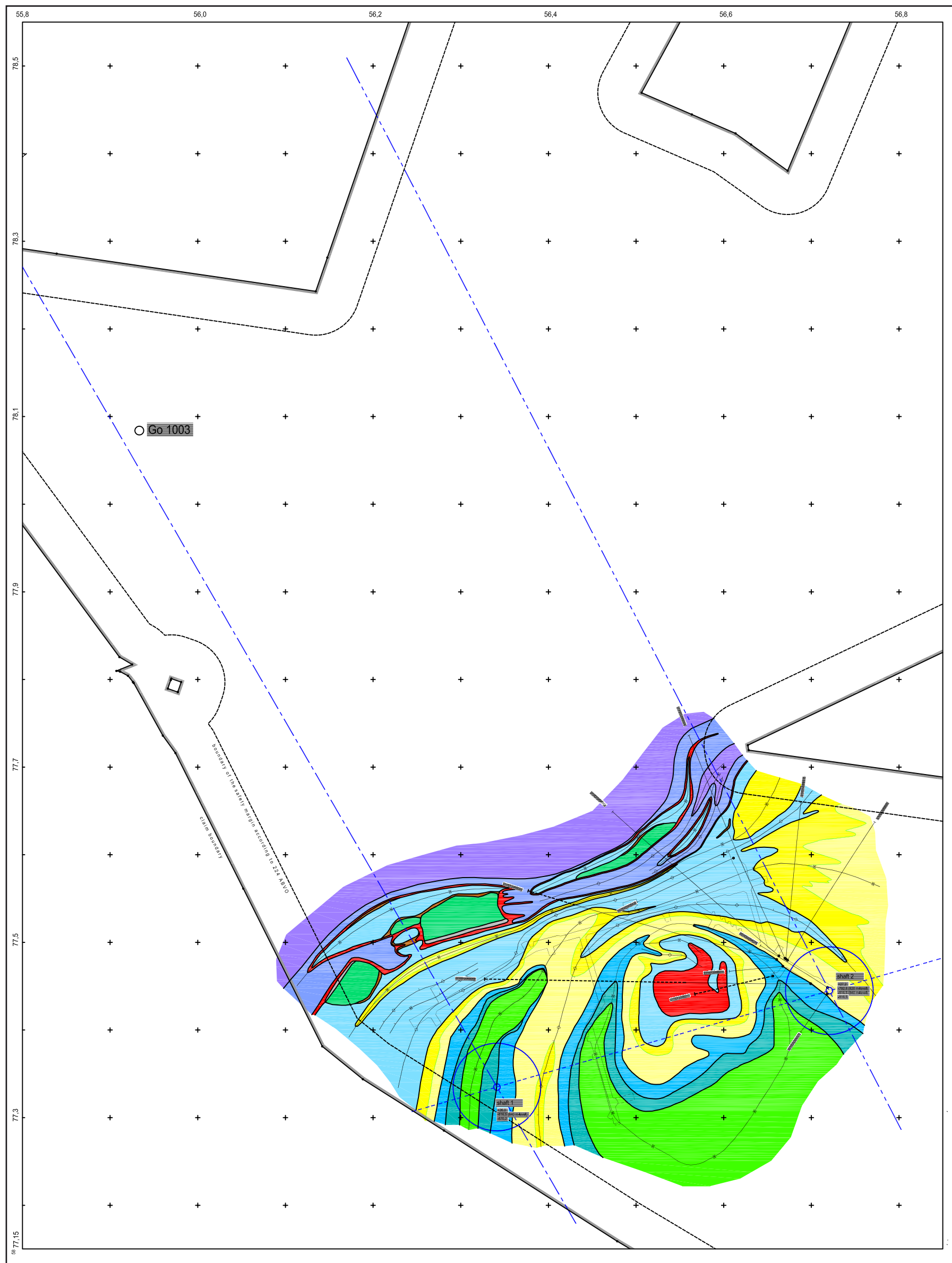
exploration borehole
with intersected mine levels



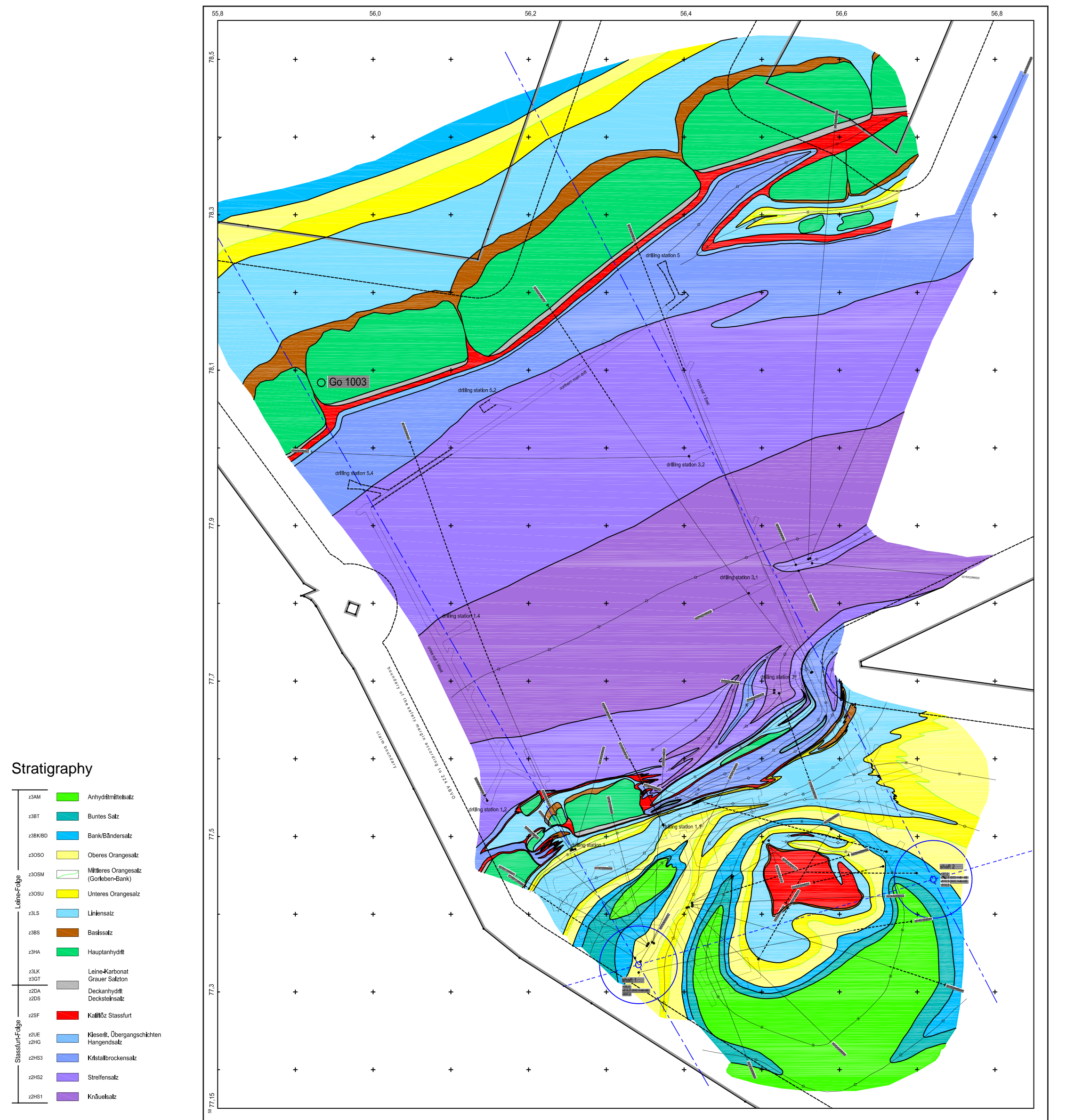
01 - 00YES02 RA274	17 - 02YEA04 RB021	33 - 02YER02 RB233
02 - 00YES01 RA777	18 - 01YEF20 RB014	34 - 02YER02 RB261
03 - 00YES02 RA272	19 - 02YEA04 RB022	35 - 02YER02 RB154
04 - 01YEF20 RB001	20 - 02YEA06 RB170	36 - 02YEQ01 RB194
05 - 01YEF20 RB015	21 - 01YEF20 RB217	37 - 02YER20 RB500
06 - 01YEF20 RB004	22 - 02YEA12 RB218	38 - 02YEQ01 RB119
07 - 01YEF20 RB002	23 - 02YEA04 RB029	39 - 02YEQ01 RB120
08 - 01YEF20 RB003	24 - 02YEA24 RB030	40 - 02YEQ01 RB427
09 - 01YEF11 RB058	25 - 02YEA04 RB023	41 - 02YER20 RB254
10 - 02YEF11 RB003	26 - 02YEA04 RB025	42 - 02YER20 RB488
11 - 02YEF11 RB012	27 - 02YEA04 RB024	43 - 02YER20 RB184
12 - 02YEF11 RB004	28 - 02YEF10 RB001	44 - 02YER20 RB186
13 - 02YEF11 RB013	29 - 02YEQ02 RB264	45 - 02YEQ01 RB208
14 - 02YEF11 RB001	30 - 02YER02 RB032	46 - 02YEQ01 RB206
15 - 02YEA06 RB171	31 - 02YER02 RB031	47 - 02YEQ01 RB210
16 - 01YEF20 RB059	32 - 02YER02 RB033	

Geological maps

820 m-level



840 m-level

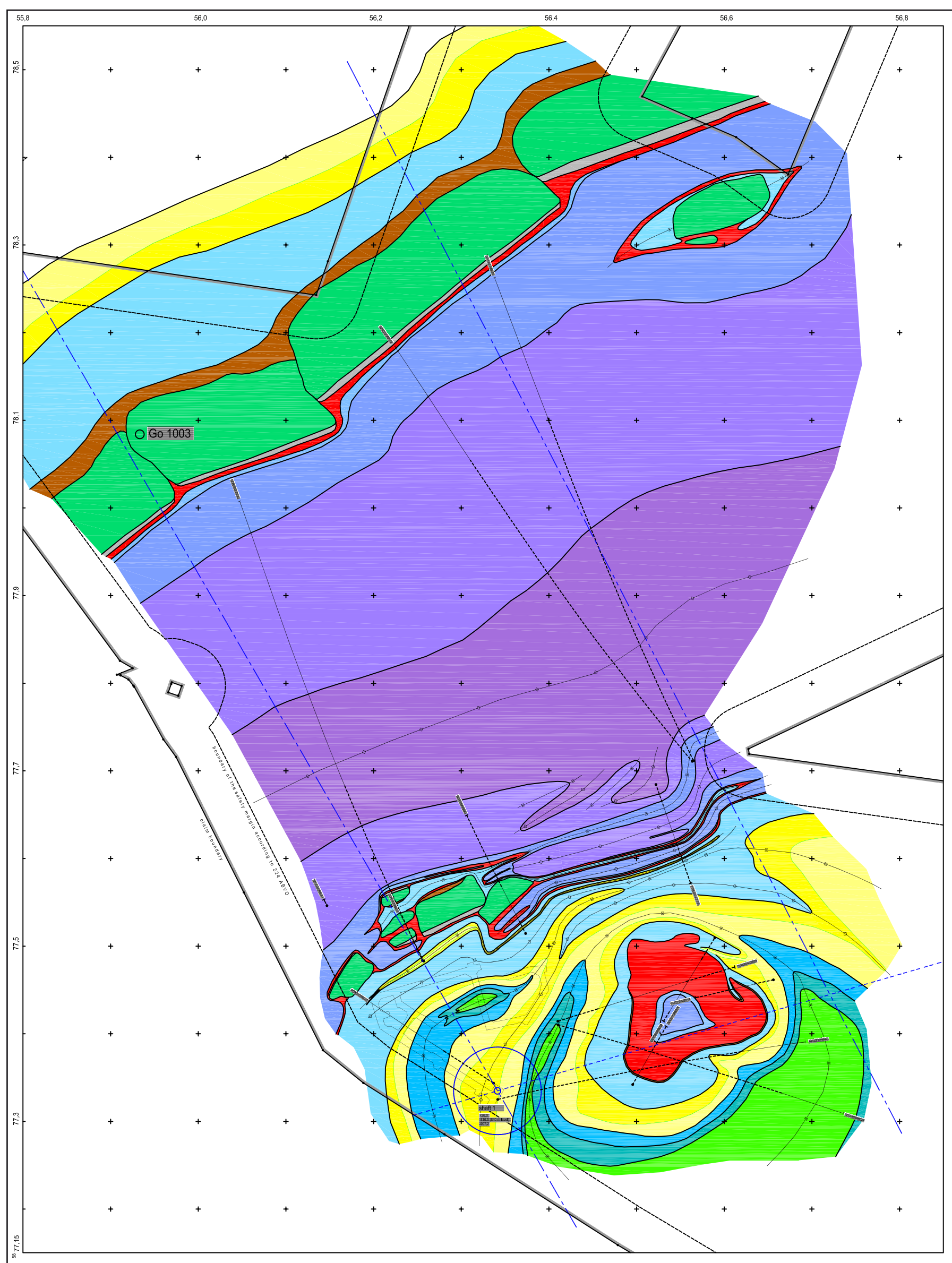


Stratigraphy

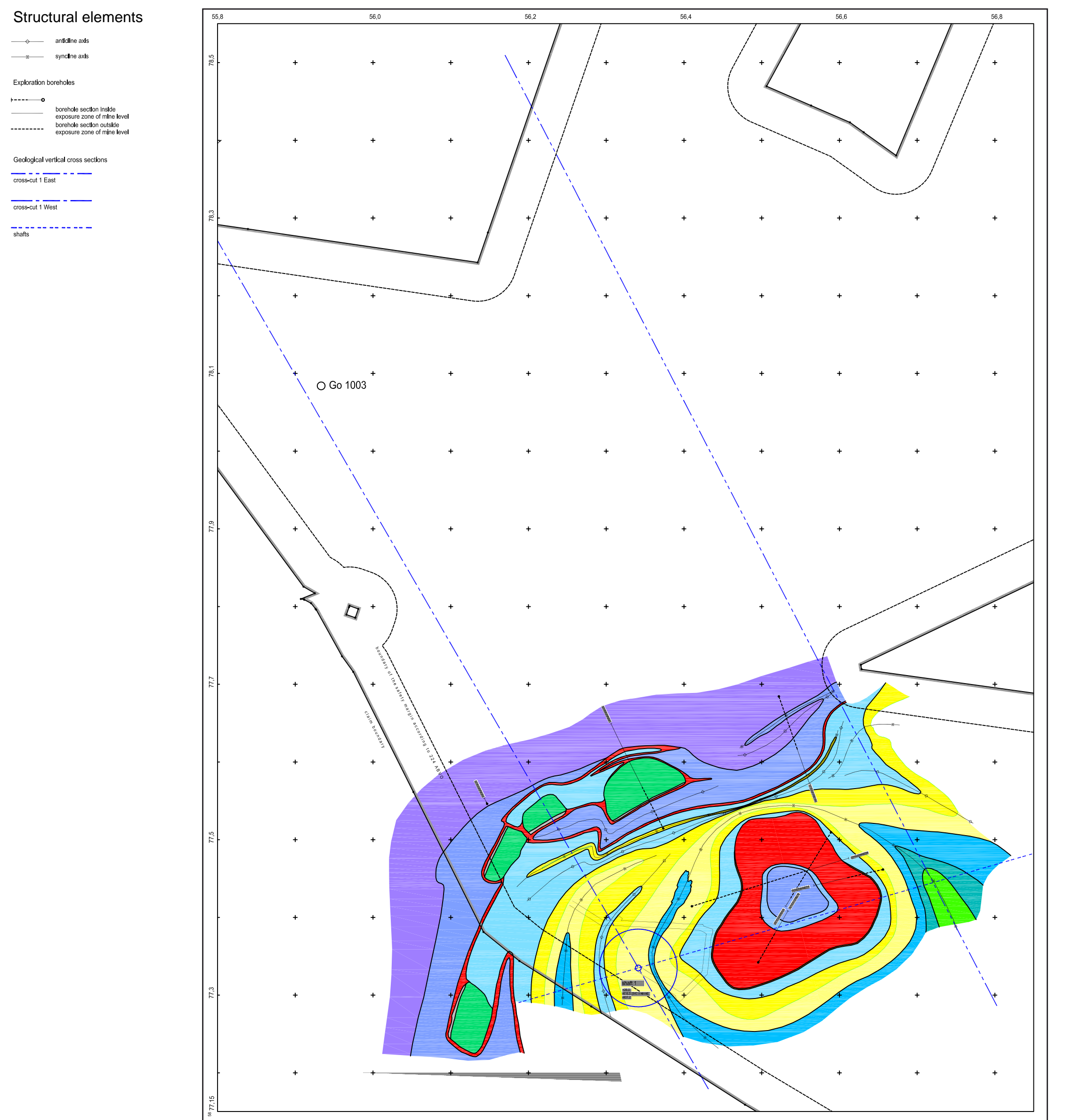
Elevation	Stratigraphic Unit
2390	Arthurschale
2387	Burtes Salz
2384/80	Bark/Schörsalz
2380	Oberes Orangeus
2378	Mittleres Orangeus (Gorkon-Bank)
2376	Unteres Orangeus
2375	Lilienus
2365	Baldus
2364	Hauptstufen
2357	Leine-Kalinal
2356	Groß-Salton
2354	Duckentuff
2353	Duckentuff
2352	Kalzig-Steinsart
2348	Neuer Übergangsschichten
2340	Hängenub
2340	Kristallrockensalz
2340	Stratonsalz
2340	Kochsalz

0 10 m

880 m-level



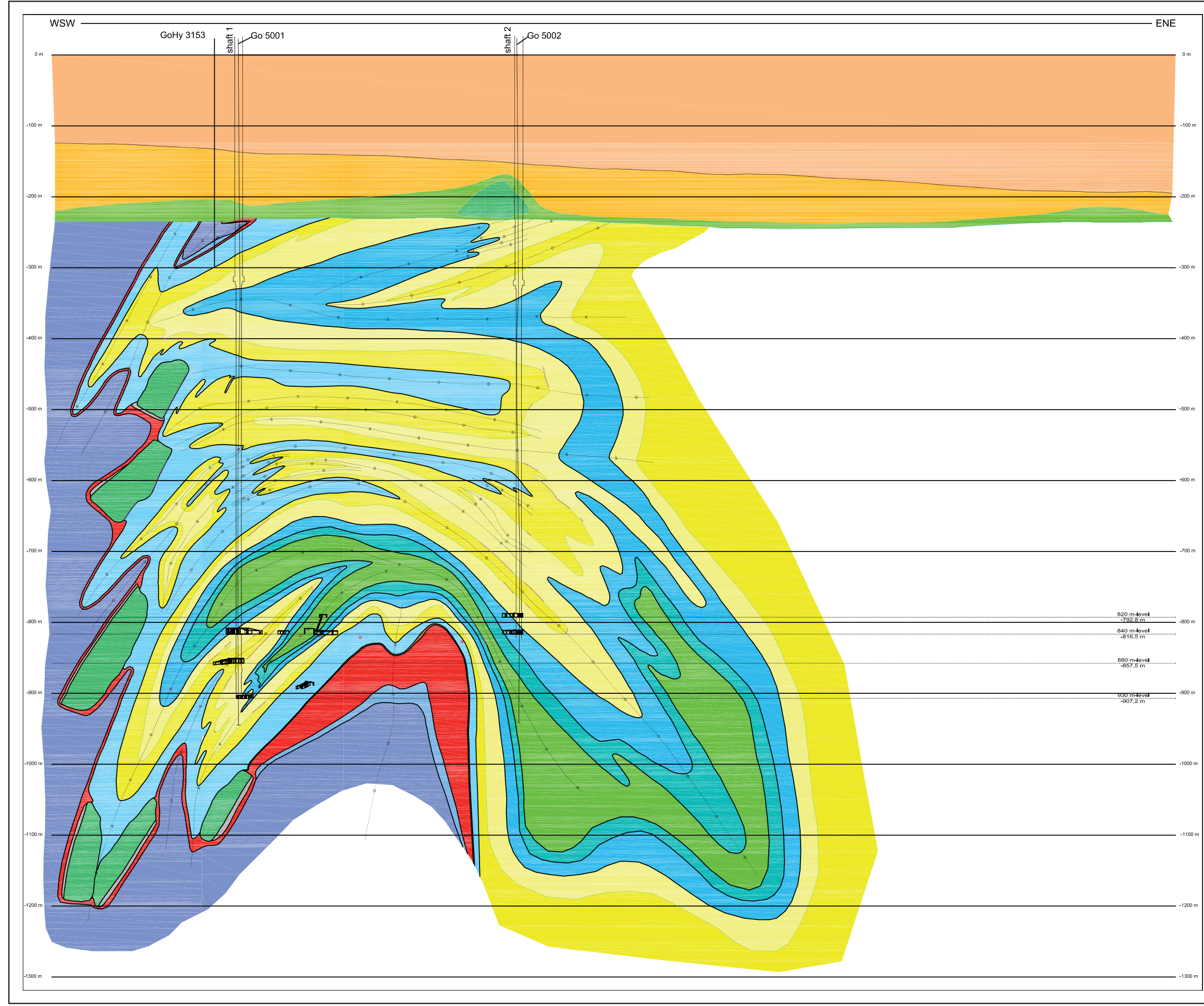
930 m-level



Structural elements

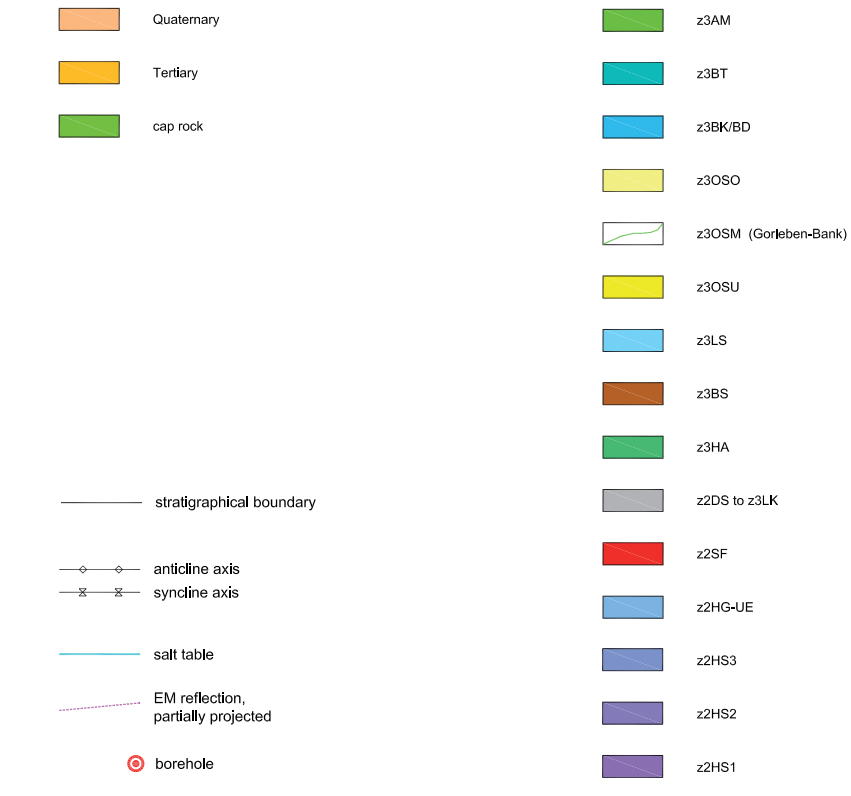
- anticline axis
- syncline axis
- Exploration boreholes
 - borehole section table
 - exposure zone of table level
 - borehole section outside
 - exposure zone of table level
- Geological vertical cross sections
 - crosscut 1 East
 - crosscut 1 West
 - stubs

shafts Gorleben 1 and 2

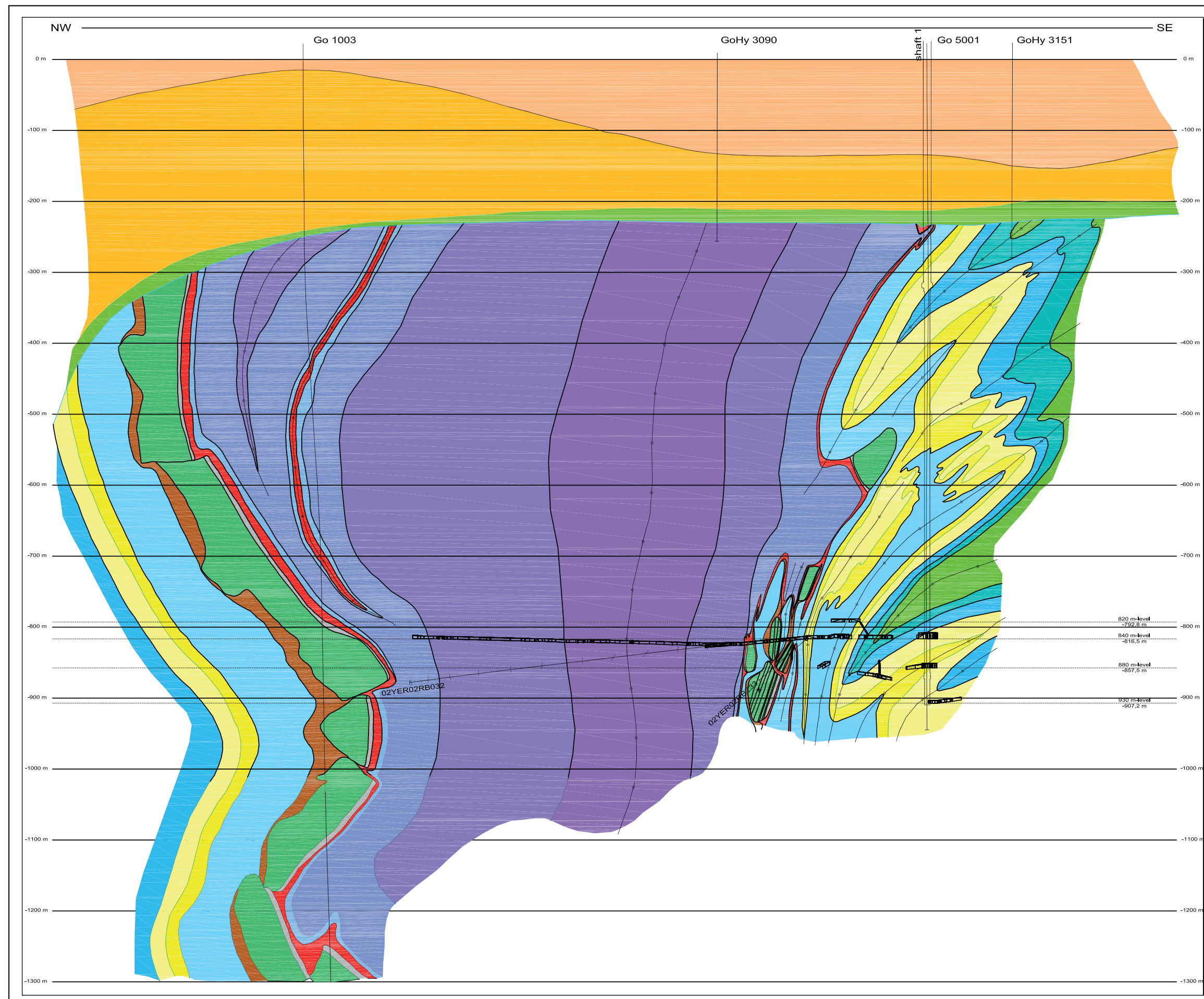


Geological cross sections

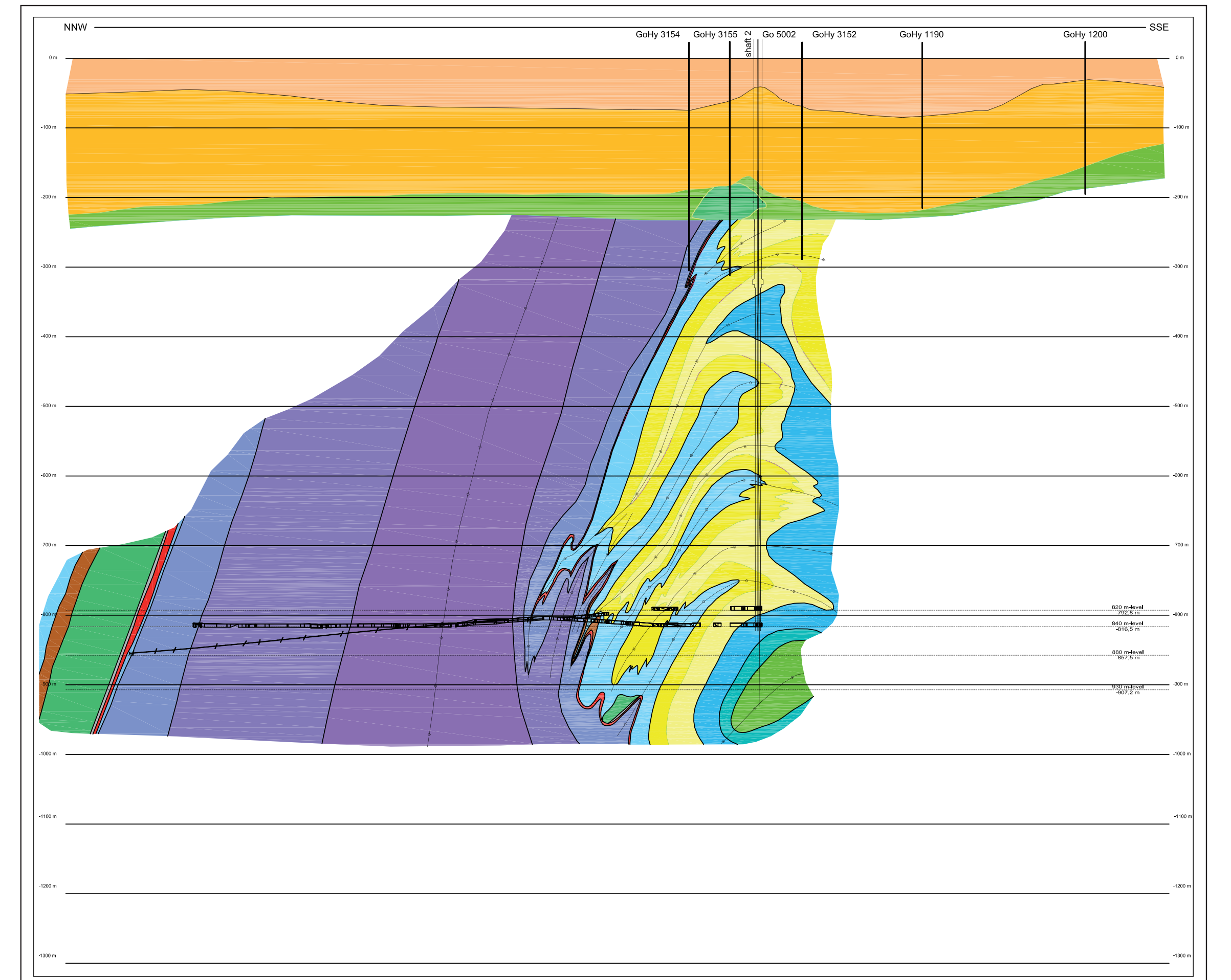
Stratigraphy



cross cut 1 West



cross cut 1 East



Stratigraphic table of the Zechstein beds, with information to the lithology and average thickness

BORNEMANN et al.:
Results of the geological surface and underground exploration of the salt formation

Table 7

Hannover 2008

Division	Group	Formation	old Symbol	new Symbol	Thickness (m)
Zechstein 7 (Möln-Folge)					
			z7	z7	
		Möln-Steinsalz		z7MS	
		Möln-Anhydrit		z7MA	
		Möln-Ton		z7MT	
Zechstein 6 (Friesland-Folge)					
			z6	z6	
		Grenzsande	zs	z6GS	
		Jüngeres Konglomerat	JK	z6KJ	
		Oberer Friesland-Ton	T6r	z6TO	
		Friesland Steinsalz	Na6	z6FS	
		Friesland-Anhydrit	A6	z6FA	
		Unterer Friesland-Ton	T6	z6TU	
		Friesland-Sandstein	S6	z6SD	
Zechstein 5 (Ohre-Folge)					
			z5	z5	
		Oberer Ohre-Ton	T5r	z5TO	
		Ohre-Steinsalz	Na5	z5OS	
		Ohre-Anhydrit	A5	z5OA	
		Unterer Ohre-Ton, Salzbrockenton	T5	z5TU	
		Ohre-Sandstein	S5	z5SD	
Zechstein 4 (Aller-Folge)					
			z4	z4	ca. 60
		Oberer Aller-Ton	T4r	z4TO	
		Aller-Grenzanhydrit	A4r	z4GA	
		Tonbanksalz	Na4tm	z4TB	
		Tonbrockensalz	Na4ß	z4TS	ca. 15
				z4TSO	
				z4TSU	
		Rosensalz	Na4y	z4RS	ca. 4
				z4RSO	
				z4RSM	
				z4RSU	
		Schneesalz	Na4ß	z4SS	ca. 4
		Basissalz	Na4α	z4BS	ca. 25
		Pegmatitanhydrit	A4	z4PA	ca. 1,5
				z4PA5	
				z4PA4	
				z4PA3	
				z4PA2	
				z4PA1	
		Aller-Karbonat	Ca4	z4AK	
		Roter Salztou	T4	z4RT	ca. 10
		Aller-Sandstein	S4	z4SD	
Zechstein 3 (Leine-Folge)					
			z3	z3	ca. 320
		Oberer Leine-Ton	T3r	z3TO	
		Grenzsatz	Na3tmg	z3GS	
		Tonmittelsalz	Na3tm	z3TM	ca. 36
				z3TM3/t	
				z3TM2/na	
				z3TM2/t	
				z3TM1/na	
				z3TM1/t	
		Kaliföz Riedel	K3Ri	z3Ri	ca. 10
		Schwadensalz	Na3ß	z3SS	ca. 12
				z3SS10	
				z3SS9	
				z3SS8	
				z3SS7	
				z3SS6	
				z3SS5	
				z3SS4	
				z3SS3	
				z3SS2	
				z3SS1	
		Anhydritmittelsalz	Na3η	z3AM	ca. 60
				z3AM9/na	
				z3AM9/ah	
				z3AM8/na	
				z3AM8/ah	
				z3AM7/na	
				z3AM7/ah	
				z3AM6/na	
				z3AM6/ah	
				z3AM5/na	
				z3AM5/ah	
				z3AM4/na	
				z3AM4/ah	
				z3AM3/na	
				z3AM3/ah	
				z3AM2/na	
				z3AM2/ah	
				z3AM1/na	
				z3AM1/ah	
		Buntes Salz	Na3ζ	z3BT	ca. 12
		Kaliföz Bergmannsseggen	K3Be	z3BE	ca. 15
		Bändersalz	Na3ε	z3BD	} ca. 14
		Banksalz	Na3δ	z3BK	
		Kaliföz Ronnenberg	K3Ro	z3RO	
		Orangesalz	Na3γ	z3OS	ca. 50
				z3OSO	
				z3OSM	0-0,7
				z3OSU	
		Linienatz	Na3β	z3LS	ca. 30
				z3LSO	
				z3LSM	
				z3LSU	
		Basissalz	Na3α	z3BS	ca. 15
		Hauptanhydrit	A3	z3HA	ca. 40-80
				z3HA13	
				z3HA12	
				z3HA11	
				z3HA10	
				z3HA9	
				z3HA8	
				z3HA7	
				z3HA6	
				z3HA5	
				z3HA4	
				z3HA3	
				z3HA2	
				z3HA1	
		Leine-Karbonat	Ca3	z3LK	ca. 1,5
		Grauer Salztou	T3	z3GT	ca. 2,5
				z3GTO	
				z3GTU	
		Leine-Sandstein	S3	z3SD	
Zechstein 2 (Staßfurt-Folge)					
			z2	z2	ca. 700-950
		Oberer Staßfurt-Ton	T2r	z2STO	
		Gebänderter Deckanhydrit	A2r	z2DA	ca. 1,5
				z2DAO	
				z2DAU	
		Decksteinsalz	Na2r	z2DS	0,2-0,5
		Kaliföz Staßfurt	K2	z2SF	15-30
		Kieseritische Übergangsschichten	Na2k	z2UE	0-2,5
		Hangendsalz	Na2y	z2HG	max. 10
		Hauptsalz	Na2ß	z2HS	
				z2HS3	ca. 60
				z2HS2	
				z2HS1	ca. 700-800
		Basissalz	Na2α	z2BS	ca. 20
		Basalanhydrit	A2	z2BA	ca. 19
				z2BA/t	
				z2BA2	
				z2BA1	
		Staßfurt-Karbonat	Ca2	z2SK	ca. 5
				z2SKO	
				z2SKU	
		Staßfurt-Ton	T2	z2ST	
Zechstein 1 (Werra-Folge)					
			z1	z1	ca. 60
		Geismarer Schichten	GS	z1GS	
		Oberstes Werra-Steinsalz	Na1r	z1SO	
		Oberer Werra-Anhydrit	A1r	z1WAO	ca. 45
		Oberes Werra-Karbonat	Ca1r	z1WKO	
		Oberer Werra-Ton (brown-red)	T1r	z1WTO	
		Tonmittel (salt-free random facies)	TM	z1TM	
		Mittleres Werra-Sulfat (salt-free random facies)	A1b	z1WAM	
		Oberes Werra-Steinsalz	Na1y	z1WSO	
				z1WSO3	
				z1WSO2	
				z1WSO1	
		Kaliföz Hessen	K1H	z1HE	
		Mittleres Werra-Steinsalz	Na1ß	z1WSM	
		Kaliföz Thüringen	K1Th	z1TH	
		Unteres Werra-Steinsalz	Na1α	z1WSU	
		Anhydritknotenschiefer	A1Ca	z1AK	
		Unterer Werra-Anhydrit	A1	z1WA	
				z1WAT	
				z1WAD	
				z1WAR	
		Stättebergsschichten	ST	z1ST	
		Zechsteinkalk	Ca1	z1ZK	ca. 5
		Kupferschiefer	T1	z1KS	ca. 0,4
		Grenzdolomit	T1Ca	z1GD	ca. 0,6
		Werra-Sandstein	S1	z1SD	
		Werra-Konglomerat	C1	z1WK	

Zechstein rocks encountered in the Gorleben exploration mine (exceptions: Kaliföz Bergmannsseggen and Kaliföz Ronnenberg)



Bundesanstalt für Geowissenschaften und Rohstoffe (BGR)
Geozentrum Hannover
Stilleweg 2
30655 Hannover
Germany

www.bgr.bund.de

ISBN 978-3-9813373-6-5

